THE UNIVERSITY
of LIVERPOOL

EXPERIMENTAL STUDY OF BEAM DEFLECTION TO IMPROVE A MODEL FOR THE EFFECTIVE SECOND MOMENT OF AREA OF ONE-WAY REINFORCED CONCRETE ELEMENTS

by

Akmaluddin
B.Sc., M.Sc.(Eng.)

Thesis submitted in accordance with the requirement of the University of Liverpool for the degree of Doctor in Philosophy

January 2004

Abstract

The effective second moment of area, I_e, is required in calculating the deflection of a reinforced concrete beam with a cracked section. Many models and equations have been presented over the years for calculating its value. Some have been derived using past experimental results and models. In this study the experimental evaluation of the deflection of beams under various form of loading have been carried out. Using these results a model previously developed in Department of Civil Engineering the University of Liverpool has been modified and verified based on these results. The beams, which varied in concrete strength and reinforcement ratio, were subjected to both two symmetrical and two unsymmetrical point loads.

The load deflection relationship for each beam was obtained experimentally. From this relationship the experimental values of initial cracking load, P_{cr}, reinforcement yield load, P_y and fully cracked load, P_u were calculated. When the maximum deflection of span/250 is adopted, the experimental value of service load can also be obtained from the load-deflection relationship.

During each test the crack propagation was marked on the side of beam for each load increment. At the end of each test the side of the beam was photographed. This enabled the crack length to be accurately measured. The results obtained experimentally showed very similar trends to the theoretical values, the experimental values being slightly less, and the degree of difference depending on the reinforcement ratio.

By considering all the above factors the calculation produce for the cracked second moment of area, I_{cr}, was modified. Also it was found that factor Φ also had to be redefined. In this study two variations of I_{cr} are proposed (I_{crm1} and I_{crm2}). The first variation produced one possible factor Φ (Φ_{m1}) and the second one offered two possible values for the factor Φ (Φ_{m2a} and Φ_{m2b}). As a result three combinations for I_e are proposed namely Case1, Case2a and Case2b that all agree well with the experimental results in this study for symmetrical and unsymmetrical two point loads.

To check whether the proposed models can be used widely, hundreds of data obtained from references with reinforcement ratio between and outside the range considered in this study were used for verification. The results showed that only Case2b gives reasonable results that are comparable with the experimental values. This model was valid when used for singly reinforced concrete with reinforcement ratios between 1% and 3%.

Acknowledgements

The author wishes to take this opportunity to express gratitude to all who made contributions to this project. In particular my supervisors, Mr. C. Thomas, for his invaluable advice and guidance throughout the course of this research.

To Tony, Martin and all the technicians for their help in casting and testing the sample beams. Also to my friends, and colleagues in Civil Engineering Department past and present and in particular Yohan for his help and support.

The author would also like to acknowledge the financial support of the EEDP (Engineering Education Development Project) of Indonesia, without which this work would not have been possible.

Finally, a deepest love and thanks goes to my wife and daughter, Dinna and Nadya respectively, for their endless support, patient and interest throughout the course of this research.

Table of Contents

List of Tables

List of Figures

List of Symbols

A_c	Area of concrete section (mm^2)
A_s	Area of steel reinforcement (mm^2)
a	Distance between support and load position (m)
b	Distance between load and support in terms of unsymmetrical point load (m)
b	Breadth of beam (mm)
d	Effective depth of beam (mm), defined as the distance from the centroid of the steel area to the outer compression fiber
d_s	Diameter of steel reinforcement (mm)
h	Total depth of beam (mm)
E_c	Concrete modulus of elasticity (GPa)
E_s	Steel modulus of elasticity (MPa)
F_{cc}	Force resultant of concrete block (kN)
F_s	Forces resultant of steel reinforcement (kN)
f_{ct}	Tensile stress of concrete (MPa)
f_{td}	Tensile strength of concrete(MPa)
f_c	Concrete strength (MPa)
f_c'	Concrete strength based on cylinder specimens (MPa)
f_{cu}	Concrete strength based on cube test results (MPa)
f_k	Characteristic strength of specimen tested (MPa)
f_m	Mean strength of specimen test results (MPa)
f_r	Modulus of rupture (the tensile stress at which cracking occurs by flexure) (MPa)
f_{st}	Tensile stress of steel reinforcement (MPa)
f_s	Stress of steel reinforcement (MPa)
f_y	Yield or proof stress of reinforcement (MPa)
I	Second moment of area (mm^4)
I_{cr}	Cracking second moment of area (mm^4)
$I_{cr(th)}$	Theoretical $I_{cr} = I_{cr}$ (mm^4)
I_{cre}	Equivalent I_{cr} proposed by Fikry (mm^4)

I_{crm1}	Modified of I_{cr} alternative 1 proposed in this study
I_{crm2}	Modified of I_{cr} alternative 2 proposed in this study
I_e	Effective second moment of area (mm^4)
I_g	Gross second moment of area neglecting steel area (mm^4)
I_{gt}	Gross second moment of area of transformed section (mm^4)
K	Factor of loading type for deflection calculation based on curvature approach
k	Factor depending on loading type for deflection in terms of second moment area method.
L	Clear span between two supports (m)
L	Length of the reinforcement (m)
L_{cr}	Cracking length (m)
M	Mass of the reinforcement (kg)
M_a	Maximum service moment (kN m)
M_{cr}	Cracking moment (kN m)
M_u	Ultimate moment (kN m)
n	Modular ratio = E_s/E_c
n_s	number of reinforcement inside concrete section
P	Service load (kN)
P_{jack}	Capacity of load cell to failure beam sample (kN)
P_u	Ultimate load (kN)
s	Standard deviation
s	Depth of stress concrete block (mm)
W	Total load on the span
w	Density of concrete (kg/m^3)
x	Neutral axis depth (mm)
x_{bal}	Neutral axis depth at balanced condition (mm)
z	Lever arm, distance between concrete force resultant and centroid of steel force
α, β	Factor depending on $n\rho$ values for calculating I_{cr}
β_1	Factor dependent upon concrete strength
Δ	Deflection
ε_a	Mean strain under upper loading stress
ε_b	Mean strain under basic loading stress
ε_{cc}	Strain on the concrete compression zone

ε_s	Actual strain on steel reinforcement
ε_{st}	Strain on the tensile zone which correspond to steel strain
ε_y	Strain on the steel reinforcement at the yield condition
Φ	Factor depending loading type, concrete grade and reinforcement ratio
Φ_{m1}	Modified factor Φ alternative 1 based on I_{crm1} proposed in this study
Φ_{m2a}	Modified factor Φ alternative 1 based on I_{crm2}
Φ_{m2b}	Modified factor Φ alternative 2 based on I_{crm2}
ϕ	Curvature
γ_f	Partial safety factor of load
γ_m	Partial factor of safety of material
ρ	Reinforcement ratio, defined as ratio of the tension steel area to the effective concrete area, *bd* (%)
ρ_b	Reinforcement ratio on the balanced condition (%)
ρ_{max}	Maximum reinforcement ratio (%)
ρ_{min}	Minimum reinforcement ratio (%)
σ_a	Upper loading stress (N/mm^2)
σ_b	Basic stress (N/mm^2)

Chapter 1

Introduction

1.1 Basic philosophy

When a point load is applied to a simply supported reinforced concrete beam, as shown in Figure 1.1, the concrete will initially be a complete (uncracked) section.

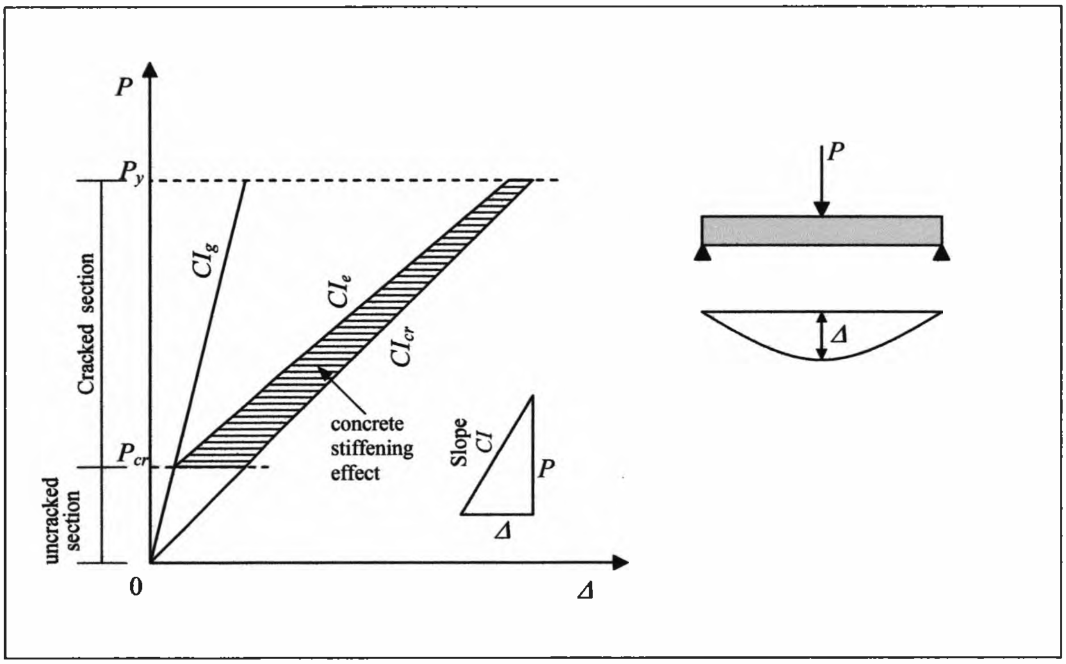

Figure 1.1 Flexural behaviour of simply supported beams

At a specific load, P_{cr}, the concrete section will start cracking, with further increases in loading producing a spread of the cracking out toward the supports.

The deflection of simply supported beam, such as Figure 1.1, is given by Equation (1.1) as below.

$$\Delta = \frac{P}{C\,I} \tag{1.1}$$

in which C is calculated as $C = 48E_c/L^3$, where E_c is the elastic modulus of concrete and L is effective span of the beam.

The value of I on the Equation above would be a variable depending on load magnitude, P. When the value of load is less than P_{cr} the deflection of the beam can be found by computing the gross cross section neglecting steel reinforcement, I_g, or the gross cross section transformed (steel area is transformed to be concrete area), I_{gt}, of the beam. In practice I_g is used commonly instead of I_{gt}.

However as the load increases above the cracking load, producing cracks along the span of the beam, a more complicated condition is produced. The cracking will occur in the tensile zone of the beam causing the beam stiffness or flexural rigidity to be reduced and eventually beam failure. The position is further complicated in that the cracked concrete will still have some part to play in carrying the load. This is usually called the concrete stiffening effect, and its effect on the deflection of the beam can be seen in Figure 1.1. This means that the second moment of area is greater than I_{cr} so that an effective second moment of area I_e must be calculated to evaluate the deflection of the beam in which the value of I_e changes along the beam span from a maximum value of I_g for uncracked section to a minimum value of I_{cr} for fully cracked transformed section.

Based on explanation above many empirical expressions for the evaluation of second moment of area I_e have been proposed. The most widely accepted of these is Branson's equation [1] where the effective second moment of area over the entire length of simply supported beam is expressed in the form

$$I_e = I_{cr} + (I_g - I_{cr}) \left(\frac{M_{cr}}{M_a} \right)^m \quad (1.2)$$

where,

I_{cr}	is cracking second moment of area
I_g	is gross second moment of area ignoring reinforcement
M_{cr}	is cracking moment
M_a	is maximum applied service moment
m	is a constant

Equation (1.2) above is used to compute the effective second moment of area, I_e, when $M_a > M_{cr}$, otherwise I_e must be taken as I_g.

Recently, an approach to calculate the effective second moment of area has been developed by Fikry [2] based on data found in the literature and given as Equation (1.3).

$$I_e = I_{cre} + (I_g - I_{cre})\ e^{\Phi} \tag{1.3}$$

Where,

Φ is function of loading intensity and reinforcement ratio. This will be explained in detail later in Chapter 4.

I_{cre} is a simplified form of I_{cr} and will be discussed in Chapter 4.

No experimental work was conducted by Fikry in developing his model, therefore, an experimental programme has been considered to verify and/ or modify the proposed Fikry's equation above.

1.2 Scope of Thesis

The goal set in this study is to verify and/ or possibly modify the previous work of Fikry [2] by experimental work in the laboratory to measure the deflection of one-way reinforced concrete elements with various concrete grades and reinforcement ratios, under different load conditions.

The main objectives of this study are:

(i) To investigate the deflection and crack development in a number of beams for various concrete grades, reinforcement ratios and load positions of two symmetrically applied point loads.

(ii) To verify and/ or modify the expression for cracking second moment of area, I_{cr}, based on experimental data obtained during the first objective above.

(iii) To verify and/ or modify factor Φ after the second objective has been reached.

(iv) To verify and/ or modify the value of the second moment of area, I_e, of the model developed by Fikry.

As the study progresses the objectives outlined above will be fully elaborated and any aspect related with the expression will be discussed.

1.3 Organization of Thesis

Chapter 1 presents a basic philosophy of beam failure in flexure. This part of the study is the development of the model. The limitations of this study and its objectives are also elaborated in this chapter. Chapter 2 gives a brief review of the previous works conducted by researches relating to this study.

The test beams considered in this study are analysed in Chapter 3. Parameters involved, mainly material properties and models used in this study, are discussed in this chapter. Effective second moment of area, I_e, is discussed in Chapter 4. Cracking second moment of area, I_{cr}, and factor Φ in the model proposed are also elaborated in this chapter.

The main aspects of the experimental method and apparatus used in this study are outlined in Chapter 5, where the calibration of the equipment is also discussed.

Chapter 6 presents the experimental results obtained from the physical testing programme, together with modification to the previous model. The modified models proposed are presented in this chapter. The proposed models are initially verified using test beams in this study with different characteristics followed by test beams obtained from journal papers. Discussion of the results and summary are also presented in this chapter.

In Chapter 7, a brief discussion for the model proposed is presented. This is then followed by the conclusion. In addition, suggestions for possible future work are given.

Chapter 2

Review of Previous Works

2.1 Introduction

The aim of this chapter is to present an overview of the work most relevant to the calculation of beam deflections. This chapter will present the research carried out by researchers, relating to this topic, over the last few years.

Deflection is normally predicted either by a using curvature coefficient or effective second moment of area approach [3]. Past publications relating to both approaches are presented and discussed. As the effective second moment of area approach is the primary concern of the current study it was thought useful to present a chronological review of the research carried out on this topic.

2.2 Methods A and B of Yu and Winter

Based on extensive studies, Yu and Winter [4] suggested in 1960 two alternative methods of flexural rigidity to predict the instantaneous deflection using the usual elastic deflection equation, Equation (1-1), as described below.

a. Method A

In this method the value of E_c in the deflection equation is suggested to be $1000f_c^{'}$ in which $f_c^{'}$ is the concrete cylinder compressive strength. The value of I in the equation be I_{cr} in which I_{cr} is second moment of area of the cracked transformed section as given by Equation (4.6) in Chapter 4.

b. Method B

The contribution of concrete section in the tension region is ignored in Method A. Method B, however, considers the contribution by replacing the value of I in the deflection equation, Equation (1-1), with

$$I = \frac{I_{cr}}{\left[1-\left(b\frac{M_1}{M_a}\right)\right]} \tag{2.1}$$

where

b is the width of beam at the tension zone

M_a is the applied moment

$M_1 = 0.1\left(f_c^{'}\right)^{\frac{2}{3}} h\left(h-x\right)$

h is the total depth

x is the depth of neutral axis as given by Equation (4.4) in Chapter 4.

In other words, to account for the contribution of the concrete in the tension side the instantaneous deflection obtained using Method A is multiplied by a correction factor, $\left[1-bM_1/M_a\right]$.

It can be seen that method B is semi-empirical as there is a factor 0.1 involved in the expression for M_1. To calculate the value of x is not an easy task which makes using the second model a lengthy process. In addition, as presented in their report, it can be seen that some beams have predicted deflections underestimating the measured deflection by more than 20%.

2.3 Branson's Equation

The equation proposed by Branson [1], Equation (1.2), has been widely used and adopted by both American and Canadian codes [5,6]. He developed his model based on experimental data. The equation proposed was initially based on results obtained by testing simple supported beams under uniform loads. He suggested that a value of 4 be taken for the power m whenever numerical integration is used to calculate I_e over the entire span. Alternatively, however, he recommended a power of 3 be used for an average I_e over the entire span and reformulated Equation (1.2) to be,

$$I_e = I_{cr} + (I_g - I_{cr}) \left(\frac{M_{cr}}{M_a}\right)^3 \leq I_g \tag{2.2}$$

The equation was also found applicable to beams continuous at one-end using an average value of second moment of area given by the following equation

$$I_{av} = \tfrac{2}{3}\left[\text{Pos.Mom. } I_e\right] + \tfrac{1}{3}\left[\text{Neg.Mom. } I_e\right] \tag{2.3}$$

For beams continuous at both-ends he suggested the following equation

$$I_{av} = \tfrac{2}{3}\left[\text{Pos.Mom. } I_e\right] + \tfrac{1}{6}\left[\text{Neg.Mom. } I_e\right] \text{ Left End} + \tfrac{1}{6}\left[\text{Neg.Mom. } I_e\right] \text{ Right End} \quad (2.4)$$

For other types of loading, i.e. concentrated load, the above equation was found to produce errors as high as 100% for the deflection of a beam [7,8].

2.4 Grossman's Equation

Nearly 20 years after Branson produced his Equation, in 1981 Grossman [9] proposed simplifications to Branson's equation in an effort to eliminate the need to calculate I_{cr}. He modified Branson's equation as follows,

a. When $M_a/M_{cr} < 1.6$

$$I_e = \left(\frac{M_{cr}}{M_a}\right)^2 I_g \leq I_g \quad (2.5)$$

b. When $M_a/M_{cr} > 1.6$

$$I_e = 0.1\left(\frac{M_a}{M_{cr}}\right) I_g \quad (2.6)$$

with a lower bound of $0.35I_g$ for I_e calculated by either Equation (2.5) or Equation (2.6).

The equations have been derived by considering the variation of $\left(I_e/I_g\right)$ against $\left(M_a/M_{cr}\right)$ for a number of beams. By dividing the curve obtained using Branson's equation into two parts the simplified equations shown above were derived. Then values of I_e produced when using these simplified equations were within 10% of the values obtained using Branson's equation.

Since no experimental results were consulted the study assumed the second moment of area as given by Branson's equation to be exact. However, because the proposed expression still did not represent the loading type and that their validity was drawn based on Branson's equation, which itself bears the drawback discussed above, there was no reason to accept the proposed expressions as a sound alternative.

2.5 Rangan's Equation

Rangan [10] in 1982 proposed two approaches. Initially, he suggested the following equation as an attempt to simplify the calculation of the effective second moment of area

$$I_e = Kbd^3 \tag{2.7}$$

where

K is a function of $n\rho$

for $n\rho > 0.045$

$$K = 0.1955\sqrt{n\rho} \quad \leq \quad 0.111$$

and

for $\quad n\rho \le 0.045$

$$K = 0.0019/n\rho \le 0.067$$

Later he proposed another approach to control the beam deflection by using an allowable span-depth ratio given by the following equation, Equation (2.8).

$$\frac{l}{d} \le K_1 K_2 \left[\frac{(\Delta_i)_{\lim}}{l} \frac{\alpha b_{ef} E_c}{(w + \lambda w_s)} \right]^{0.33} \qquad (2.8)$$

where

l	is the span of the beam
d	is the effective depth of section
$(\Delta_i)_{lim}$	is the maximum permissible total deflection
b_{ef}	is the effective width of the compressive face at mid-span region
E_c	is the modulus of elasticity of concrete
α	is a number depend on the value of $n\rho$ and given by the following equation for $n\rho > 0.045$, $\alpha = 15\sqrt{n\rho} \le 8$ and for $n\rho \le 0.045$, $\alpha = 1/7n\rho \le 5$
n	is the modular ratio
ρ	is the reinforcement ratio at mid-span
w	is the service load per unit length
w_s	is the sustained load per unit length

λ is the long-time deflection multiplier

K_1 is a coefficient that depends on support condition

K_2 is a coefficient that relies on the shape of the section

Again no experimental work was carried out in developing the proposed models above but the results were compared with the values obtained using Branson's equation. Therefore, this equation also produced similar errors to Branson's equation for other type of loading. In addition, Equation (2.8) is dependent upon a number of factors and coefficients which have to correctly evaluated to produces an accurate value of the deflection.

2.6 Model of Duan et al

Duan et al [11] in 1989 proposed an equation in an effort to simplify Branson's equation using a form of flexural rigidity, B_d, as a replacement for EI_e which is given by

$$B_d = (1 + 0.3\gamma_1)\frac{M_n}{\alpha\phi_y} \qquad (2.9)$$

where

$$\gamma_1 = \frac{(b_i - b)h_f}{bd} \qquad (2.10)$$

$$\alpha = 0.75 + 0.5\frac{M}{M_n} \tag{2.11}$$

$$\phi_y d = (0.7 + 2.8\frac{a}{d}) \times 10^{-3} + \frac{f_y}{E_s} \tag{2.12}$$

in which

b_i is the width of tension flange

h_f is the thickness of tension flange.

α is the stiffness modification factor which can be calculated from Equation (2.11)

ϕ_y is the curvature of a section at first yield of tension steel and can be derived from Equation (2.12)

M_n is the moment at the position where deflection is required.

M is the maximum applied moment

a is the depth of the rectangular compression stress distribution

d is the effective depth

f_y is the yield steel strength

E_s is the elastic modulus of steel

Although the equations derived above produce slightly better accuracy compare to Branson's equation as reported but the methods are not easy and simple to use. This method is also based on the concept adopted by the Chinese Code for concrete [11].

Again this method did not take into account the effect of loading type and as a result the error produced is the same as Branson's Equation.

2.7 Model of Al-Zaid et al

In 1991, Al-Zaid et al [12] modified Branson's equation by studying the effect of loading type acting on the beam. A 200 mm square cross section with 2500 mm clear span simply supported beam with a reinforcement ratio of 0.4 ρ_b was used. The number of beams tested was eight, with four different types of loading.

From the results obtained they proposed that the power m in Branson's equation, Equation (1-2), should be replaced by 2.8, 2.3 and 1.8 for uniform load, two point loads at third span, and central point load respectively. They also proposed an alternative equation to calculate the second moment of area as follows

$$I_e = \left(\frac{L_{cr}}{L}\right)^{m'} I_{cr} + \left[1 - \left(\frac{L_{cr}}{L}\right)^{m'}\right] I_g \tag{2.13}$$

where

$$m' = \frac{M_{cr}}{M_a}$$

L_{cr} is the length of the span over which the applied moment exceeds M_{cr} (usually known as the cracking length)

L is the clear span of the beam.

Although, the effect of loading type has been incorporated in this model it still produced considerable error [2,13].

2.8 Model of Al-Shaikh et al

In 1993 Al-Shaikh et al [14] initially modified Branson's equation by incorporating the effect of reinforcement ratio. Eighteen test beams were used in the experimental programme. The beams were simply supported, subjected to a single point load at mid-span, with various reinforcement ratios. It showed that the effect of reinforcement ratio changed the value of *m* in Branson's equation and that it should be replaced by $3-0.8\rho$ so that the equation becomes

$$I_e = I_{cr} + (I_g - I_{cr}) \left(\frac{M_{cr}}{M_a} \right)^{3-0.8\rho} \quad (2.14)$$

This modified form of Equation (1-2) only slightly improved the accuracy in comparison to Branson's original equation [13].

The previous model proposed by Al-Zaid et al [12], Equation (2.13), was then modified by redefining the factor m' producing the following equation for the effective second moment of area

$$I_e = I_g + (I_{cr} - I_g) \left(\frac{L_{cr}}{L} \right)^{0.8\rho \frac{M_{cr}}{M_a}} \quad (2.15)$$

where,

ρ is the reinforcement ratio in %

Although the effect of reinforcement ratio was studied it was limited to a central point load acting on the beam. Studies of two unsymmetrical point loads, acting at various distances between supports had still not been considered.

2.9 Fikry's model

Fikry [2,13] developed a new form of equation as a replacement for Branson's equation based on test data found in the literature [15] as stated in Chapter 1. His proposed equation is restated here for convenience

$$I_e = I_{cre} + (I_g - I_{cre})\ e^{\Phi} \tag{2.16}$$

The Fikry model was not directly compared with experimental work and its verification and possible modification is the objective of this present study.

2.10 Gilbert's model

In 1999, Gilbert [16,17] proposed three alternatives for calculating the deflection of a beam.

- Alternative 1

To account for the loss of tension stiffening effect under long-term or cyclic loads, the following modification to Branson's equation was suggested

$$I_e = \beta\left(\frac{M_{cr}}{M_a}\right)^3 I_g + \left[1-\beta\left(\frac{M_{cr}}{M_a}\right)^3 I_{cr}\right] \le I_g \tag{2.17}$$

where

β = 1.0 for immediate deflection

= 0.4 for long term or cyclic loading

- Alternative 2

Here his proposal was to use the same equation to calculate the effective second moment of area but using a modified value of the cracking moment for long-term deflection, which is obtained from the equation below

$$M_{cr} = Z(f_r - f_{sc}) \text{ but } \ge 0.0 \tag{2.18}$$

Where

Z	is the section modulus of the un-cracked section
f_r	is the modulus of rupture
f_{sc}	is the maximum shrinkage induced tensile stress in the uncracked section which can be obtained from the following equation

$$f_{sc} = \frac{2.5\overline{\rho}}{1+50\overline{\rho}} E_s \varepsilon_{sc}$$

in which E_s is the steel elastic modulus, ε_{sc} is the concrete shrinkage strain and $\overline{\rho}$ is the ratio of the tension steel area to the gross area of the concrete section.

- Alternative 3

He suggested the following equation be used to calculate the time-dependent deflection

$$\kappa(t) = \kappa_i \left(1 + \frac{\phi_c}{\alpha}\right) \tag{2.19}$$

where

κ_i is the initial curvature due to the sustained service moment M, and may be taken as $\kappa_i = \dfrac{M}{E_c I_e}$, in which I_e is the value calculated using the cracking moment of Equation (2.18).

ϕ_c is the creep coefficient at time t

α is the term that accounts for the effect of cracking and the bonding action of the reinforcement and is typically in the range 1.0 to 1.6 for the uncracked section and 4.0 to 10.0 for the cracked section.

The curvature induced by shrinkage on a reinforced concrete section is approximated by Equation (2.20) for an uncracked section and Equation (2.21) for cracked section.

$$\kappa_{sc} = \left[\frac{0.7\varepsilon_{sc}}{D}\right]\left[1 - \frac{A_s'}{A_s}\right] \tag{2.20}$$

$$\kappa_{sc} = \left[\frac{1.2\varepsilon_{sc}}{D}\right]\left[1 - \frac{A_s'}{A_s}\right] \tag{2.21}$$

where D is the overall depth of the beam.

The total deflection, for a continuous member, is calculated by assuming a parabolic curvature variation diagram along the span L so that

$$\Delta = \frac{L^2}{96}(\kappa_L + 10\kappa_m + \kappa_R) \tag{2.22}$$

where

κ_L is the total curvature, Equation (2.19) + either Equation (2.20) or (2.21), at the left support

κ_M is the total curvature at the mid span

κ_L is the total curvature at the right support

2.11 Ashours's model

In 2000, Ashour [18] studied both the effect of concrete compressive strength and tensile reinforcement ratio on the flexural behaviour of reinforced concrete beams. This study was again an effort to modify Branson's equation so that it could be applied to high strength concrete. This study showed that the value of the cracking second moment of area varied between 75 and 93 % of the theoretical second moment of area of a cracked transformed section. This is given by the following equation.

$$I_{cr} = I_{cr(th)}\left[1.129 - 0.0011 f_c' - 0.1133\rho\right] \tag{2.23}$$

where,

$I_{cr(th)}$ is theoretical I_{cr} as used in Branson's equation.

f_c' and ρ are cylindrical concrete strength and reinforcement ratio respectively.

By changing the model for the second moment of area of a cracked section, such as Equation (2.23), he suggested that the effect of concrete strength could be included by redefining *m* in Branson's equation, Equation (1-2), as

$$m = 3 - 0.8\rho\sqrt{\frac{33}{f_c'}} \qquad (2.24)$$

2.12 Summary

From the papers discussed above two approaches have been used in evaluating the deflection of a beam;

(a) Curvature

(b) Effective second moment of area.

The second approach is a more direct approach and in all probability easiest to use. The curvature approach requires a great number of calculations. Initially the effective second moment of area approach consisted of Branson's equation and modification of the equation. These modifications did show that the reinforcement ratio, concrete strength and cracked length did affect the value of the second moment of area. Fikry's model also showed that the load(s) type and position(s) affected the value of I_e.

Therefore in this study all the above parametric variations have been considered in the experimental programme. As the equation produced by Fikry already considered most of these variables, it was considered reasonable to modify his equation in terms of the experimental results.

Chapter 3

Analysis and Design of Test Beams

3.1 Introduction

This chapter aims to discuss the test beams considered in this study. Parameters involved in the calculation of the test beams are reviewed and discussed. Section considered of the test beams to resist applied load were analysed. This was to allow the beam to fail in flexure before the maximum capacity of load-cell available in the Laboratory.

Once moment capacities of the beams had been obtained, deflections were computed. Curvature and second moment of area approach were used to calculate the deflections. Fikry's method was adopted as part of second moment of area approach in the deflection calculation.

3.2 Beam properties

3.2.1 Concrete and steel strength

The strength test results of either concrete, f_{cu}, or steel, f_y will vary. The strength considered, however, is their characteristics value not their minimum value. The characteristic strength is defined as the value taken as 5% below the average value of all possible test results. This is given by

$$f_k = f_m - 1.64s \tag{3.1}$$

where

f_k is characteristic strength

f_m is mean strength

s is standard deviation.

In terms of concrete cube strength the term f_k is f_{cu} while for tension steel strength the term is f_y.

The strength of concrete is required to calculate the strength of the sections and their deflections. To obtain the strength of concrete specified, BS 1881-116 [19] has been adopted. By making three cubes of 100x100x100 mm and a cylinder of 150 mm diameter x 300 mm height, cube concrete compressive strength, f_{cu}, and cylinder concrete compressive strength, f_c', were determined for each batch of concrete mix. The cylinder specimen was also used to determine the static modulus of elasticity experimentally with reference to BS 1881 part 121 [20].

Mild steel and high-yield steel have the approximate values of modulus of elasticity of 200 kN/mm^2. However, the specified strength of the mild steel used in the design is based on the yield stress, whereas for high yield steel the strength is based on the specified proof stress of 0.2 per cent, the stress causing a residual strain of 0.2%, of the real proof stress value [21,22].

3.2.2 Concrete modulus of elasticity

Due to the non linearity of the stress-strain curve of concrete as shown in Figure 3.1, the secant modulus is used as the modulus of elasticity, E_c, by taking the slope of the straight line that connects the origin to a given stress of $0.4f'_c$. This satisfies the practical assumption that strain occurring during loading can be considered basically elastic [23].

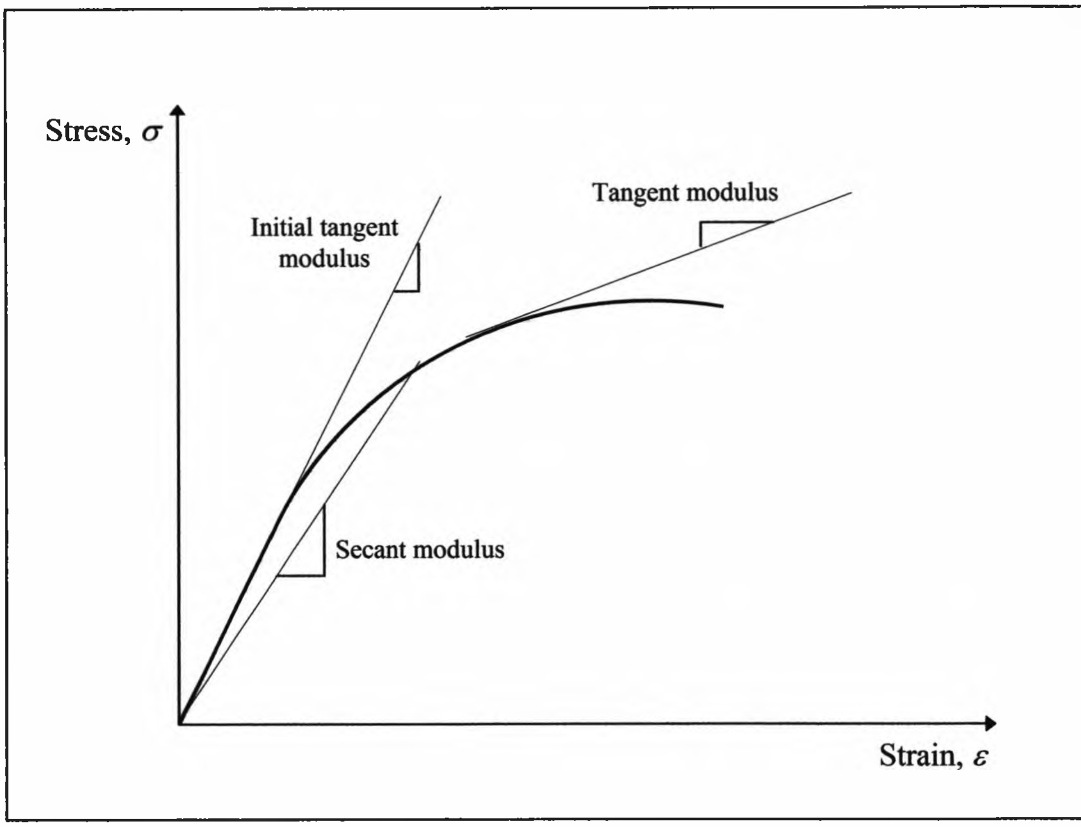

Figure 3.1 Tangent and secant modulus of concrete

Based on experimental data, the ACI code gives the following expression for calculating the elastic modulus of concrete for f'_c up to 41 MPa,

$$E_c = 0.0143 w^{1.5} \sqrt{f_c'} \tag{3.2}$$

where E_c is the elastic modulus of concrete in MPa, w is the density of concrete in Kg/m^3 and f'_c is the cylinder compressive strength in MPa.

For normal-weight concrete Equation (3.2) is replaced by Equation (3.3).

$$E_c = 4730\sqrt{f_c'} \qquad \text{MPa} \tag{3.3}$$

Carrasquillo et al [24] suggested to replace the ACI equation for normal-weight concrete with compressive strength from 41 to 82 MPa, by the following,

$$E_c \text{ (MPa)} = (3.32\sqrt{f_c'} + 6895)\left(\frac{w}{2320}\right)^{1.5} \tag{3.4}$$

where terms and units are defined as those for Equation (3.2).

On the other hand, BS 8110 part 2 [25] specifies the following equation for the elastic modulus of normal weight concrete,

$$E_c = (20 + 0.2 f_{cu}) \tag{3.5}$$

where

E_c is the concrete elastic modulus in GPa (10^3 MPa)

f_{cu} is the cubic compressive strength in MPa.

British Standard, BS 1881-121 [20] gives a guide to determine the static modulus of elasticity experimentally, E_c. Determination of the concrete strength, f_c, is first needed as part of static modulus evaluation. Alternatively, the compressive strength may be estimated from cube strengths, f_{cu}. By referring to the British Standard [20] regarding the detail in determining the static modulus of elasticity, E_c, the mean strain ε_a and ε_b can be obtained. Thus, the static modulus of elasticity in compression, E_c, (in MPa) is given by the following equation.

$$E_c = \frac{\sigma_a - \sigma_b}{\varepsilon_a - \varepsilon_b} \tag{3.6}$$

where, σ_a is the upper loading stress (in MPa) equal to $0.8 f_{cu}/3$. Whilst, σ_b is the basic stress and is taken as 0.5 MPa. ε_a and ε_b are the mean strain under upper loading stress and the mean strain under the basic stress respectively. This is illustrated in Figure 3.2.

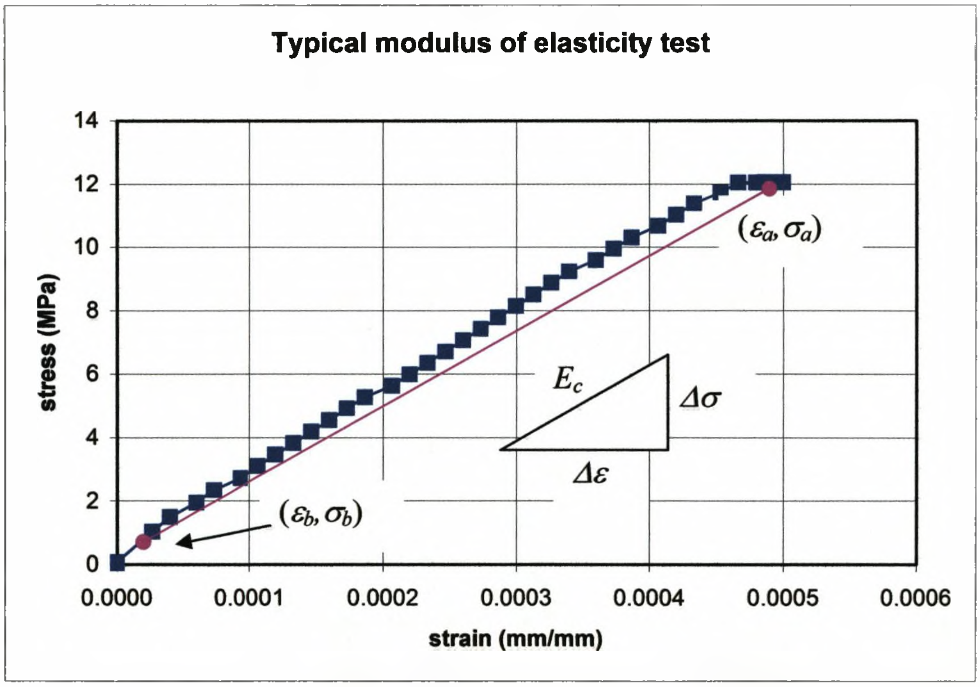

Figure 3.2 Stress-strain relationship to determine E_c experimentally

All test beams considered in this study have f'_c values less than 41 MPa or f_{cu} (cube strength) less than about 55 MPa, therefore there is no need for Equation (3.4) and only equations, (3.3) or (3.5) will be applied. Values of f'_c less than 41 MPa are consistent with the usual practice since f'_c values higher than 41 MPa are usually used in compression elements, which are rarely investigated for deflection, and in which cracking is not a major effect [26,27,28].

3.2.3 The modulus of rupture

Normally, the tensile strength of concrete is ignored in the calculations for the strength of flexural members. However, it is very important to take it into account in the serviceability consideration such as deflection calculations. This parameter is important in determining when the first flexural crack may develop. Concrete tensile strength considered in these cases is called the modulus of rupture (f_r).

Empirically, the equation for calculating the concrete tensile strength or modulus of rupture is given as a function of the compressive concrete strength. In terms of cylindrical compressive strength the equation as below

$$f_r = 0.62\sqrt{f_c'} \quad \text{where } f_r \text{ and } f_c' \text{ in MPa} \qquad (3.7)$$

The code also specifies that 75% and 85% of the values of Equation (3.7) can be used for the modulus of rupture of all light-weights concrete and sand-lightweight concrete, respectively.

Since there is no expression for the flexural tensile strength of concrete as a function of the compressive strength given in the British Standard, Equation (3.7) is used throughout this study. When the compressive cube strength is specified Equation (3.7) has to be modified. Generally the following ratio holds for most types of concrete,

$f_c^{'} / f_{cu} = 0.8$, so that the equation becomes,

$$f_r = 0.56\sqrt{f_{cu}} \quad \text{where } f_r \text{ and } f_{cu} \text{ in MPa} \tag{3.8}$$

where f_{cu} is cube concrete strength in MPa.

3.3 Detailing and requirements

3.3.1 Test beam details

The section of all reinforced concrete beams considered was 150 mm width and 230 mm height. 40 mm high plastic props were embedded in the concrete sections to support the main reinforcement away from the sofit. Rounded mild steel bars of 6 mm diameter were used as links. Thus, the nominal cover to all reinforcement (including links) is $40-6=34$ mm. This value is within the range specified by British Standard [29]. Deformed bars were used as the main reinforcement with a yield stress of 460 MPa. Two hanger bars of 6 mm diameter were placed at the top of the beam with a yield stress of 250 MPa.

Unlike a round bar, the diameter of a deformed bar cannot be measured directly. Therefore, a method using the mass of a known length of bar as given in BS 4482 [30] is used. For any steel section the following equation applies

$$A_s = \frac{M}{0.00785L} \tag{3.9}$$

where

A_s is area of the reinforcement (mm^2)

M is the mass of the reinforcement (kg)

L is the length of the reinforcement (m)

Once the area of the deformed bar is obtained, the diameter can be approximated to by using Equation (3.10).

$$d_s = \sqrt{\frac{4A}{\pi}} \tag{3.10}$$

Since all the bars are positioned at the same depth from the neutral axis the bar spacing has to be checked to ensure sufficient space for the aggregate between the bars. Therefore,

$$\text{bar spacing} = (b - (2 \times cover\ side + 2 \times diameter\ link + n_s \times diameter\ bar))/(ns - 1)$$

with n_s = number of the bar.

The critical section for this case is that section with $n_s = 4$

$$\text{bar spacing} = (150 - (2 \times 20 + 2 \times 6 + 4 \times 12))/(4 - 1)$$

$$= 16.67 \text{ mm}$$

The code specified that bar spacing must be bigger than maximum aggregate size plus 5 mm. Thus maximum aggregate used in all cases was 10 mm which gives a maximum bar spacing of 15 mm.

3.3.2 Ductility

The term ductility describes the ability of a member to experience large deformation without rupture. Ductile structure may bend and deform excessively under load but they remain intact. This capability prevents total structural collapse and provides protection to occupant of building. On the other hand, a member that fails suddenly, completely with little warning is termed brittle.

The ability of a ductile structure to undergo large deformation before collapse produces visible evidence of the imminence of collapse and may give occupants the opportunity to relieve distress by reducing loads. In contrast, brittle failures occur suddenly, without warning and with no time for measures to be taken to prevent damage. Therefore, the ductility condition is always required in designing a flexural reinforced concrete member.

By limiting the percentage of reinforcing steel, it moves the neutral axis toward the compression zone. As a result, the strain in the steel will increase more rapidly than the strain in the concrete, and the beam will fail in a ductile manner by yielding of the steel before the concrete crushes.

As discussed above, clearly, the presence of steel in a concrete member plays an important role when designing the concrete member to ensure adequate ductility.

Depending on the type of failure, namely, yielding of the steel or crushing of the concrete, analysis of the strain state in the tension reinforcement becomes the determinant in the measure of ductility in the reinforced concrete element. The percentage of the tension reinforcement would, therefore, determine the magnitude of strain, and whether failure develops by initial yielding of steel (a ductile type of failure) or by initial crushing of the concrete (a brittle mode of failure).

If failure by yielding of the tensile reinforcement and the crushing of the concrete extreme compression fibers occur simultaneously, such a mode of failure is termed as balanced failure. In such a case, the corresponding limit strain, ε_y, in the tensile reinforcement is reached at the same time that the limit strain, ε_c, is reached in concrete (0.0035 in terms of BS or 0.003 in terms of ACI).

In order to prevent such a state of behaviour in flexural members, a strain greater than ε_y in the extreme tensile reinforcement has to be required in design.

To ensure ductile performance, the percentage of reinforcement should be in the range of 50 to 60% of the percentage needed for the limit balanced behaviour. Such a lower percentage of reinforcement would also prevent congestion of the reinforcement in the concrete section. However, a minimum percentage of reinforcement has also to be maintained, so that the reinforced concrete element does not behave as a plain concrete section.

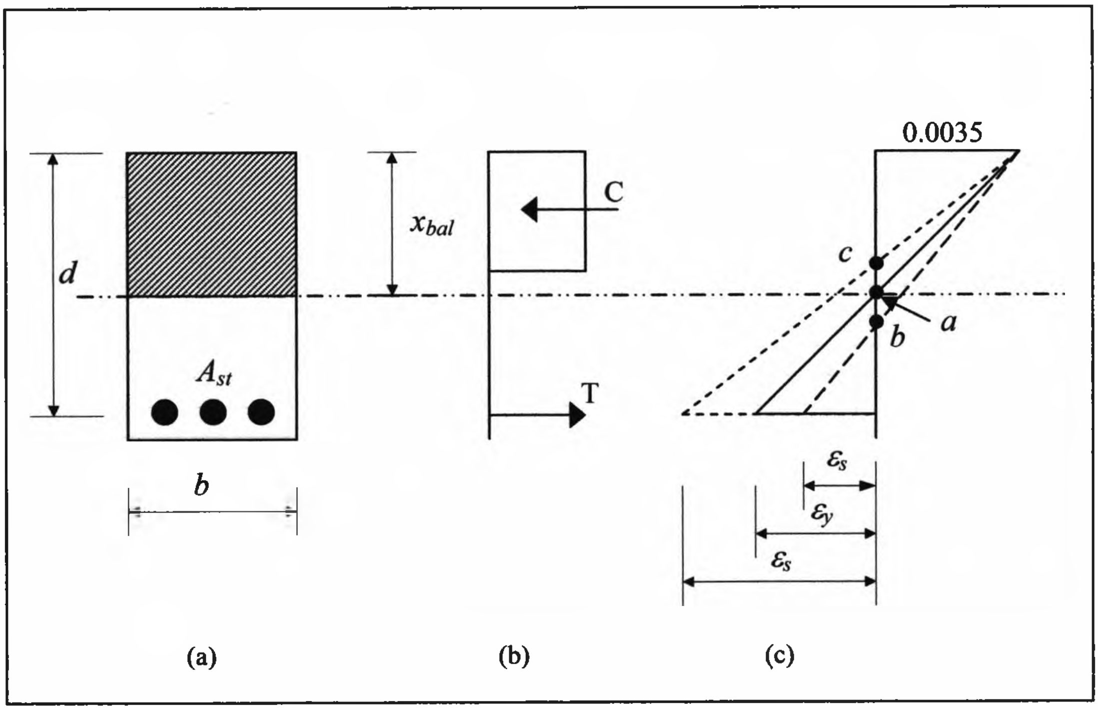

Figure 3.3 Strain distribution across depth: (a) beam cross-section; (b) stress diagram; (c) strain distribution for various mode of flexural failure

If ρ less than ρ_b the tensile force T is smaller than that at balanced condition, and as a result the compressive force C is also smaller, requiring less compressive area. Consequently, the neutral axis rises in the beam as shown in Figure 3-3c.

Neutral axis at point *c*; under reinforced

$$\rho < \rho_b$$

$$\varepsilon_s > \varepsilon_y$$

$$f_s = f_y$$

Neutral axis at point b; over reinforced

$$\rho > \rho_b$$

$$\varepsilon_s < \varepsilon_y$$

$$f_s < f_y$$

- *Ductility check*

The ductility of a member depends primarily on the magnitude of the maximum strain in the concrete as the tension steel is stressed just to its yield point. Ductility disappears when the percentage of steel, called balanced steel, A_{sb}, is large enough to position the neutral axis so that the strain in the concrete reaches 0.003 just as the steel is strained to its yield points ($\varepsilon_s = \varepsilon_y$). This is known as a balanced condition.

The ACI code established an equation to compute the upper limit of the reinforcing steel ratio, ρ (defined in the current study as the ratio of the tension steel area to the effective concrete area, *bd* where *b* is the width of the section and *d* is its effective depth taken as the distance from the centroid of the steel area to the outer compression fiber) to prevent the beam become over reinforced. The equation is given below.

$$\rho_{\max} = 0.75\rho_b \tag{3.11}$$

in which

$$\rho_b = 0.85\beta_1 \frac{f_c^{'}}{f_y} \frac{600}{600 + f_y} \tag{3.12}$$

where β_1 is a factor dependent upon the concrete strength, as given below.

$$\beta_1 = \begin{cases} 0.85 \quad \text{for} \quad f_c^{'} \leq 28 \\ 0.85 - 0.00725 \dfrac{f_c^{'} - 28}{1000} \\ 0.65 \quad \text{for} \quad f_c^{'} > 56 \end{cases} \tag{3.13}$$

For the lower limit of reinforcing steel the code gives the equation below.

$$\rho_{\min} = \frac{1.4}{f_y} \tag{3.14}$$

Units for all equation described above is in SI where $f_c^{'}$ and f_y are in MPa.

The British Standard [29] derives the limitations as well based on balanced failure. However, the strain of the concrete used is 0.0035 instead of 0.003 as used in the ACI code [5]. The limitation is specified on the depth of the neutral axis, x, of the section.

From the strain diagram, Figure 3-3c, of the balanced failure condition, the neutral axis of the section is given by

$$x_{bal} = \frac{d}{1 + \frac{\varepsilon_y}{0.0035}} \tag{3.15}$$

where the yield strain is given by

$$\varepsilon_y = \frac{f_y / \gamma_m}{E_s} \tag{3.16}$$

At the ultimate limit state for this case (f_y = 460 MPa, E_s = 200 000 MPa), and γ_m = 1.05 $\varepsilon_y = 0.00219$

Therefore,

$$x_{bal} = 0.615 \times d \tag{3.17}$$

The upper limit of the neutral axis

$$x = 0.111 \times d \tag{3.18}$$

while the lower limit is given as

$$x = 0.500 \times d \tag{3.19}$$

The British Standard also specifies the minimum reinforcement for a rectangular section in flexure as

$$\frac{100A_s}{A_c} > 0.13\% \qquad (3.20)$$

Fikry has summarised the upper bound value of ρ as well as $n\rho$ for normal range of concrete strength as shown in Table 3.1 to ensure the section remains in the ductile condition at all values.

Table 3.1 Upper Bound value of ρ and $n\rho$

Cube strength f_{cu} (MPa)	**Modular ratio n**	**Reinforcement ratio $\rho_{(max)}$ (%)**	**$n\rho_{(max)}$ (%)**
(1)	(2)	(3)	(4)=(2)x(3)
25	8	2.31	18.48
30	7.7	2.77	21.33
35	7.4	3.23	23.90
40	7.1	3.7	26.27
45	6.9	4.16	28.70
50	6.7	4.62	30.95

The minimum value of ρ also has to be satisfied so that the beam behaves in a ductile manner, and is given by Equation (3.14).

All the limitations discussed above will now be applied to the test beams. The concrete section specified in this study will now be checked for ductility requirements.

As this study designed based on the concrete cube strength so for the ACI approach the concrete cylinder strength is obtained by multiplied the concrete cube strength with factor 0.8. This factor has been discussed in the Section 3.2.3. The next step is applying Equation (3.11) to (3.14) and the results are shown in Table 3.2.

Table 3.2 Ductility check using ACI 318

Cylinder strength f'_c *) (MPa)	Steel		b (mm)	d (mm)	ρ (%)	ρ_{min} (%)	ρ_b (%)	ρ_{max} (%)	$\rho_{min}<\rho<\rho_{max}$
	d_s (mm)	n_s							
(1)	(2)	(3)	(4)	(5)	(6)	(7)	(8)	(9)	(10)
20	12	2	150	184	0.82	0.30	1.78	1.33	Ok
	12	3	150	184	1.23	0.30	1.78	1.33	Ok
	12	4	150	184	1.64	0.30	1.78	1.33	No
28	12	2	150	184	0.82	0.30	2.49	1.87	Ok
	12	3	150	184	1.23	0.30	2.49	1.87	Ok
	12	4	150	184	1.64	0.30	2.49	1.87	Ok
36	12	2	150	184	0.82	0.30	3.20	2.40	Ok
	12	3	150	184	1.23	0.30	3.20	2.40	Ok
	12	4	150	184	1.64	0.30	3.20	2.40	Ok

*) f'_c is theoretical value of cylinder concrete strength

Having defined upper and lower limit of ductility based on BS 8110 as discussed above, the Equations above are applied and results are shown in Table 3.3.

Table 3.3 Ductility check using BS 8110

f_{cu} *) (MPa)	Steel		b (mm)	d (mm)	ρ (%)	100*As/bh* < 4 %	100*As/bh* > 0.13%	x (mm)	x/d < 0.50	x/d <0.615
	d_s (mm)	n_s								
(1)	(2)	(3)	(4)	(5)	(6)	(7)	(8)	(9)	(10)	(11)
25	12	2	150	184	0.82	Ok	Ok	65.08	Ok	Ok
	12	3	150	184	1.23	Ok	Ok	97.63	No	Ok
	12	4	150	184	1.64	Ok	Ok	130.17	No	No
35	12	2	150	184	0.82	Ok	Ok	46.49	Ok	Ok
	12	3	150	184	1.23	Ok	Ok	69.73	Ok	Ok
	12	4	150	184	1.64	Ok	Ok	92.98	No	Ok
45	12	2	150	184	0.82	Ok	Ok	36.16	Ok	Ok
	12	3	150	184	1.23	Ok	Ok	54.24	Ok	Ok
	12	4	150	184	1.64	Ok	Ok	72.32	Ok	Ok

*) f_{cu} is theoretical value of cube concrete strength

The beams sections are also checked using upper and lower limit summarised in Table 3.1. The results are shown in Table 3.4.

Table 3.4 Ductility check based on Table 3-1

f_{cu} *) (MPa)	Steel		b (mm)	d (mm)	ρ (%)	n	$n\rho$ (%)	$n\rho_{max}$ (%)	$n\rho < n\rho_{(max)}$
	d_s (mm)	n_s							
(1)	(2)	(3)	(4)	(5)	(6)	(7)	(8)	(9)	(10)
25	12	2	150	184	0.82	8.00	6.56	18.48	Ok
	12	3	150	184	1.23	8.00	9.83	18.48	Ok
	12	4	150	184	1.64	8.00	13.11	18.48	Ok
35	12	2	150	184	0.82	7.41	6.07	23.9	Ok
	12	3	150	184	1.23	7.41	9.11	23.9	Ok
	12	4	150	184	1.64	7.41	12.14	23.9	Ok
45	12	2	150	184	0.82	6.90	5.65	28.7	Ok
	12	3	150	184	1.23	6.90	8.48	28.7	Ok
	12	4	150	184	1.64	6.90	11.30	28.7	Ok

*) f_{cu} is theoretical value of cube concrete strength

From the results presented through Table 3.2 to 3.4, it can be said that all beams section are ductile in terms of limitation provided by Fikry. However, eight out of nine beams are ductile according to ACI and six out of nine beams are ductile based on BS 8110. Therefore, it can be said that the test beams specified are representative for the purpose of this study.

3.4 Section analysis

The basic principle of the bending theory for reinforced concrete is that the concrete will crack in the tensile region. After cracking all tension is carried by the reinforcement. It also assumes that plane sections of a structural member remain plane after straining, so that across the section there must be a linear distribution of strains.

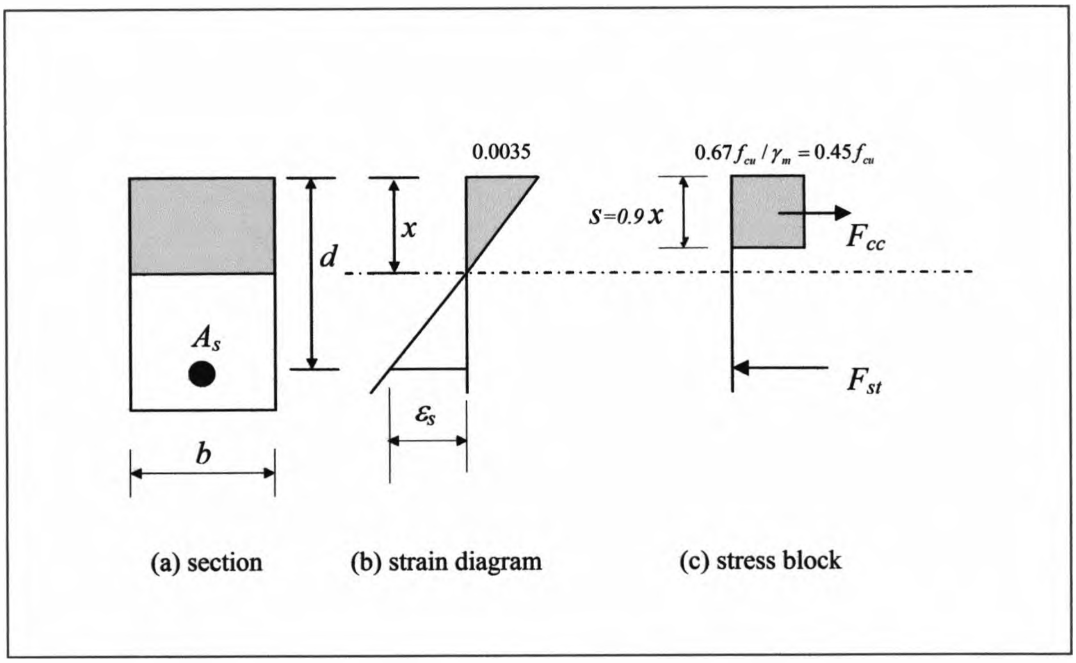

Figure 3.4 Stress and strain distribution for singly reinforced concrete beam according to BS 8110

In designing concrete structures, it is usual to design for the ultimate limit state (ULS) condition first, then to checks whether the serviceability limit state (SLS) is also satisfied. This ensures that no excessive deflection or cracking of the concrete will occur. BS 8110 [29] also simplifies the stress block of the concrete section from parabolic to be rectangular, Figure 3-4c, to make simple computation. This approach is adopted when analysing the section used for the experimental models.

From Figure 3.4c,

$$F_{cc} = F_{st}$$

or

$$0.45 f_{cu} b \times s = 0.95 f_y A_s$$

Therefore the depth of the stress block is given by

$$s = \frac{0.95 f_y A_s}{0.45 f_{cu} b}$$

and

$$x = s/0.9$$

Therefore ultimate moment of resistance of the section is

$$M_u = F_{st} \times z$$

$$= 0.95 f_y A_s (d - s/2)$$

$$= 0.95 f_y A_s \left(d - \frac{0.95 f_y A_s}{0.45 f_{cu} b} \right)$$

These equations assume the tension reinforcement has yielded, which will be the case if x is not greater than 0.615*d*. Otherwise it can only be solved by applying successive values of x until $F_{cc} = F_{st}$ with the steel strain and hence stresses being determined from the equations below to be used instead of $0.95 f_y$.

$$\varepsilon_{st} = \varepsilon_{cc} \left(\frac{d - x}{x} \right) \text{ and}$$

$$f_{st} = E_s \times \varepsilon_s$$

3.4.1 Ultimate loads and moments of resistance

The above analysis of the section was for the ultimate limit state condition using partial factors of safety for the materials, γ_m, when failure in flexure of 1.5 and 1.05 for concrete and steel respectively.

There are nine combinations of the basic reinforced beam section, as discussed in the previous section but only one will be analysed in this section and the results for the others presented in a tabular form.

Consider a beam section of 150 mm width and 230 mm height with a 40 mm clear cover to main reinforcement (or 34 mm to the links). The cube strength of the concrete is 35 MPa with three deformed bars, diameter 12 mm and f_y =460 MPa, as the tensile reinforcement.

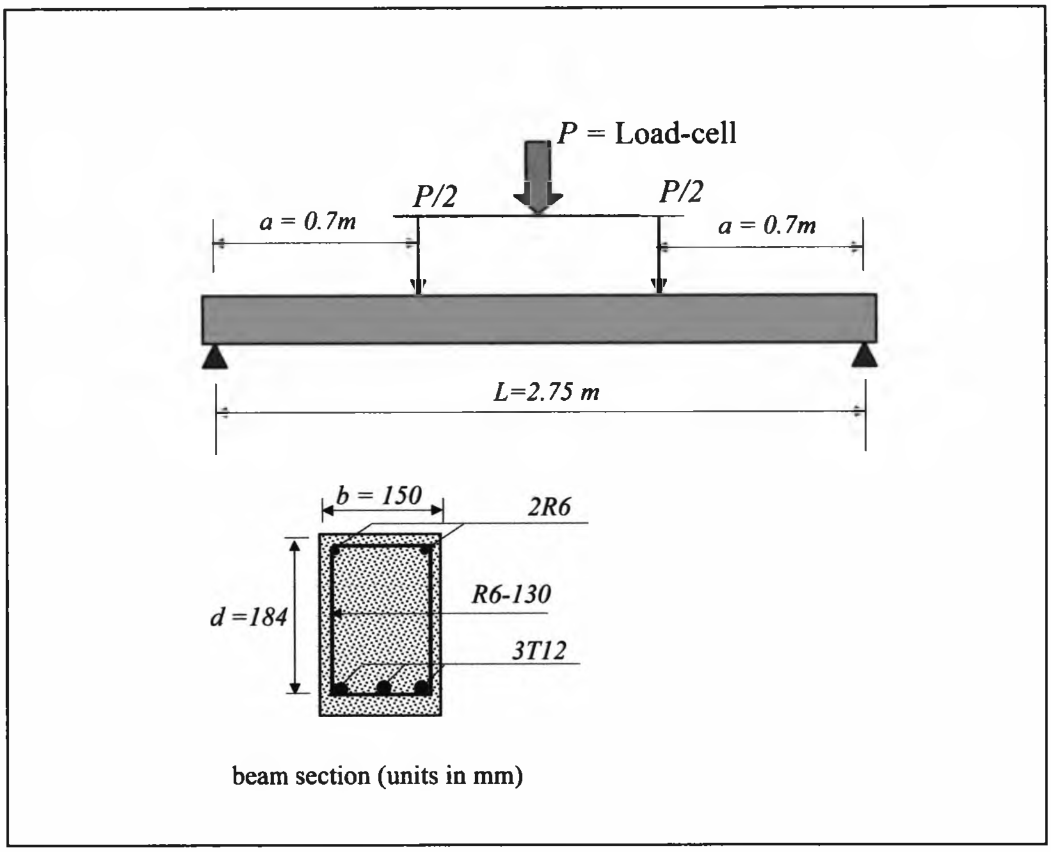

Figure 3.5 Loading arrangement and section considered for example calculation

The steel area is given by

$$A_s = n_s \times \tfrac{1}{4}\pi \times d_s^{\,2}$$

$$= 339,3 \ \ \text{mm}^2$$

producing an effective depth, *d*

$$d = 230 - 40 - \tfrac{1}{2} \times 12$$

$$= 184 \text{ mm}$$

The depth of stress block of the section is

$$s = 0.95 f_y \frac{A_s}{0.45 f_{cu} b}$$

$$= 62.76 \text{ mm}$$

Thus the neutral axis $x = \dfrac{s}{0.9} = 69.7$ mm.

As $\dfrac{x}{d} = 0.379 < 0.615$ the tension steel will have yielded.

The forces in the concrete and steel are

$$F_{cc} = 0.45 f_{cu} b \times s$$
$$= 1.483 \times 10^5 \text{ N}$$

$$F_{st} = 0.95 f_y A_s$$
$$= 1.483 \times 10^5 \text{ N}$$

The moment of resistance of the concrete section is

$$M_u = 0.45 f_{cu} b \times s\left(d - \tfrac{1}{2}s\right) \times 10^{-6}$$
$$= 22.6 \ \ \text{kNm}$$

The span between the supports of the beam is 2.75 m with two symmetrical point loads applied as shown in Figure 3.3, the distance between loads and supports indicated by *a*. When the distance *a* is taken as 0.7 m the total load needed to fail the beam is

$$P_u = \frac{2M_u}{a}$$

$$= \frac{2 \times 22.6}{0.7}$$

$$= 64.6 \text{ kN}$$

Thus load cell capacity, *P*, has to be greater than 64.6 kN.

In the same way for various value of a, reinforcement ratio and concrete strength, the required values of P_u are calculated and shown in Table 3.5.

Table 3.5 Load capacity of the section specified for various load positions

f_{cu} (MPa)	Steel		*b* (mm)	*h* (mm)	*d* (mm)	*ρ* (%)	M_u (kNm)	P_u (kN) for various *a* (m)			
	d_s (mm)	n_s						0.7	0.92	1.15	1.375
(1)	(2)	(3)	(4)	(5)	(6)	(7)	(8)	(9)	(10)	(11)	(12)
25	12	2	150	230	184	0.82	15.29	43.69	33.25	26.60	22.24
	12	3	150	230	184	1.23	20.77	59.34	45.15	36.12	30.21
	12	4	150	230	184	1.64	24.80	70.84	53.90	43.12	36.07
35	12	2	150	230	184	0.82	16.12	46.06	35.04	28.03	23.45
	12	3	150	230	184	1.23	22.63	64.65	49.19	39.35	32.91
	12	4	150	230	184	1.64	28.10	80.30	61.10	48.88	40.88
45	12	2	150	230	184	0.82	16.58	47.37	36.04	28.83	24.12
	12	3	150	230	184	1.23	23.66	67.61	51.44	41.15	34.42
	12	4	150	230	184	1.64	29.94	85.55	65.09	52.07	43.55

3.4.2 Service loads

The concrete compressive stresses under service loads are always elastic. Because of this, and because the stresses in the steel reinforcement are also elastic the linear theory always applies.

When a section is analysed for this type of load, the partial factor of safety for both materials (γ_m) when failure is in flexure, is taken as 1.0. As service loads are a part of the ultimate loads therefore the global factor of safety for this condition has to be applied. In this case, a beam failure caused by yielding of the ensile reinforcement would have a factor of

$$\gamma_m \times \gamma_f = 1.05 \times 1.4 = 1.47$$

Therefore the service load can be approximated as the ultimate load divided by its global factor of safety.

Thus $$M_s = \frac{M_u}{1.47} = 0.68\ M_u$$

Using the above approximation the full results are presented in Table 3-6.

Table 3.6 Load and moment assumed in serviceability condition

f_{cu} (MPa)	Steel		b (mm)	h (mm)	d (mm)	ρ (%)	M_s (kNm)	P_s (kN) for various a (m)			
	d_s (mm)	n_s						0.7	0.92	1.15	1.375
(1)	(2)	(3)	(4)	(5)	(6)	(7)	(8)	(1)	(2)	(3)	(4)
25	12	2	150	230	184	0.82	10.40	29.71	22.61	18.09	15.13
	12	3	150	230	184	1.23	14.12	40.35	30.70	24.56	20.54
	12	4	150	230	184	1.64	16.86	48.17	36.65	29.32	24.53
35	12	2	150	230	184	0.82	10.96	31.32	23.83	19.06	15.94
	12	3	150	230	184	1.23	15.39	43.97	33.45	26.76	22.38
	12	4	150	230	184	1.64	19.11	54.60	41.55	33.24	27.80
45	12	2	150	230	184	0.82	11.27	32.21	24.51	19.61	16.40
	12	3	150	230	184	1.23	16.09	45.97	34.98	27.98	23.40
	12	4	150	230	184	1.64	20.36	58.17	44.26	35.41	29.62

3.5 Deflection of concrete members

The deflection of a member is calculated by double integrating the curvature along the span length. For an elastic member, the curvature, ϕ, may be calculated as $\phi = M/EI$, where *EI* is the flexural stiffness of the cross section of the member. When the integration is completed it can be seen that the deflection of a member is a function of the span length , support, or end conditions, such as simple support or restraint due to continuity, the type of loading such as concentrated or distributed load and the flexural stiffness, *EI*.

In general the maximum deflection in an elastic member due to uniformly distributed load can be expressed as

$$\Delta = k_1 \frac{WL^3}{EI} \tag{3.21}$$

where, W is total load on the span

L is clear span length

E is elastic modulus

I is second moment of area of the section

k_1 is a factor depending on the degree of fixity of the support and load pattern. For this particular case k_1 = 5/384

Equation (3.21) can also be written in term of moment such that the deflection at mid span of the member is

$$\Delta = k_2 \frac{ML^2}{EI} \tag{3.22}$$

in which k_2 = 5/48

If the *EI* value is constant the calculation is a relatively routine process. For the reinforced concrete beam, however, three different values of *EI* must be considered. This will be discussed later in Chapter 4.

The total deflection of a reinforced concrete beam is caused by the change of curvature and shear deformation. The latter can be neglected when span/depth ratio > 10 [31]. In the case of these test beams, deflection due to shear deformation is ignored as the beams have a span/depth ratio of 11.9.

3.5.1 Curvature approach

Using small-deflection theory, the curvature at any point x along the span can be written as,

$$\frac{1}{r_x} = \frac{d^2\delta}{dx^2} \tag{3.23}$$

where,

$1/r_x$ is the curvature at any point x along the span.

δ is the deflection at the point considered.

Using the boundary conditions of the span Equation (3.23) is then double integrated by any convenient numerical integration technique to obtain the desired deflection.

The method outlined above is simplified by the code [29] using an approximate method where the maximum deflection is evaluated as follows,

$$\delta_{max} = KL^2\left(\frac{1}{r_b}\right) \tag{3.24}$$

where,

K is a loading type factor and for the loading condition shown in Figure 3.5 is given by.

$$K = 0.125 - \frac{a^2}{6L^2} \quad (3.25)$$

L is the effective span

$1/r_b$ is the curvature at the mid-span of beams or at the support of cantilevers.

3.5.1.1 Uncracked section

In this case the gross concrete area with all steel areas (both tension and compression if any) transformed into an equivalent area of concrete are considered. The curvature is then calculated as

$$\left(\frac{1}{r}\right)_{tr} = \frac{M}{E_c I_{gt}} \quad (3.26)$$

where I_{gt} is the second moment of area of the gross section.

3.5.1.2 Cracked Section

This is a section in which the concrete in the tension zone below the neutral axis is assumed to sustain a triangular stress distribution as shown in Figure 3.6. Unlike the concrete compressive stresses above the neutral axis and the tensile stress of the steel, these concrete tensile stresses are not related to the strains. In addition, the tensile stress in the concrete at the level of the tension steel, denoted by f_{ct}, is function of neutral axis and its tensile strength, f_{td}, The tensile strength is assumed to have respectively values of 1 and 0.55 MPa for short and long-term loadings.

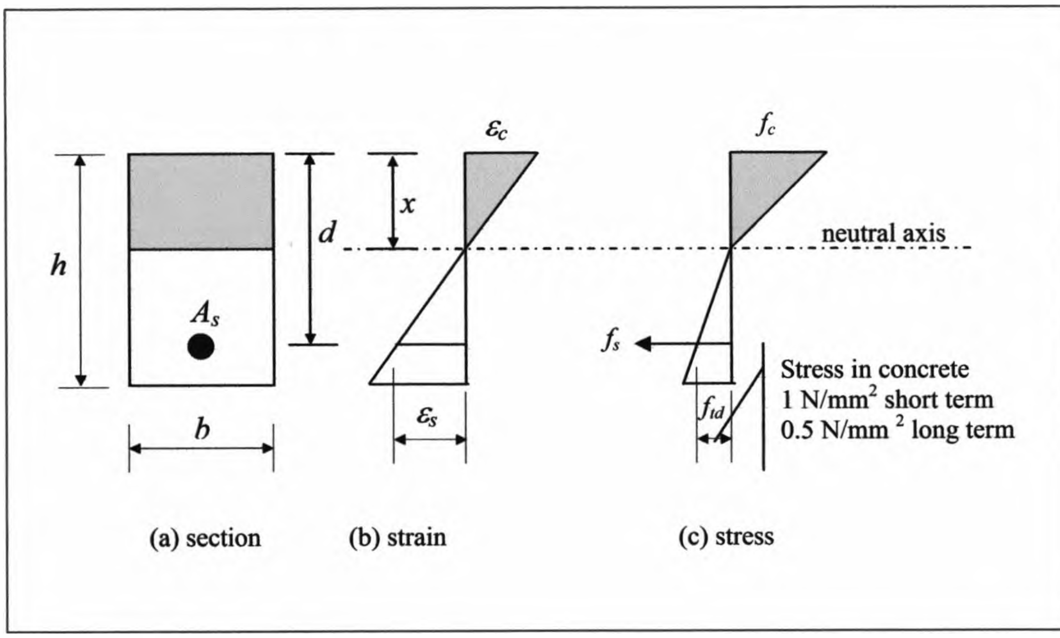

Figure 3.6 Strain and stress distribution for cracked section according to BS 8110

3.5.2 Second moment of area approach

The deflection due to a load on a cracked reinforced concrete beam is based on the calculation of an effective second moment of area, I_e, to be assumed constant over the full length of the beam. Several empirical expressions have been suggested as discussed in Chapter 2. In this section the form of equation developed by Fikry, Equation (1-3), will be used.

$$I_e = I_{cre} + (I_g - I_{cre})\ e^{\Phi} \tag{3.27}$$

where I_{cre} is the cracked second moment of area. I_g is the gross second moment of area of concrete section ignoring steel. Φ is the factor depends on loading type. This expression will be explained in detail in Chapter 4.

Equation (3.27) above is substituted into Equation (3.28) to find the deflection at specified load.

$$\delta = \frac{M_a(3L^2 - 4a^2)}{24E_c I_e} \tag{3.28}$$

3.6 Computation of deflections

3.6.1 Based on curvature approach

The design moment at mid span is taken from Table 3.6. The moment curvature of uncracked section is considered first, then the moment curvature of the cracked section is calculated. The largest value of moment curvature from both conditions is taken for calculating deflection.

(a) Calculate short-term curvature un-cracked section

$$E_c = (20 + 0.2 f_{cu}) \text{ GPa}$$

$$= (20 + 0.2 \times 35) \times 10^3$$

$$= 27 \times 10^3 \text{ MPa}$$

$$\frac{1}{r_b} = \frac{M}{E_c I}$$

$$= \frac{15.39 \times 10^6}{27 \times 10^3 \times \frac{1}{12} \times 150 \times 230^3}$$

$$= 3.75 \times 10^{-6} /\text{mm}$$

(b) Calculate short-term curvature cracked section

Assume $x = 50$ mm

Maximum tensile stress allowed in the concrete

$$f_{ct} = \left(\frac{h-x}{d-x}\right) f_{td}$$

f_{td} is taken as 1 for short-term deflection

$$f_{ct} = \left(\frac{230-50}{184-50}\right) \times 1$$

$$= 1.34$$

$$M = A_s f_s \left(d - \frac{x}{3}\right) + \tfrac{1}{3} b h f_{ct} (h-x)$$

$$f_s = \frac{M - \tfrac{1}{3} b h f_{ct} (h-x)}{A_s \left(d - \frac{x}{3}\right)}$$

$$= \frac{15.39 \times 10^6 - \tfrac{1}{3} \times 150 \times 230 \times 1.34 (230-50)}{\tfrac{1}{4} \pi \times 12^2 \left(184 - \frac{50}{3}\right)}$$

$$= 221.97 \quad \text{N/mm}^2$$

Concrete stress is given by

$$f_c = f_{c1} = \frac{x}{(d-x)} \frac{E_c}{E_s} f_s \qquad (3.29)$$

therefore

$$f_c = f_{c1} = \frac{50}{(184-50)} \frac{25000}{200000} \times 221.97$$

$$f_c = f_{c1} = 11.18 \quad \text{N/mm}^2$$

but f_c is also given by

$$f_c = f_{c2} = \frac{f_s A_s + \frac{1}{2} b(h-x) f_{ct}}{\frac{1}{2} bx} \qquad (3.30)$$

therefore

$$f_c = f_{c2} = \frac{221.97 \times \frac{1}{4}\pi \times 12^2 + \frac{1}{2} \times 150(230-50) \times 1.34}{\frac{1}{2} \times 150 \times 50}$$

$$f_c = f_{c2} = 24.93 \quad \text{N/mm}^2$$

These values of f_c do not agree, therefore further depth of the neutral axis are tried.

Substituting the values of x into Equation (3.29) giving f_{c1} as follows

$x = 50$ $\quad f_{c1} = 11.18$

$x = 65$ $\quad f_{c1} = 17.07$

$x = 80$ $\quad f_{c1} = 25.08$

Substituting the same value of x as above into Equation (3.30) giving f_{c2}

$x = 50$ $\quad f_{c2} = 24.93$

$x = 65$ $\quad f_{c2} = 19.64$

$x = 80$ $\quad f_{c2} = 16.37$

These values are plotted in Figure 3.7 produces two lines intersecting at a point which is correspond to $x = 68.532$ mm and $f_c = 18.74$ N/mm^2.

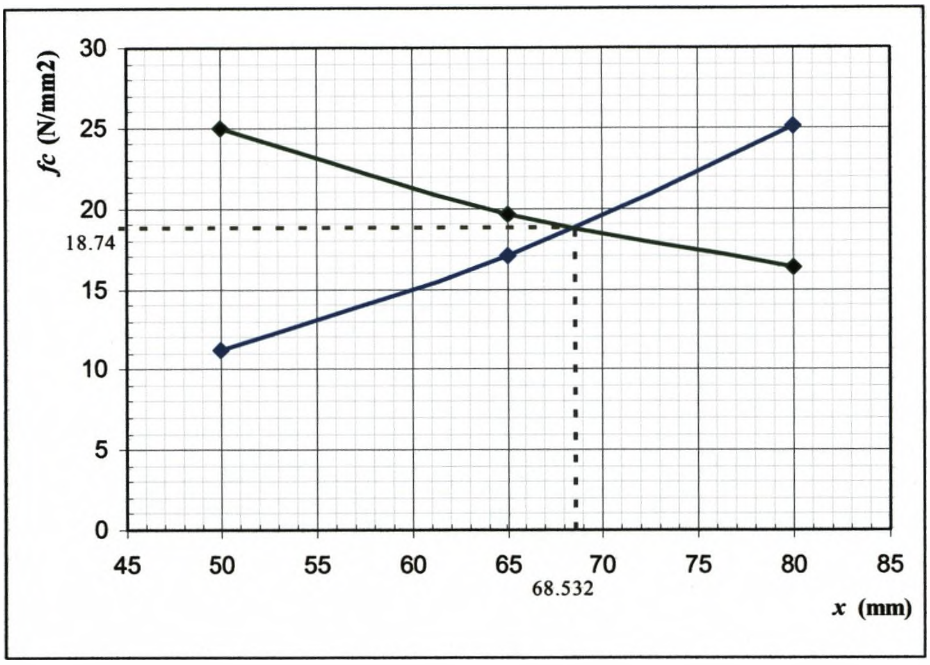

Figure 3.7 Plotting points between compressive strength and neutral axis

Hence,

$$\frac{1}{r_b} = \frac{f_c}{xE_c}$$

$$\frac{1}{r_b} = \frac{18.74}{68.532 \times 27 \times 10^3}$$

$$= 11.2 \times 10^{-6} \text{ /mm}$$

Since this curvature is greater than the un-cracked value, it is not necessary to check the concrete tensile stress for that case, the cracked value of 11.2×10^{-6} /mm being used to determine the deflection.

Referring to Figure 3.5 the factor load, *K*, value is given by Equation (3.25) as

$$K = 0.125 - \frac{a^2}{6L^2}$$

$$K = 0.125 - \frac{0.7^2}{6 \times 2.75^2}$$

$$= 0.114$$

Thus,

$$\delta = \frac{1}{r_b} K L^2$$

$$= 1.12 \times 10^{-5} \times 0.114 \times (2.75 \times 10^3)^2$$

$$\delta = 8.75 \quad \text{mm}$$

Similarly, for other variations of the section specified the deflection calculations are summarised in Table 3.7.

To calculate the value of x for other test beams a computer program has been written to speed the calculation. Typical computer program, Program B-1, can be seen in Appendix B-2.

Table 3.7 Deflection calculation using curvature approach

f_{cu} (MPa)	ρ (%)	M_s (kNm)	1/rb * (10^{-6})	x (mm)	fc1 (N/mm²)	fc2 (N/mm²)	1/rb ** (10^{-6})	a (m)	δ (mm)
25	0.82	10.4	2.735	63.09	13.70	13.70	8.69	0.70	7.50
								0.92	6.99
								1.15	6.30
								1.38	5.48
	1.23	14.12	3.714	71.02	16.67	16.67	9.39	0.70	8.11
								0.92	7.55
								1.15	6.81
								1.38	5.92
	1.64	16.86	4.434	77.79	18.36	18.37	9.44	0.70	8.16
								0.92	7.60
								1.15	6.85
								1.38	5.95
35	0.82	10.96	2.669	60.83	14.91	14.92	9.08	0.70	7.84
								0.92	7.30
								1.15	6.58
								1.38	5.72
	1.23	15.39	3.748	68.53	18.74	18.74	10.1	0.70	8.75
								0.92	8.15
								1.15	7.34
								1.38	6.38
	1.64	19.11	4.654	75.10	21.44	21.45	10.6	0.70	9.14
								0.92	8.51
								1.15	7.67
								1.38	6.67
45	0.82	11.27	2.555	58.96	15.77	15.77	9.23	0.70	7.97
								0.92	7.42
								1.15	6.69
								1.38	5.81
	1.23	16.09	3.648	66.48	20.12	20.12	10.4	0.70	9.01
								0.92	8.39
								1.15	7.56
								1.38	6.58
	1.64	20.36	4.616	72.90	23.44	23.44	11.1	0.70	9.58
								0.92	8.92
								1.15	8.04
								1.38	6.99

* = Uncracked section
**= Cracked section

3.6.2 Based on Fikry's method

Unlike the moment curvature approach the deflection calculation using the second moment of area approach is more straight forward. The transition between cracked and uncracked section takes place when the ratio of applied moment to cracking moment becomes greater than unity.

Calculate the cracking moment for the same beam as discussed in Section 3.6.1. Cracking moment is given by Equation

$$M_{cr} = \frac{f_r I_g}{y_t} \tag{3.31}$$

where modulus of rupture is calculated using

$$f_r = 0.56\sqrt{f_{cu}}$$

$$f_r = 0.56\sqrt{35}$$

$$= 3.313 \text{ N/mm}^2$$

thus

$$M_{cr} = \frac{3.313 \times \frac{1}{12} \times 150 \times 230^3}{115} \times 10^{-6}$$

$$= 4.381 \text{ kN m}$$

$$\frac{M_a}{M_{cr}} = \frac{15.390}{4.381} = 3.51 > 1 \qquad \text{section cracked}$$

Cracked second moment of area is calculated using Equation below (see Eq. 4.7)

$$I_{cr} = (\alpha + \beta\, n\rho)\frac{bd^3}{12}$$

for this case $n\rho = 9.11\ \%$ and $\alpha = 0.16$

$\beta = 0.05$

thus

$$I_{cr} = (0.16 + 0.05 \times 9.11)\frac{150 \times 184^3}{12}$$

$$= 4.79 \times 10^7 \text{ mm}^4$$

The value of gross second moment of area ignoring steel is given by

$$I_g = \frac{1}{12}bh^3 = \frac{1}{12} \times 150 \times 230^3 = 1.52 \times 10^8$$

Factor Φ is calculated using Equation below

$$\Phi = -\left(\frac{M_a}{M_{cr}} - 2\frac{a}{L}\right)\rho$$

$$= -(3.51 - 2 \times 0.7 / 2.75) \times 1.23$$

$$\Phi = -3.69$$

Therefore,

$$I_e = I_{cr} + \left(I_g - I_{cr}\right) e^{\Phi}$$

$$I_e = 4.79 \times 10^7 + \left(1.52 \times 10^8 - 4.79 \times 10^7\right) e^{-3.69}$$

$$= 5.05 \times 10^7 \text{ mm}^4$$

The I_e value above is then substituted into Equation (3.28) which give desired deflection.

$$\delta = \frac{M_a(3L^2 - 4a^2)}{24E_cI_e}$$

$$\delta = \frac{15.39 \times 10^6 \times \left(3 \times (2.75 \times 10^3)^2 - 4 \times (0.7 \times 10^3)^2\right)}{24 \times 27000 \times 5.05 \times 10^7}$$

$$= 9.75 \text{ mm}$$

Similarly, the above example is applied to calculate all beams considered which is presented in Table 3-8.

Table 3.8 Deflection calculation using Fikry's Method

f_{cu} (MPa)	ρ (%)	M_a (kNm)	M_a/M_{cr}	I_{cr} (mm^4)	a (m)	Φ	I_e (mm^4)	δ (mm)
25	0.82	10.4	2.81	3.80E+07	0.70	-1.88	5.53E+07	6.49
					0.92	-1.75	5.77E+07	5.79
					1.15	-1.62	6.07E+07	4.97
					1.38	-1.48	6.39E+07	4.10
	1.23	14.12	3.81	5.95E+07	0.70	-4.06	6.11E+07	7.98
					0.92	-3.87	6.15E+07	7.39
					1.15	-3.66	6.19E+07	6.61
					1.38	-3.46	6.24E+07	5.70
	1.64	16.86	4.55	6.35E+07	0.70	-6.63	6.36E+07	9.15
					0.92	-6.37	6.37E+07	8.52
					1.15	-6.09	6.37E+07	7.67
					1.38	-5.82	6.38E+07	6.66
35	0.82	10.96	2.50	3.61E+07	0.70	-1.63	5.88E+07	5.97
					0.92	-1.50	6.19E+07	5.27
					1.15	-1.36	6.57E+07	4.48
					1.38	-1.23	7.00E+07	3.66
	1.23	15.39	3.51	4.79E+07	0.70	-3.69	5.05E+07	9.75
					0.92	-3.50	5.11E+07	8.98
					1.15	-3.29	5.18E+07	7.98
					1.38	-3.09	5.27E+07	6.82
	1.64	19.11	4.36	5.97E+07	0.70	-6.31	5.99E+07	10.21
					0.92	-6.05	5.99E+07	9.50
					1.15	-5.78	6.00E+07	8.55
					1.38	-5.51	6.01E+07	7.42
45	0.82	11.27	2.57	3.45E+07	0.70	-1.69	5.62E+07	5.98
					0.92	-1.56	5.92E+07	5.28
					1.15	-1.42	6.28E+07	4.48
					1.38	-1.29	6.69E+07	3.66
	1.23	16.09	3.67	4.55E+07	0.70	-3.89	4.77E+07	10.06
					0.92	-3.69	4.81E+07	9.27
					1.15	-3.49	4.87E+07	8.25
					1.38	-3.29	4.95E+07	7.07
	1.64	20.36	4.65	5.65E+07	0.70	-6.78	5.66E+07	10.72
					0.92	-6.52	5.66E+07	9.97
					1.15	-6.25	5.67E+07	8.98
					1.38	-5.98	5.67E+07	7.80

3.6.3 Comparison between two methods

The results obtained between two methods are compared and their deflection ratios are presented in the last column of Table 3-9.

Table 3.9 Comparison between Fikry's and BS 8110

f_{cu} (MPa)	ρ (%)	M_a (kNm)	a (m)	Fikry	BS 8110	ratio
25	0.82	10.4	0.70	6.49	7.5	0.87
			0.92	5.79	6.99	0.83
			1.15	4.97	6.3	0.79
			1.38	4.1	5.48	0.75
	1.23	14.12	0.70	7.98	8.11	0.98
			0.92	7.39	7.55	0.98
			1.15	6.61	6.81	0.97
			1.38	5.7	5.92	0.96
	1.64	16.86	0.70	9.15	8.16	1.12
			0.92	8.52	7.6	1.12
			1.15	7.67	6.85	1.12
			1.38	6.66	5.95	1.12
35	0.82	10.96	0.70	5.97	7.84	0.76
			0.92	5.27	7.3	0.72
			1.15	4.48	6.58	0.68
			1.38	3.66	5.72	0.64
	1.23	15.39	0.70	9.75	8.75	1.11
			0.92	8.98	8.15	1.10
			1.15	7.98	7.34	1.09
			1.38	6.82	6.38	1.07
	1.64	19.11	0.70	10.21	9.14	1.12
			0.92	9.5	8.51	1.12
			1.15	8.55	7.67	1.11
			1.38	7.42	6.67	1.11
45	0.82	11.27	0.70	5.98	7.97	0.75
			0.92	5.28	7.42	0.71
			1.15	4.48	6.69	0.67
			1.38	3.66	5.81	0.63
	1.23	16.09	0.70	10.06	9.01	1.12
			0.92	9.27	8.39	1.10
			1.15	8.25	7.56	1.09
			1.38	7.07	6.58	1.07
	1.64	20.36	0.70	10.72	9.58	1.12
			0.92	9.97	8.92	1.12
			1.15	8.98	8.04	1.12
			1.38	7.8	6.99	1.12

The results show that for reinforcement ratio more than 1%, both approaches give similar values. However, for low reinforcement ratio the results show significant differences. The theoretical results using both approaches will be compared with the actual values obtained experimentally which will be discussed in Chapter 6.

Chapter 4

Effective Second Moment of Area

4.1 Introduction

The second moment of area is an important value, which is used to calculate the stress in a section, the resistance to buckling and the deflection of a beam. The deflection calculations required for a reinforced concrete element has been presented in Chapter 3.

The second moment of area (also sometimes called the moment of inertia) is a term used to describe the capacity of the cross section to resist bending. It is expressed mathematically as

$$I_{x-x} = \int y^2 dA \tag{4.1}$$

In which:

I_{x-x} is second moment of area around the x axis

y is the distance between the centroid of the section and the x axis

A is area of the section

4.2 Second moment of area of reinforced concrete beam

Since concrete is a brittle material weak in tension and strong in compression, when a concrete beam is loaded the beam deflection will cause a tensile region to be formed below the neutral axis. In this tensile region the beam cracks causing the effective concrete section area to decrease. It also produces a non-uniform section along the length of the beam, therefore as a result of these cracks occurring along the span of the beam an average value of the cracked and un-cracked section is taken into account in deflection calculations. It is known as the effective second moment of area.

This will produce two conditions in the reinforced concrete section, which will be described in detail below.

The first condition is when no cracks appear in the beam section. At this stage two values of the second moment of area can be calculated, allowing for the presence of reinforcement and ignoring reinforcement.

The second condition is that of a fully cracked section. The second moment of area of a cracked section will be explained from both the theoretical and the experimental point of view.

4.2.1 Uncracked section

When the concrete section, with steel reinforcement, as shown in Figure 4.1a, has not cracked the second moment of area of the section can be computed as the sum of second moment of area of concrete about its own centroidal axis and the second moment of area of the transformed steel reinforcement. This area is obtained by multiplying the steel area with the modular ratio, *n*, then applying the transfer formula. Therefore,

$$I_{gt} = \tfrac{1}{12}bh^3 + bh\,(x - \tfrac{1}{2}h)^2 + (n-1)A_s\left(d - x\right)^2 \qquad (4.2)$$

where,

I_{gt}	is gross second moment of area of uncracked transformed section
b	is cross-section width of beam
d	is effective depth
h	is height of the beam cross section
x	is centroidal of section
n	is modulus ratio, $n = \dfrac{E_s}{E_c}$
A_s	is area of steel

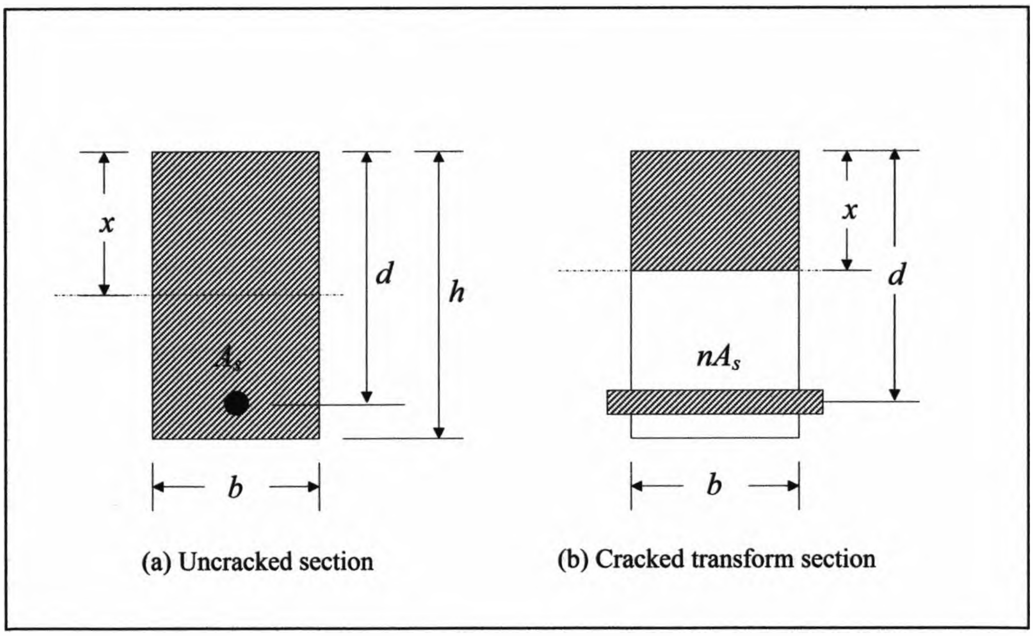

Figure 4.1 Section assumption of singly reinforced beam

Since the area of steel reinforcement in flexure is small, of the order of 1% of the gross cross-sectional area, the flexural stresses in the uncracked concrete are small and may be neglected [32]. Therefore, in beam deflection calculations most designers use the simplified procedure by ignoring the additional stiffness contributed by the steel reinforcement. Thus only the gross concrete section is considered, this generally is called the gross second moment of area, I_g.

Hence,

$$I_g = \tfrac{1}{12} bh^3 \tag{4.3}$$

where terms and units are same as mentioned in Equation (4.2) above.

4.2.2 Cracked section

4.2.2.1 Theoretical

Consider the single reinforced section with concrete cracked as shown in Figure 4.1b. To determine the cracked second moment of area, I_{cr}, of the section, the steel area have been converted into an equivalent area of concrete using the modular ratio, *n*. Thus, equivalent area of concrete, $A_f = nA_s$

The depth of neutral axis, x, can be determined from the equivalent transform section as shown in Figure 4.1b.

Taking the area moment about the upper edge

$$x = \frac{\sum Ax}{\sum A}$$

$$x = \frac{b\,x\,x/2 + nA_s\,d}{b\,x + nA_s} \qquad \text{or}$$

$$\tfrac{1}{2}bx^2 + nA_s\,x - nA_s\,d = 0$$

Solving the quadratic equation gives

$$x = \frac{-nA_s \pm \sqrt{(nA_s)^2 + 2b\,nA_s\,d}}{b}$$

Expressing A_s as ρbd, therefore

$$x = \frac{-n\rho bd \pm \sqrt{(n\rho bd)^2 + 2b\,n\rho bd\,d}}{b}$$

$$x = -n\rho d \pm d\sqrt{(n\rho)^2 + 2n\rho} \qquad (4.4)$$

As x is the depth of section thus the negative value will be meaningless, hence

$$x = -n\rho d + d\sqrt{(n\rho)^2 + 2n\rho}$$

Taking $k = -n\rho + \sqrt{(n\rho)^2 + 2n\rho}$

give

$$x = k\,d$$

Taking second moment of area of equivalent transform section about their neutral axis gives,

$$I_{cr} = \tfrac{1}{12} b x^3 + (bx)(\tfrac{1}{2} x)^2 + n A_s (d - x)^2 \qquad (4.5)$$

Substituting $k\,d$ for x into the above I_{cr} equation gives

$$I_{cr} = \tfrac{1}{12} b d^3 k^3 + \tfrac{1}{4} b d^3 k^3 + n \rho b d (d - kd)^2$$

$$I_{cr} = \tfrac{1}{12} b d^3 [4k^3 + 12 n \rho (1 - k)^2] \qquad (4.6)$$

where,

I_{cr} = cracked second moment of area

ρ = reinforcement ratio $= \dfrac{A_s}{bd}$

k = a constant depend upon $n\,\rho$

Fikry [2] has linearised Equation (4.6) and expressed it in the form below

$$I_{cre} = (\alpha + \beta\, n \rho)\ \tfrac{1}{12} b d^3 \qquad (4.7)$$

where,

I_{cre} is a simplified form of I_{cr}

α and β are factors dependent upon $n\rho$ and given as follows:

$\alpha = 0.003 \qquad \beta = 0.095 \quad \text{for } n\rho \leq 1.9\ \%$

$\alpha = 0.05 \qquad \beta = 0.07 \quad \text{for } 1.9\ \% < n\rho \leq 5\ \%$

$\alpha = 0.16 \qquad \beta = 0.05 \quad \text{for } 5\ \% < n\rho \leq 17\ \%$

$\alpha = 0.50 \qquad \beta = 0.03 \quad \text{for } 17\ \% < n\rho \leq 32\ \%$

$\alpha = 0.80 \qquad \beta = 0.02 \quad \text{for } n\rho > 32\ \%$

4.2.2.2 Experimental

The cracked second moment of area can be defined as the slope of the line connecting the origin and the point of initial yield of the tensile reinforcement in the moment-curvature curve [8]. Therefore experimentally it can be calculated by measuring strain in the tension and compression zones of the concrete beam under loading and applying the equation below [18].

$$I_{cr(\exp)} = \frac{M_y}{E_c \phi_y} \tag{4.8}$$

where

$$\phi_y = \frac{\varepsilon_{cy} + \varepsilon_{sy}}{d}$$

ε_{cy} is the measured compression strain in the concrete at yielding of steel reinforcement

ε_{sy} is the measured tensile strain in steel reinforcing at yielding stage

M_y is applied moment at yielding stage

For particular load arrangement such as Figure 3.5 the experimental cracked second moment of area can also be obtained by considering the equation below.

$$I_{cr(\exp)} = \frac{P_y\, a\left(3L^2 - 4a^2\right)}{48E_c\Delta_{\exp}} \tag{4.9}$$

where

P_y	is applied load at yield stage
a	is distance between support and load position
L	is span length
$\Delta_{\exp}$	is measured deflection

In terms of applied yield moment Equation (4.9) can be written as

$$I_{cr(\exp)} = \frac{M_y\left(3L^2 - 4a^2\right)}{24E_c\Delta_{\exp}} \tag{4.10}$$

where M_y is moment applied at yield stage.

The latter technique, either Equation (4.9) or (4.10), is adopted in this project to calculate the cracked second moment of area experimentally rather than Equation (4.8). Ashour [18] has reported that the second technique was a more realistic assumption than the first technique and gave smaller error compared to the theoretical value to the result produced by applying Equation (4.9).

When the concrete section is partially cracked, the second moment of area will be somewhere between I_g and I_{cr}. Therefore, the effective second moment of area, I_e, is the term used to define the value.

4.3 Effective Second Moment of Area

The distribution of *EI* along a simply supported beam can be seen in Figure 4.2. The *EI* varies from the uncracked values at points where the applied moment is less than cracking moment, to a partially cracked value at points of high moment.

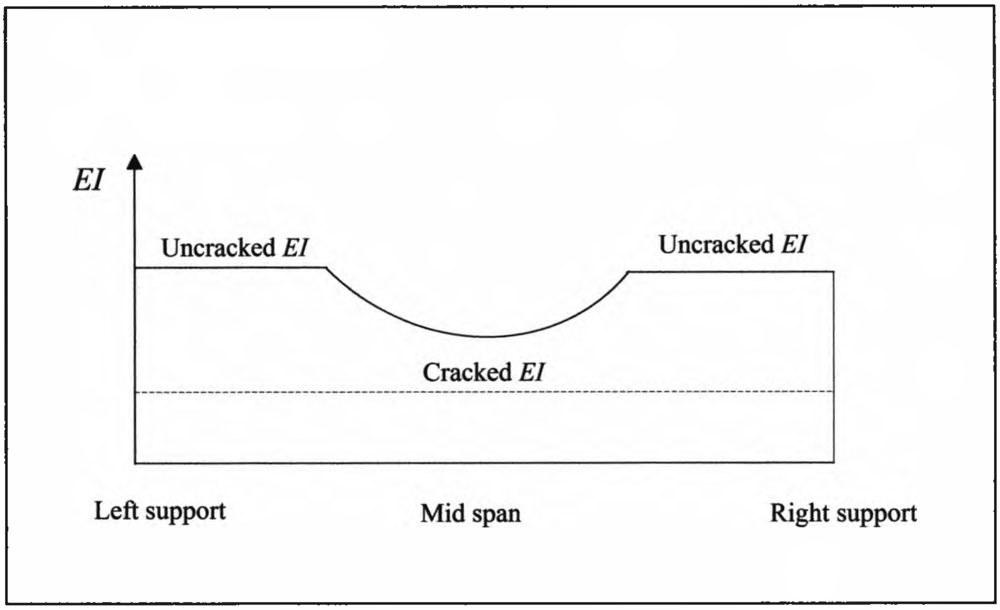

Figure 4.2 Variation of *EI* along the span beam

Since the use of such a distribution of *EI* value would make the deflection calculations tedious, an overall average or effective *EI* values is used. The effective second moment of area must account for both tension stiffening and the variation of *EI* along the member.

Branson derived Equation (1-2) to explain the transition from I_g to I_{cr} that is observed in experimental data [1].

Fikry [2] developed a new equation, Equation (1.3), as a replacement for Branson's equation based on data found in the literature. For convenient the equation represented below

$$I_e = I_{cre} + (I_g - I_{cre})\ e^{\Phi} \tag{4.11}$$

where,

I_{cre} is simplified form of I_{cr} as Equation (4.7)

I_g is gross second moment of area

Φ is a factor representing the type of load and its intensity. This factor is explained below.

The factor Φ in Equation (4.11) is dependant on the load condition, reinforcement ratio and the strength of the concrete. The value of Φ for two unsymmetrical point loads, two symmetrical point loads, and central point load are derived. The value of Φ for single point load acting at any point of beam is also discussed below.

The general expression for factor Φ is shown in Equation (4.12) below.

$$\Phi = -\left(\frac{M_a}{M_{cr}}\right)\left(\frac{L_{cr}}{L}\right)\rho \text{ for } \rho \geq 1\% \tag{4.12}$$

otherwise,

$$\Phi = -\left(\frac{M_a}{M_{cr}}\right)\left(\frac{L_{cr}}{L}\right) \tag{4.13}$$

in which

M_a is applied maximum moment

L_{cr} is span of concrete element in which cracks occur

M_{cr} is cracking moment, as given by Equation (3.31)

Different types of load acting on a beam will have different values of L_{cr}, depending upon bending moment diagram, and therefore to simplify the factor Φ the ratio of $\frac{L_{cr}}{L}$ will be derived for two unsymmetrical points load initially and factor Φ itself in the latter section.

4.3.1 Cracked length to span ratio

The cracked length to span ratio is defined as the ratio of the length over which the applied moment exceeds the cracking moment to the length of span considered.

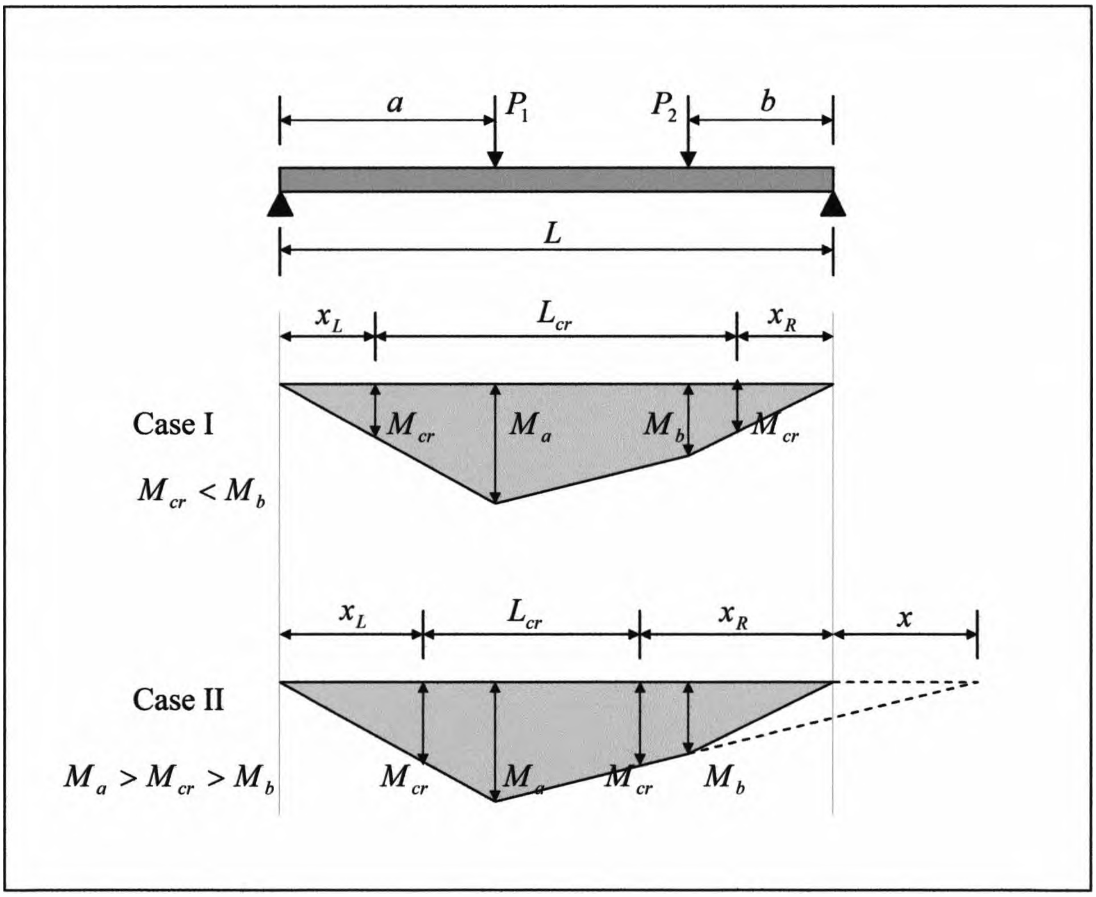

Figure 4.3 General condition of two points load to derive L_{cr}

4.3.1.1 Two unsymmetrical points load

Considering Figure 4.3 with two unsymmetrical point loads acting on the beam with P_1 greater than P_2, therefore moment diagram is shown as the dark area in Figure 4.3.

Let cracking moment, M_{cr}, be less than M_b (see Case I on the Figure 4.3 above)

Therefore $\quad L_{cr} = L - (x_L + x_R)$

in which $\quad x_L = a\dfrac{M_{cr}}{M_a}$ and $x_R = b\dfrac{M_{cr}}{M_b}$

Thus $\quad L_{cr} = L - \dfrac{M_{cr}}{M_a}\left(a + b\dfrac{M_a}{M_b}\right)$

Therefore cracked length and span ratio can be written as Equation (4.14).

$$\frac{L_{cr}}{L} = 1 - \frac{M_{cr}}{M_a}\left(\frac{a}{L} + \frac{b}{L}\frac{M_a}{M_b}\right) \tag{4.14}$$

If cracking moment, $M_a > M_{cr} > M_b$ (see case II in Figure 4.3 above)

The length of x in Figure 4.3 it can be found from similar triangles whose side is (x+b) with altitude M_b and a triangles having side of (L-a+x) with M_a depth and we can say that

$$\frac{x+b}{M_b} = \frac{(L-a)+x}{M_a}$$

therefore,

$$x = \frac{M_b(L-a) - b\,M_a}{M_a - M_b} \tag{4.15}$$

From the Figure also L_{cr} can be written as

$$L_{cr} = L - (x_L + x_R)$$

where

$$x_L = a\frac{M_{cr}}{M_a} \quad ;$$

$$x_R = \frac{M_{cr}}{M_a}(L - a + x) - x$$

thus

$$L_{cr} = L - \left(a\frac{M_{cr}}{M_a} + \frac{M_{cr}}{M_a}(L - a + x) - x \right)$$

$$L_{cr} = L - \frac{M_{cr}}{M_a}\big(a + (L - a + x)\big) + x$$

$$L_{cr} = L + x - \frac{M_{cr}}{M_a}(L + x)$$

$$L_{cr} = (L + x)\left(1 - \frac{M_{cr}}{M_a}\right)$$

Hence, the cracked length to span ratio is given by Equation (4.16).

$$\frac{L_{cr}}{L} = \frac{L + x}{L}\left(1 - \frac{M_{cr}}{M_a}\right) \tag{4.16}$$

4.3.1.2 Two symmetrical points load

The equation for this case can be obtained by making the value of a equal to b as well as P_1 equal to P_2 and subsequently M_a equal to M_b.

Rewriting Equation (4.14) produces

$$\frac{L_{cr}}{L}=1-\frac{M_{cr}}{M_a}\left(\frac{a}{L}+\frac{a}{L}\frac{M_a}{M_a}\right)$$

hence

$$\frac{L_{cr}}{L}=1-\frac{M_{cr}}{M_a}\left(\frac{2a}{L}\right) \tag{4.17}$$

4.3.1.3 Central point load case

Rewriting Equation (4.14) by substituting the value of *a*, *b* as $\frac{L}{2}$ and M_b equal to M_a.

Then

$$\frac{L_{cr}}{L}=1-\frac{M_{cr}}{M_a}\left(\frac{L}{2L}+\frac{L}{2L}\frac{M_a}{M_a}\right)$$

hence

$$\frac{L_{cr}}{L}=1-\frac{M_{cr}}{M_a} \tag{4.18}$$

4.3.1.4 Single point load at any point case

Referring to Figure 4.1 P_2 coincides with P_1, therefore $b=L-a$ and $M_b=M_a$ and $x=0$

Again rewriting Equation (4.14) and substituting all the value where they are appropriate.

Therefore,

$$\frac{L_{cr}}{L}=1-\frac{M_{cr}}{M_a}\left(\frac{a}{L}+\frac{L-a}{L}\frac{M_a}{M_a}\right) \text{ or } \qquad \frac{L_{cr}}{L}=\frac{L+0}{L}\left(1-\frac{M_{cr}}{M_a}\right)$$

Hence, the equations above give

$$\frac{L_{cr}}{L}=\left(1-\frac{M_{cr}}{M_a}\right) \tag{4.19}$$

4.3.2 Factor Φ

4.3.2.1 Two unsymmetrical points load case

- When Case I in Figure 4.3 above happen

  Rewriting Equation (4.12) then substitute $\frac{L_{cr}}{L}$ of Equation (4.14) above

$$\Phi=-\left(\frac{M_a}{M_{cr}}\right)\left(\frac{L_{cr}}{L}\right)\rho$$

$$\Phi=\left(\frac{M_a}{M_{cr}}\right)\left[1-\frac{M_a}{M_{cr}}\left(\frac{a}{L}+\frac{b}{L}\frac{M_a}{M_b}\right)\right]\rho$$

$$\Phi=-\left[\frac{M_a}{M_{cr}}-\frac{a+b}{L}\frac{M_a}{M_b}\right]\rho \tag{4.20}$$

- If cracking moment, $M_a > M_{cr} > M_b$ (see case II in Figure 4.3)

Therefore

$$\Phi=-\left(\frac{M_a}{M_{cr}}\right)\left(\frac{L_{cr}}{L}\right)\rho$$

$$\Phi=-\left(\frac{M_a}{M_{cr}}\right)\left[\frac{L+x}{L}\left(1-\frac{M_{cr}}{M_a}\right)\right]\rho$$

$$\Phi=-\left(\frac{L+x}{L}\right)\left[\left(\frac{M_a}{M_{cr}}-1\right)\right]\rho \qquad (4.21)$$

with x refers to Equation (4.15).

4.3.2.2 Two symmetrical points loads case

Rewriting Equation (4.12) and replacing $\frac{L_{cr}}{L}$ with Equation (4.17)

$$\Phi=-\left(\frac{M_a}{M_{cr}}\right)\left(\frac{L_{cr}}{L}\right)\rho$$

$$\Phi=-\left(\frac{M_a}{M_{cr}}\right)\left(1-\frac{M_{cr}}{M_a}\frac{2a}{L}\right)\rho$$

hence

$$\Phi=-\left(\frac{M_a}{M_{cr}}-\frac{2a}{L}\right)\rho \qquad (4.22)$$

4.3.2.3 Central point load case

Again rewriting Equation (4.12) and substituting $\frac{L_{cr}}{L}$ of Equation (4.18)

$$\Phi = -\left(\frac{M_a}{M_{cr}}\right)\left(\frac{L_{cr}}{L}\right)\rho$$

$$\Phi = -\left(\frac{M_a}{M_{cr}}\right)\left(1-\frac{M_{cr}}{M_a}\right)\rho$$

thus

$$\Phi = -\left(\frac{M_a}{M_{cr}}-1\right)\rho \qquad (4.23)$$

4.3.2.4 Single point load at any point case

For the case of single point load at any position the cracked length to span ratio has the same value as the cracked length to span ratio of the case of central point load as Equation (4.18). Therefore, the factor Φ will also be the same as central point load case as given by Equation (4.23).

Thus for single point load at any point, the factor Φ is given by

$$\Phi = -\left(\frac{M_a}{M_{cr}}-1\right)\rho \qquad (4.24)$$

4.4 Summary

- Effective second moment of area will have a value between I_{gt} which is the section is in uncracked condition and I_{cr} in which the section is in the fully cracked condition.
- Crack length to span ratio equation is dependent upon the load condition. Fikry's equation used this factor in his model and has found that they have the

same value for load act in the middle of the beam and for a single point load acting at any point of the beam. As a result, the values of factor Φ in Fikry's equation are equal for this type of load.

- In brief, the results for L_{cr}/L and Φ are presented in Table 4.1.

Table 4.1 Various equation form of L_{cr}/L and factor Φ

Load position	L_{cr}/L	Factor Φ
#1. 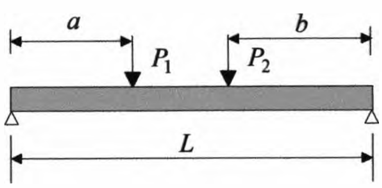	*If* $P_1 > P_2$ *and* $M_{cr} < M_b$ $\frac{L_{cr}}{L} = 1 - \frac{M_{cr}}{M_a}\left(\frac{a}{L} + \frac{b}{L}\frac{M_a}{M_b}\right)$ *For* $P_1 > P_2$ and $M_a > M_{cr} > M_b$ $\frac{L_{cr}}{L} = \frac{L+x}{L}\left(1 - \frac{M_{cr}}{M_a}\right)$	*If* $P_1 > P_2$ *and* $M_{cr} < M_b$ $\Phi = -\left[\frac{M_a}{M_{cr}} - \frac{a+b}{L}\frac{M_a}{M_b}\right]\rho$ *For* $P_1 > P_2$ and $M_a > M_{cr} > M_b$ $\Phi = -\left(\frac{L+x}{L}\right)\left[\left(\frac{M_a}{M_{cr}} - 1\right)\right]\rho$
#2. 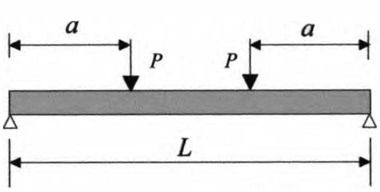	$\frac{L_{cr}}{L} = 1 - \frac{M_{cr}}{M_a}\left(\frac{2a}{L}\right)$	$\Phi = -\left[\frac{M_a}{M_{cr}} - 2\frac{a}{L}\right]\rho$
#3. 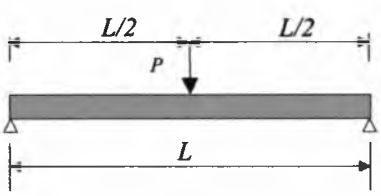	$\frac{L_{cr}}{L} = \left(1 - \frac{M_{cr}}{M_a}\right)$	$\Phi = -\left[\frac{M_a}{M_{cr}} - 1\right]\rho$
#4. 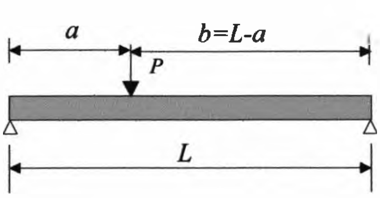	$\frac{L_{cr}}{L} = \left(1 - \frac{M_{cr}}{M_a}\right)$	$\Phi = -\left[\frac{M_a}{M_{cr}} - 1\right]\rho$

Chapter 5

Experimental Apparatus and Procedures

5.1 Introduction

This Chapter describes the experimental test procedures used in testing the singly reinforced concrete beams. The equipment used in the testing and calibration is also described together with the preparation of the specimens. The test programme and the specimen designation are also explained.

5.2 Experimental Procedure

5.2.1 Flexural test

The experimental set-up is shown diagrammatically in Figure 5.1. Each concrete beam is placed on two supports as shown and subjected to either a central concentrated load or equal loads at the same distance from the supports. The latter was achieved by using a steel beam to transfer the applied load to the point of application. The load was applied to the beam via a load cell with a maximum capacity of 100 kN. At each load increment the value of load was read off a load cell, which was also connected to the computer package Picolog.

The deflection of the beams were measured at the mid span of the beams and also at both third span positions. This was done by placing displacement transducers with dial gauge attached, in contact with the soffit of the beams. These transducers were also connected to the computer package.

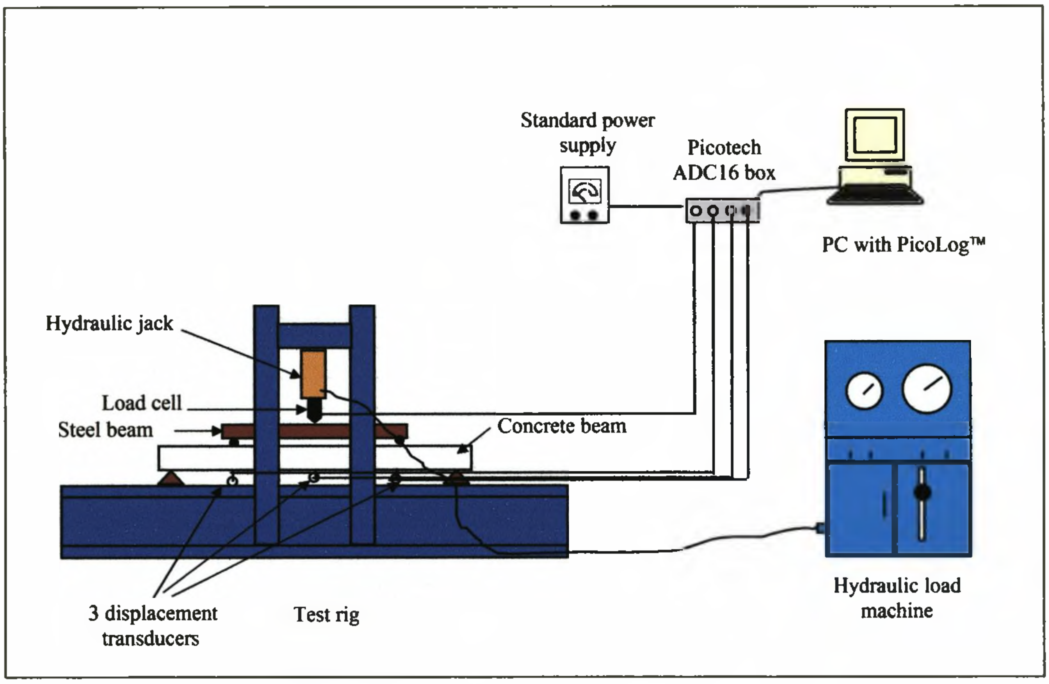

Figure 5.1 Experimental set-up for the flexural tests

To see easily the crack propagation in the beams one side of each beam was painted with white paint. At load increment each new crack or crack extension was traced using black ink pens for maximum contrast. At the end of load test the beam sides were photographed for a permanent record.

5.2.1.1 Crack detection using plastic optical fibre alongside flexural test

Plastic optical fibre (POF) sensor has the ability to detect initial crack on the small-scale concrete specimen as shown in Ref. [33]. Therefore it was decided to use it in terms of full-scale reinforced concrete specimen. Flexural test set-up for this purpose is shown diagrammatically in Figure 5.2 below.

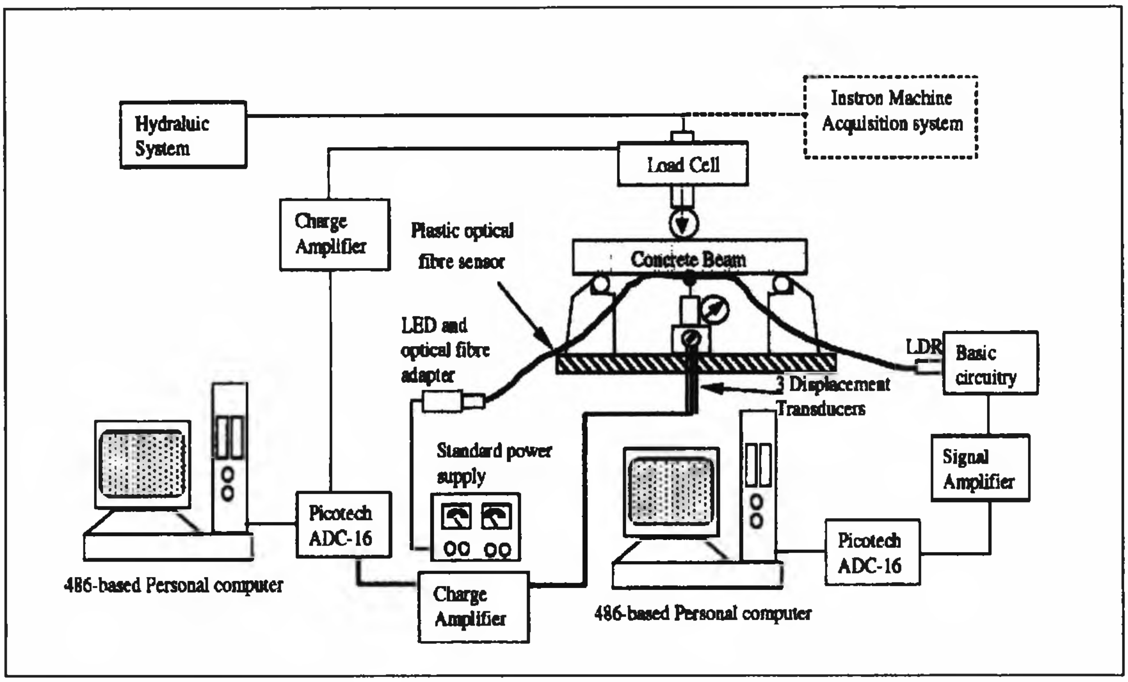

Figure 5.2 Experimental set-up of crack detection using POFs in flexural test

5.2.1.2 Attachment of the POF sensors to the concrete specimen

The POFs were attached to the concrete beams specimen as shown in Figure 5.3. The surfaces of the concrete specimens were initially ground using 180 and 320-grit size grinding papers to remove any unevenness. The prepared surface was then dusted and cleaned with a damp cloth to remove any residual concrete. After drying, the proposed position of the sensors was marked out on the sample and the sensor was temporarily held in position by securing the fibre to the edge of the concrete specimen using masking tape. A cynoacrylate-based adhesive was then used to bond the fibre to the surface of the concrete. The adhesive was carefully applied along the interface between the fibre and the surface of the concrete. The adhesive was allowed to harden for 5 minute before proceeding to sensitize the fibre.

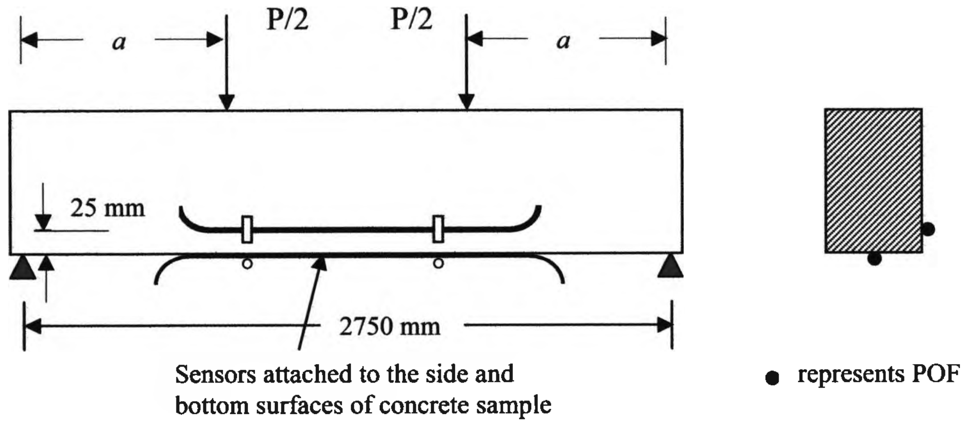

Beam section (see Figure)	f_{cu} (MPa)	a (m)	Location and number	
			side	bottom
1 (Fig. 5.4a)	35	1.375	0	1
2 (Fig. 5.4c)	45	1.375	1	1
3 (Fig. 5.4c)	45	0.7	0	1

Figure 5.3 Detail of POF attached on the surface of reinforced concrete specimen

A total of three beams were tested under central and two point loads conditions (see Figure 5.3). In specimen 1 and 3, only one sensor was used initially. A second sensor was attached to the side surface of the beam for specimen 2 in addition to the sensor attached to the lower surface of the beam. Locating the sensor on the side of the surface facilitates a visual inspection of the crack surface. This allows the operator to ascertain whether changes in the sensor signal are result of crack initiation in the vicinity of the sensor or otherwise. Since the crack is expected to propagate upwards from the lower surface of the beam, the sensor on the side of the beam was located as close as possible to the bottom edge of the beam (approximately 25 mm from lower surface). This was done to minimize time delay between the detection of a crack by the sensor (attached to the side of the beam) and the actual moment when cracks initiate from the lower surface.

5.2.2 Specimen preparation

Initially five beams were cast using reinforcing cages used in the undergraduate laboratory classes. They had the disadvantage of having the main tensile steel made out of mild steel (yield strength 250 N/mm^2). They were considered as suitable for carrying out preliminary test to sort out the experimental set up, the range of variable etc.

The main part of the testing programme load tested a total of 36 beams over 2750 mm span. Three reinforcement ratios were used together with three concrete grade and 36 reinforcement cages. The details of reinforcement are shown in Figure 5.4. One overall beam section was used to facilitate the casting of the beam.

The main tensile reinforcement was 12 mm diameter, deformed bars (f_y = 460 N/mm^2). The stirrups were 6 mm diameter bar placed at 130 mm along the length of the span. The hanging bars were plain 6 mm diameter bars.

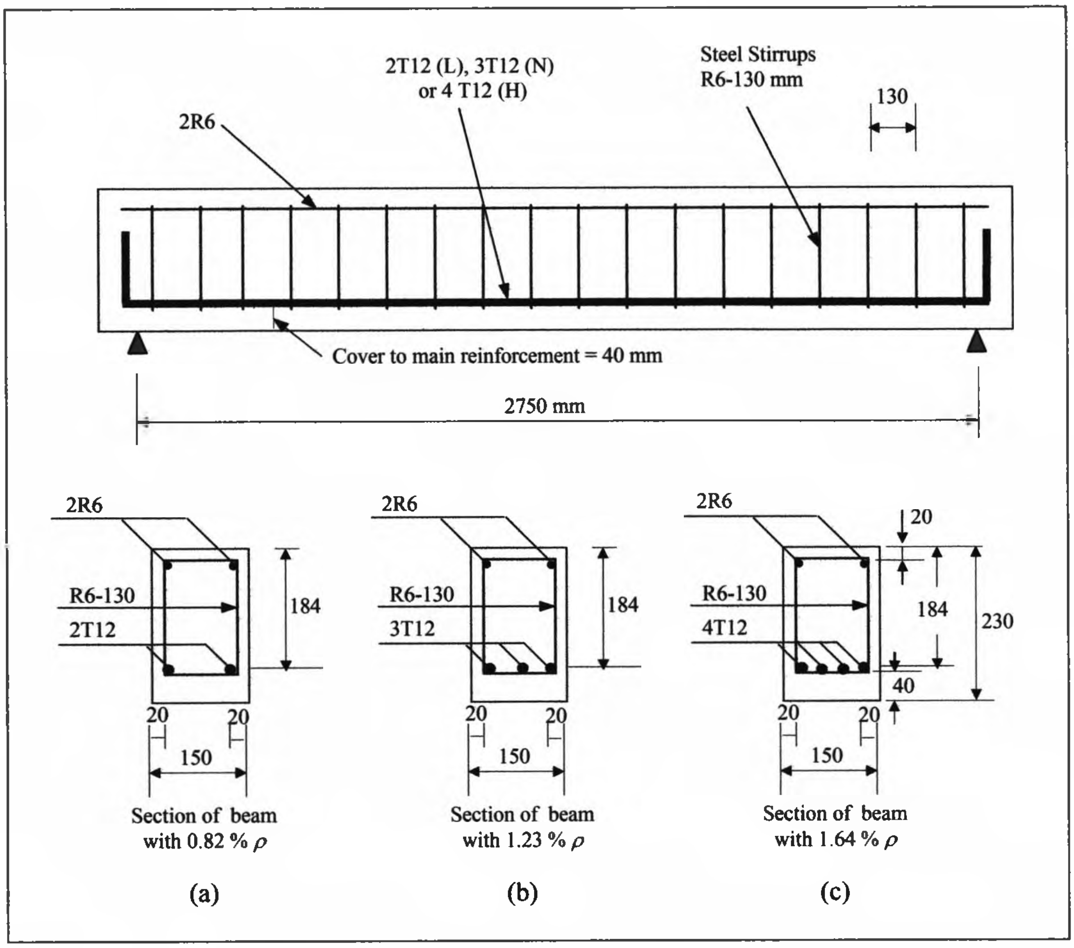

Figure 5.4 Reinforcement detail of beams considered in this study

The three variation of concrete cube compressive strength (f_{cu}) used were *25*, 35 and *45* MPa. Ordinary Portland cement (*Castle Type I*), sand aggregate (*Hope*) with fine grade of 60% passing 600 μm sieve and uncrushed coarse aggregate (Staffordshire pink) of 10 mm maximum size were used. Relative density of the aggregate (SSD) was 2.63. Building Research Establishment [34] procedure was adopted for making mix design of concrete, but factor standard deviation slightly adjusted based on experience results obtained in laboratory. After all, care was taken to ensure the appropriate mix proportion of the OPC, sand, and coarse aggregate as shown in Table 5-1.

The concrete mixture was poured into moulds and covered with wet burlaps and plastic sheets after casting. The beams were released from the moulds after 3 days and stored under laboratory condition for 25 days.

Table 5.1 Mix proportion of concrete material by weight

Cube concrete strength, f_{cu} (MPa)	Cement	Water	Fine aggregate	Coarse aggregate
				10 mm
25	1	0.84	3.6	4.20
35	1	0.70	2.79	3.56
45	1	0.59	2.18	3.02

With the casting of each beam, sample cubes and cylinder from each batch of the concrete mixture were also cast. Three 100 mm cube and one 150 mm diameter x 300 mm length cylinder sample were cast. These were tested after water curing for 28 days to determine cube concrete strength, cylinder strength and the static modulus of elasticity.

Table 5.2 Initial deflection to check the effect of different cured

Beam	Load (kN)	Measured defl. (mm)	Average f_{cu1} * (MPa)	Calculated defl.1 (mm)	Average f_{cu2} ** (MPa)	Calculated defl.2 (mm)	ratio1	ratio2
(1)	(2)	(3)	(4)	(5)	(6)	(7)	(8)=(5)/(3)	(9)=(7)/(3)
B4H35	35	11.35	39	9.08	36	9.15	0.80	0.81
B2H35	60	15.36	37	13.72	35	13.76	0.89	0.90

* standard cured cube
** cured cube similar with beam specimen

A number of sample cubes were also cured using the same technique as that for the beam. The different between the results of this method compared to those of the standard method is insignificant in terms of deflection calculation results as shown in Table 5.2. Therefore it was considered to use sample cube with standard curing for the rest of the beam to determine strength of the beam specimen.

5.3 Test Programme

As mentioned previously that a series of preliminary tests were carried out. Based on these preliminary test results it was decided to investigate a total of thirty-six beams. Three concrete grades, three reinforcement ratios and four load positions were considered. The section of each beam was 150 mm x 230 mm by 3000 mm length and a 2750 mm span as shown in Figure 5.4.

Table 5.3 Properties of the additional beams used to validate the proposed model

Beam	f_{cu} (MPa)	b (mm)	h (mm)	d (mm)	Tension steel	ρ (%)	L (m)	Load arrangement
X_1	45	150	240	208	3T16	1.96	2.5	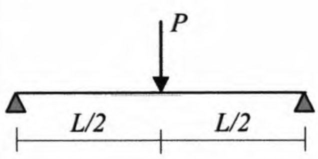
X_2							3.3	
X_3							4.0	
X_4					2T12	0.73	3.3	
X_5					3T12	1.09	3.6	
X_6					2T12	0.73	3.3	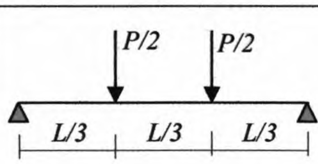
X_7					2T12	0.73	2.75	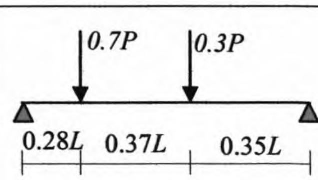
X_8					3T12	1.09	2.75	

After the above beams were tested and the theoretical model was developed, eight more beams with different properties and spans were tested to show that the model could be applied to any simply supported beams. The details of these additional beams are given in Table 5.3.

5.4 Beam Designations

In this section, the designation system for the beams used in developing the proposed model is explained.

- Beam is designated by letter B
- Number 1, 2, 3 and 4 designate distance between load acting and support position. Number 1 represent distance of 700 mm, number 2 for 910 mm while 3 and 4 represent distance of 1150 and 1375 mm respectively.
- Reinforcement ratio is designated by letter L for low reinforcement ratio of 0.82 %, N of normal reinforcement ratio of 1.23 % and H represent heavy reinforcement ratio of 1.64 %.
- Number 25, 35 and 45 represent the concrete grade used in this study.

For example B1L35 means a beam with load positions 700 mm from support and a low reinforcement ratio of 0.82 % with 35 MPa cube concrete strength. Complete list of beam designation is presented in Table 5.4.

Table 5.4 Beam designation of the main beam sample

Beam	Load position from support, *a* (m)	Reinforcement ratio, (%)			f_{cu}, (MPa)	Beam designation		
		L	N	H				
B1	0.7	0.82	1.23	1.64	25	B1L25	B1N25	B1H25
					35	B1L35	B1N35	B1H35
					45	B1L45	B1N45	B1H45
B2	0.92	0.82	1.23	1.64	25	B2L25	B2N25	B2H25
					35	B2L35	B2N35	B2H35
					45	B2L45	B2N45	B2H45
B3	1.15	0.82	1.23	1.64	25	B3L25	B3N25	B3H25
					35	B3L35	B3N35	B3H35
					45	B3L45	B3N45	B3H45
B4	1.375	0.82	1.23	1.64	25	B4L25	B4N25	B4H25
					35	B4L35	B4N35	B4H35
					45	B4L45	B4N45	B4H45

5.5 Equipment

5.5.1 Denison machine – universal test rig

Denison universal test rig machine with maximum load capacity of 100 kN was used. This machine is fully equipped with its own computer and printer. The machine was used to calibrate the load cell and dial gauges. Figure 5.5 shows the machine while running tension test of reinforcement specimen.

Figure 5.5 Denison universal test rig is testing tensile of steel reinforcement

5.5.2 TONIPAC – compression machine

Maximum load capacity of 3000 kN was available with TONIPAC compression machine. This machine is used for compression test of material with adjustable loading rate provided which depends upon the material and size of specimen tested.

This machine is also connected into a portable computer with PicoLog™ computer software package using Microsoft windows 98. A unit device attached to the machine, with three transducers, can be connected to the computer software to measure concrete strain and strength of cylinder specimens. Once strain and strength of the specimens were obtained, concrete modulus of elasticity could then be calculated.

Figure 5.6 shows the TONIPAC compression machine whilst running a compression test on a concrete cylinder specimen.

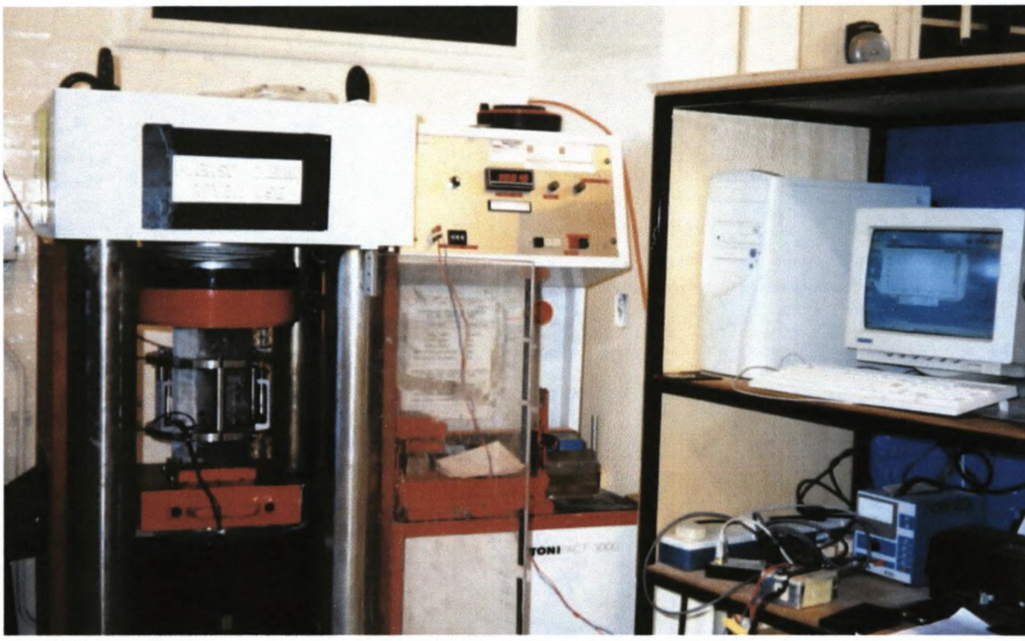

Figure 5.6 TONIPAC compression machine connected to PC for strength and strain test of cylinder specimen

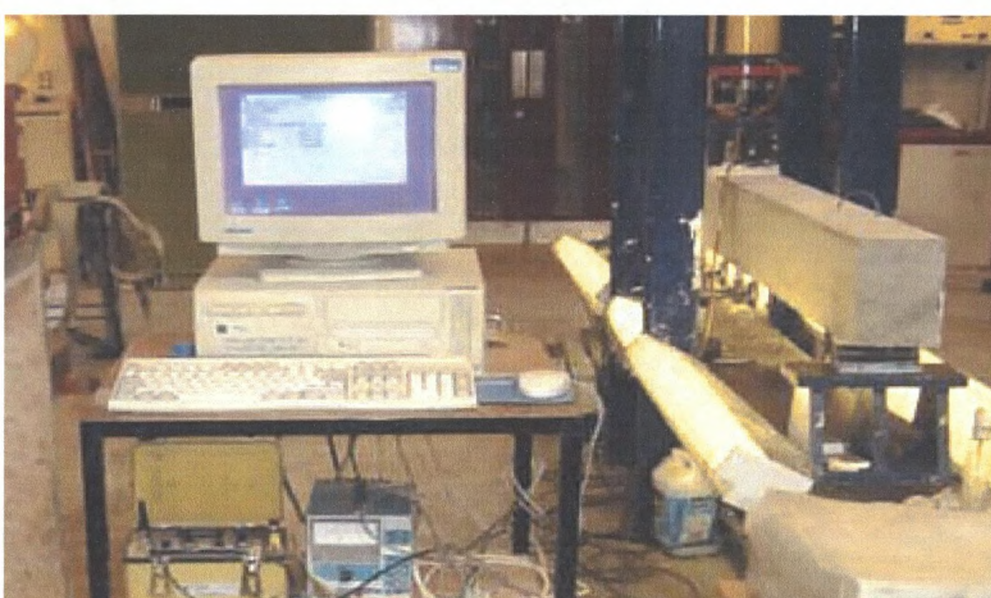

Figure 5.7 Flexural test in progress using Pico computer software

5.5.3 Flexural test equipment

A control station connected to the main power supply provides a means of controlling the load applied to the hydraulic jack as shown in Figure 5.1. The load cell, attached to the hydraulic jack, is connected to the Picotech software by means of a transducer. The precise load applied to the load cell was determined based on the reading obtained from the computer display, which was generated by PicoLog software as shown in Figure 5.7.

5.6 Calibration of Equipment

In order to produce data that can be accepted as accurate the equipment used must be calibrated. The main devices used in measuring the data were a load cell and three dial gauges. The devices were connected into PicoLog™ computer software with eight channels box provided. A 10 Volt DC power supplier was used to motorize the transducers that were connected to the load cell and three dial gauges. The load cell was calibrated first then followed by the dial gauges.

A full explanation of calibration process for each device is discussed in the section below.

5.6.1 Sensonic Load Cell

The calibration of the load cell was undertaken as follow. Firstly, Denison machine with proof strength computer software was switch on. Load cell, which has been connected with PicoLog™ computer software, was placed on the Denison test rig and loaded. As load cell was compressed by the machine with certain load level, it influences load reading on the PicoLog™ computer software. Readings from Denison machine and the PicoLog™ computer software were referred to as Load reference and Sensonic cell respectively.

Secondly, load reading from "load reference" could be paused at any level to allow the load reference and the sensonic cell reading to be taken. Both load reading of 'load reference' and 'Sensonic cell' were written down and then tabulated in Table 5.5.

Table 5.5 Data input for calibration load cell

Load reference (kN)	Sensonic cell (kN)
0.001	-1.068
0.645	-1.831
1.213	-2.518
2.621	-4.196
4.126	-5.989
6.147	-8.507
10.095	-13.390
20.050	-25.139
30.080	-36.774
40.110	-48.333
50.090	-59.968
60.970	-72.595
70.070	-83.085
80.030	-94.682
90.000	-106.355
100.060	-117.914

In addition, in order to obtain "Sensonic cell" that has the same value as "load reference", on the experimental test, the load reading on the table above can be re-written into the scale column available in the PicoLog™ software. Otherwise linear relationship between the Load reference and the Sensonic cell can be performed such as Figure 5.8.

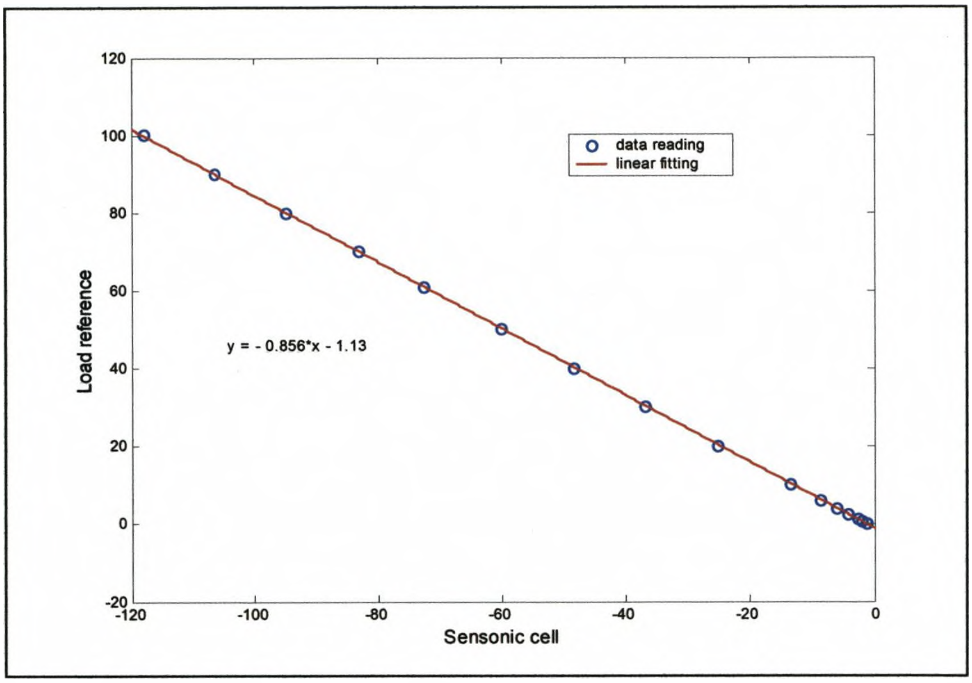

Figure 5.8 Linear relationship between load cell and load reference

Furthermore, to enter either the data in Table 5.5 or the results in Figure 5.8, the instruction through the windows screen of the PicoLog software could be followed.

5.6.2 Dial Gauges

Similarly as above, a mechanical dial gauge has been placed on the Denison test rig machine and pressed with a certain level of displacement. Other type of dial gauge with 0.01 mm accuracy of meter reading were pressed by hand and paused at 5 mm displacement increment. All dial gauges were connected to a computer by means of three transducers. Displacements reading from three dial gauges (Gauge1, Gauge2, and Gauge3) and PicoLog software (Trans1, Trans2, Trans3) were read and note were taken on each all together. The reading is presented in Table 5.6.

Table 5.6 Data read from dial gauges and picolog

Gauge1	Trans1	Gauge2	Trans2	Gauge3	Trans3
0.000	-0.139	0.000	-1.622	0.000	-0.148
5.000	2.224	5.000	1.355	5.000	2.145
10.000	4.825	10.000	3.875	10.000	4.515
15.000	7.269	15.000	6.470	15.000	7.190
20.000	9.637	20.000	8.990	20.000	9.331
25.000	12.157	25.000	11.433	25.000	11.700
30.000	14.601	30.000	13.876	30.000	14.299
				35.000	16.669
				40.000	19.039
				50.000	24.007

Again linear relationship between dial gauges (Gauge) and Picolog software (Trans) are performed using data in Table 5.6 to obtain linear equations to be put into picolog software.

Figure 5.9, 5.10 and 5.11 show the linear relationship between picolog software and dial gauge 1, 2 and 3 respectively.

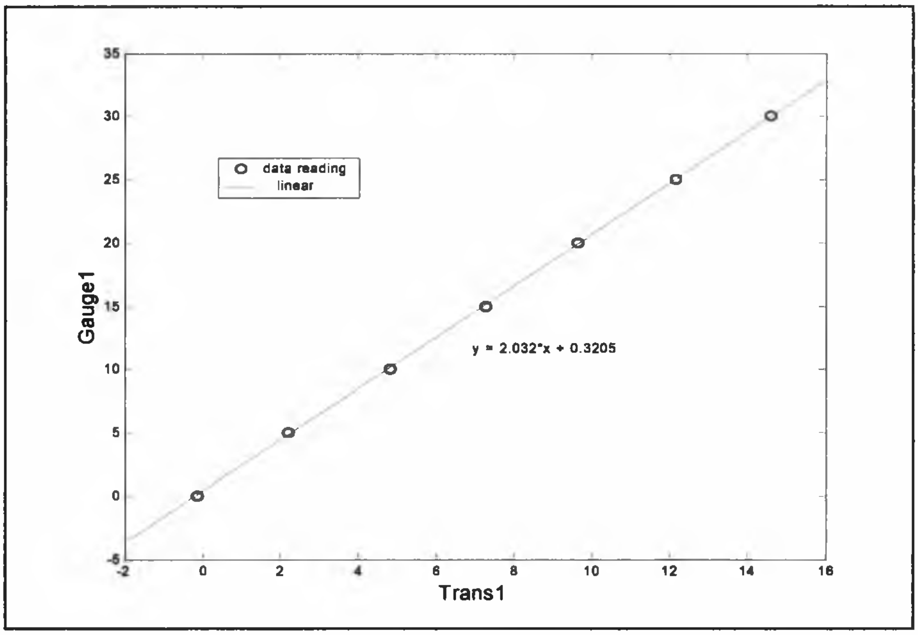

Figure 5.9 Linear relationship between Gauge1 and Trans1

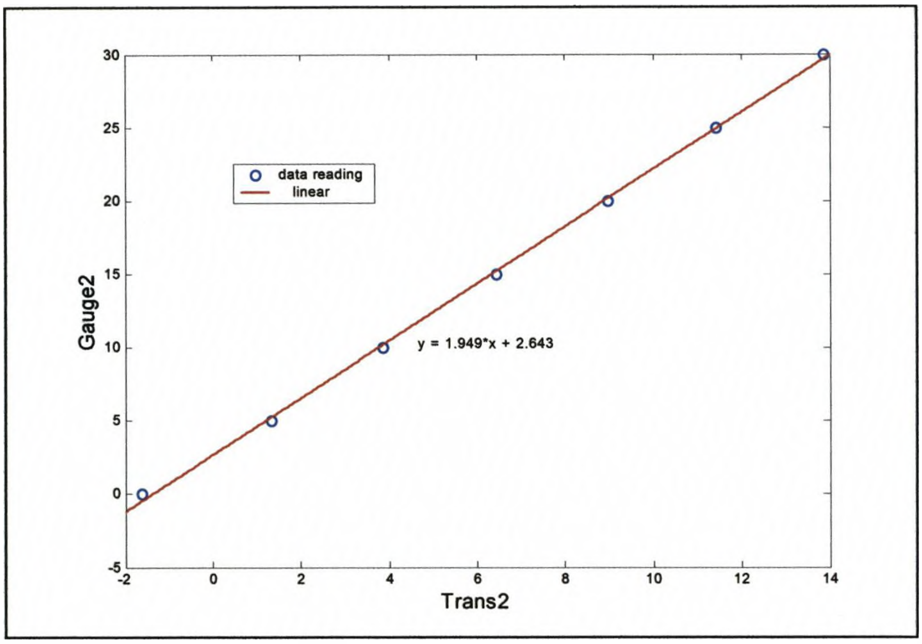

Figure 5.10 Linear relationship between Gauge2 and Trans2

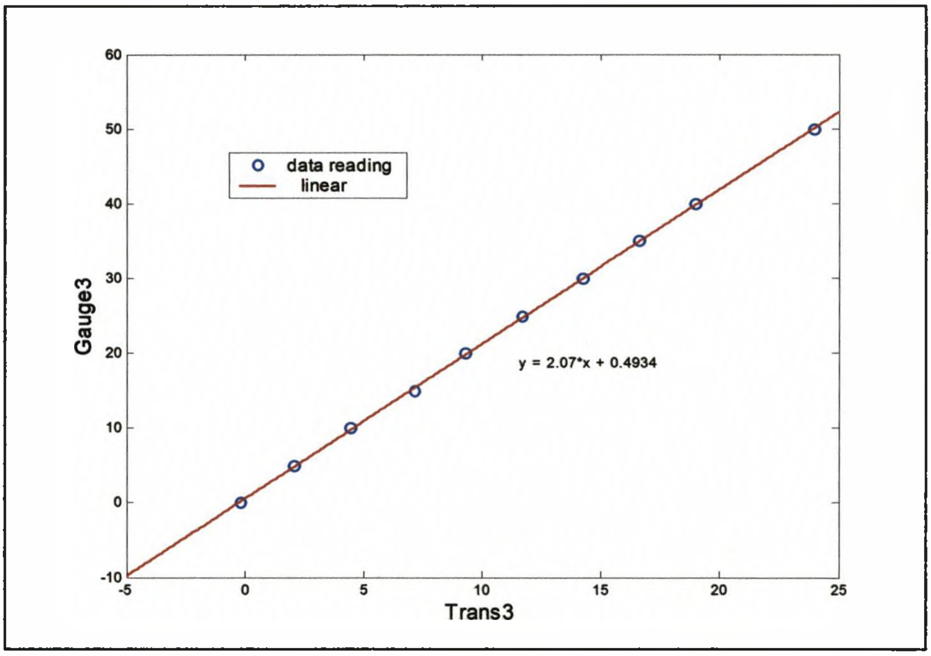

Figure 5.11 Linear relationship between Gauge3 and Trans3

5.7 Data acquisition

5.7.1 Flexural test

Once the calibration of the devices has been completed, data was captured and stored using a PC with Pico software. This software was installed under Microsoft windows 3.1.

In this experiment the software was set-up to record one data each second with the maximum number of data of a million. From the window displayed on Figure 5.12 the value of load and displacements of transducers can be read easily. The main window in the figure is called PLW-Recorder. From the main window can be viewed any sub windows of PLW XY-Graph and PLW Spreadsheet.

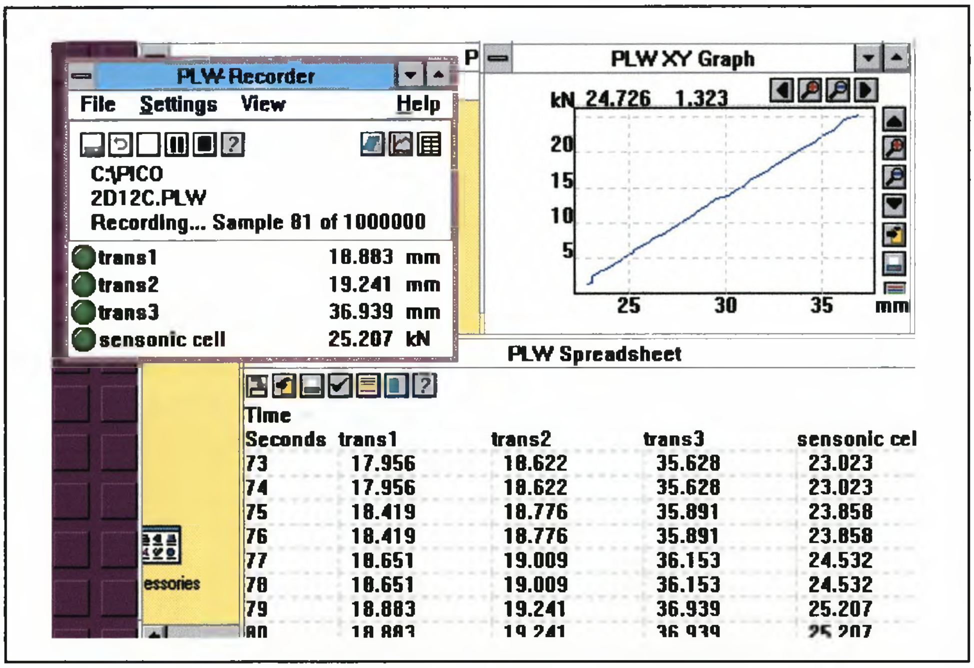

Figure 5.12 Typical monitor screen while recording data

5.7.2 Optical fibre sensors

A standard voltage supply was used to power the ultra-high luminescent LED (centred at 612nm). The light detection system consisted of a light-dependent resistor (LDR) and a fixed resistor in the form of a voltage divider circuit. As the incident light on the LDR varied, the voltage signal across the fixed resistor varied accordingly. The data from the optical fibre were automatically collected by the computer at a sampling rate of 1 Hz and this information was displayed graphically in real time.

5.7.3 Compression and modulus of elasticity test

Three 100mm cube specimens from each batch of concrete mixture were tested to determine the cube compressive stress. The stress value was then used to predict compression strength value of a cylinder specimen in which one-third of its value is required to determine modulus of elasticity. At the end, a cylinder specimen was tested until failure (specimen crash).

The modulus of elasticity was calculated based on the strain and strength of the cylinder specimen. The data was captured by Pico software after it has been connected with the TONIPAC compression machine.

Cube concrete strength of each specimen was read from the TONIPAC compression machine, Figure 5.6, from the displayed value. For this test the loading rate was 30 kN/s. The machine can be set-up to stop automatically after a specimen crashes. Data obtained can then be recorded by filling in the form provided. Tension reinforcement data was stored and collected from the print out of the Denison machine test, Figure 5.5.

Chapter 6

Results and Discussions

6.1 Basic properties

6.1.1 Concrete strength

The procedure for mix design has been explained in Chapter 5, great care being taken to produce concrete with a normal strength of 25, 35 and 45 MPa. In order to verify the strengths the required cube tests were carried out on three different mixes. The concrete strengths variations are shown in Figure 6.1, 6.2 and 6.3 where all can be seen to follow a normal distribution. Using basic statistical analysis the normal 25 MPa strength concrete had an average strength of 28.621, with standard deviation of 2.006. Therefore using Equation (3-1) the concrete strength is given by

$$f_{cu} = 28.621 - 1.64 \times 2.006$$

$$= 25.33 \text{ MPa}$$

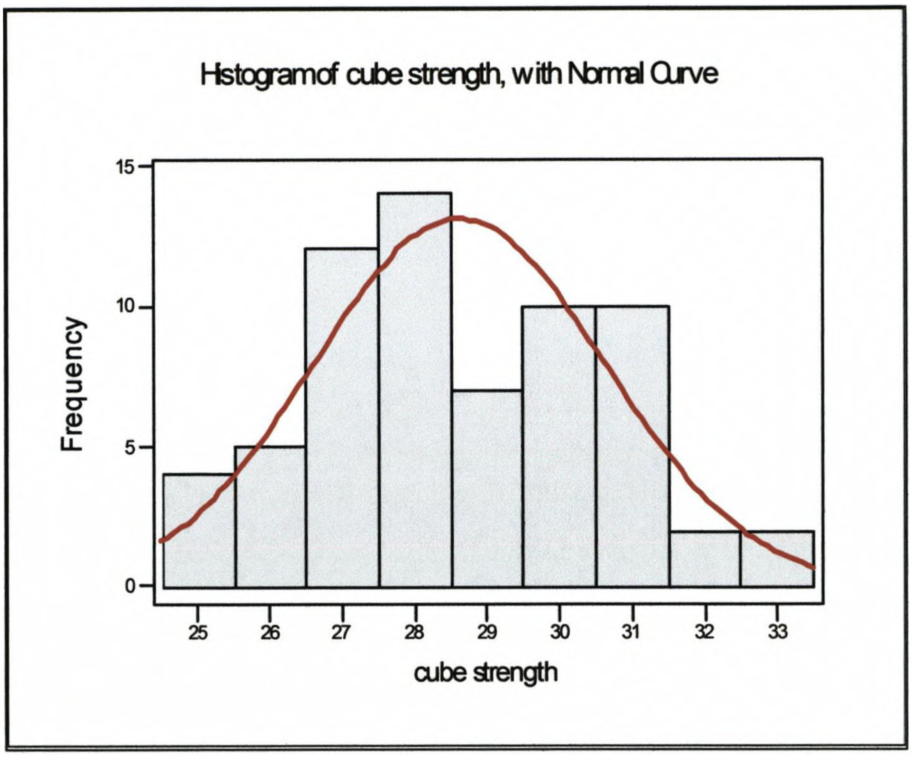

Figure 6.1 Test cube result for mix design of 25 MPa

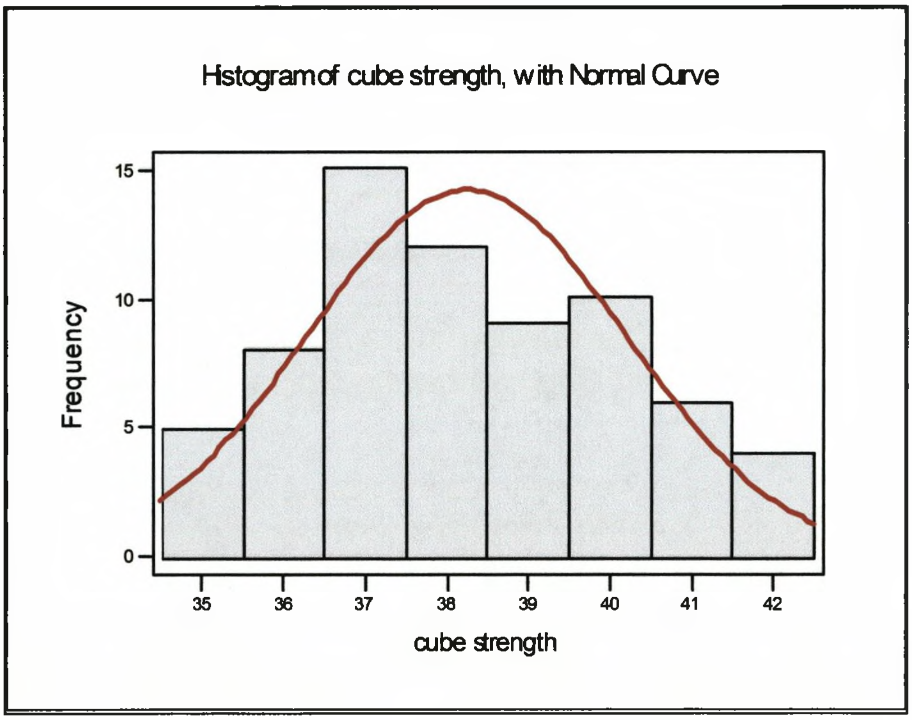

Figure 6.2 Test cube result for mix design of 35 MPa

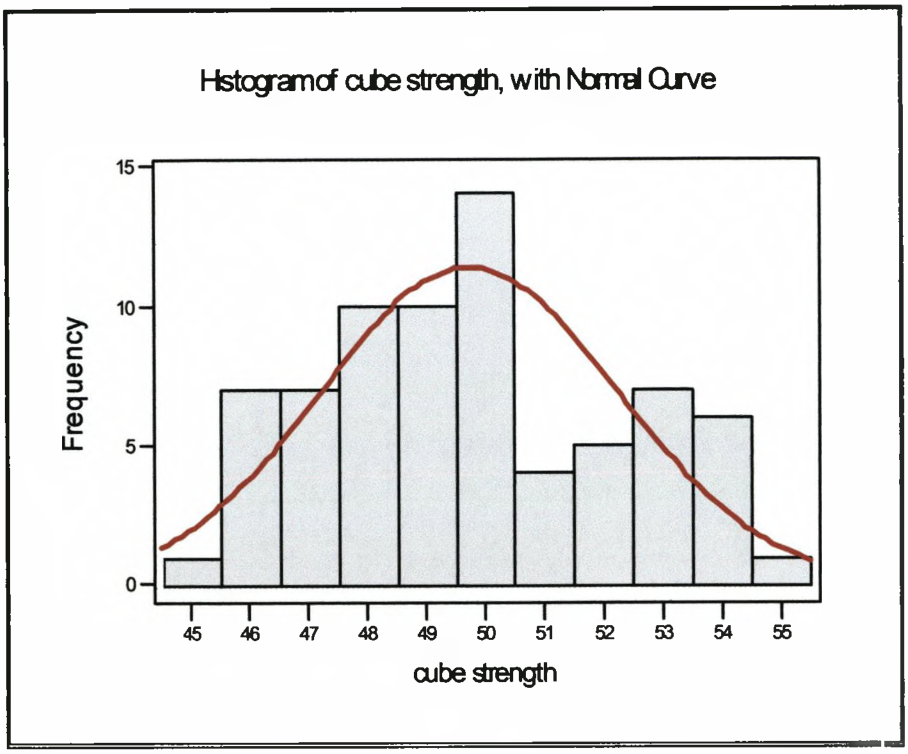

Figure 6.3 Test cube result for mix design of 45 MPa

Similarly, for mix designs of 35 and 45 MPa it was found that the mean strengths were 38.246 and 49.722 with standard deviations of 1.936 and 2.524 which give f_{cu} value of 35.07 and 45.58 respectively.

From the test results, it can be seen that few test cubes have the minimum values of 25, 35 and 45 MPa as shown in Figure 6.1, 6.2 and 6.3 respectively. However, in terms of average cube strength for each concrete beam specimen, the minimum values were above those values as shown in Table 6.1 column 3.

Table 6.1 Concrete strength test result for each beam specimen

Designation	Average f_c' * (MPa)	Average f_{cu} (MPa)	ratio
(1)	(2)	(3)	(4)=(2)/(3)
B1H25	21	30	0.70
B2H25	20	26	0.77
B3H25	-	26	-
B4H25	21	26	0.81
B1L25	-	29	-
B2L25	22	29	0.76
B3L25	-	28	-
B4L25	22	31	0.71
B1N25	24	31	0.77
B2N25	21	28	0.75
B3N25	-	31	-
B4N25	21	28	0.75
B1N35	-	38	-
B4N35	-	37	-
B1H35	30	39	0.77
B2H35	-	37	-
B3H35	30	39	0.77
B4H35	-	39	-
B1L35	28	36	0.78
B2L35	29	38	0.76
B3L35	28	39	0.72
B2N35	28	38	0.74
B3N35	31	41	0.76
B4L35	28	38	0.74
B1H45	39	50	0.78
B2H45	36	48	0.75
B3H45	37	49	0.76
B4H45	36	48	0.75
B1L45	39	48	0.81
B2L45	41	49	0.84
B3L45	38	50	0.76
B4L45	40	52	0.77
B1N45	42	53	0.79
B2N45	39	50	0.78
B3N45	41	52	0.79
B4N45	41	47	0.87

* Cylinder strength is obtained from the specimen that initially used for testing modulus of elasticity

6.1.2 Reinforcement

Random samples have been tested to check the strength of the steel used as the main reinforcement in the concrete beam specimens. Results show that the reinforcement strength varies between 499 and 530 MPa. Therefore the reinforcement can be classified as high yield steel (HYS).

With reference to British Standard [29] two values of steel strength are commonly used in design practice. They are hot rolled mild steel (HRS) and high yield steel (HYS) with characteristic strengths of 250 MPa and 460 MPa respectively. The yield strength of the reinforcement has indirect effect on the calculation of deflections. The modulus of elasticity and the bar diameter, however, contribute directly to the value of the beam deflection. Therefore it was considered sufficient to use a value of 460 MPa in the calculation of the resistance strength of beam specimens.

Table 6.2 Reinforcement test results

Sample #	Length (mm)	Weight (g)	A_s * (mm^2)	D ** (mm)	Es (GPa)	0.2% proof stress (MPa)
(1)	(2)	(3)	(4)	(5)	(6)	(7)
1	175	152	110.6	11.87	203	561
2	328	327	110.2	11.85	195	532
3	358	317	112.8	11.98	201	560
4	366	323	112.4	11.96	192	499
5	398	356	113.9	12.04	196	570
6	405	361	113.5	12.02	199	572
7	413	369	113.8	12.04	196	570
8	380	329	110.3	11.85	192	533
9	405	362	113.9	12.04	196	572
10	390	343	112.0	11.94	192	512
Average				11.96	196	548

* A_s is produced automatically from 'DENISON' software and similar to Equation (3-9)
** D is calculated using Equation (3-10)

Table 6.2 shows the test reinforcement results that include the predicted diameter of the reinforcement, since this sample consisted of deformed bars. From the table it can be seen that the average bar diameter of 11.96 mm. Thus, it is reasonable to use a bar diameter of 12 mm in the calculation.

6.1.3 Modulus of elasticity

6.1.3.1 Steel

The steel modulus of elasticity test results are presented in column 6 of Table 6.2. An average value of 196000 MPa was obtained. This value is about 0.98 of the value normally used in the theory which is 200000 MPa.

6.1.3.2 Concrete

Test results for the concrete modulus of elasticity, E_c, are summarised in Table 6.3, 6.4 and 6.5. For 25 MPa concrete its value varies between 26000 and 28000 MPa which gives an average value of 27000 MPa as shown in Table 6.3. It can be seen in Table 6.4 that for 35 MPa concrete the value varies between 27000 and 29000 MPa, which gives an average value of 28000. For 45 MPa the value varies between 29000 and 33000 MPa, which gives average value of 30500 MPa as shown in Table 6.5. These average values are close to the values calculated using Equation (3.5). The ratios between the experimental average values and the calculated values being 1.07, 1.04 and 1.05 for 25, 35 and 45 MPa respectively.

Table 6.3 Modulus of elasticity test results for 25 MPa concrete strength

Beam	σ_a (MPa)	σ_b (MPa)	ε_a	ε_b	E_c (MPa)	Average E_c (MPa)	Rounded E_c (MPa)	E_c (MPa) Eq.(3-5)	Ratio (8)/(9)
(1)	(2)	(3)	(4)	(5)	(6)	(7)	(8)	(9)	(10)
B1H25	6.822	0.843	0.00024	0.00001	26573	27150.30	27000		1.08
	6.921	0.821	0.00022	0.00000	27727				
B2H25	6.685	0.857	0.00021	0.00000	27752	27739.83	28000		1.12
	6.921	0.821	0.00022	0.00000	27727				
B4H25	6.833	0.283	0.00024	0.00000	27292	26629.92	27000		1.08
	6.683	0.97	0.00024	0.00002	25968				
B2L25	6.788	0.785	0.00023	0.00000	26100	26452.27	26000		1.04
	6.791	0.894	0.00022	0.00000	26805				
B3L25	6.654	1.091	0.00023	0.00002	26490	26883.33	27000	25000	1.08
	6.964	1.236	0.00023	0.00002	27276				
B4L25	6.788	0.785	0.00023	0.00000	26100	25778.26	26000		1.04
	6.687	0.832	0.00023	0.00000	25457				
B1N25	6.788	0.801	0.00022	0.00000	27214	26477.65	26000		1.04
	6.858	0.68	0.00024	0.00000	25742				
B2N25	6.757	0.551	0.00024	0.00000	25858	26562.5	27000		1.08
	6.719	0.993	0.00023	0.00002	27267				
B4N25	6.687	1.091	0.00023	0.00003	27980	26670.43	27000		1.08
	6.649	0.816	0.00023	0.00000	25361				
Average						26704.94	27000	25000	1.07

Table 6.4 Modulus of elasticity test results for 35 MPa concrete strength

Beam	σ_a (MPa)	σ_b (MPa)	ε_a	ε_b	E_c (MPa)	Average E_c (MPa)	Rounded E_c (MPa)	E_c (MPa) Eq.(3-5)	Ratio (8)/(9)
(1)	(2)	(3)	(4)	(5)	(6)	(7)	(8)	(9)	(10)
B1H35	9.301	1.055	0.00033	0.00004	28832	28832.00	29000		1.07
B3H35	11.273	0.903	0.00038	0.00001	28027	27985.14	28000		1.04
	11.307	0.968	0.00038	0.00001	27943				
B1L35	9.44	0.803	0.0003	0.00000	28790	28070.81	28000		1.04
	9.407	0.928	0.00032	0.00001	27352				
B2L35	9.398	0.752	0.00034	0.00002	27019	27349.38	27000		1.00
	9.364	1.06	0.00032	0.00002	27680				
B3L35	9.337	1.057	0.00032	0.00003	28552	28585.86	29000		1.07
	9.494	0.908	0.00032	0.00002	28620			27000	
B4L35	9.44	0.562	0.00033	0.00002	28639	28006.85	28000		1.04
	9.4	0.64	0.00035	0.00003	27375				
B1N35	9.373	1.028	0.00030	0.00002	29804	29076.79	29000		1.07
	9.335	0.83	0.00031	0.00001	28350				
B2N35	9.335	0.948	0.00031	0.00000	27055	27180.65	27000		1.00
	9.337	0.872	0.00031	0.00000	27306				
B3N35	9.438	0.555	0.00034	0.00002	27759	27787.5	28000		1.04
	9.546	0.645	0.00035	0.00003	27816				
Average						28097.22	28000	27000	1.04

Table 6.5 Modulus of elasticity test results for 45 MPa concrete strength

Beam	σ_a (MPa)	σ_b (MPa)	ε_a	ε_b	E_c (MPa)	Average E_c (MPa)	Rounded E_c (MPa)	E_c (MPa) Eq.(3-5)	Ratio (8)/(9)
(1)	(2)	(3)	(4)	(5)	(6)	(7)	(8)	(9)	(10)
B1H45	12.085	0.658	0.00037	0.00000	30884	31867.61	32000	29000	1.10
	12.149	0.651	0.00035	0.00000	32851				
B2H45	12.051	0.799	0.00037	0.00000	30411	30639.19	31000		1.07
	12.063	0.642	0.00038	0.00001	30868				
B3H45	12.047	0.718	0.00036	0.00000	31469	31316.67	31000		1.07
	12.031	0.812	0.00036	0.00000	31164				
B4H45	12.011	1.017	0.00036	0.00002	32335	32852.5	33000		1.14
	12.045	1.033	0.00035	0.00002	33370				
B1L45	12.923	0.888	0.00039	0.00001	31671	31410.53	31000		1.07
	12.457	0.620	0.00040	0.00002	31150				
B2L45	12.491	0.801	0.00040	0.00001	29974	29898.94	30000		1.03
	12.486	0.825	0.00040	0.00001	29824				
B3L45	12.997	0.968	0.00040	0.00001	30844	30764.29	31000		1.07
	13.037	0.763	0.00040	0.00000	30685				
B4L45	12.136	0.821	0.00039	0.00000	29013	29024.5	29000		1.00
	12.036	0.799	0.00040	0.00001	29036				
B1N45	11.924	0.908	0.00039	0.00001	28989	29310.93	29000		1.00
	12.455	0.928	0.00040	0.00001	29632				
B2N45	12.016	0.890	0.00038	0.00000	29279	29848.93	30000		1.03
	12.054	0.799	0.00037	0.00000	30419				
B3N45	12.074	0.670	0.00041	0.00002	29241	29775.92	30000		1.03
	12.016	0.801	0.00037	0.00000	30311				
B4N45	12.054	0.957	0.00039	0.00001	29203	29286.45	29000		1.00
	12.016	1.149	0.00039	0.00002	29370				
Average						30499.705	30500	29000	1.05

6.1.4 Discussion

Both modulus of elasticity discussed above have significant effect on the calculation of deflection. Modulus of elasticity ratio between steel and concrete, called modular ratio and denoted by 'n', plays an important role in the calculation of cracked second moment of area, as a result it influences the value of effective second moment of area.

The ratio value obtained for concrete modulus of elasticity as mentioned in Section 6.1.3.2 shows that Equation (3.5) given in the British Standard [29] is valid.

The elastic modulus of steel is slightly lower than the nominal value used in the design as discussed in Section 6.1.3.1. When the experimental value is used the modular ratio becomes smaller thus cracked second moment of area is lower than the theoretical one. This agrees with the result as shown in Figure 6.18 in Section 6.7.1.

6.2 Deflection test results

6.2.1 Introduction

A typical load deflection curve, for all the beams tested, is shown in Figure 6-4. Displacement transducers were placed at the mid span location of each beam and also at both third span locations. Transducer No. 3 was placed at mid span with transducer No. 1 and No.2 placed at third span locations.

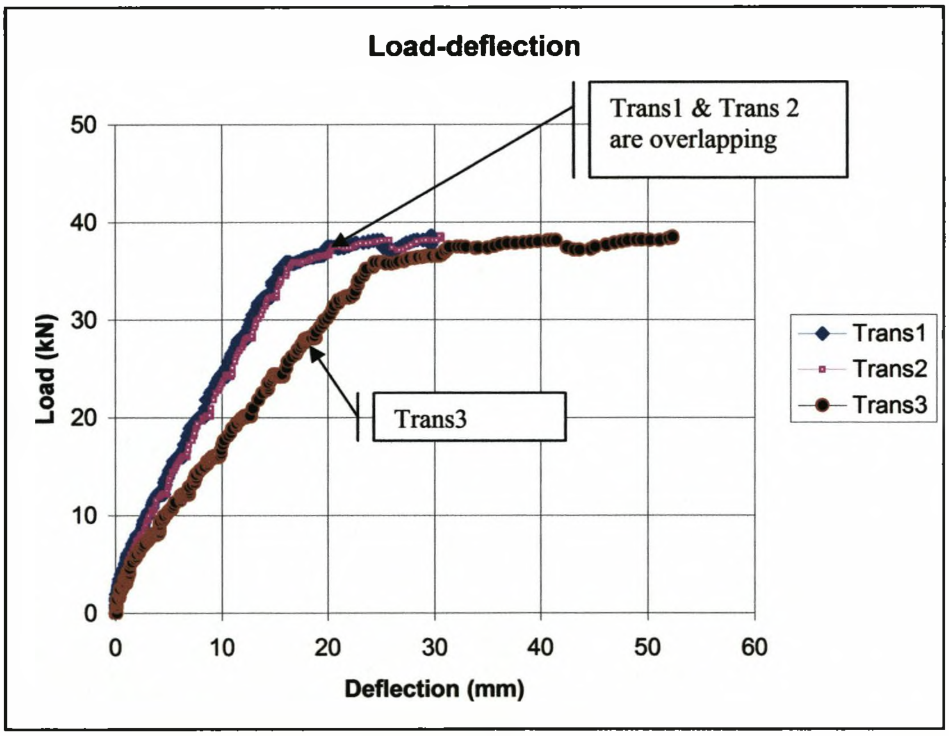

Figure 6.4 Typical deflection reading of three transducers captured by PicoLog software

From Figure 6.4 it can be seen for this particular beam, as well as the other symmetrically loaded beams, symmetrical deformation of the beam was achieved. In verifying the model developed only the mid span deflection is required.

6.2.2 Beams behaviour

Nine combinations, one combination consisting of four different load positions, of reinforced concrete beams as discussed in Chapter 3 are analysed. Only one of the combinations showed clearly different trend and presented along with other combinations with similar concrete strength of 25 MPa as shown in Figure 6.5.

Figure 6.5a shows the behaviour of four beams during testing. Beam B1H25 did not fail since the maximum load cell available was insufficient to cause failure. Three other beams (B2, B3 and B4), however, were loaded until failure occurred.

A general conclusion can therefore be deduced from these three beams that all beams of the same combination may have similar trends. At a certain load, called cracking load, cracking will start in beam. As the loading is increased the cracking spreads along the beam. This means that the steel reinforcement will be required to resist the tension forces alone. As the load was increased the beams suddenly failed. The behaviour of these beams shows that forces in the concrete compression zone have reached their limiting values while the steel reinforcements have not yet reached its yield stresses.

As explained previously in Chapter 3 beams that behave in this way are called over-reinforced concrete beams. These beams are normally avoided in the design since as they are not only uneconomical but also as steel yielding does not take place a sudden brittle collapse will occur.

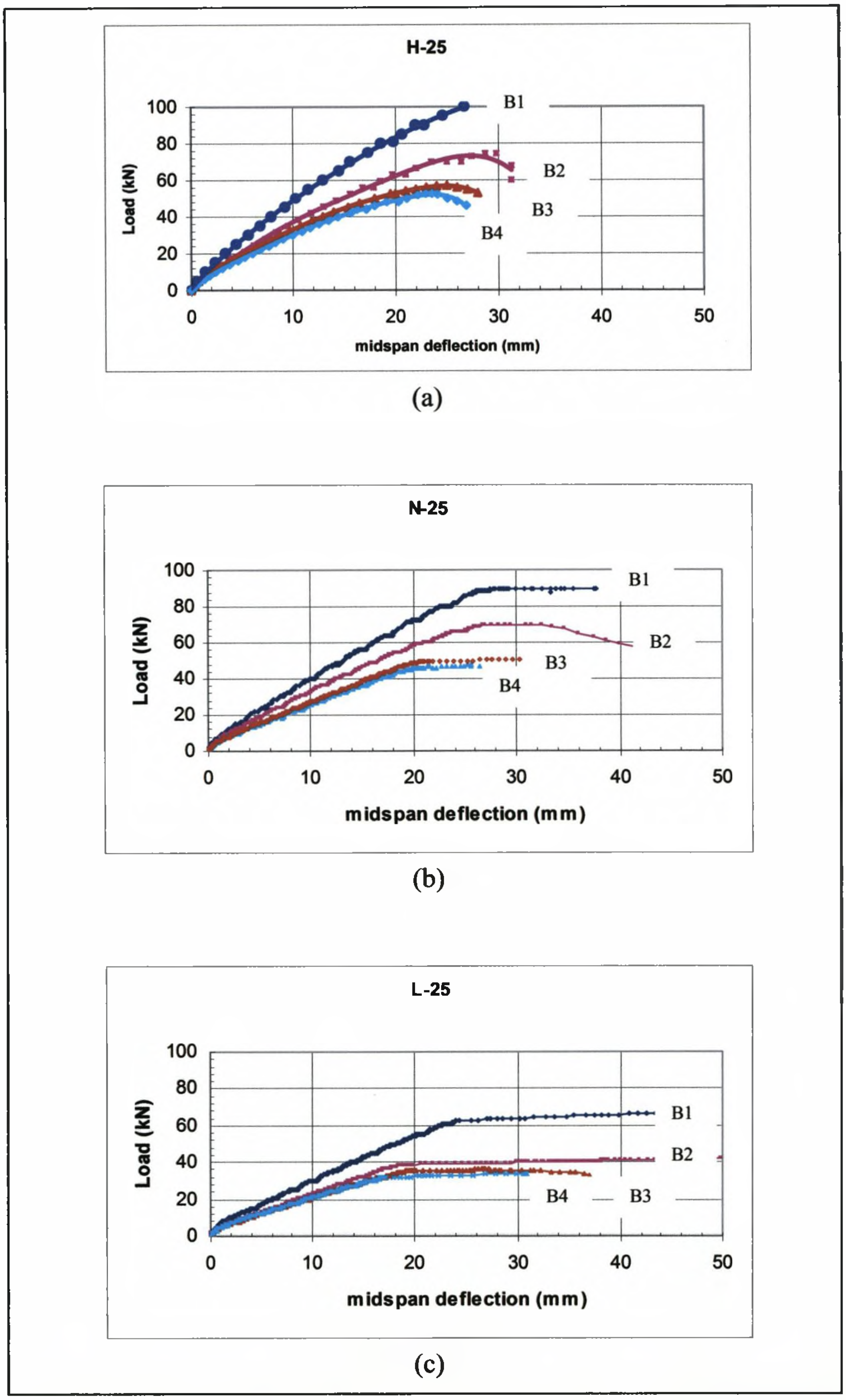

Figure 6.5 Beams deflection behaviour for various load position for 25 MPa concrete strength with: (a) Heavy reinforcement, (b) Normal reinforcement, (c) Low reinforcement

Figure 6.5b shows load deflection curves for beams with similar concrete strength but different reinforcement ratios (N25). Beam behaviour with low reinforcement ratio (L25) and similar concrete strength are shown in Figure 6-5c.

At an early stage, before cracking, the deflection is virtually in direct proportion to the applied load and the behaviour of the beam is primarily determined by its cross section and the characteristic strength of the concrete. The reinforcement has little effect as it is lightly stressed.

Once cracking has occurred in the tension zone the ability of the concrete to make any significant contribution to resist the tensile force has ceased. The tensile force is thus transferred completely to the main longitudinal reinforcement, causing a considerable increase in the steel strain. As the load is increased further the strain in the reinforcement and the deflection of the beam still increases in more or less direct proportion to the load, but at a faster rate than in the uncracked state. This stage is called the service condition of the beam.

The third and final stage of the beam's reaction to load is initiated when the strain in the longitudinal tensile reinforcement in the region of maximum bending moment reaches the value corresponding to yielding of the steel reinforcement. This can be seen from the beam's behaviour in Figure 6.5b and 6.5c where the curves begin to deviate somewhat from their earlier linear pattern. Once this happens, the increase in the applied load can no longer be balanced by the increase of the force in the steel. The concrete compressive zone can resist considerable deformation during this last stage and the central part of the beam becomes in effect a plastic hinge where the beams have excessive deflection with very little increase to the applied load. This form of behaviour has the advantage in that it can be seen and acts as a warning of impending failure. The beam is called an under-reinforced beam and is strongly recommended in design. The beams behaviour similar to those discussed above are presented in Figure A-1 and A-2 in Appendix A for 35 and 45 MPa concrete strength respectively.

In terms of behaviour of concrete beams with combination between heavy reinforcement (1.64%) and low concrete strength (25 MPa) which gives over-reinforced behaviour as discussed above and this behaviour similar to design concrete member as discussed in Chapter 3. This, therefore, can be used as further check for mix design of concrete strength. Thus, this beam behaviour indicates that design strength of 25 MPa in this study is reasonable due to reinforcement ratio can be measured accurately.

6.3 Cracking load, $P_{cr(exp)}$

6.3.1 Analysis and results

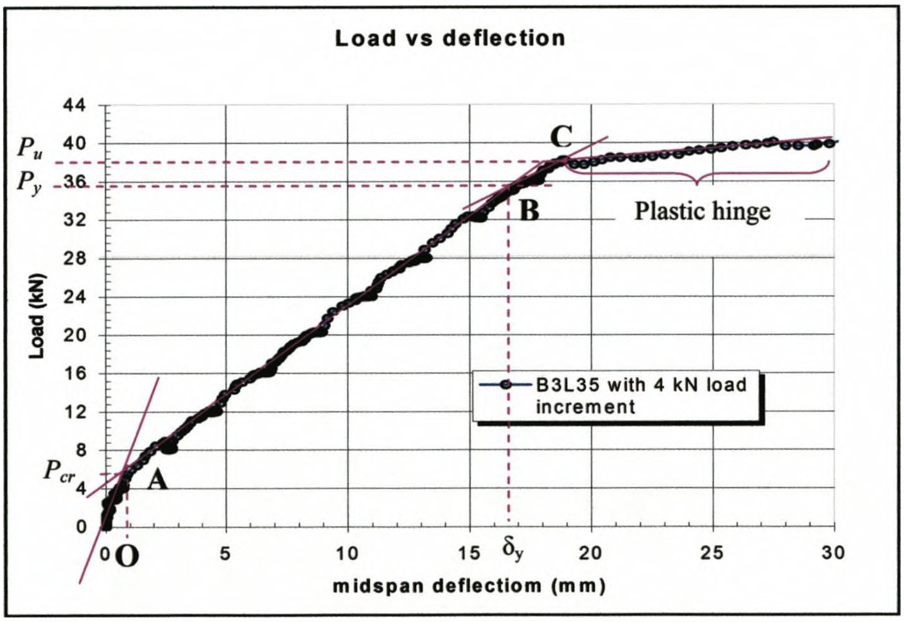

Figure 6.6 First cracked, yield and ultimate load

The crack load is defined as the load that produces the first crack(s) in the section. This can be seen as a point on the load-deflection curve at which the form of the curve becomes nonlinear [35]. Knowing the value of $P_{cr(exp)}$, by using simple bending theory, the value of $M_{cr(exp)}$ can be obtained.

When a crack is formed in a concrete beam the second moment of area is reduced. The effect of this can be seen on the load-deflection curve for beam B3L25 in Figure 6.6. At point A on the curve there is a change in the shape of the curve, so that the value of load at point A on the curve is $P_{cr(exp)}$. As the load is increased a further change in shape occurs at point B. At this load, $P_{y(exp)}$, the steel reinforcement is yielding. The slope at the curve then changes gradually until point C is reached. At this load, $P_{u(exp)}$, a plastic hinge is formed in the concrete beam and very little further increment in load can be achieved.

In order to evaluate $P_{cr(exp)}$, a procedure was adopted where the load-deflection curve was simplified to three linear portions OA, AB and BC where the two lines OA and AB intersected the load value was taken as $P_{cr(exp)}$. From Figure 6.6 it can be seen for this particular beam that the value of $P_{cr(exp)}$ is 6 kN.

During the testing of the beam the crack formation and propagation was noted by the use of a marker pen, as can be seen in Figure 6.7.

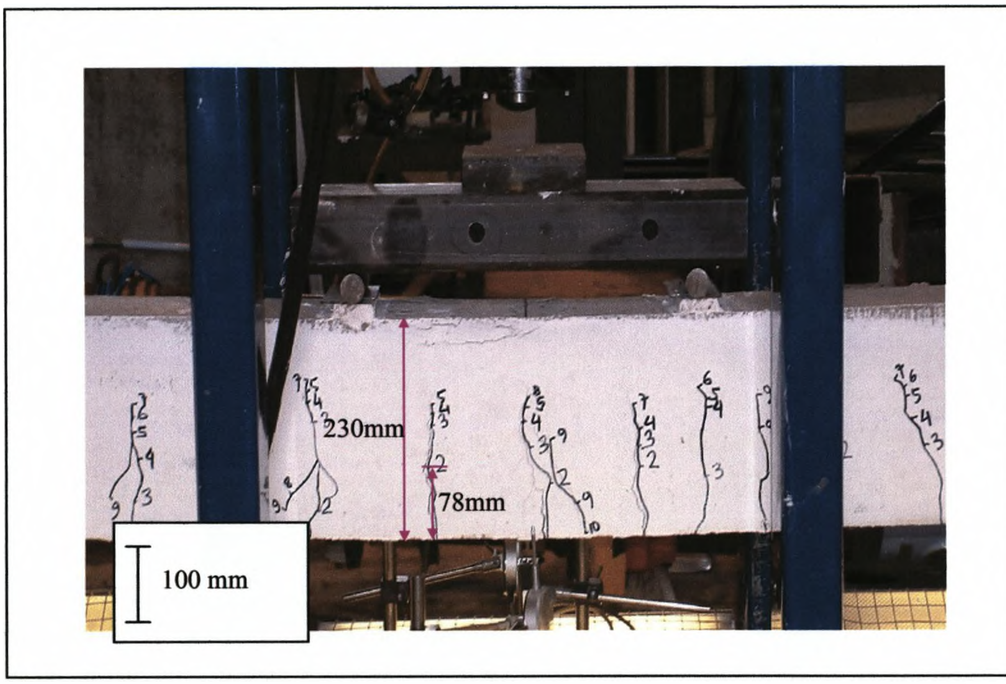

Figure 6.7 Crack propagation on the tested beam

Load was applied to the beam in increments of 4 kN. At a load of 4 kN no cracks were visible on the surface of the beam. When the load was increment to 8 kN (increment 2) several cracks appeared on the surface of the beam. The total propagation of the cracks were denoted by 2 on the beam surface. From Figure 6.7 it can be seen that the crack propagation value up to a maximum of 78 mm.

The results of the POF analysis give good agreement with the procedure adopted in this study to evaluate $P_{cr(exp)}$. The results are shown in Figure 6.8, 6.9 and 6.10 for B4L35, B4H35 and B4H45 respectively. It can be seen from the figures that the POF signal intensity is almost constant before cracking occurs on the concrete beam. The signal, however, start to decrease once the concrete beam crack(s). This is corresponding with the change of slope of load-deflection curve.

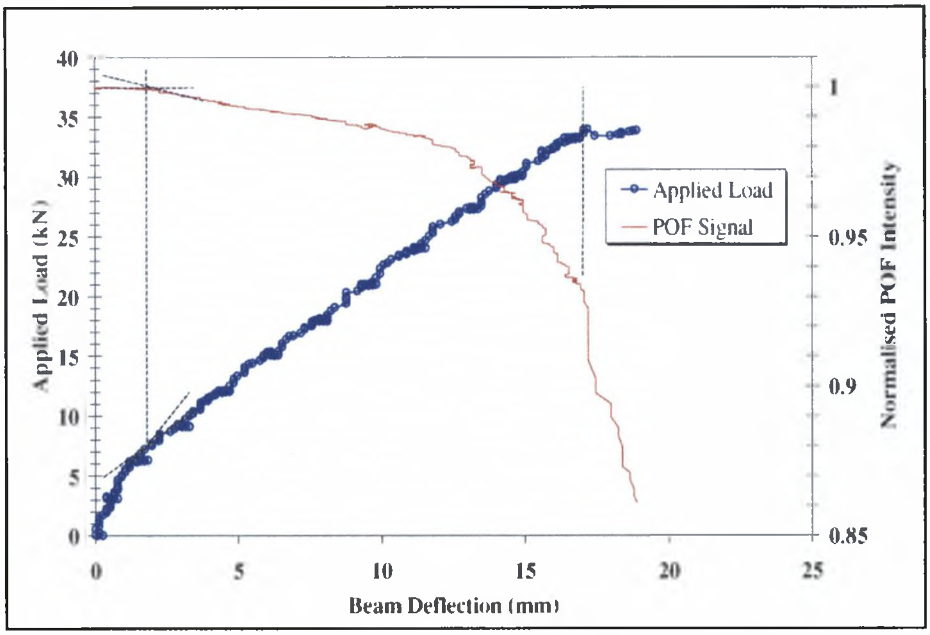

Figure 6.8 Load-deflection curve and the sensor response of POF during flexural tests on beam 1 (B4L35)

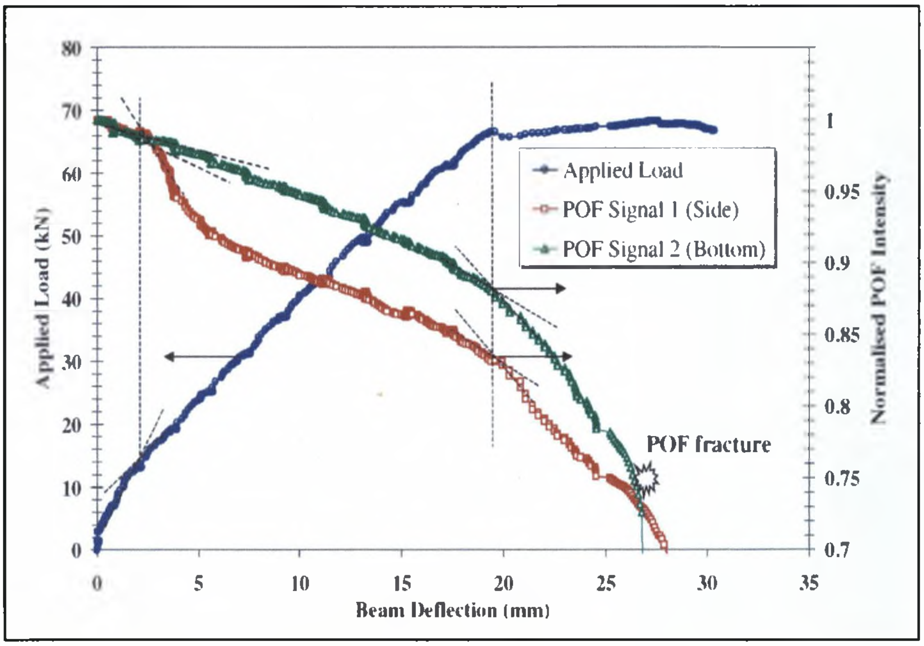

Figure 6.9 Load-deflection curve and the sensor response of POF during flexural tests on beam 2 (B4H35)

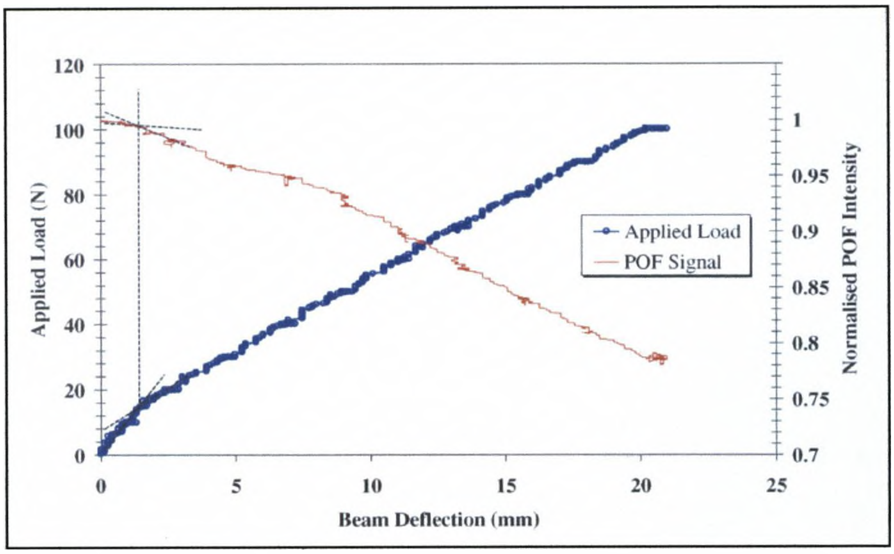

Figure 6.10 Load-deflection curve and the sensor response of POF during flexural tests on beam 3 (B4H45)

Details of the experimental results from these tests are given in Table 6.6. The table summarizes the sensor accuracy in detecting initial crack propagation in these specimens. In addition, the predicted values of load and beam deflection at which cracking initiates, $P_{cr(th)}$ and $\delta_{cr(th)}$ respectively, have been determined using Equation (6.3). It is clear from the table that the sensors offers a high level of detectability and reliability (less than 1 mm error in beam deflection in all specimen) and shows good agreement with the corresponding computed values.

Table 6.6 A summary of the initial crack as detected from the load-displacement curve and the POF signal

Beam	Experimental values				Theoretical values	
	$P_{cr(exp)}$ (kN)	$\delta_{cr(exp)}$ (mm)	$\delta_{cr(pof)}$ (mm)	error (mm)	$P_{cr(th)}$ (kN)	$\delta_{cr(th)}$ (mm)
1 (B4L35)	6	0.9	1.7	0.8	6.37	0.61
2 (B4H35)	10	1.2	2.2	1	7.23	1.38
3 (B1H45)	18	1.6	1.3	0.3	14.19	1.44

Table 6.7 Cracking load, P_{cr} and Cracking Moment, M_{cr}

No.	Beam	$P_{cr(exp)}$ (kN)	$M_{cr(exp)}$ (kNm) Eq. (6-1)	$M_{cr(th)}$ (kNm) Eq. (6-3)	$\frac{M_{cr(\exp)}}{M_{cr(th)}}$	Average for different ρ
(1)	(2)	(3)	(4)	(5)	(6)	(7)
1	B1L25	9.00	3.15	3.70	0.851	0.735
2	B1L35	9.00	3.15	4.38	0.719	
3	B1L45	9.00	3.15	4.97	0.634	
4	B1N25	10.00	3.50	3.70	0.945	1.051
5	B1N35	10.00	3.50	4.38	0.799	
6	B1N45	20.00	7.00	4.97	1.409	
7	B1H25	16.00	5.60	3.70	1.512	1.379
8	B1H35	17.00	5.95	4.38	1.358	
9	B1H45	18.00	6.30	4.97	1.268	
10	B2L25	8.00	3.68	3.70	0.994	0.99
11	B2L35	10.00	4.60	4.38	1.050	
12	B2L45	10.00	4.60	4.97	0.926	
13	B2N25	11.00	5.06	3.70	1.366	1.240
14	B2N35	11.00	5.06	4.38	1.155	
15	B2N45	13.00	5.98	4.97	1.204	
16	B2H25	12.00	5.52	3.70	1.491	1.349
17	B2H35	12.00	5.52	4.38	1.260	
18	B2H45	14.00	6.44	4.97	1.296	
19	B3L25	6.00	3.45	3.70	0.932	0.804
20	B3L35	6.00	3.45	4.38	0.787	
21	B3L45	6.00	3.45	4.97	0.694	
22	B3N25	8.00	4.60	3.70	1.242	1.111
23	B3N35	8.00	4.60	4.38	1.050	
24	B3N45	9.00	5.18	4.97	1.042	
25	B3H25	9.00	5.18	3.70	1.398	1.358
26	B3H35	10.00	5.75	4.38	1.312	
27	B3H45	11.80	6.79	4.97	1.366	
28	B4L25	6.00	4.13	3.70	1.114	0.962
29	B4L35	6.00	4.13	4.38	0.941	
30	B4L45	6.00	4.13	4.97	0.830	
31	B4N25	6.00	4.13	3.70	1.114	1.159
32	B4N35	8.00	5.50	4.38	1.255	
33	B4N45	8.00	5.50	4.97	1.107	
34	B4H25	6.00	4.13	3.70	1.114	1.448
35	B4H35	10.00	6.88	4.38	1.569	
36	B4H45	12.00	8.25	4.97	1.661	

In the model developed a theoretical value of M_{cr} was developed. This can now be compared with the experimental value given by

$$M_{cr(\exp)} = \frac{P_{cr(\exp)}}{2} a \tag{6.1}$$

The value of $M_{cr(th)}$ and $M_{cr(exp)}$ are shown in Table 6.7 for all the beams tested in this study.

Average values, for different ρ values, have been calculated for the ratio ($M_{cr(exp)}$/ $M_{cr(th)}$). These values show that variation occurs with different reinforcement ratios. This variation can be approximated to

$$M_{cr} = f(\rho)\ M_{cr(th)} \tag{6.2}$$

6.3.2 Discussion of the results

The cracking moment, M_{cr}, was evaluated using the beams tested in flexure. This method was considered to be more logical than to carry out indirect tensile tests. Comparison between the theoretical cracking moment and the experimental cracking moment, obtained using Equation (6.1), can be seen in Figure 6.11. When the average value of $M_{cr(th)}/M_{cr(exp)}$ for each concrete cube strength is taken and plotted against f_{cu} in Figure 6.11, the results show that the values are close to the line $M_{cr(th)}/M_{cr(exp)}$ = 1. Desayi [36] also reported that the coefficient of variation of cracking moment was 30%. These results are sufficient reason why the theoretical M_{cr} can be used through out this study.

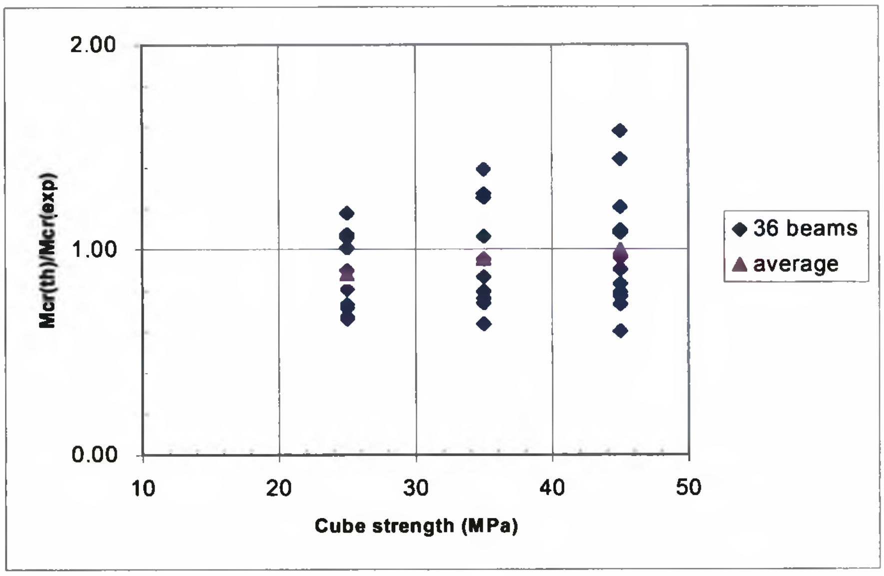

Figure 6.11 Comparison between theoretical and experimental M_{cr} against f_{cu}

The theoretical cracking moment is obtained from equation

$$M_{cr} = \frac{f_r}{y_t} I_g \tag{6.3}$$

Replacing M_{cr} with $M_{cr(exp)}$ taken from Equation (6.1), the experimental modulus of rupture can be obtained from relationship

$$f_{r(\exp)} = \frac{M_{cr(\exp)}}{I_g} y_t \tag{6.4}$$

From the equation above it can be said that I_g and y_t are only slightly affected by the presence of reinforcement in concrete section as shown on Table 6.6. Thus f_r is assumed only affected by concrete strength. However the effect of reinforcement ratio on the cracking moment is not taken into account separately, instead it will be considered later in analysing the factor Φ as M_{cr} is part of the factor Φ in the complete equation.

The modulus of rupture, f_r, were taken from ACI formula then converted into SI unit in terms of cube concrete strength as given in the Equation (3-8). This equation is used to calculate cracking moment in Equation (6.3).

To check whether the equation can be accepted in this study, $f_{r(exp)}$ derived from Equation (6.4) and plotted against concrete strength. Since the instant at which cracking occurs is not easy to determine in a test, a large scatter in the results is to be expected. This is shown in Figure 6.12.

The results show that average value of f_r for each concrete strength is very close the curve representing $0.56\sqrt{f_{cu}}$. This was also found to be the case by other researchers [15, 24] using a greater number of samples. Therefore the theoretical value of f_r will be used in this study.

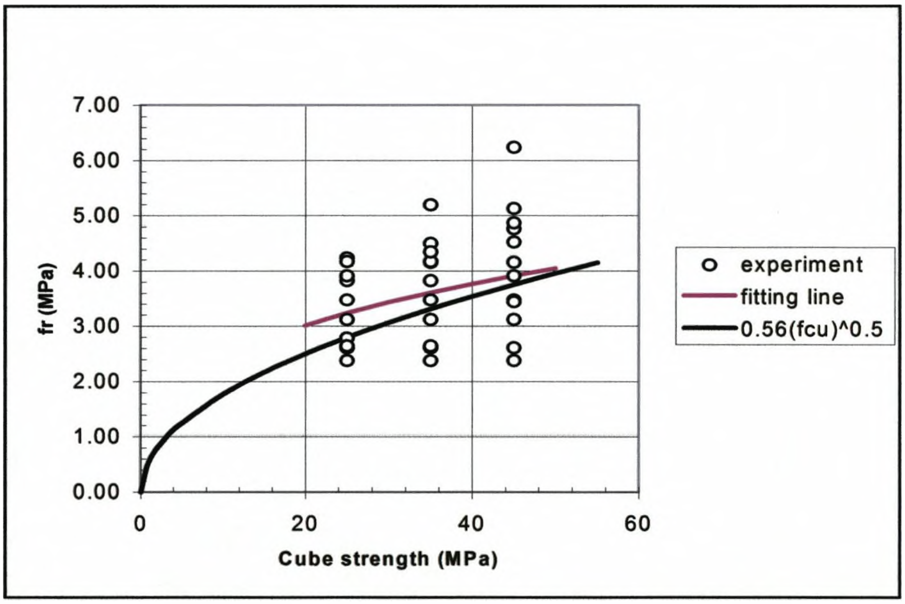

Figure 6.12 Modulus of rupture against cube strength

6.4 Load conditions

The analysis of the ultimate moment of resistance has been done using characteristic value of fcu in Chapter 3. However, the actual material properties have been obtained based on experiment and was given in Table 6.1 and 6.2 for concrete and steel stress respectively. In this section, the ultimate moment of resistance will be reanalysed based on the actual material properties using the same method as that used in Chapter 3. The results of this analysis are given in Table 6.8.

6.4.1 Yield load, $P_{y(exp)}$ and Ultimate Load, $P_{u(exp)}$

Using the same technique as described in the previous section at point B and C on the load-deflection curve, Figure 6.6, the values of $P_{y(exp)}$ and $P_{u(exp)}$ were obtained. The experimental and the theoretical values of both P_y and $P_{u(th)}$ are shown in Table 6.8. The ratio of $(P_{u(th)}/P_{u(exp)})$ is also shown in column 6. This ratio varies between 0.74 and 0.94, indicating that the theoretical model will always provide a safe value P_u.

6.4.2 Service load, $P_{s(exp)}$

Serviceability is controlled by the permissible crack width and deflection under working load as determined by the codes. If deflection is taken as the criterion in this study, and assuming deflection under service load not to exceed $L/250$ of span as a requirement [25] then the service load value can be determined from load-deflection curve relationship such as Figure 6-6, and the results are presented in column 7, Table

6.9. The ratio of experimental service load and ultimate load, $P_{s(\exp)}/P_{u(\exp)}$, is also tabulated in column 8. This ratio varies between 0.51 and 0.74 with mean ratio of 0.6.

Table 6.8 Ultimate moment and load resistance based on actual concrete strength and steel stress

Beam	b (mm)	h (mm)	d (mm)	a (mm)	A_s (mm^2)	Actual strength		M_u (kNm)	P_u (kN)
						f_{cu} (MPa)	f_y (MPa)		
B1L25	150	230	184	0.70	226.19	29	548	18.13	51.79
B1L35				0.70	226.19	36		18.81	53.75
B1L45				0.70	226.19	48		19.53	55.79
B1N25				0.70	339.29	31		25.05	71.56
B1N35				0.70	339.29	38		26.42	75.48
B1N45				0.70	339.29	53		28.14	80.40
B1H25				0.70	452.39	30		29.64	84.68
B1H35				0.70	452.39	39		32.80	93.71
B1H45				0.70	452.39	50		35.12	100.34
B2L25				0.92	226.19	29		18.13	39.40
B2L35				0.92	226.19	38		18.96	41.23
B2L45				0.92	226.19	49		19.57	42.55
B2N25				0.92	339.29	28		24.25	52.71
B2N35				0.92	339.29	38		26.42	57.43
B2N45				0.92	339.29	50		27.88	60.61
B2H25				0.92	452.39	26		27.53	59.85
B2H35				0.92	452.39	37		32.23	70.07
B2H45				0.92	452.39	48		34.77	75.60
B3L25				1.15	226.19	28		18.00	31.30
B3L35				1.15	226.19	39		19.03	33.10
B3L45				1.15	226.19	50		19.61	34.11
B3N25				1.15	339.29	31		25.05	43.56
B3N35				1.15	339.29	41		26.86	46.72
B3N45				1.15	339.29	52		28.06	48.79
B3H25				1.15	452.39	26		27.53	47.88
B3H35				1.15	452.39	39		32.80	57.04
B3H45				1.15	452.39	49		34.95	60.78
B4L25				1.38	226.19	31		18.35	26.70
B4L35				1.38	226.19	38		18.96	27.58
B4L45				1.38	226.19	52		19.69	28.64
B4N25				1.38	339.29	28		24.25	35.27
B4N35				1.38	339.29	37		26.25	38.19
B4N45				1.38	339.29	47		27.58	40.12
B4H25				1.38	452.39	26		27.53	40.05
B4H35				1.38	452.39	39		32.80	47.71
B4H45				1.38	452.39	48		34.77	50.58

Table 6.9 Service load, Yield and Failure load

No.	Beam	$P_{y(exp)}$ (kN)	$P_{u(th)}$ (kN)	$P_{u(exp)}$ (kN)	$P_{u(th)}/P_{u(exp)}$	$P_{s(exp)}$ (kN)	$P_{s(exp)}/P_{u(exp)}$
(1)	(2)	(3)	(4)	(5)	(6)	(7)	(8)
1	B1L25	60	51.79	64	0.81	34	0.53
2	B1L35	60	53.75	65	0.83	36	0.55
3	B1L45	60	55.79	68	0.82	38	0.56
4	B1N25	86	71.56	86	0.83	44	0.51
5	B1N35	90	75.48	90	0.84	47	0.52
6	B1N45	90	80.40	92	0.87	52	0.57
7	B1H25	*	84.68			54	
8	B1H35	*	93.71			56	
9	B1H45	*	100.34			61	
10	B2L25	40	39.40	42	0.94	25	0.60
11	B2L35	44	41.23	46	0.90	30	0.65
12	B2L45	44	42.55	48	0.89	32	0.67
13	B2N25	70	52.71	70	0.75	36	0.51
14	B2N35	70	57.43	70	0.82	38	0.54
15	B2N45	70	60.61	70	0.87	40	0.57
16	B2H25	-	59.85	76	0.79	41	0.54
17	B2H35	90	70.07	90	0.78	46	0.51
18	B2H45	92	75.60	94	0.80	50	0.53
19	B3L25	37	31.30	37	0.85	22	0.59
20	B3L35	39	33.10	40	0.83	25	0.63
21	B3L45	38	34.11	41	0.83	28	0.68
22	B3N25	44	43.56	49	0.89	29	0.59
23	B3N35	51	46.72	52	0.90	29	0.56
24	B3N45	60	48.79	56	0.87	35	0.63
25	B3H25	-	47.88	56	0.86	36	0.64
26	B3H35	65	57.04	66	0.86	37	0.56
27	B3H45	74	60.78	75	0.81	45	0.60
28	B4L25	33	26.70	33	0.81	22	0.67
29	B4L35	34	27.58	34	0.81	24	0.71
30	B4L45	32	28.64	35	0.82	26	0.74
31	B4N25	46	35.27	44	0.80	30	0.68
32	B4N35	46	38.19	45	0.85	29	0.64
33	B4N45	46	40.12	47	0.85	33	0.70
34	B4H25	-	40.05	54	0.74	32	0.59
35	B4H35	60	47.71	61	0.78	37	0.61
36	B4H45	66	50.58	66	0.77	44	0.67

* Insufficient load cell capacity
\- Over reinforced beam

When the ratio of $P_{u(\exp)}/P_{s(\exp)}$, called serviceability factor, is calculated it can be seen that a value of 1.66 is obtained. This value is slightly larger than the serviceability factor obtained from the global factor of safety explained previously in Section 3.4.2 which was 1.47. This indicates that experimental service loads obtained in this study can be accepted.

6.5 Cracked length of beam

6.5.1 Analysis and results

Previous researchers [12] have used the cracked length of the beam to differentiate between the different types of load. It is used for this purpose in this study. The theoretical derivation of the cracked length of the beam has been explained in Chapter 4.

Basically, the cracked length of the beam is the distance between the extreme cracks at any load.

The cracking pattern was recorded for each beam on a digital camera, a typical photograph is shown in Figure 6.13. Knowing the distance between the supports then by scaling the cracked length of the beam can be measured. Although the picture in Figure 6.13 is taken after completion of testing, cracked length at any load level still can be measured as the crack developments at each load number (load number showing load increment) have been marked.

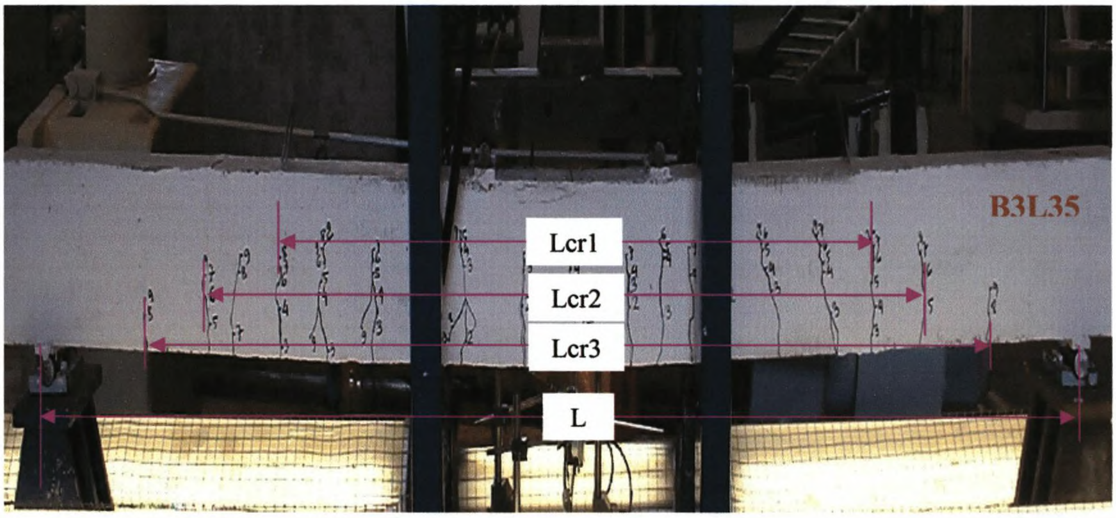

Figure 6.13 Scaling cracked length of the tested beam

There is no guarantee that a load increment to the testing beam will produce a new crack on beam but instead produce an extension to a previous crack. This allows different load numbers (levels) sometimes to produce the same cracked length as shown in the picture. As an example three cracked lengths in each test beam are measured and denoted as Lcr1, Lcr2 and Lcr3 as shown in Figure 6.13. Both load number 3 (12 kN) and load number 4 (16 kN) produce a crack length, Lcr1, of 1.58 m, load number 5 (20 kN), load number 6 (24 kN) and load number 7 (28 kN) produce a cracked length, Lcr2, of 1.90 m. Cracked length, Lcr3, of 2.24 is caused by load number 8 (32 kN) and 9 (36 kN).

However, theoretically different load levels produce different cracked lengths therefore to allow comparison between theoretical and experimental value of the cracked length the average value of theoretical cracked lengths is taken as shown in column 5 of Table 6.10.

Table 6.10 Typical cracked length of beam

Beam	Load #	$L_{cr(exp)}$ (m)	$L_{cr(th)}$ (m)	Average $L_{cr(th)}$ (m)	ratio	mean ratio
(1)	(2)	(3)	(4)	(5)	(6)	(7)
B3L35	3	1.58	1.29	1.47	1.07	1.01
	4		1.65			
	5	1.90	1.87	2.00	0.95	
	6		2.02			
	7		2.12			
	8	2.24	2.20	2.23	1.00	
	9		2.26			

The results for theoretical and experimental cracked lengths for all the beams tested are given in Appendix A-2.

6.5.2 Discussion

Adopting the above approach a comparison can be made between experimental and theoretical cracked lengths and is shown in Figure 6.14. This Figure shows that the majority of experimental cracked lengths are lower than the theoretical values.

When the mean ratio of the experimental to the theoretical cracked length is taken, column 7 in Table 6.10, and plotted against reinforcement ratio, ρ, as shown in Figure 6.15 it can be seen that the cracked length decreases as reinforcement ratio increases.

This variation can be approximated to

$$L_{cr} = f(\rho)\ L_{cr(th)} \tag{6.5}$$

Again this suggests that the equation for Φ needs to be modified since the cracked length, L_{cr}, is function of Φ equation, see Equation (4.12).

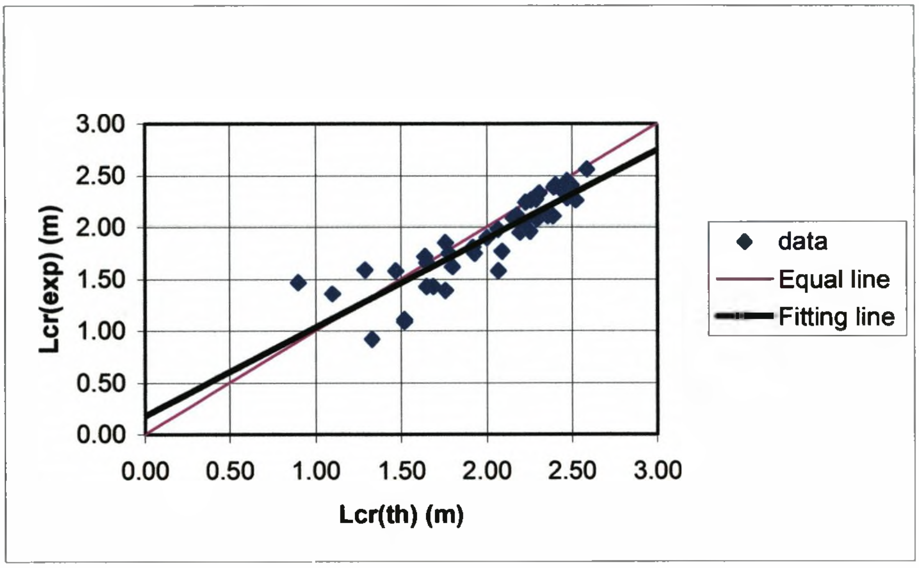

Figure 6.14 Comparison between experimental and theoretical cracked length

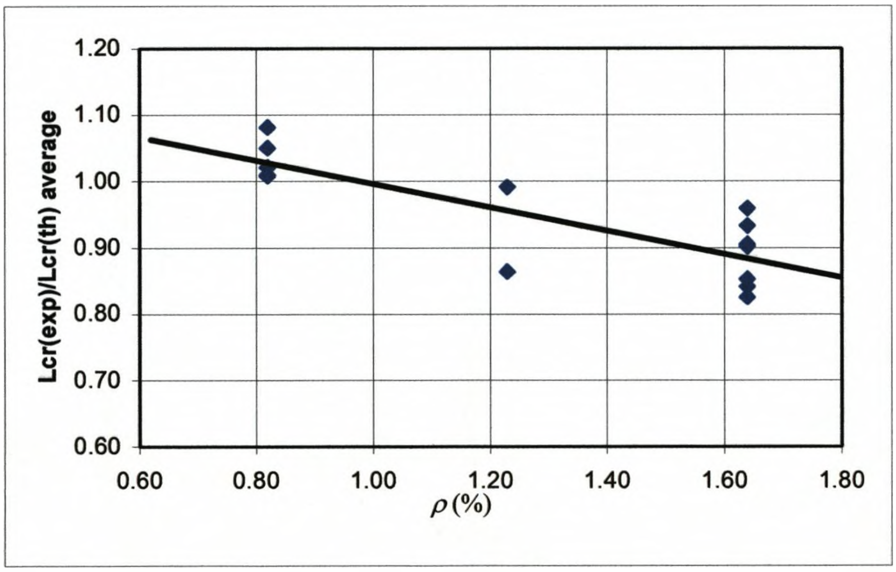

Figure 6.15 Effect of reinforcement ratio on cracked length

6.6 Model verification

The model developed by Fikry [2] was the effective second moment of area (I_e) to calculate the deflection of a beam. The deflection, at mid span, for each beam and load case is calculated using the following equation

$$\Delta = \frac{Pa\left(3L^2 - 4a^2\right)}{48E_cI_e} \tag{6.6}$$

where the terms in the equation are defined in Chapter 3.

For a typical beam the difference between the experimental deflection and the theoretical deflection, calculated using Equation (6.6), can be seen in Figure 6.16. In all cases it was found that the theoretical model underestimated the actual experimental model. This is a condition that must be avoided for safety reasons.

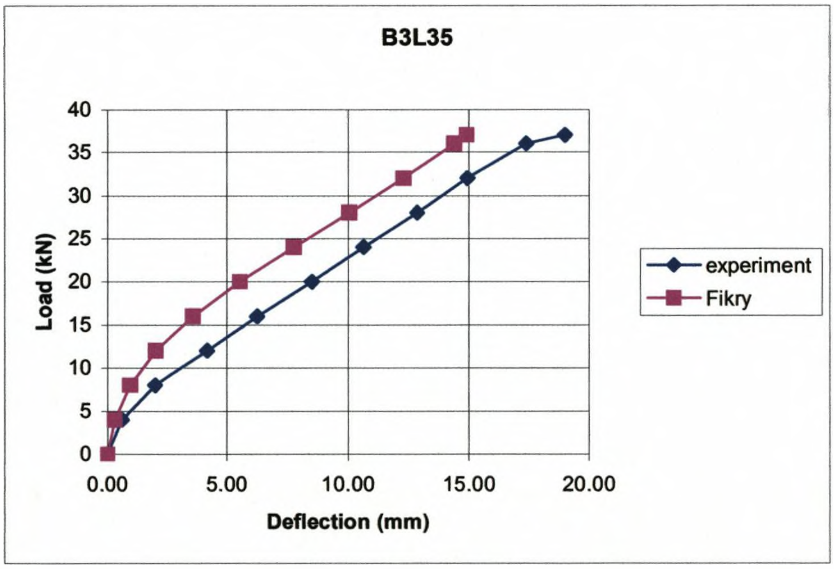

Figure 6.16 Load–deflection curve for typical beam

In order to show the overall effect for the 36 beams the theoretical deflection is plotted against experimental deflection for all load cases. The result can be seen in Figure 6.17

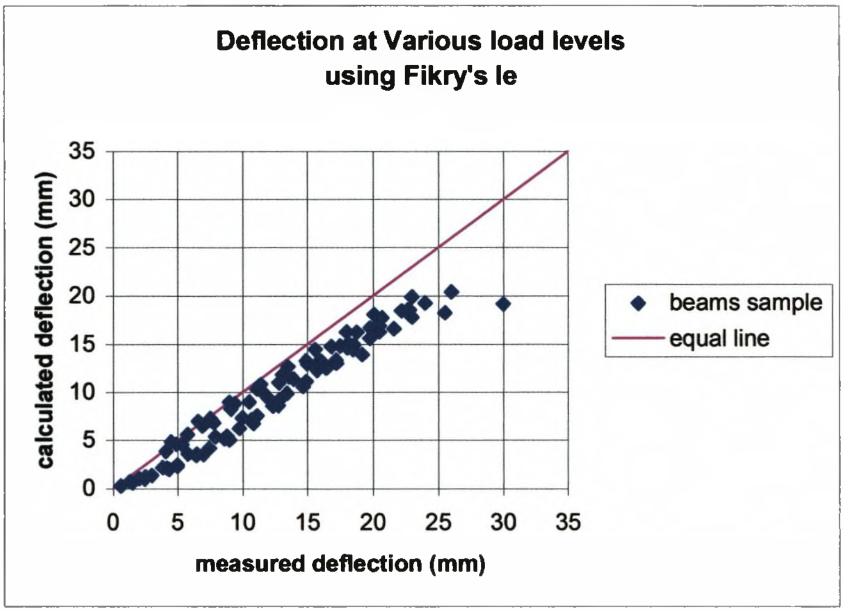

Figure 6.17 Deflection comparison of test beams at various load levels

It is evident from Figure 6.17 that the model proposed by Fikry underestimates the actual deflection in the vast majority of cases. Even allowing for spurious results the extent of difference varies considerably. Therefore, it can be assumed that a number of factors need to be considered in modifying the theoretical model.

6.7 Modification of I_e

6.7.1 Modification of I_{cr}

In Equation (6.6) the value of span, distance between load application points and supports and applied load can be measured accurately. The only uncertainty is the evaluation of I_e.

Rearranging Equation (6.6) produces the following equation for the experimental evaluation of I_e.

$$I_{e(\exp)} = \frac{P\,a\,(3L^2 - 4a^2)}{48 E_c \Delta_{\exp}} \tag{6.7}$$

where

$\Delta_{\exp}$ is the measured deflection at mid span.

As can be seen from Figure 6.17 all the beam deflection followed the same trend. Therefore, to illustrate the need for modification one beam, B2N25, can be used as an example. As the formula for the evaluation of I_e involves the ratio (M_a/M_{cr}) this is plotted against I_e in Figure 6.18. As well as the theoretical and experimental values of I_e the value of I_{cr} and I_g are also plotted.

From the figure, two important observations can be made.

(a) the theoretical values of I_e are always higher than the experimental values

(b) the theoretical value of I_{cr} is greater than the experimental value of I_e over a large position of the range of M_a/M_{cr}

Therefore the modification of the model needs to consider the theoretical evaluation of I_{cr}.

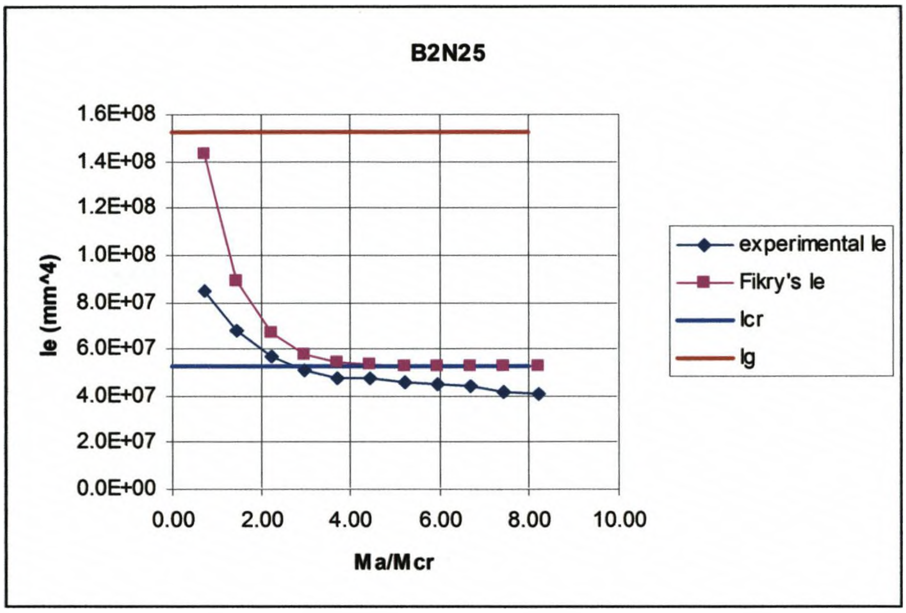

Figure 6.18 The effective second moment of area at various value of Ma/Mcr

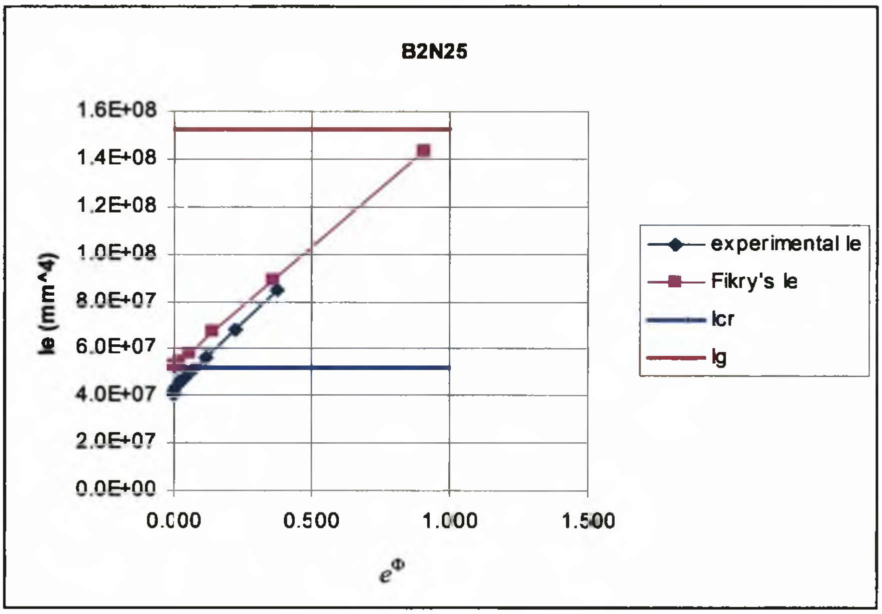

Figure 6.19 The effective second moment of area at various value of e^{Φ}

For the same beam the results can be presented in a different form. This is shown in Figure 6.19 where the variation of I_e is plotted against e^{Φ}. This figure again shows that the theoretical model of I_{cr} needs to be redefined.

6.7.1.1 Analysis and results

Rewriting Equation (1-3) using experimental values

$$I_{e(\exp)} = I_{cr(\exp)} + (I_g - I_{cr(\exp)})\ e^{\Phi}$$

or rearranging

$$I_{cr(\exp)} = \frac{I_{e(\exp)} - I_g e^{\Phi}}{1 - e^{\Phi}} \tag{6.8}$$

As the value of load approaches the yield load then the value of I_{cr} approaches the value of I_e. The value of e^{Φ} also approaches zero so that $(1-e^{\Phi})$ approaches unity.

Therefore to a very close approximation

when $\quad P = P_y \qquad\qquad I_{e(\exp)} = I_{cr(\exp)}$

so that Equation (6.7) can be modified to

$$I_{cr(\exp)} = \frac{P_y\ a\left(3L^2 - 4a^2\right)}{48E_c\Delta_{\exp}} \tag{6.9}$$

The values for $I_{cr(exp)}$ for all the beam tested, using the above equation, are shown in Table 6-11. The last column on the right shows the ratio $(I_{cr(exp)}/I_{cr(th)})$.

Table 6.11 Yield load analysis showing ratio of I_{cr}

Beam	P_y (kN)	Δ_y (mm)	$I_{cr(exp)}$ (mm^4)	$I_{cr\,(th)}$ (mm^4)	Ratio (4)/(5)
(1)	(2)	(3)	(4)	(5)	(6)
B1L25	55.00	20.00	3.33E+07	3.84E+07	0.865
B2L25	35.00	16.50	3.14E+07	3.84E+07	0.817
B3L25	31.00	15.50	3.33E+07	3.84E+07	0.867
B4L25	28.00	14.80	3.28E+07	3.84E+07	0.853
B1N25	71.00	19.00	4.52E+07	5.22E+07	0.866
B2N25	54.00	18.00	4.44E+07	5.22E+07	0.851
B3N25	48.00	18.00	4.45E+07	5.22E+07	0.852
B4N25	44.00	17.50	4.36E+07	5.22E+07	0.835
B1H25	67.00	14.50	5.59E+07	6.41E+07	0.872
B2H25	43.00	11.50	5.53E+07	6.41E+07	0.864
B3H25	37.00	11.50	5.36E+07	6.41E+07	0.837
B4H25	30.00	9.50	5.47E+07	6.41E+07	0.854
B1L35	52.00	19.00	3.06E+07	3.62E+07	0.846
B2L35	38.00	16.00	3.25E+07	3.62E+07	0.899
B3L35	36.00	16.00	3.47E+07	3.62E+07	0.959
B4L35	32.00	15.80	3.25E+07	3.62E+07	0.898
B1N35	70.00	20.00	3.92E+07	4.93E+07	0.795
B2N35	57.00	19.00	4.11E+07	4.93E+07	0.834
B3N35	49.00	19.70	3.84E+07	4.93E+07	0.779
B4N35	44.00	18.50	3.82E+07	4.93E+07	0.774
B1H35	80.00	17.00	5.27E+07	6.07E+07	0.868
B2H35	60.00	15.40	5.34E+07	6.07E+07	0.879
B3H35	53.00	16.50	4.96E+07	6.07E+07	0.817
B4H35	47.00	16.20	4.66E+07	6.07E+07	0.767
B1L45	52.00	17.50	3.10E+07	3.42E+07	0.905
B2L45	42.50	17.80	3.05E+07	3.42E+07	0.890
B3L45	36.00	15.80	3.27E+07	3.42E+07	0.957
B4L45	30.00	14.00	3.20E+07	3.42E+07	0.935
B1N45	76.00	18.00	4.40E+07	4.68E+07	0.941
B2N45	62.00	19.00	4.16E+07	4.68E+07	0.890
B3N45	53.00	18.00	4.23E+07	4.68E+07	0.905
B4N45	44.00	15.80	4.16E+07	4.68E+07	0.890
B1H45	97.00	19.70	5.13E+07	5.77E+07	0.889
B2H45	70.00	16.40	5.45E+07	5.77E+07	0.944
B3H45	62.00	17.10	5.21E+07	5.77E+07	0.903
B4H45	59.00	16.70	5.28E+07	5.77E+07	0.915

As can be seen in all cases the ratios are below unity, and vary between 0.74 and 0.93. This variation suggests that a number of factors affect the value. Considering the variations studied by other authors, it was decided to consider the effect of f_{cu}, and ρ on the value of $I_{cr(exp)}$.

The average ratio $I_{cr(\exp)}/\frac{1}{12}bd^3$ for load position was plotted against ρ for all beams. The results obtained are shown in Figure 6.20. It can be seen that three lines are obtained dependent upon the value of concrete strength.

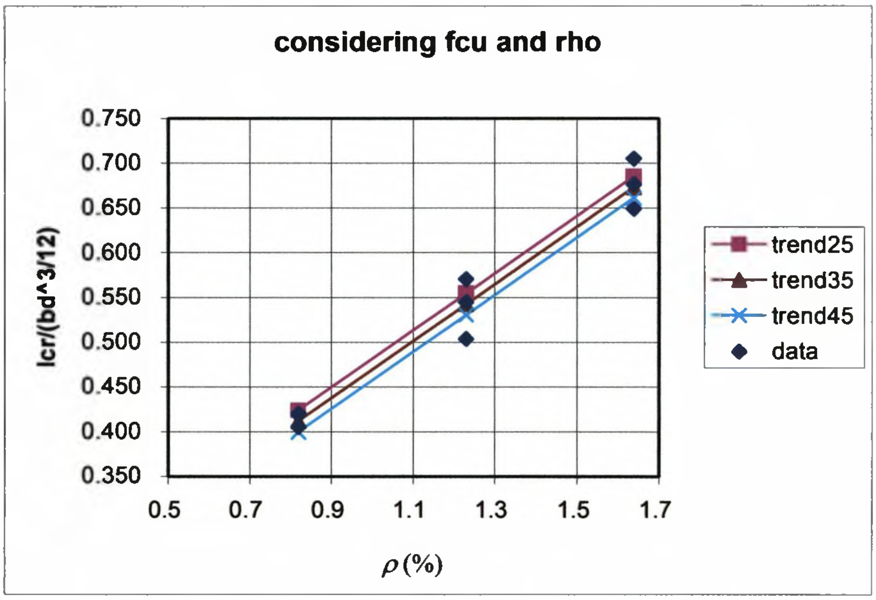

Figure 6.20 Ratio of I_{cr} against ρ for various f_{cu} values

Applying a regression analysis the following equation is obtained for I_{cr} and denoted as I_{crm1}.

$$I_{crm1} = (0.1914 - 0.0012 f_{cu} + 0.3195\rho)\tfrac{1}{12}bd^3 \qquad (6.10)$$

An alternative regression analysis was carried out replacing f_{cu} and ρ by one term $n\rho$ as the result shown in Figure 6.21.

This time the equation for I_{cr} is denoted as I_{crm2}

$$I_{crm2} = \left(0.1618 + 0.0418\ n\rho\right)\tfrac{1}{12}bd^3 \qquad (6.11)$$

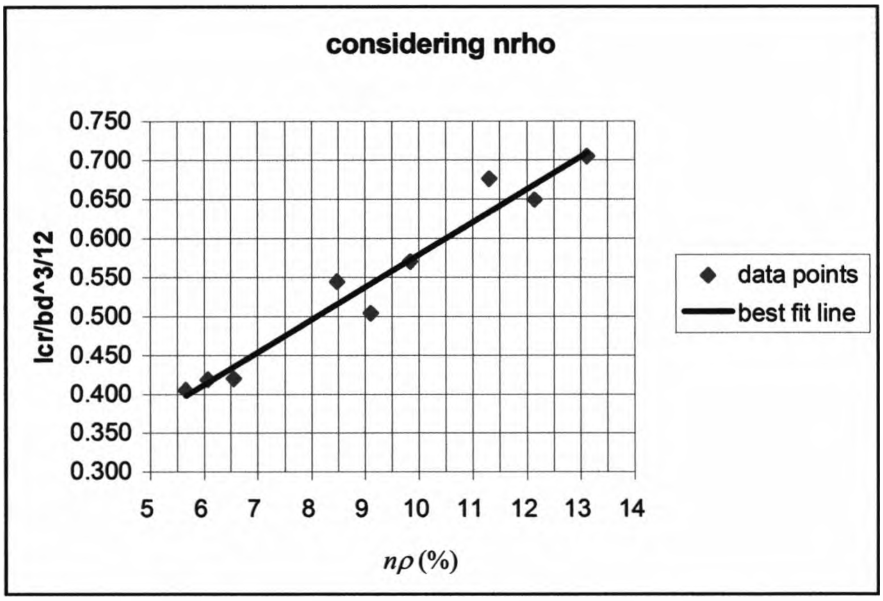

Figure 6.21 Ratio of I_{cr} against $n\rho$ values

6.7.1.2 Discussion of the results

The modified value of I_{cr} obtained from Equations (6.10) and (6.11) above are presented in Table 6.12 in column 6 and 7 respectively. The cracked second moment of area is calculated using Fikry's equation is given in column 5 of Table 6.12.

From the table it can be seen that the value of both equations are less than the theoretical value. The values vary from 0.84 to 0.91 for Equation (6.10) and 0.88 to 0.91

for Equation (6.11). This means that the neutral axis lies slightly above the theoretical neutral axis. This might happen due to variation of the concrete and steel reinforcement. Al-Shaikh [18] also reported that the value of cracked second moment of area varied from 0.7 to 0.9 of the theoretical value.

Equation (6.11) has similar form to the equation proposed by Fikry in part of his model but with slightly different coefficient.

Table 6.12 Cracking second moment of area

Beam	ρ (%)	f_{cu} (MPa)	$n\rho$ (%)	I_{cre} (mm^4)	I_{crm1} (mm^4)	I_{crm2} (mm^4)	ratio1	ratio2
(1)	(2)	(3)	(4)	(5)	(6)	(7)	(8)	(9)
BL25	0.820	25	6.56	3.80E+07	3.297E+07	3.395E+07	0.87	0.89
BN25	1.230	25	9.84	5.08E+07	4.317E+07	4.463E+07	0.85	0.88
BH25	1.640	25	13.	6.35E+07	5.337E+07	5.530E+07	0.84	0.87
BL35	0.820	35	6.07	3.61E+07	3.203E+07	3.237E+07	0.89	0.88
BN35	1.230	35	9.11	4.79E+07	4.223E+07	4.226E+07	0.88	0.90
BH35	1.640	35	12.15	5.98E+07	5.244E+07	5.214E+07	0.88	0.87
BL45	0.820	45	5.66	3.45E+07	3.110E+07	3.101E+07	0.90	0.91
BN45	1.230	45	8.48	4.55E+07	4.130E+07	4.021E+07	0.88	0.90
BH45	1.640	45	11.31	5.65E+07	5.150E+07	4.941E+07	0.91	0.87

6.7.2 Modification of Φ

6.7.1.1 Analysis and results

Rewriting Equation (1.3) using $I_{e(exp)}$ and I_{crm} and $e^{\Phi} = e^{\Phi\exp}$

$$I_{e(\exp)} = I_{crm} + (I_g - I_{crm})e^{\Phi_{\exp}} \tag{6.12}$$

$$e^{\Phi_{exp}} = \frac{I_{e(\exp)} - I_{crm}}{I_g - I_{crm}}$$

$$\Phi_{\exp} = \ln\left|\frac{I_{e(\exp)} - I_{crm}}{I_g - I_{crm}}\right| \tag{6.13}$$

Originally Φ was defined by the following equation

$$\Phi = -\rho\left(\frac{M_a}{M_{cr}}\right)\left(\frac{L_{cr}}{L}\right)$$

Considering Equation (6.2) and (6.5) discussed previously for M_{cr} and L_{cr} respectively in which both rely on the reinforcement ratio, therefore

$$\Phi = -\rho\left(f(\rho)\frac{M_a}{M_{cr}}\right)\left(f(\rho)\frac{L_{cr}}{L}\right)$$

In this study the equation above is simplified by eliminating $f(\rho)$ in M_a/M_{cr} and L_{cr}/L but use only one $f(\rho)$ in the whole expression instead. Thus, the basic definition was redefined as

$$\Phi = -f(\rho)\left(\frac{M_a}{M_{cr}}\right)\left(\frac{L_{cr}}{L}\right)$$

$$\Phi = -C\left(\frac{M_a}{M_{cr}}\right)\left(\frac{L_{cr}}{L}\right) \tag{6.14}$$

Equating the two value of Φ produces the following equation

$$C = -\frac{\ln\left|\dfrac{I_{e(\exp)} - I_{crm}}{I_g - I_{crm}}\right|}{\left(\dfrac{M_a}{M_{cr}}\right)\left(\dfrac{L_{cr}}{L}\right)} \tag{6.15}$$

Using the value of I_{crm} given by Equation (6.10) the value of C for all 36 beams is obtained.

The value of C for all beams is shown in Figure 6.19. Two possibilities were initially considered for the variation of C with ρ, linear and polynomial. However, for this case it only a linear variation, as shown in Figure 6.22, is considered.

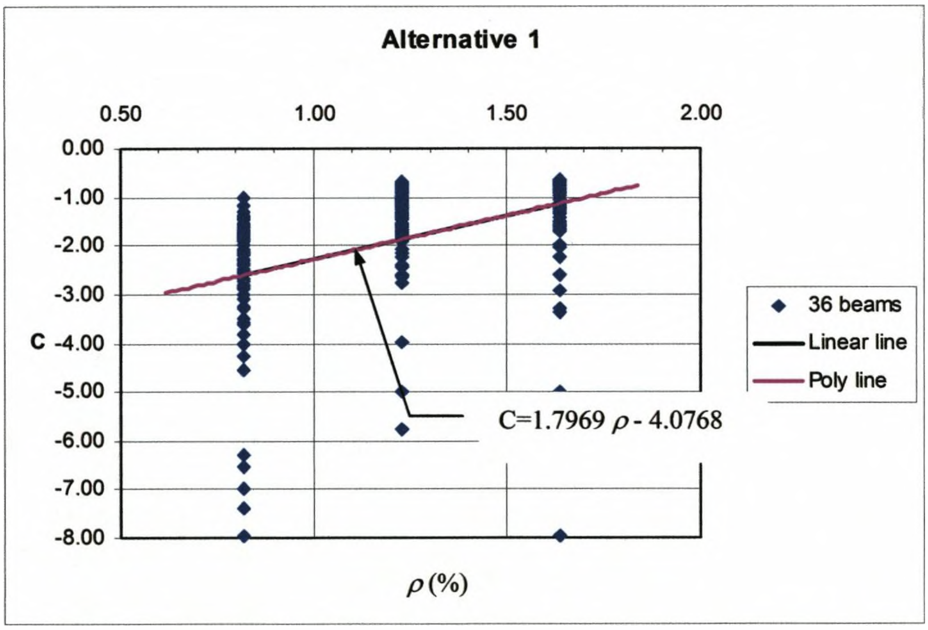

Figure 6.22 Regression of coefficient C against ρ for I_{crm1}

Assuming linear variation and applying a regression analysis, the following variation is obtained.

$$C = -4.0768 + 1.7969\,\rho$$

giving the following value for Φ

$$\Phi_{m1} = -\left(\frac{M_a}{M_{cr}}\right)\left(\frac{L_{cr}}{L}\right)(4.0768 - 1.7969\rho) \qquad (6.16)$$

Assuming the value of I_{cr} given in Equation (6.11) the variation of C with ρ is shown in Figure 6.23.

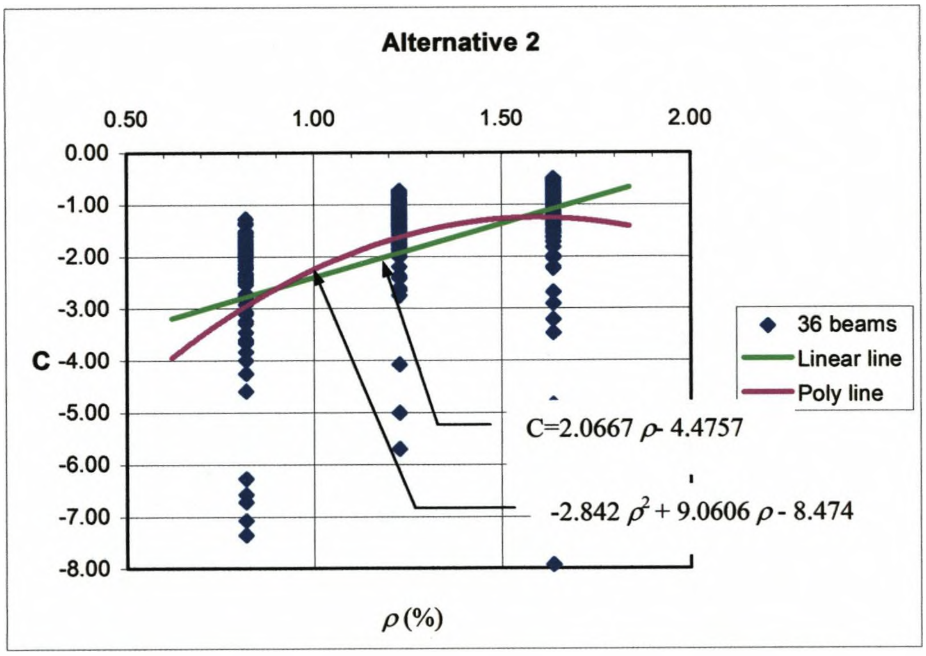

Figure 6.23 Regression of coefficient C against ρ for I_{crm2}

Assuming a linear variation of C with ρ and applying a regression analysis, the following relationship is obtained.

$$C = -4.4757+2.0667\rho$$

hence

$$\Phi_{m2a} = -\left(\frac{M_a}{M_{cr}}\right)\left(\frac{L_{cr}}{L}\right)(4.4757-2.066\rho) \tag{6.17}$$

Similarly with an assumed polynomial variation the following relationship is produced

$$C = -8.474+9.0606\rho-2.842\rho^2$$

hence

$$\Phi_{m2b} = -\left(\frac{M_a}{M_{cr}}\right)\left(\frac{L_{cr}}{L}\right)(8.474-9.0606\rho+2.842\rho^2) \tag{6.18}$$

6.7.2.2 Discussion of the results

The factor Φ has a direct relationship with ratios M_a/M_{cr}, L_{cr}/L and the reinforcement ratio. As discussed previously, the cracking moment, M_{cr}, was slightly affected by the presence of reinforcement. The cracked length, L_{cr}, is also a function of the reinforcement ratio, ρ. Therefore, for the derivation of factor Φ it was convenient to consider a plot of Φ against the reinforcement ratio.

Three alternatives for Φ were suggested. One for I_{cr} Equation (6.10) and two for I_{cr} Equation (6.11) as discussed above.

Two different values of Φ obtained for I_{crm2} are used to demonstrate the effect of I_e on the factor Φ as shown in Figure 6.24.

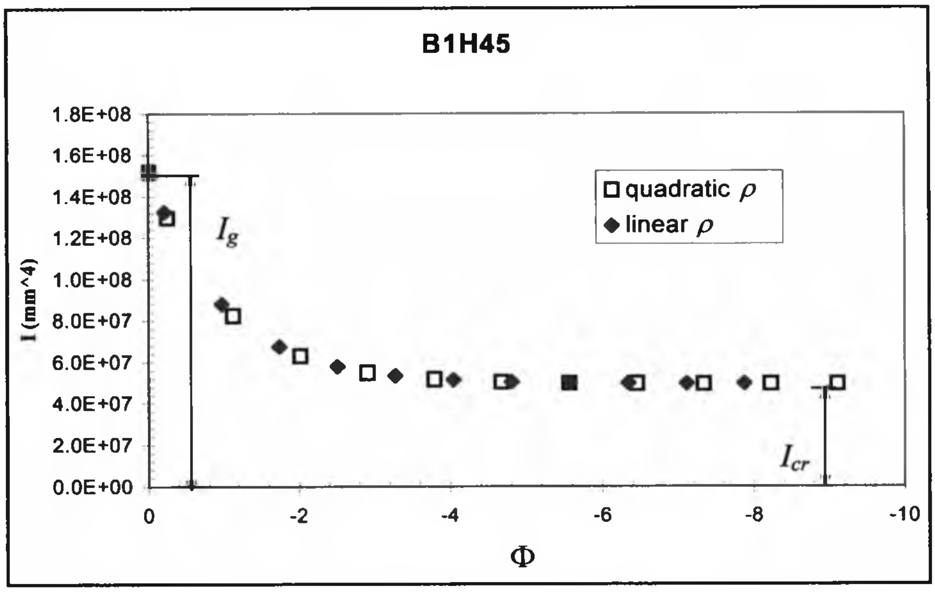

Figure 6.24 Variation of I_e values for different factor Φ

It should be noted that a limit is needed for these equation due to the possibility of the factor Φ reaching a value bigger than zero. This normally happens in the early stages when the concrete has not begun to crack.

The limit suggested is that if Φ is bigger than zero then Φ should be taken as equal to zero. This limit will give the value of effective second moment of area, I_e, equal to gross second moment of area, I_g, when the concrete has not cracked.

The factor Φ becomes smaller (bigger in negative sign) as the applied load increases and will reach its peak value when the concrete section completely cracks. This value will give the effective second moment of area equal to the cracked second moment of area, I_{cr}.

From a typical result presented in Figure 6.24, it can be seen that factor Φ obtained from the quadratic ρ variation have slightly bigger value than Φ obtained from the linear one. This also give the effective second moment of area slightly smaller than that produced by linear Φ and as a result deflection values are slightly bigger when quadratic Φ is used compared to linear Φ.

6.8 Verification of proposed I_e

6.8.1 Using main data considered

With the development of the equations for I_{cr} and Φ in the previous section Table 6.13 shows the possible combinations for calculating I_e. Case 1 is combination between I_{crm1} and Φ_{m1}.

For Case 2 there are two possibilities. Combination of I_{crm2} and Φ_{m2a} is termed Case 2a and combination of I_{crm2} and Φ_{m2b} is expressed as Case 2b.

Table 6.13 The possible combinations for calculating I_e

Case 1	Case 2
I_{crm1}	I_{crm2}
Φ_{m1}	Either Φ_{m2a} or Φ_{m2b}

To show the effect of the above modifications one typical beam, B2N25, will be considered in detail. For all the beams the results are given in Figure C-1 to C-36 in Appendix C.

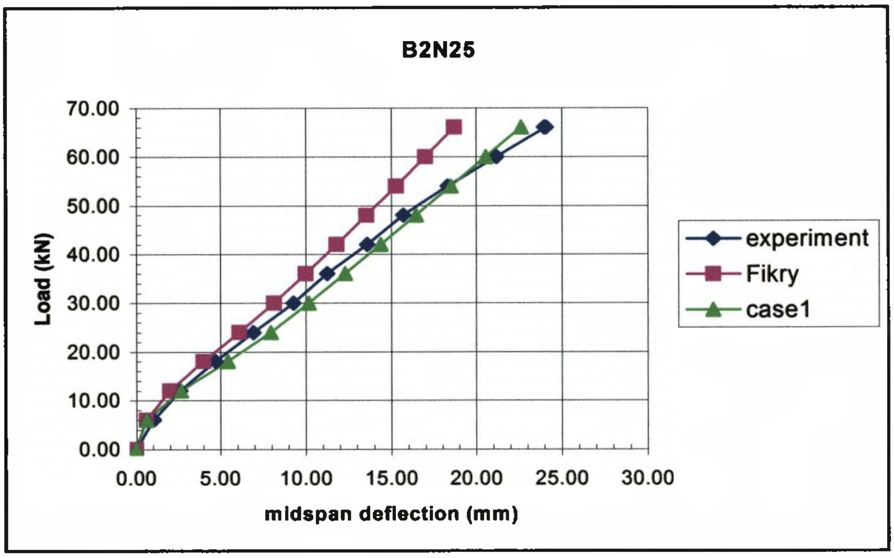

Figure 6.25 Comparison of three deflection values of B2N25 by applying Casel

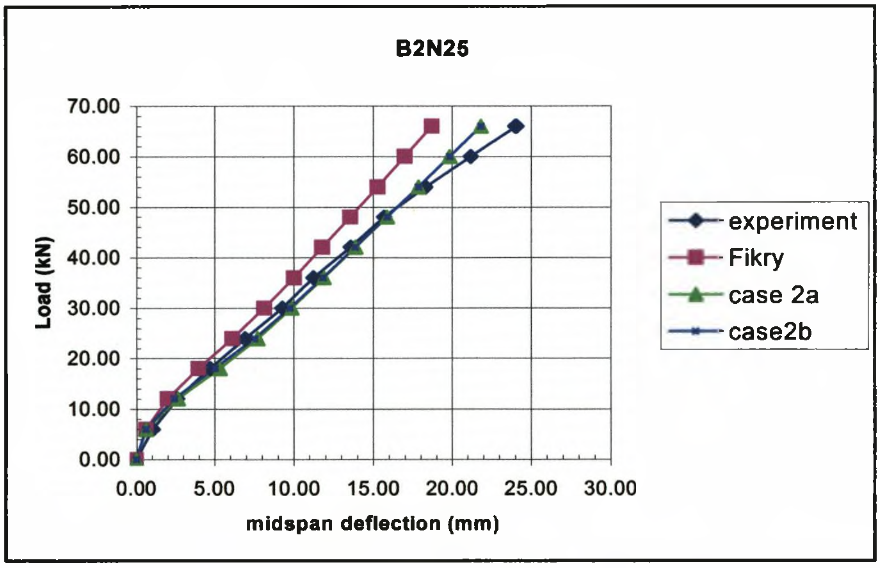

Figure 6.26 Comparison of four deflection values of B2N25 by applying Case 2

In Figure 6.25 the experimental load deflection curve is compared with the curves produced using Fikry's method and the curves using Case 1 with linear C variation.

In Figure 6.26 the same comparison is made between the experimental load deflection curves, Fikry's curve and the curves produced by Case 2 with different C variation.

The following conclusions can be made

(a) For both cases the linear and polynomial variations of C produce virtually the same load deflection curve.

(b) The curves produced by the modified values are safe in that they overestimate the deflection

(c) The curves produced by the modified equations give a more accurate value than the original Fikry's curve.

As explained in a previous section deflection is normally checked for the service load which is normally between 50 and 70% of their ultimate load, therefore overall results from these experiments are presented to compare the actual and calculated deflections at load levels of $0.50\ P_u$, and $0.70\ P_u$.

In Figure 6.27 the actual deflections are compared with analytical deflections using Case 1 with a linear C variation. In Figure 6.28 the same comparison is made between actual and analytical deflections calculated using Case 2 with two variation of C.

For overall beams the following conclusions can be drawn:

(a) In all cases the vast majority of calculated deflections are overestimated.

(b) For both cases C with linear and polynomial variation show slightly different results.

(c) All of the deflections predicted produced by Case 1 and 2 are less than 20% error in which the limit are still acceptable.

To draw a more comprehensive conclusion for the modified I_e, beams with different properties such as span length, reinforcement ratio as well as unsymmetrical applied load were observed and will be discussed in the next section.

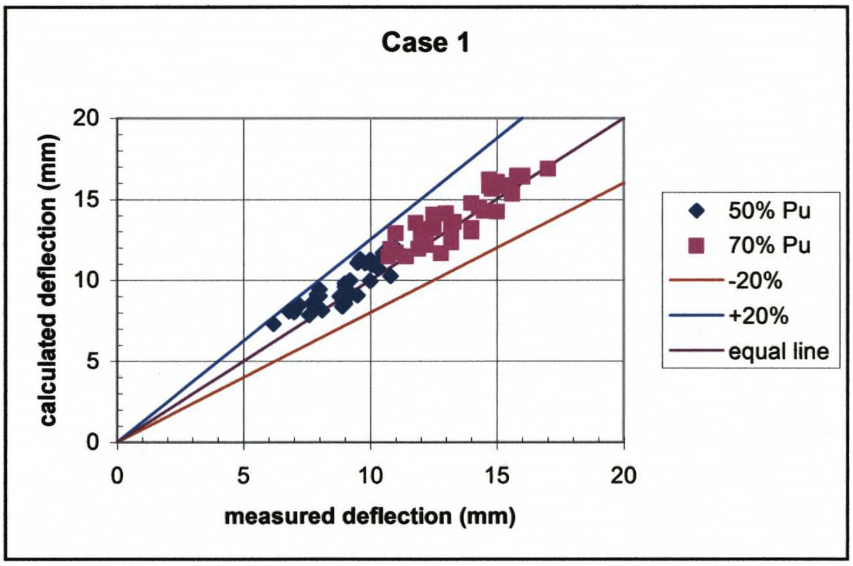

Figure 6.27 Comparison between actual and analytical deflection for overall 36 beams by applying case 1 with C linear

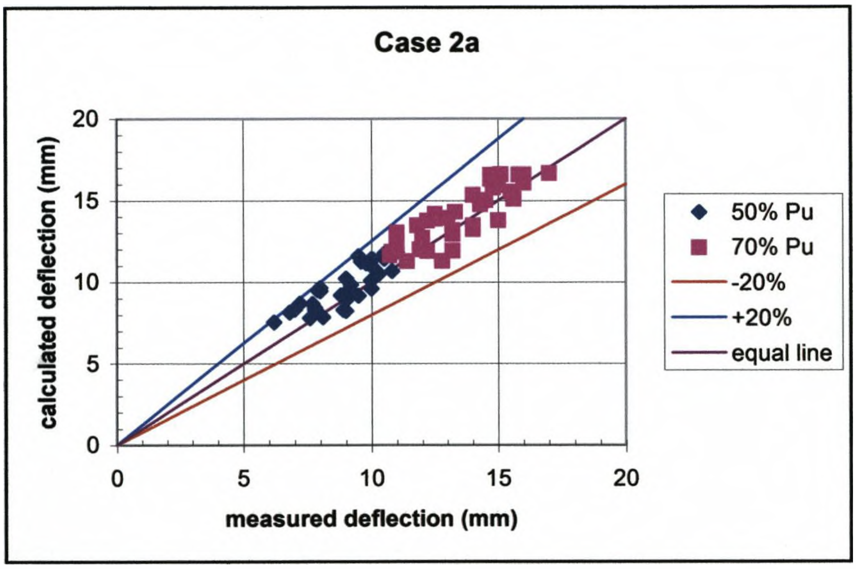

(a)

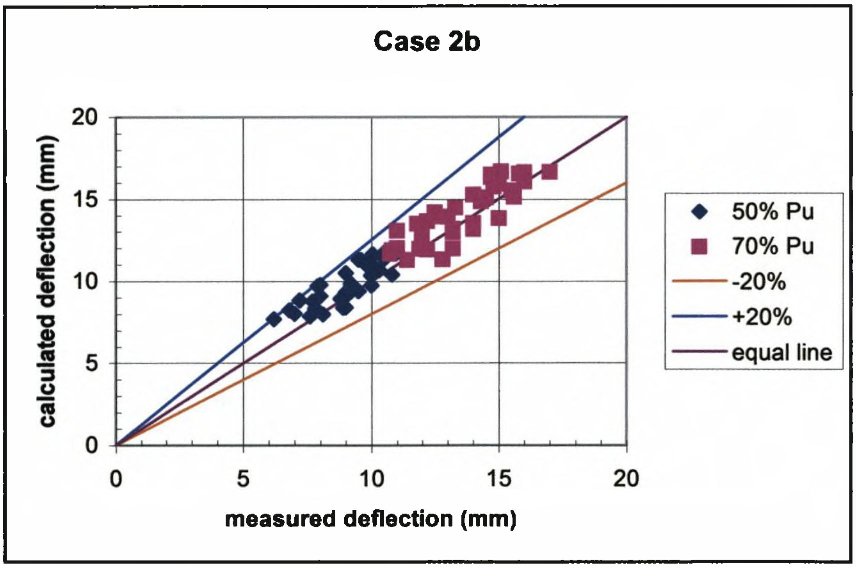

(b)

Figure 6.28 Comparison between observed and computed deflection for overall 36 beams by applying Case 2 with (a) C linear and (b) C polynomial

6.8.2 Using beams with various spans

In this section beam with various span lengths, i.e. X_1, X_2 and X_3 as presented in Table 5.3, are considered. In Figure 6.29 load-deflection curves using case 1 are compared with experimental curve and curve produced by Fikry's method for beam X_1. Comparison of load-deflection curve produced by case 2 for the same beam is presented in Figure 6.30.

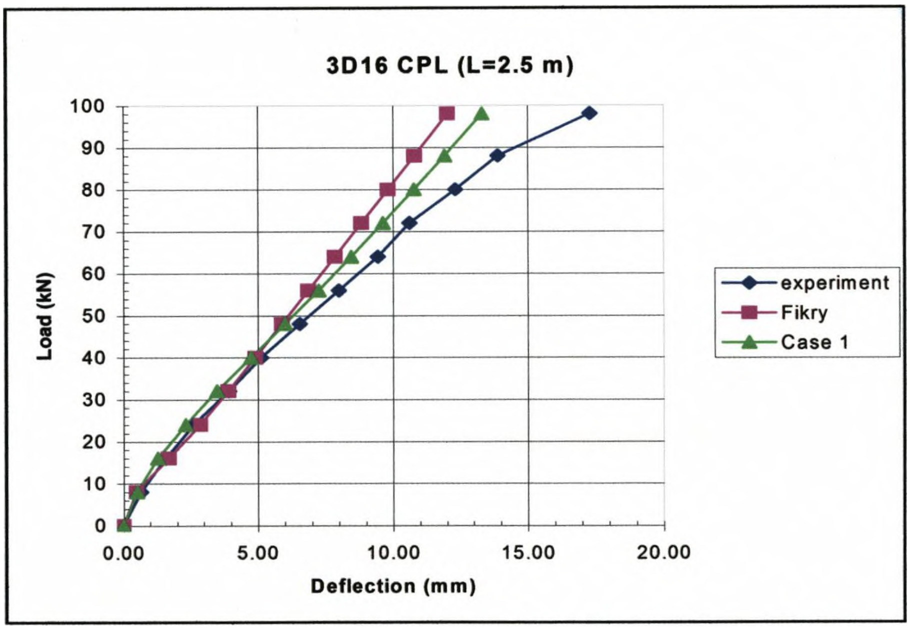

Figure 6.29 Comparison of three load-deflection curves of X_1 using Case 1

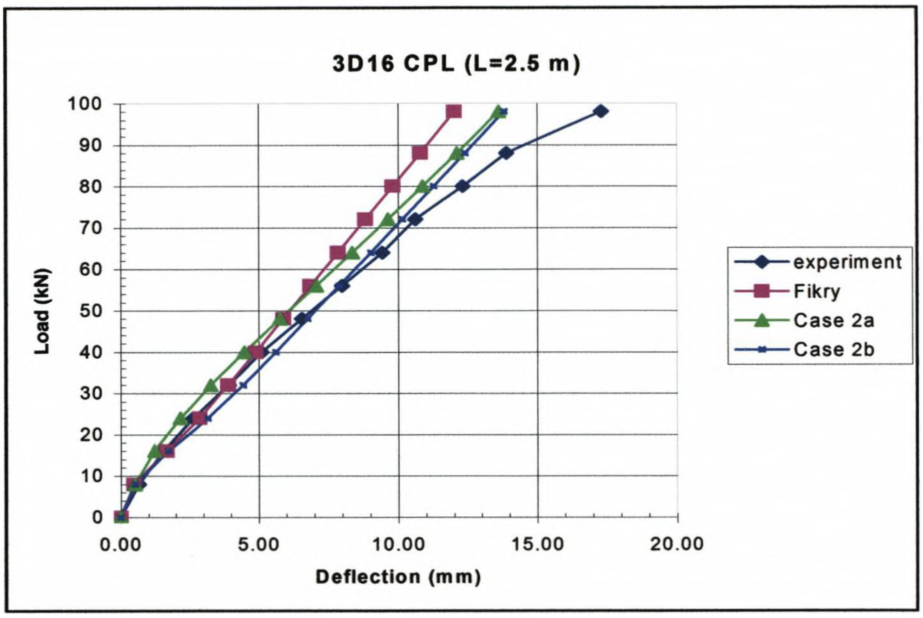

Figure 6.30 Comparison of four load-deflection curves of X_1 using Case 2

In Figure 6.31 and 6.32 the same comparison is made for beam X_2 using Case 1 and Case 2 respectively.

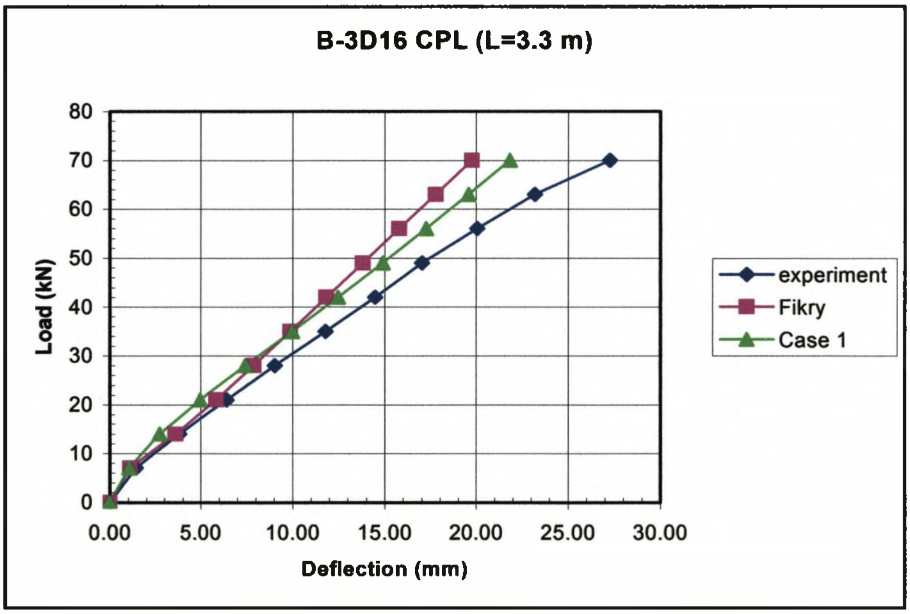

Figure 6.31 Comparison of three load-deflection curves of X_2 using Case 1

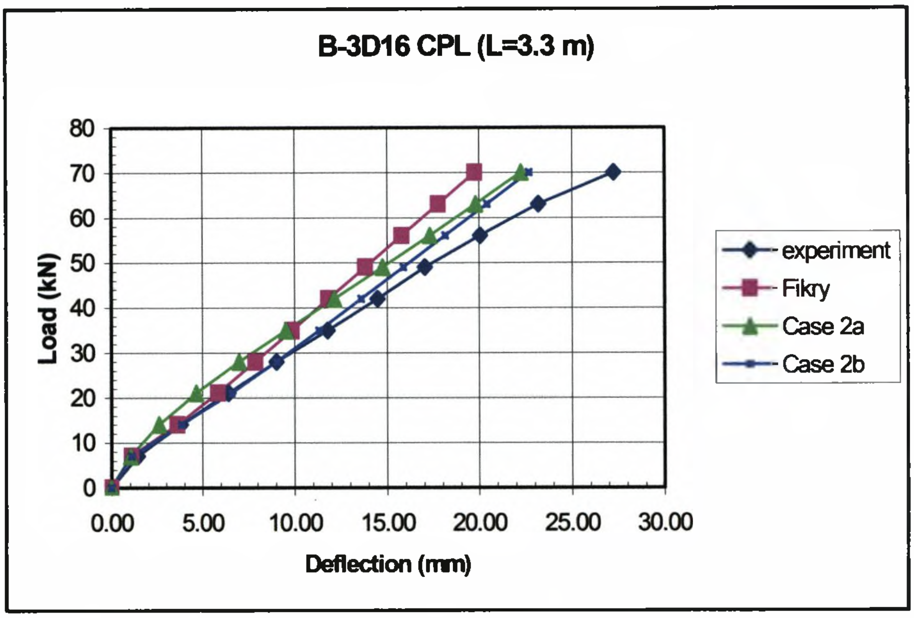

Figure 6.32 Comparison of four load-deflection curves of X_2 using Case 2

Again the same comparison is made for beam X_3. Figure 6.33 and 6.34 are respectively the deflection produced by Case 1 and Case 2.

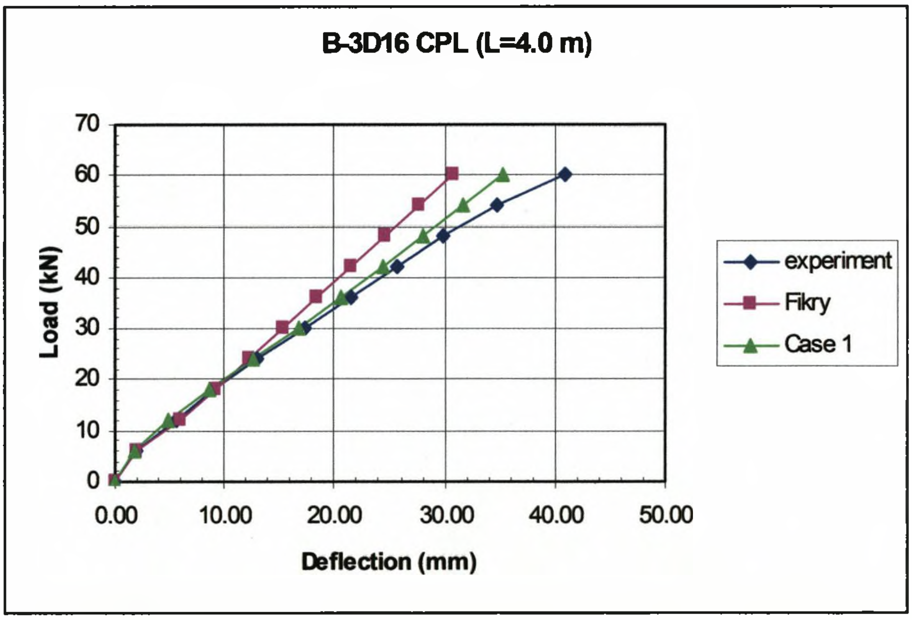

Figure 6.33 Comparison of three load-deflection curves of X_3 using Case 1

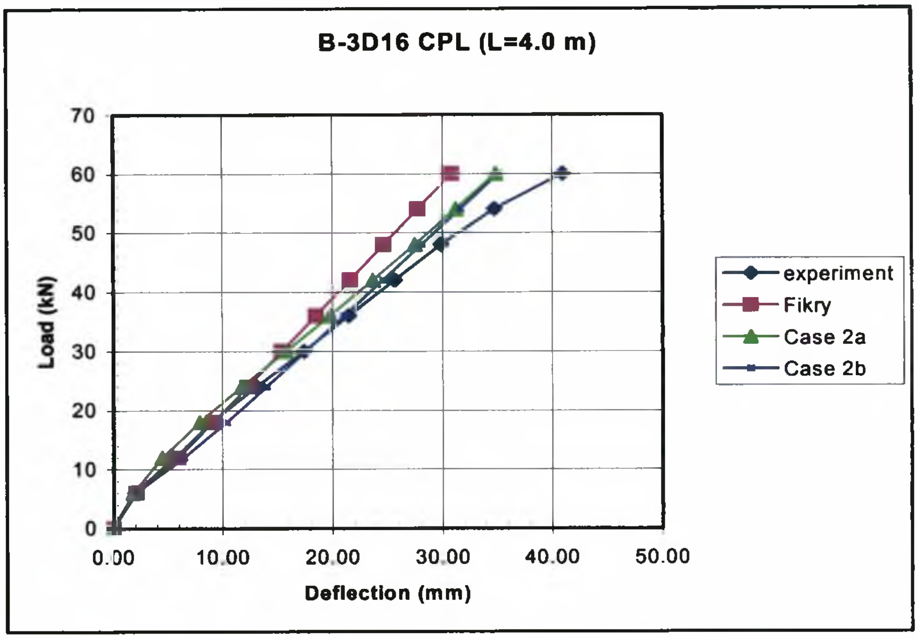

Figure 6.34 Comparison of four load-deflection curves of X_3 using Case 2

From the results presented in the Figures above the following conclusions can be drawn:

(a) Both deflection curves produced by the modified model show the same trend for different spans.

(b) Deflection curves using both the modified models with linear variation of C underestimate the actual deflection.

(c) Polynomial C variation in the modified model produces a deflection curve that overestimates the actual deflection, below 50% of ultimate load, for all different spans.

(d) The modified model with polynomial variation of C gives a more accurate deflection prediction than linear variation of C.

6.8.3 Using beams with various ρ, L and a

Beams combinations between reinforcement ratio, span length and load condition are considered. Table 5.3 shows detail of these beams namely X_4, X_5 and X_6.

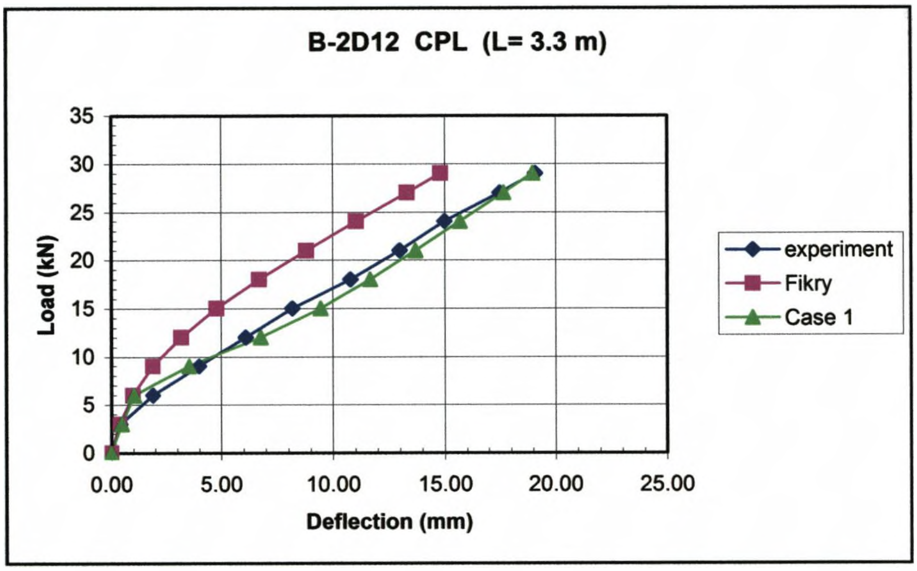

Figure 6.35 Comparison of three load-deflection curves of X_4 using Case 1

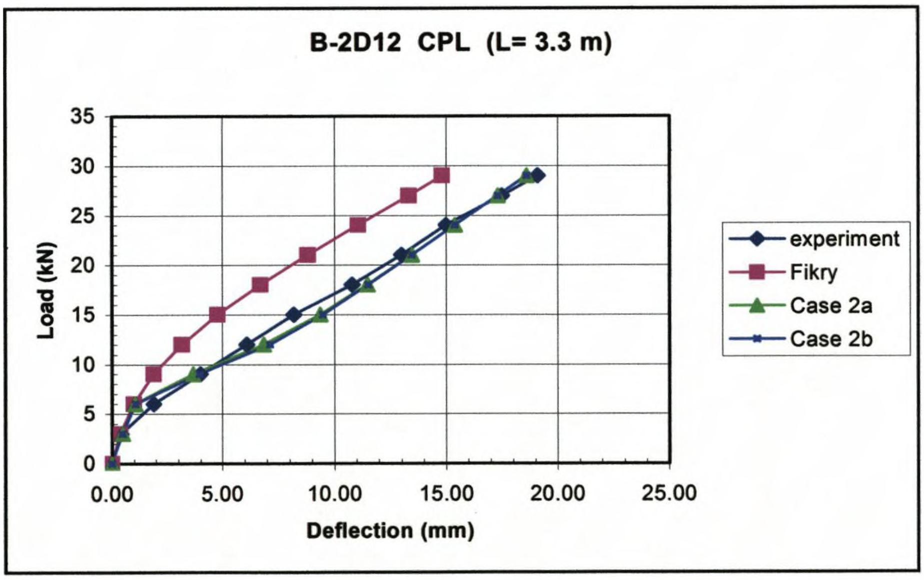

Figure 6.36 Comparison of four load-deflection curves of X_4 using Case 2

Figure 6.35 shows the load-deflection curves for beam X_4 produced by Fikry's method, experimental, and a curve calculated by Case 1 with linear C variation. In Figure 6.36 the same comparison is made for both curves produced by Case 2 with two C variations.

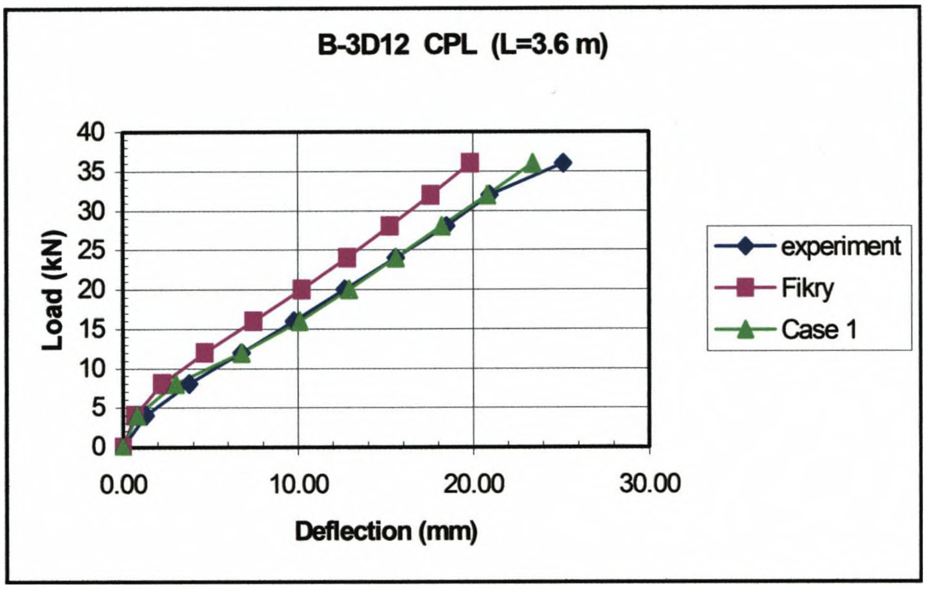

Figure 6.37 Comparison of three load-deflection curves of X_5 using Case 1

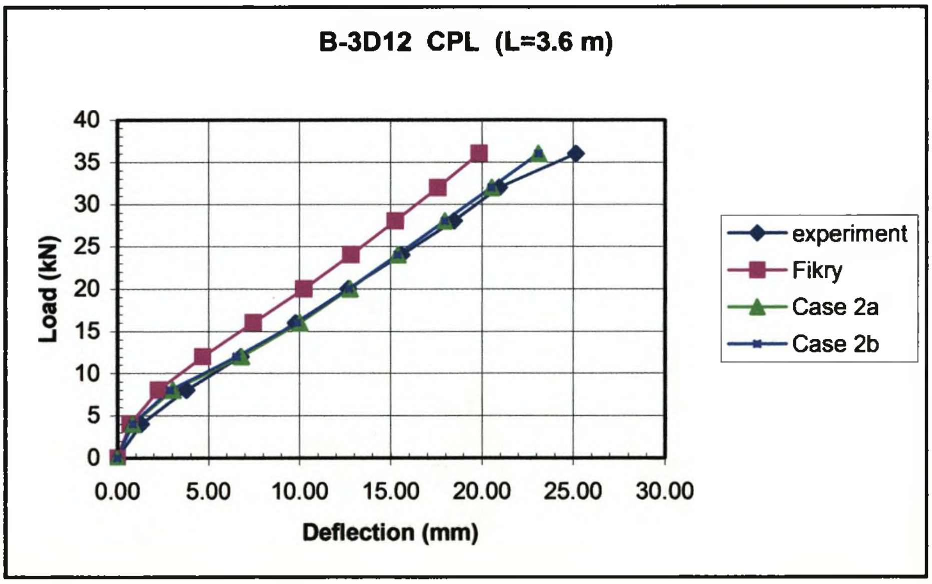

Figure 6.38 Comparison of four load-deflection curves of X_5 using Case 2

In Figure 6.37 comparison of load-deflection curves of beam X_5 is presented. A load deflection curve using Case 1 with a linear variation of C is compared with Fikry's and the experimental deflection curve. The same comparison is made for curves produced by Case 2 with two variation of C and are presented in Figure 6.38.

In Figure 6.39 a comparison is shown for the beam X_6. The result from the experiment on this beam is also compared with Fikry's, and with the result obtained from case 1 with a linear variation of C. This comparison is presented in Figure 6.36. In Figure 6.40 the same comparison for this beam is made but for Case 2 with two C variation.

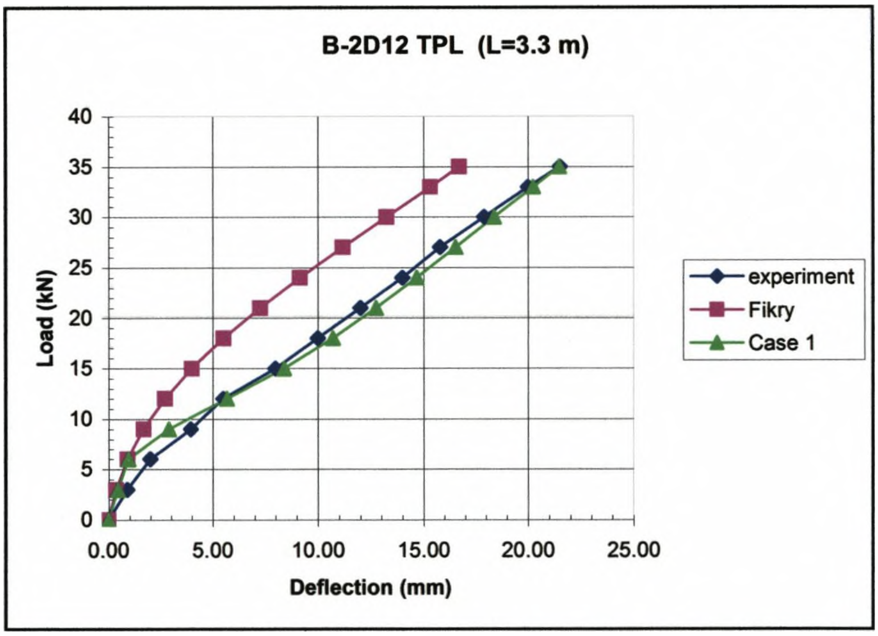

Figure 6.39 Comparison of three load-deflection curves of X_6 using Case 1

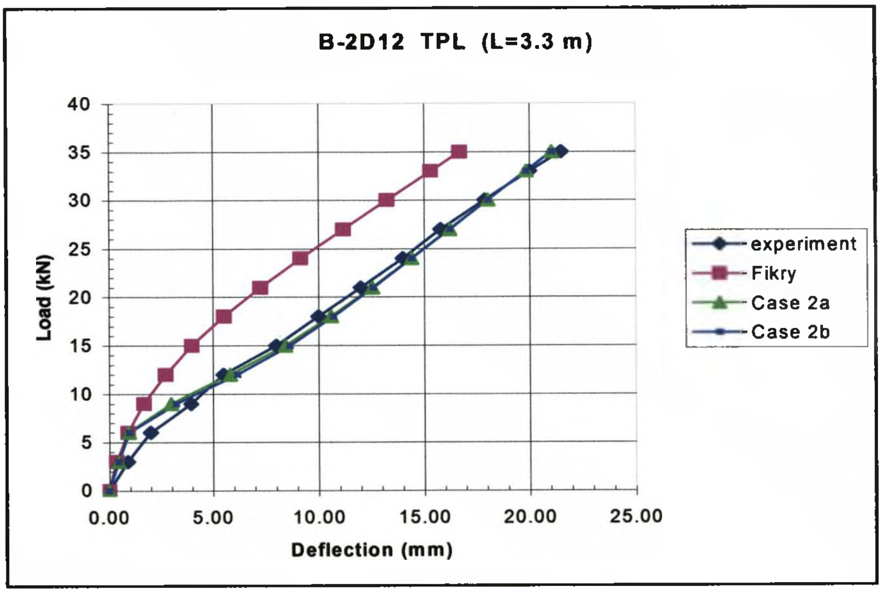

Figure 6.40 Comparison of four load-deflection curves of X_6 using Case 2

From the graph presented above the following conclusions can be made:

(a) Deflection curve produced by Fikry underestimates the actual deflection. This should always be avoided in design.

(b) Deflection curve for all beam combinations produced by both the modified model with linear and polynomial C variation give accurate predictions.

(c) In the early stage of load application, the deflection curves calculated by both modified models underestimate the actual deflection. However, this is not a critical case as the deflection is normally controlled at service loads which have values from 50 to 70% of maximum design loads.

6.8.4 Unsymmetrical point loads

Two unsymmetrical point loads i.e. beam X_7 and X_8 in Table 5.3 are considered. The maximum deflection equation has been derived in Appendix B-1 using the usual analytical method and given by Equation (6.19).

$$\Delta_{max} = \{-\tfrac{1}{6}V_A x^3 + \tfrac{1}{6}P_1(x-a)^3 + \left(\tfrac{1}{3}P_1 aL + \tfrac{1}{6}P_2 bL - \tfrac{1}{2}P_1 a^2 + \frac{P_1}{6L}a^3 - \frac{P_2}{6L}b^3\right)x\} / EI_e \quad (6.19)$$

The position where the maximum deflection occurs is at a distance of x = 1.31 m from the left support (See Table 5.3 for detail of beam X_7 and X_8).

Using Equation (6.19), a comparison of load-deflection curves can be made and is shown in Figure 6.41 and 6.42 for beam X_7.

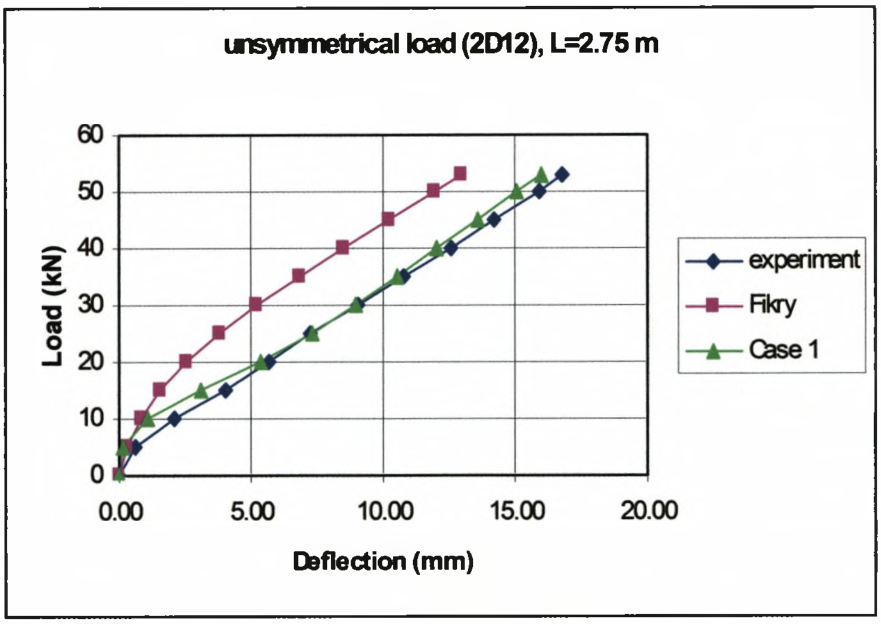

Figure 6.41 Comparison of three load-deflection curves of X_7 using Case 1

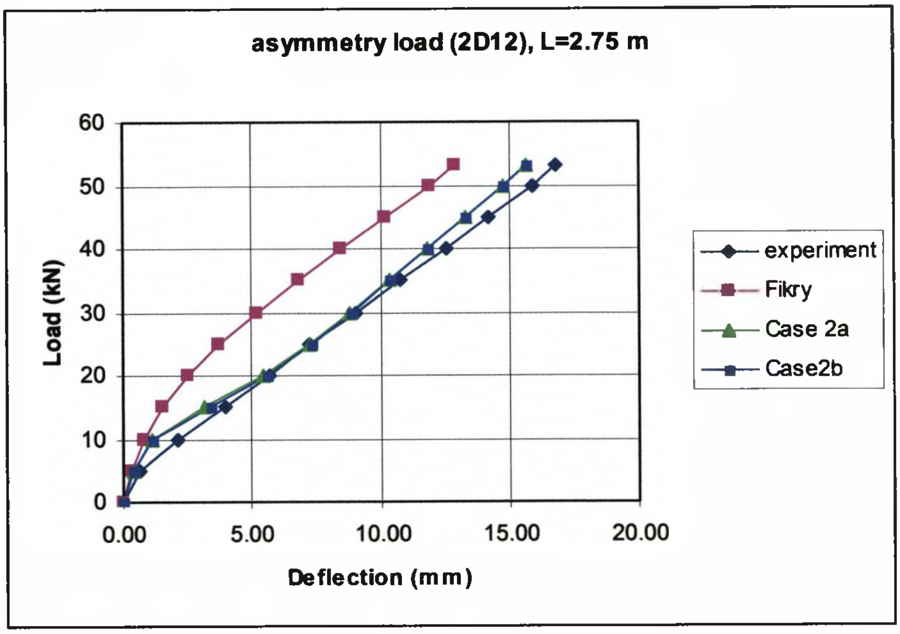

Figure 6.42 Comparison of four load-deflection curves of X_7 using Case 2

Finally, a comparison is made for a beam X_8 and is shown in Figure 6.43 and 6.44

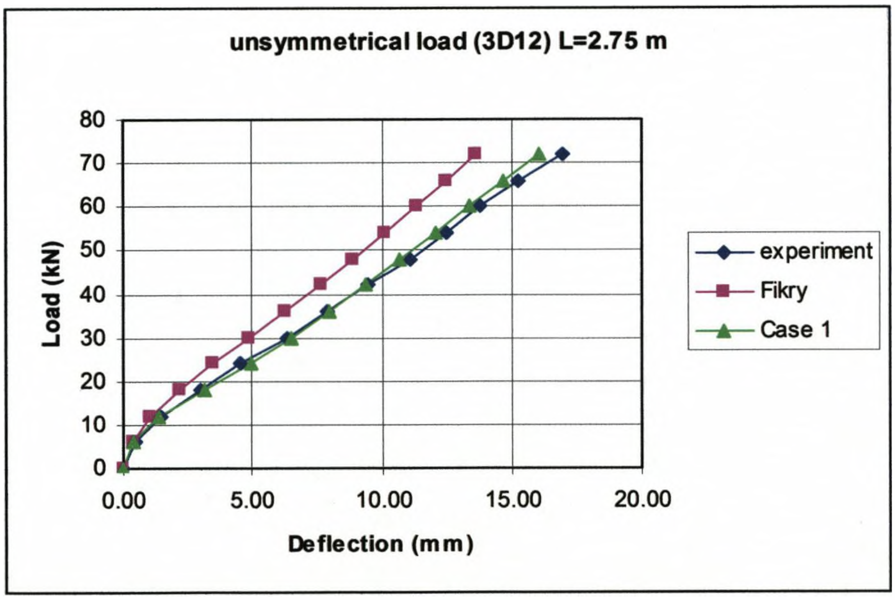

Figure 6.43 Comparison of three load-deflection curves of X_8 using Case 1

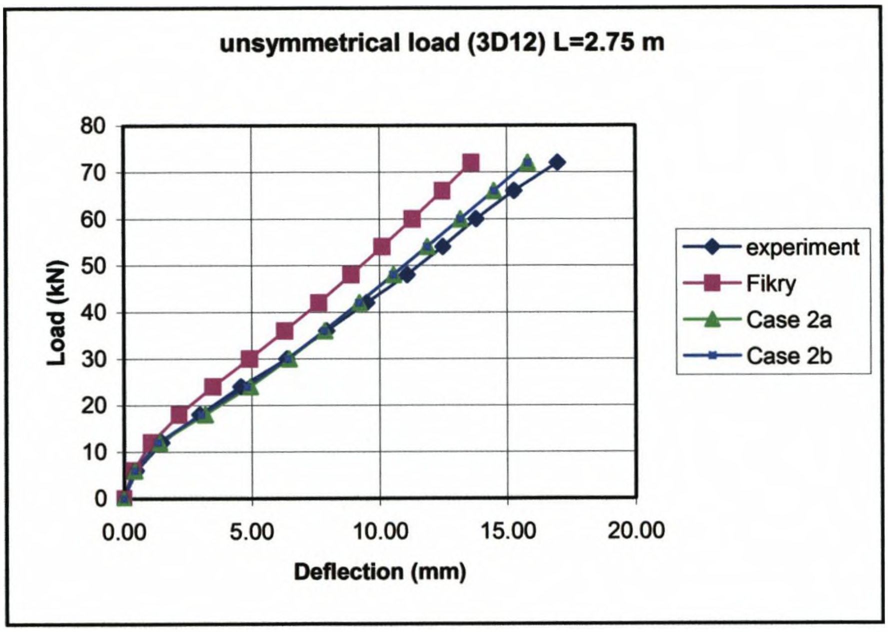

Figure 6.44 Comparison of four load-deflection curves of X_8 using Case 2

From the curves for unsymmetrical point loads the following observations can be made:

(a) Deflection curves produced by Fikry's method underestimate the actual deflections.

(b) Both modified models with two C variations, give very close prediction of the actual deflections.

(c) Different load conditions have no effect on the modified model

6.9 Validation of proposed I_e

6.9.1 Comparison between proposed and various theoretical models

A computer program "Program B-2" using Matlab has been written to calculate the deflections in this study. A typical program and complete output results is presented in Appendix B-3 and B-4 respectively.

A comparison between experimental load-deflection curves obtained in this study and those predicted by Fikry, ACI, BS and proposed model are presented in Figure 6.45a to 6.45d respectively

It can be seen that the three methods, Fikry's method, ACI and BS, produce an underestimate of the deflection as shown in Figures 6.45a, b and c, respectively. The three alternative methods proposed in this study show good agreement with the experimental values, as shown in Figure 6.45d.

As discussed previously, deflections are critical at working load, which occurs at about 70% of the ultimate load. Therefore, to make an easy comparison for all the beams calculated using the four different methods discussed above, the deflections at 50% and 70% of their ultimate load shown in Figure 6.46 and 6.47, respectively.

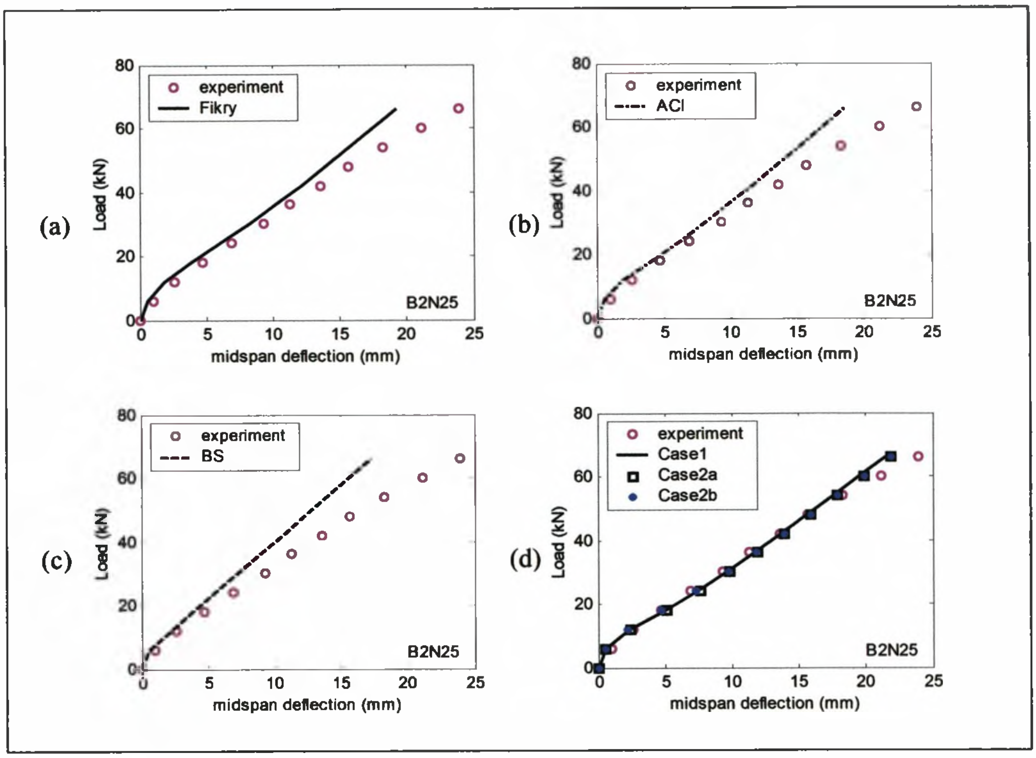

Figure 6.45 Typical output of deflection computation using various methods

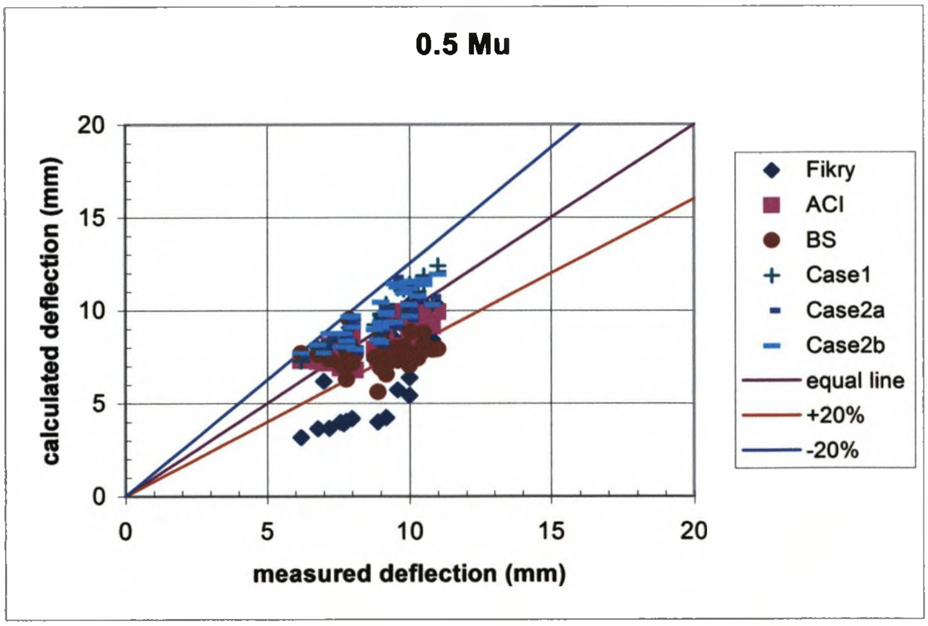

Figure 6.46 Comparison between measured and calculated deflection at 0.5Mu

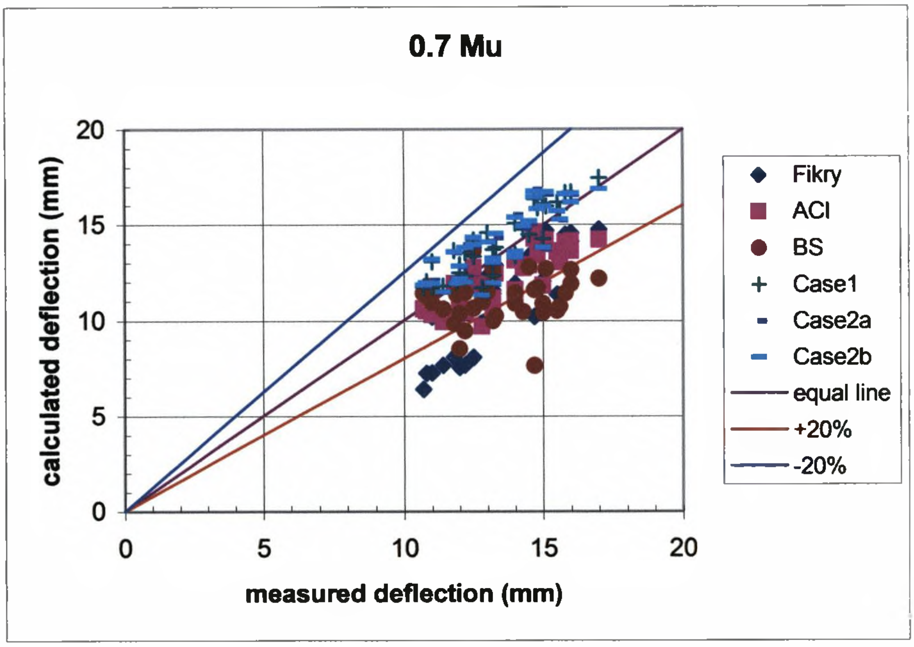

Figure 6.47 Comparison between measured and calculated deflection at 0.7Mu

Normally, predictions of deflections within a limit range of ± 20% error are allowed. When this limit is adopted it can be said that all three equations suggested in this study give accurate predictions for 50% ultimate load as shown in Figure 6.46. Fikry's method, however, gives prediction which is lower than the 20% limit for a few numbers of beams and in general the prediction underestimates the experimental deflections measured in this study. Similar results to Fikry's method are also produced by the British Standard method. The ACI method gives a much better prediction compared to Fikry's method and also the British Standard method. The ACI method gives values within the range specified, even though it still produces an underestimated prediction.

The same trend of deflection predictions obtained from various methods explained above, are shown in Figure 6.47 for 70% ultimate load.

6.9.2 Comparison with experimental results

As discussed previously, this study has been confined to use reinforcement ratios within the range of 0.82 to 1.64%, usually used in practice. Therefore the modified model produced should be checked to see whether it can be applied to reinforcement ratios outside the range considered.

Data was available from Beeby's technical report [15] consisting of 133 beams with various reinforcement ratios and concrete grades. Yield strength of steel reinforcement varied between 215 MPa and 493 MPa. The beams were all singly reinforced, sectional geometries were varied along with the effective depth. The beams were simply supported and loaded with two points load at a distance of 0.28 of the span from each support. Reinforcement ratios varied from a minimum of 0.86% to a maximum of 2.67%. This data will be used to check the modified models proposed in this study.

At 50% of ultimate applied loads, the three equations proposed in this study do not all agree with Beeby's experimental results. One equation, however, gives a closer result, which is the combination of I_{crm2} and Φ_{m2b} (Case 2b). This equation produces results quite similar to the ACI method but the majority of the predicted values slightly overestimate the deflection values as shown in Figure 6.48, which gives a safe condition for design.

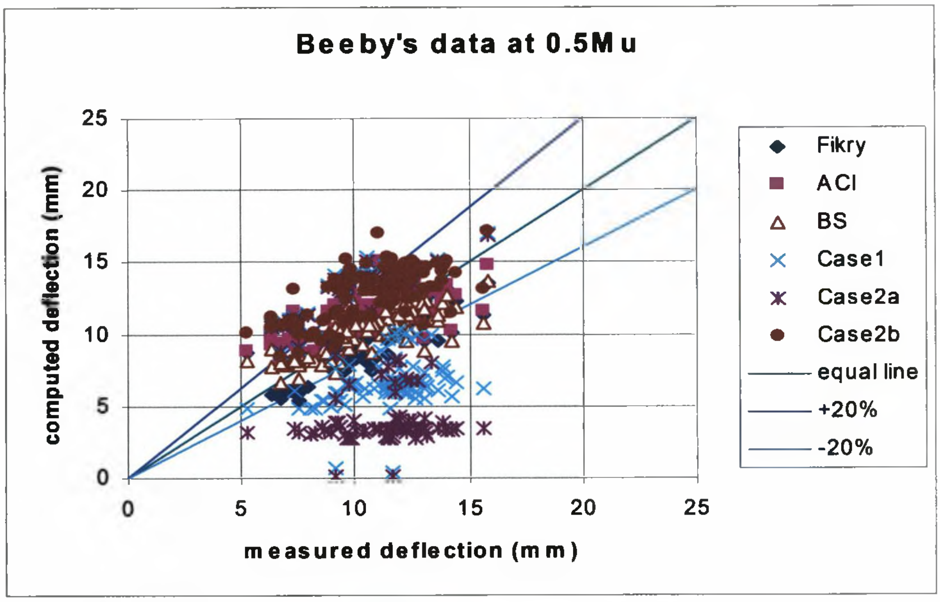

Figure 6.48 Comparison between measured and computed deflection of Beeby's data at 0.5Mu

The two other modified equations give poor results as majority of the deflection predictions are out of the 20% limit range specified. These equations are Case 1 and Case 2a.

The majority of results produced by Fikry's equation lie on the range specified but below the equal line which means that his equation will underestimate the value of deflection.

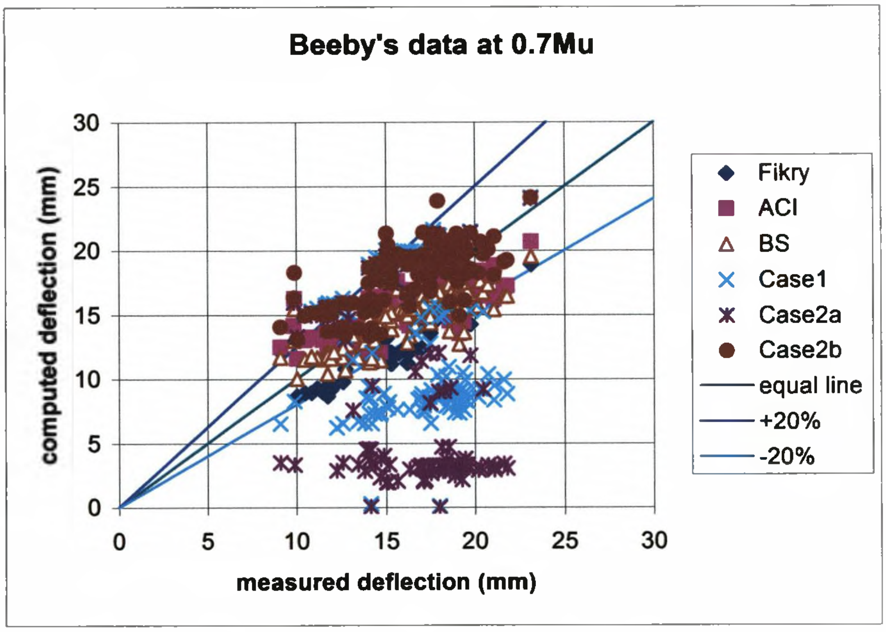

Figure 6.49 Comparison between measured and computed deflection of Beeby's data at 0.7Mu

At 70% of applied load, all the various methods used have a similar trend with deflection predictions obtained from the 50% of the applied load as shown in Figure 6.49.

In Beeby's report is also available data supplement carried out by Best et al and Perchat et al. The data that consists of 230 singly reinforced beams with various load positions, concrete strengths and reinforcement ratios was selected. The reinforcement ratio varies from 0.3% to 3.25%. The three proposed model are applied to these data. Only Case2b produces results within the 20% limit, as can be seen clearly in output of the computer programme in Appendix B-6. The results calculated using Fikry's, ACI, BS methods and Case2b are presented in Figure 6.50, 6.51, 6.52 and 6.53 respectively.

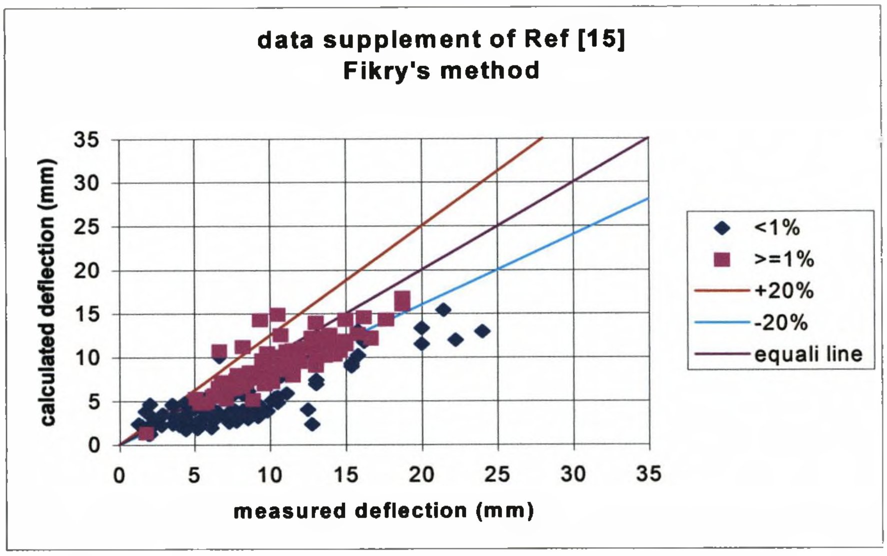

Figure 6.50 Comparison between measured and computed deflection for data supplement of Ref. [15] using Fikry's method

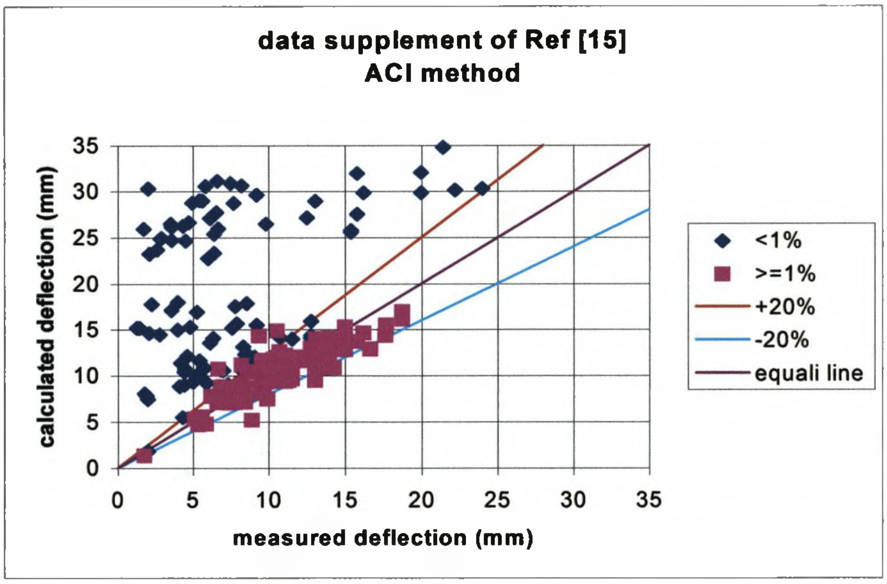

Figure 6.51 Comparison between measured and computed deflection for data supplement of Ref. [15] using ACI method

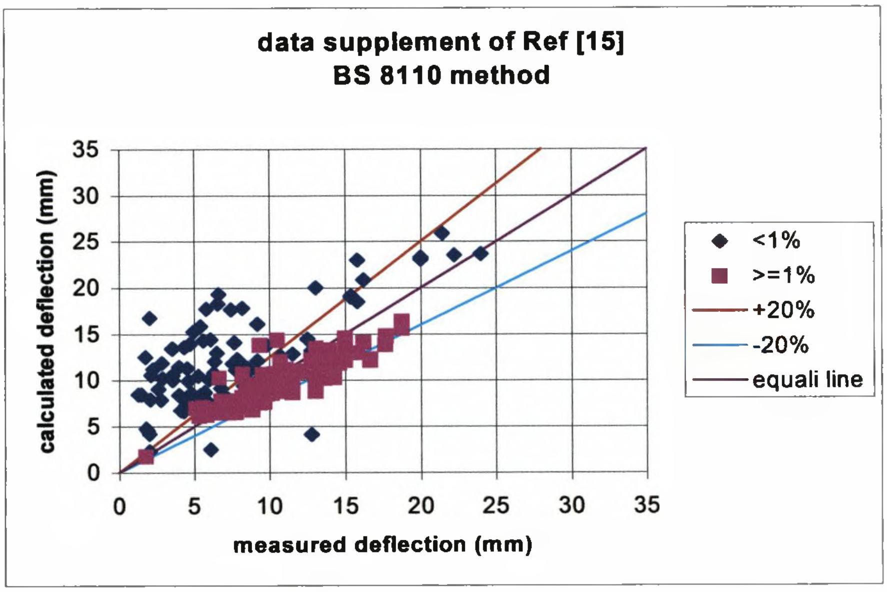

Figure 6.52 Comparison between measured and computed deflection for data supplement of Ref. [15] using BS8110 method

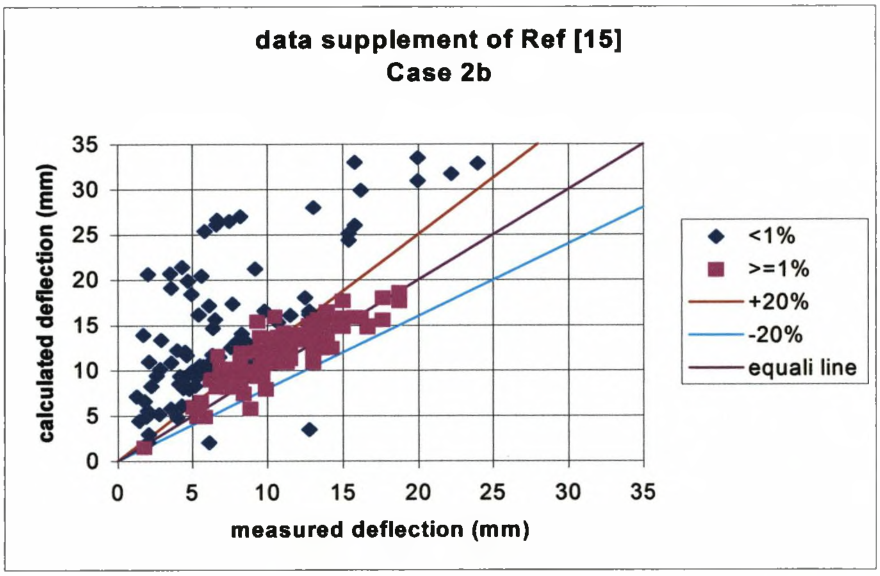

Figure 6.53 Comparison between measured and computed deflection for data supplement of Ref. [15] using Case2b

6.9.3 Discussion

The proposed model (Case1, Case2a and Case2b) discussed in Section 6.8 give a better prediction compared with ACI, BS and Fikry's method in terms of the sample beams considered in this study as shown in Figure 6.46 and 6.47.

When the proposed model was applied to data obtained from Reference [15], only Case 2b produced a prediction that agreed well with the ACI predictions as shown in Figure 6.48 and 6.49. This is due to the beams from this reference having reinforcement ratios higher than the beams considered in this study. It can be seen that the factor Φ in the proposed model produces different results. This can be explained as follows. Case1 and Case2a have different I_{cr}, Eq. (6.10) and (6.11), with similar linear ρ variation of factor Φ that produce results which are not valid for ρ out side range of this study. On the other hand, Case2b has the same I_{cr} as Case2a but the factor Φ variation is quadratic ρ, which produces different results from that of Case 2a. By referring to Figure 6.20 where two possibility of factor Φ are presented, it can be seen that when the linear line is extended it will produce the line intersect at C equal to zero at a specific value of ρ. This means that the value of factor Φ will be equal to zero. When the value of ρ exceeds the specific value, it will produce positive value of the factor Φ. When these values are used in Equation (1.2) they will produce $I_e \geq I_g$ causing deflection values that are smaller. The quadratic variation of ρ, however, always produces negative values of the factor Φ, which provides a value of I_e between I_{cr} and I_g. Therefore, by increasing the reinforcement ratio this case is still applicable as demonstrated by Figure 6.48 and 6.49.

For $\rho < 1\%$ the modified model is consistently at overestimate. This clearly can be seen in output of the computer programme in Appendix B-6.

Since Case 2b gives good agreement with the experimental results obtained from Reference [15], therefore only results calculated by Case 2b are presented alongside Fikry's, ACI and BS method as shown in Figure 6.50 to 6.53. The complete results for other cases can be seen in output of the computer programme in Appendix B-8.

The results from Figure 6.50 to 6.53 show that almost all of deflections calculated using Fikry's method underestimate the experimental results. The ACI method produces underestimated values for the deflections for ρ higher than 1% but the majority of deflection calculations overestimate the experimental results for ρ less than 1%. The British Standard produces similar trend of deflection values with the ACI method in terms of reinforcement ratio higher than 1% but give better prediction for reinforcement ratio lower than 1%. The proposed model, Case 2b, produces results that overestimate the measured deflections for most values of ρ. When the reinforcement ratio is higher than 1% most deflection calculations are within the 20% limit. For reinforcement ratio less than 1%, however, the results are outside the 20% limit but overestimate the experimental values, which give a safe design.

From the above discussion, it can be said that the proposed model, Case 2b, is valid to be used for beams with reinforcement ratio between 1% and 3%.

6.10 Summary

From the experimental results presented in the previous sections the following can be summarised:

(a) Experimental and theoretical cracking moment ratio varies considerably. This very much depends upon the reinforcement ratio. When their average ratio value was taken, the value of the ratio increases from lower to higher reinforcement ratio.

(b) Theoretical ultimate load values varied significantly between 0.65 and 0.85 of the value of the experimental ultimate load.

(c) Yield loads obtained experimentally have been used to modify cracked second moment of area value. The new I_{cr} was used to produce a modified factor Φ.

(d) Experimental service load values varied from 0.51 to 0.74 of the experimental ultimate load. This variation gave an average factor of safety of 1.66 which is bigger than global factor of safety of 1.47 obtained from the code.

(e) Cracked lengths produced experimentally give the same trend as the theoretical values. The experimental values were always slightly less than the theoretical values.

(f) The different results obtained between theoretical and experimental values of cracked lengths (L_{cr}) and cracking moments (M_{cr}) meant the factor Φ had to be modified to allow for this.

(g) The new I_{crm} and Φ_m that have been produced and used as a substitution for effective second moment of area of Fikry's model. The modified model produces accurate predictions in term of deflections almost in all cases. The factor Φ, with polynomial C variation, gave more accurate results for deflection prediction of high reinforcement ratio.

Chapter 7

Conclusions and Recommendations

7.1 Introduction

In Chapter 6 three possibilities to improve the evaluation of the second moment of area based on Fikry's model were developed. Initially, two models for the approximation of I_{cr} were proposed. The theoretical models proposed were validated by comparison with beams tested during this study and also test results obtained from a number of papers. In developing the model the practicality of using it in a design procedure was always considered.

In this chapter, the results of the study presented in Chapter 6 are summarized followed by conclusions and suggestions for possible future research.

7.2 Improvement on the previous model

The three proposed model mentioned above consist of a combination between two possible models of proposed I_{cr} and three possible models of proposed factors Φ.

Each modified I_{cr} produced a different Φ equation. The details of this improvement are discussed in section below.

7.2.1 Cracked second moment of area

Originally, the cracked second moment of area was calculated using Equation (4-7) in Chapter 4, and denoted as I_{cre}. The value of I_{cre} varies depending on the value of $n\rho$, which consists of five different ranges. In this study, however, the range containing the greatest range of $n\rho$ was considered. This range covers the values used in practice.

Two possible models of I_{cre} were proposed. I_{cre} considering f_{cu} and ρ and I_{cre} with $n\rho$ factor. The first model is given by Equation (6-10) and denoted as I_{crm1}. The second model has similar form with the previous proposed model but slightly different coefficient as given by Equation (6-11) and denoted as I_{crm2}. Basically, both models are an attempt to take into account the effect of the concrete strength and the reinforcement ratio. In the first model the concrete strength appears directly in the equation, but in the second model its effect is represented by the modular ratio, n. The modular ratio represents the ratio of the steel modulus of elastic to concrete modulus of elasticity. The concrete modulus being a function of the concrete strength.

Two models of the proposed cracked second moment of area, I_{crm1} and I_{crm2}, discussed above produce a smaller value of I_{cr} compared with the I_{cre} value of the previous model. This value varies from 0.84 to 0.91 of the previous model value as can be seen in Table 6-12. The result of this study also agrees with the result obtained from reference [18] in terms of the experimental value of I_{cr} being lower than the theoretical value.

7.2.2 Factor Φ

As the value I_{cre} was modified the factor Φ also had to be modified. The original form of factor Φ is given by Equation (4-12) which is a function of M_a/M_{cr}, L_{cr}/L and ρ. From the experimental results in Chapter 6 it was found that the values of M_{cr} and L_{cr} vary depending upon the reinforcement ratio, ρ, which can be seen in Equation (6-2) and Equation (6-5) respectively. However as the factor Φ is directly a function of ρ in order to obtain a practical equation the variation of ρ against Φ was considered assuming the original theoretical values of M_{cr} and L_{cr} only.

For each proposed I_{crm}, discussed in Section 7.2.1, a different equation for factor Φ is produced. The combinations between the proposed cracked second moment of area, I_{crm}, and factor Φ are summarised in Table 6-13.

As a result of the combinations discussed above three modified models for I_e are proposed, namely Case1, Case2a and Case 2b. All the Cases in this study gave good agreement with the experimental results. However, Case 2b, I_{crm2} when combined with Φ_{m2b} which has quadratic ρ variation, gave good agreement when the model is applied to beams which have reinforcement ratio larger than those considered in this study. This means that the Φ prediction in this study is valid for ρ outside the range considered in this study as long as within range of $n\rho < 23\%$.

7.3 Concluding remarks

Since conclusions have been given at the end of each chapter, only the main points are highlighted here.

1. From a simple graph of load against deflection four variables can be observed. Load causing first crack, load when the steel reinforcement yielded, ultimate load and load at the service condition as tabulated in Table 6-7 and 6-8.
2. The results showed that cracking moment varies depending upon the amount of reinforcement as shown in Table 6.7.
3. The ultimate loads obtained in this study were higher than the calculated ultimate loads. This means that the theoretical ultimate load provides a safe value.
4. The ratio of experimental service load to experimental ultimate load varies between 0.51 and 0.74. From this result it can be said a serviceability factor of 1.66 was obtained. This also agrees with the factor used in practice by many researches who have compared their results at 0.5 P_u and 0.7 P_u.
5. A new technique to measured L_{cr} was introduced using recorded photograph. The results showed that a similar trend to the theoretical one was obtained.
6. Two possible models for I_{cre} were proposed. Both showed the value varies from 78 to 98 % of the previous model. Three variations for the factor Φ have also been proposed.
7. With developing the new I_{cr} and factor Φ consequently a new model for I_e, namely I_{em}, was proposed. In general the value I_{em} was lower than the previous model which produced a larger deflection than the previous model.
8. Using the model proposed in this study the vast majority of the deflections over estimated the experimental values but within a 20% error range.
9. The model also agrees with the experimental results when applied to a simple supported beam with two unsymmetrical point loads.

7.4 Suggestions for future works

Due to the limited time and funds available, the experiments carried out for this research only focuses on single-reinforced beams. Fikry's modified model for this type of beams is presented in this thesis. There are two significant modifications i.e. I_{cr} and the factor Φ as discussed in the previous section.

Single-reinforced beams are probably the simplest element in the structure of a building. A significant amount of time, however, is required to calculate the value of their I_{cr}. More effort is therefore necessary to determine the I_{cr} of the more complicated beam sections such as double-reinforced beams, single reinforced and double-reinforced T-sections, etc.

From the above discussion, some suggestions for future research can therefore be proposed as follows:

1. Experiment to verify the applicability of the proposed model on other beam sections e.g. double-reinforced beams, single- and double-reinforced T-sections, etc. is necessary.

2. Beam deflection calculation for continuous beams is based on the same principle as that of the simple supported beam. In theory, therefore, the proposed model should be valid to the continuous beam cases. Nevertheless, the author suggests that some experiment is needed to confirm this argument.

3. More research is also necessary to extend the applicability of the proposed model to fibre reinforced concrete beams. It is desirable to maintain the same general

expression for the calculation of I_e. However, the addition of fibre reinforcement would have an effect on the value of I_{cr} and the factor Φ. Experimental work is therefore needed to determine these values.

References

[1] Branson, D.E., "Instataneous and Time dependent Deflection of simple and Continues Reinforced Concrete Beams", *HPR Report No. 7, Part 1, Alabama, Highway Departement/US Bureau of Public Roads*, Augustus 1963 (1965), pp 1-78.

[2] Fikry, A. M., "Development of a model to estimate the effective second moment of area of one-way reinforced concrete flexural element", PhD Thesis, University of Liverpool, 1996

[3] Ghali, A., Favre, R., and Elbadry, M., "Concrete Structure Stresses and Deformations" 3td Ed., *Spn Press* , London, 2002

[4] Yu, W. and Winter, G., "Instantaneous and Long-Time Deflection of Reinforced Concrete Beams Under Working Loads", *ACI Journal Proceedings*, V. 57, No.1, July 1960, pp29-50.

[5] ACI Committee 318 "Building Code Requirement for RC and Commentary (ACI 318-89/ACI 318R-89), *American Concrete Institute*, Detroit, 1989, 353 pp.

[6] Design of Concrete Structures for Buildings (CAN 3-A233-M84), "Canadian Standards Associations", Rexdale, 1984, 281 pp.

[7] Al-Shaikh, A.H., Al-Zaid, R.Z., "Effect of Reinforcement Ratio of Reinforced Concrete Beams", *ACI Structural Journal*, V 90, No. 2, March-April, 1993, pp. 144-148

[8] Ghali, A., "Deflection of Reinforced Concrete Members: A Critical Review", *ACI Structural Journal*, V 90, No. 4, July-August, 1993, pp. 364-373

[9] Grossman, J. S., "Simplified Computations for Effective Moment of Inertia Ie and Minimum Thickness to avoid Deflection Computations", *ACI Structural Journal*, V 78, Nov-Dec, 1981, pp. 423-439

[10] Rangan V. B., "Control of Beam Deflections by Allowable Span-Depth Ratio", *ACI Structural Journal*, V 79, Sept-October, 1982, pp. 372-377

[11] Duan, L., Wang, F., and Chen, W., "Flexural Rigidity of Reinforced Concrete Members", *ACI Structural Journal*, V 86, July August, 1989, pp. 419 427

[12] Al-Zaid, R. Z., Al-Shaikh, A. H. and Abu-Hussein, M. M., "Effect of Loading Type on the Effective Moment of Inertia of Reinforced Concrete Beams", *ACI Structural Journal*, V 88, March-April 1991. pp. 184-190

[13] Abdullah M. Fikry and Cledwyn Thomas, "Development of a model for the effective moment of inertia of one-way reinforced concrete elements", *ACI Structural Journal*, V 95, No. 4, July-August, 1998, pp. 444-455

[14] Al-Shaikh, A.H., Al-Zaid, R.Z., "Effect of Reinforcement Ratio of Reinforced Concrete Beams", *ACI Structural Journal*, V 90, No. 2, March-April, 1993, pp. 144-148

[15] Beeby, A. W. "Short-term Deflection of Reinforced Concrete Members" Technical Report No. TRA-408, *Cement and Concrete Association*, London, March, 1968.

[16] Gilbert, R. I., "Deflection Calculation for Reinforced Concrete Structures-Why We Sometimes Get It Wrong", *ACI Structural Journal*, V 96, November-December 1999, pp. 1027-1032

[17] Gilbert, R. I., "Shrinkage, Cracking and Deflection - the Serviceability of Concrete Structures", *Electronic Journal of Structural Engineering*, V 1, 2001, pp. 15-37

[18] Ashour, S. A., "Effect of Compressive strength and Tensile Reinforcement ratio on flexural behaviour of high-strength concrete beams", *Engineering Structures*, V 22., 2000, pp. 413-423

[19] BS 1881 part 116, "Method for determination of compressive strength of concrete cube", *British Standard*, 1983

[20] BS 1881 part 121, "Method for determination of Static modulus of elasticity in Compression", *British Standard*, 1983

[21] Mosley, W. H., Bungey, J. H., & Hulse, R., "Reinforced Concrete Design", 5th Ed., *Macmillan Press Ltd.*, 1999

[22] Regan, P. E. and Yu, C. W, "Limit State Design of Structural Concrete", *Chatto & Windus*, London, 1973

[23] Nawy, E. G., Reinforced Concrete a Fundamental Approach, 5th Ed., *Printice Hall*, New Jersey, 2003

[24] Carrasquillo, R. L., Nilson , A. H., and Slate, F. O., "Properties of High Strength Concrete Subject to Short-Term Loads", *ACI Structural Journal*, V 78, May-June, 1981, pp. 171-178

[25] BS 8110 part 2, "Structural use of concrete – Code of practice for special circumstances", *British Standard*, 1985

[26] ACI Committee 340, "Design Handbook in Accordance with the Strength Design Method of ACI 318-84. Vol 1 – Beams, One-way Slabs, Brackets,

Footings, and Pile Caps [SP-17(84)]", 4th Ed. Detroid, *American Concrete Institute*, 1984

[27] Arther H. Nilson and Winter G., "Design of Concrete Structure", 11th Ed., *McGraw-Hill*, Singapore, 1991

[28] Wang C. and Salmon, C. G., "Reinforced Concrete Design", 5th Ed., *HarperCollins*, NewYork, 1992

[29] BS 8110 part 1, "Structural Use of Concrete-Code of Practice for Design and Construction", *British Standard*, 1997

[30] BS 4482, "Specification for Cold Reduced Steel Wire for the Reinforcement of Concrete", *British Standard online*, 1985

[31] Numbergerova, T., Krizma, M. and Hajek, J., "Theoretical model of the determination of deformation rates of RC beams", *Construction and Building Material*, V 15, 2001, pp. 169-176

[32] Leet K., "Reinforced Concrete Design", *McGraw-Hill*, USA, 1982

[33] Kuang, K S C., Akmaluddin, Cantwell, W. J. and Thomas C., "Crack Detection and Deflection monitoring using Plastic Optical Fibre Sensors", *Measurement Science and Technology*, V 14, 2003, pp. 205-216

[34] Building Research Establishment Report, Design of Normal Concrete Mixes, *Department of Environment*, 1992

[35] MacGregor, J. G., "Reinforced Concrete: Mechanism and Design", 3rd edition, Prentice Hall, 1997

[36] Desayi, P. and Rao K B., "Probabilistic analysis of Cracking Moment of Reinforced Concrete Beams", *ACI Structural Journal*, V 86, May-June 1989, pp. 235-241

Appendix A

- **Experimental load-deflection curves**
- **Crack length measurements**

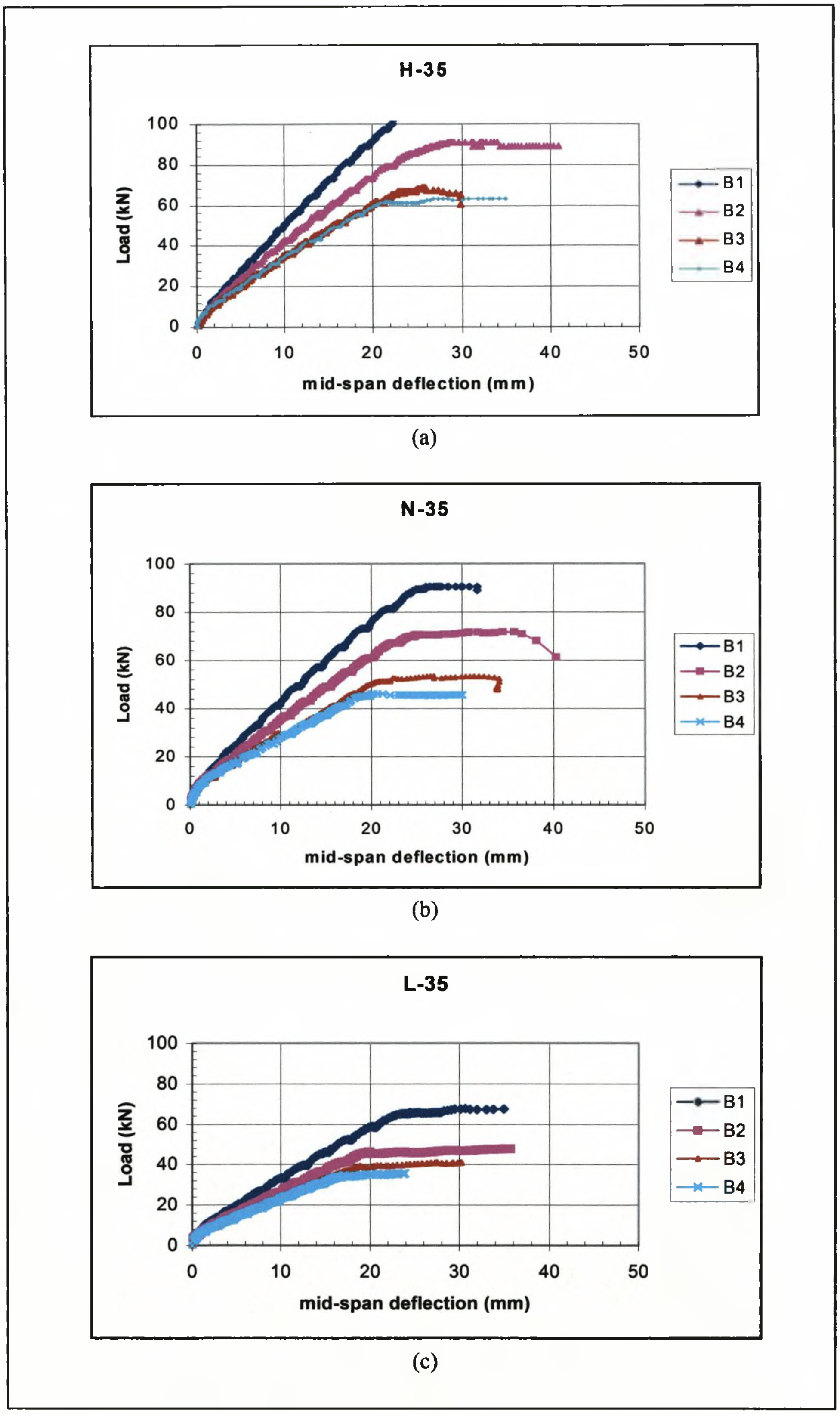

Figure A-1 Beams deflection behaviour for various load position for 35 MPa concrete strength with : (a) Heavy reinforcement, (b) Normal reinforcement, (c) Low reinforcement

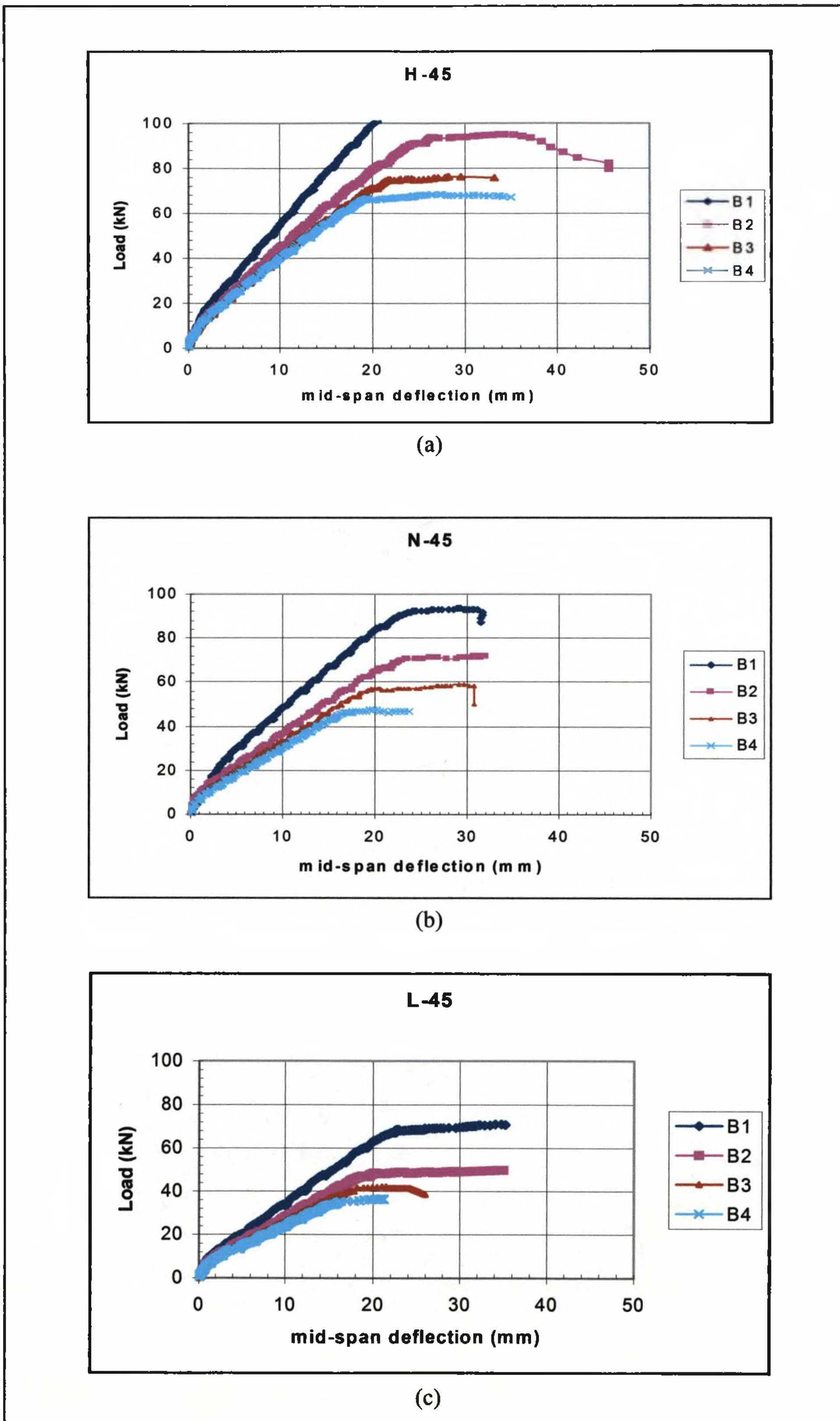

Figure A-2 Beams deflection behaviour for various load position for 45 MPa concrete strength with : (a) Heavy reinforcement, (b) Normal reinforcement, (c) Low reinforcement

Table A- 1 Comparison between the experimental and the theoretical crack length

Beam	Load #	$L_{cr(exp)}$ (m)	$L_{cr(th)}$ (m)	Average $L_{cr(th)}$ (m)	ratio	Average ratio
B1L25	3	1.85	1.76	1.76	1.05	1.01
	4	2.12	2.01	2.18	0.97	
	5		2.16			
	6		2.36			
	7	2.39	2.33	2.40	1.00	
	8		2.38			
	9		2.42			
	10		2.45			
B1L35	3	1.75	1.78	1.78	0.98	1.02
	5	2.05	2.17	2.22	1.08	
	6		2.26			
	7	2.41	2.33	2.41	1.00	
	8		2.38			
	9		2.43			
	10		2.48			
B1N25	1	1.07	0.9	0.9	1.18	1.05
	4	2.27	2.29	2.29	0.99	
	5	2.45	2.38	2.47	0.99	
	6		2.44			
	7		2.49			
	8		2.52			
	9		2.54			
B1H45	2	1.39	1.76	1.76	0.79	0.85
	3	1.77	2.09	2.09	0.85	
	5	2.28	2.35	2.475	0.92	
	6		2.42			
	7		2.47			
	8		2.5			
	9		2.53			
	10		2.58			
B1H25	3	2.12	2.2	2.32	0.91	0.93
	4		2.34			
	5		2.42			
	6	2.26	2.48	2.525	0.90	
	7		2.51			
	8		2.54			
	9		2.57			
	10	2.56	2.59	2.59	0.99	1.05
B2L35	2	1.59	1.00	1.29	1.23	
	3		1.58			
	5	2.09	2.05	2.16	0.97	
	6		2.17			
	7		2.25			
	8	2.33	2.31	2.31	1.01	

Table A- 1 Continued

Beam	Load #	$L_{cr(exp)}$	$L_{cr(th)}$	Average $L_{cr(th)}$	ratio	Average ratio
B2N25	2	1.09	1.52	1.52	0.72	0.86
	3	1.75	1.93	1.93	0.91	
	7	2.36	2.40	2.44	0.97	
	8		2.44			
	9		2.48			
B2H25	2	1.43	1.69	1.69	0.85	0.90
	3	1.95	2.04	2.20	0.89	
	4		2.22			
	5		2.33			
	7	2.42	2.45	2.47	0.98	
	8		2.49			
B2H45	2	1.66	1.65	1.65	1.01	0.96
	4	2.08	2.20	2.30	0.91	
	5		2.31			
	6		2.38			
	8	2.41	2.47	2.50	0.96	
	9		2.50			
	10		2.53			
B3L35	3	1.58	1.29	1.47	1.07	1.01
	4		1.65			
	5	1.90	1.87	2.00	0.95	
	6		2.02			
	7		2.12			
	8	2.24	2.20	2.23	1.00	
	9		2.26			
B3H45	2	0.92	1.33	1.33	0.69	0.82
	3	1.62	1.80	1.80	0.90	
	7	2.11	2.34	2.39	0.88	
	8		2.40			
	9		2.43			
B4L25	3	1.36	1.10	1.10	1.24	1.08
	4	1.72	1.52	1.64	1.05	
	5		1.76			
	6	1.98	1.93	2.07	0.96	
	7		2.04			
	8		2.13			
	9		2.20			
B4H25	3	1.11	1.52	1.52	0.73	0.84
	5	1.58	2.01	2.07	0.76	
	6		2.13			
	7	1.96	2.22	2.26	0.87	
	8		2.29			
	11	2.26	2.26	2.26	1.00	
B4H45	3	1.43	1.65	1.65	0.87	0.90
	4	1.81	1.92	1.92	0.94	
	8	2.11	2.34	2.36	0.89	
	9		2.38			

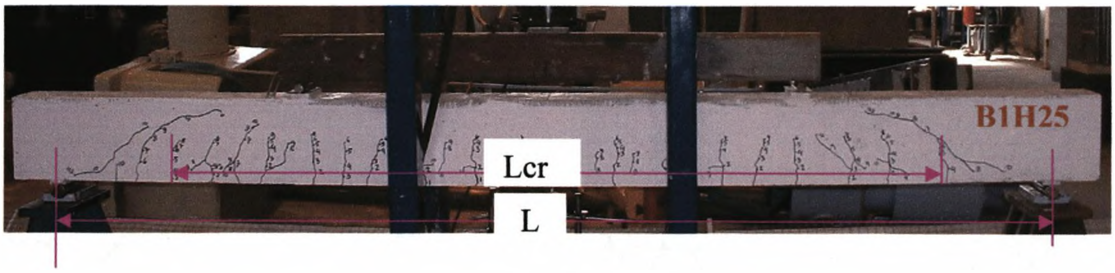

(a)

Scaling from picture (a) for load #3,4,5:

L = 13.15 cm	actual size	L= 2.75 m
Lcr = 10.16 cm	therefore,	Lcr = 2.75x(10.16/13.15) = 2.12 m

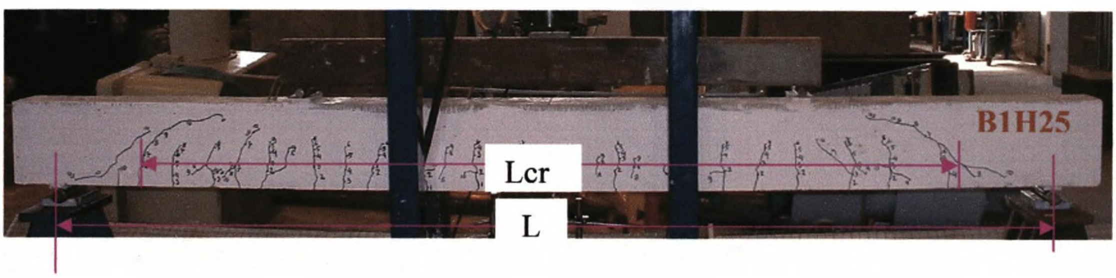

(b)

Scaling from picture (b) for load #6,7,8,9:

L = 13.15 cm	actual size	L= 2.75 m
Lcr = 10.80 cm	therefore,	Lcr = 2.75x(10.80/13.15) = 2.26 m

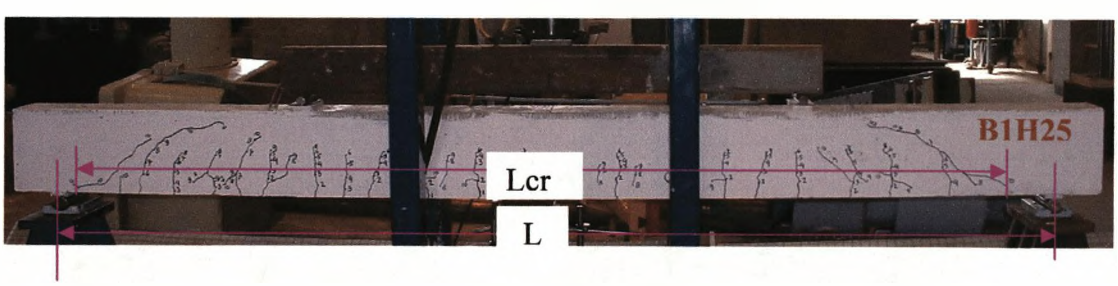

(c)

Scaling from picture (c) for load #10:

L = 13.15 cm	actual size	L= 2.75 m
Lcr = 12.25 cm	therefore,	Lcr = 2.75x(12.25/13.15) = 2.56 m

Figure A-1 Experimental cracked length of beam B1H25

(a)

Scaling from picture (a) for load #2:

L = 13.44 cm	actual size	L= 2.75 m
Lcr = 6.99 cm	therefore,	Lcr = 2.75x(6.99/13.44) = 1.43 m

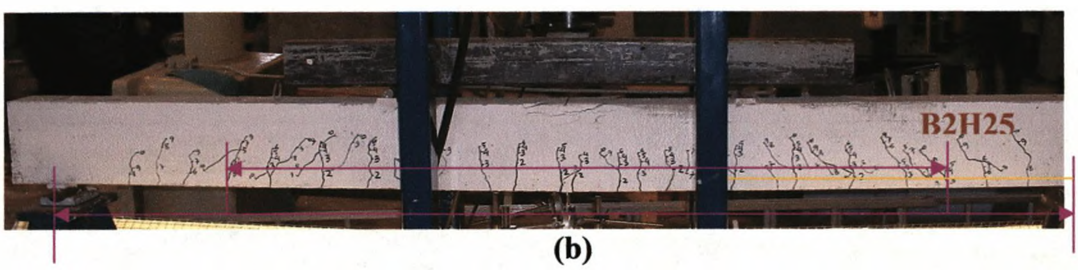

(b)

Scaling from picture (b) for load #3,4,5:

L = 13.44 cm	actual size	L= 2.75 m
Lcr = 9.53 cm	therefore,	Lcr = 2.75x(9.53/13.44) = 1.95 m

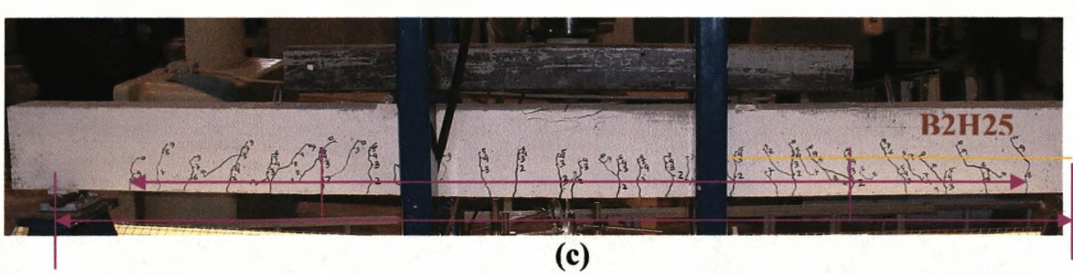

(c)

Scaling from picture (c) for load #7,8:

L = 13.44 cm	actual size	L= 2.75 m
Lcr = 11.85 cm	therefore,	Lcr = 2.75x(11.85/13.44) = 2.42 m

Figure A-2 Experimental cracked length of beam B2H25

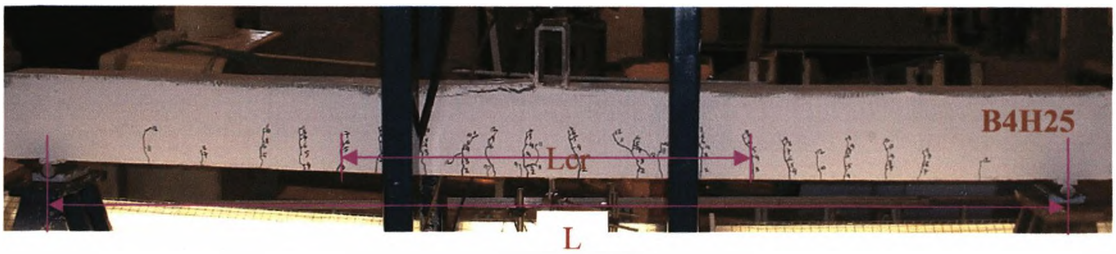

(a)

Scaling from picture (a) for load #3:

L = 13.39 cm	actual size	L= 2.75 m
Lcr = 5.40 cm	therefore,	Lcr = 2.75x(5.40/13.39) = 1.11 m

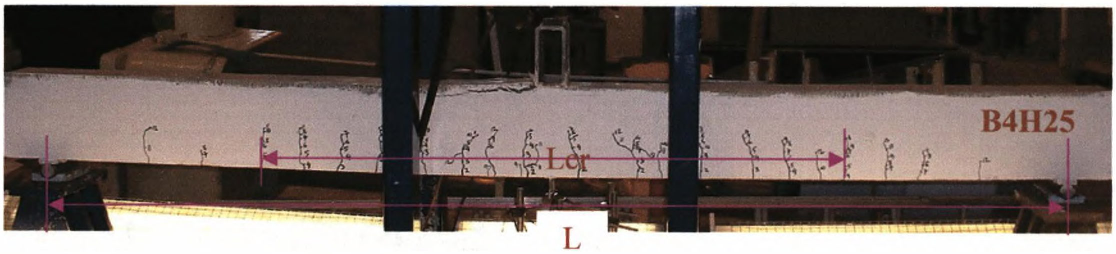

(b)

Scaling from picture (b) for load #5,6:

L = 13.39 cm	actual size	L= 2.75 m
Lcr = 7.70 cm	therefore,	Lcr = 2.75x(7.70/13.39) = 1.58 m

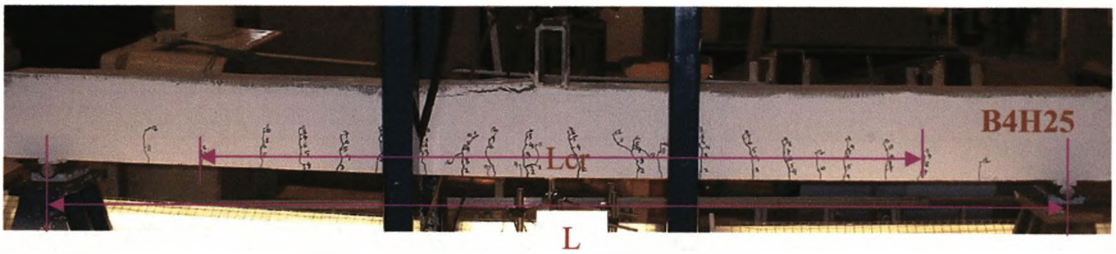

(c)

Scaling from picture (c) for load #7,8:

L = 13.39 cm	actual size	L= 2.75 m
Lcr = 9.53 cm	therefore,	Lcr = 2.75x(9.53/13.39) = 1.96 m

Figure A-3 Experimental cracked length of beam B4H25

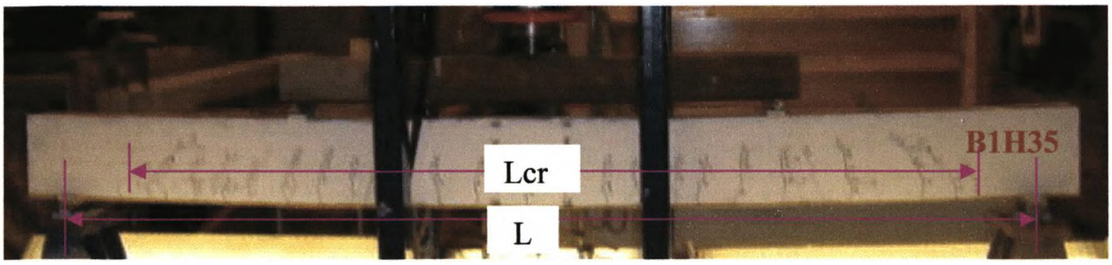

(a)

Scaling from picture (a) for ultimate load :

L = 12.80 cm	actual size	L= 2.75 m
Lcr = 11.20 cm	therefore,	Lcr = 2.75x(11.20/12.80) = 2.41 m

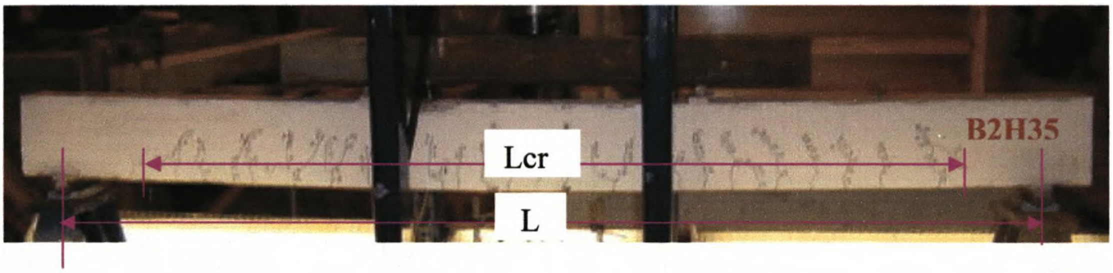

(b)

Scaling from picture (b) for ultimate load :

L = 13.01 cm	actual size	L= 2.75 m
Lcr = 10.85 cm	therefore,	Lcr = 2.75x(10.08/13.01) = 2.13 m

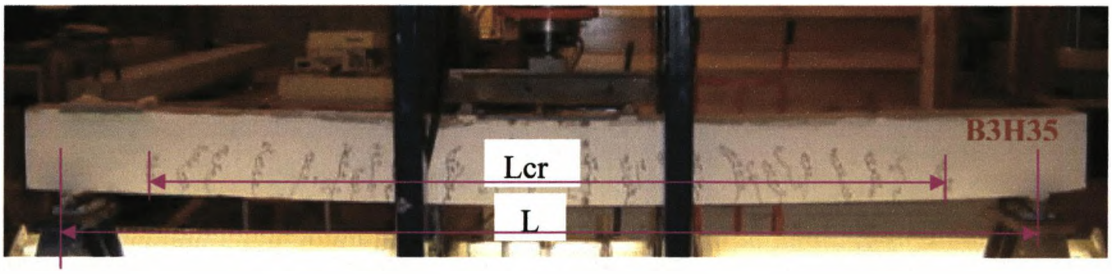

(c)

Scaling from picture (c) for ultimate load load :

L = 12.96 cm	actual size	L= 2.75 m
Lcr = 10.56 cm	therefore,	Lcr = 2.75x(11.38/13.00) = 2.24 m

Figure A-4 Experimental cracked length of beam B1H35, B2H35, and B3H35 at their ultimate load

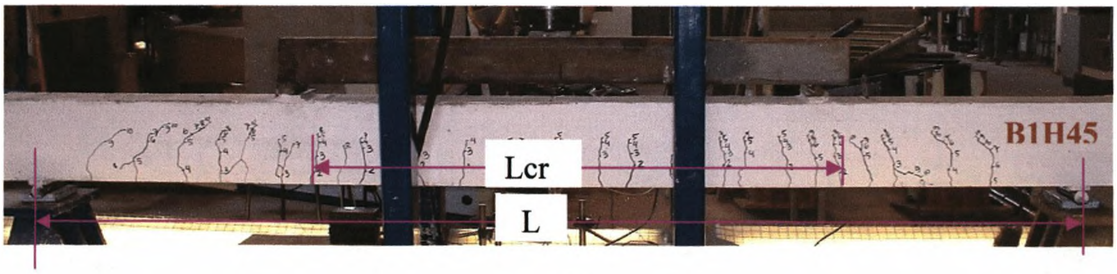

(a)

Scaling from picture (a) for load #2:

L = 13.80 cm	actual size	L= 2.75 m
Lcr = 6.99 cm	therefore,	Lcr = 2.75x(6.99/13.80) = 1.39 m

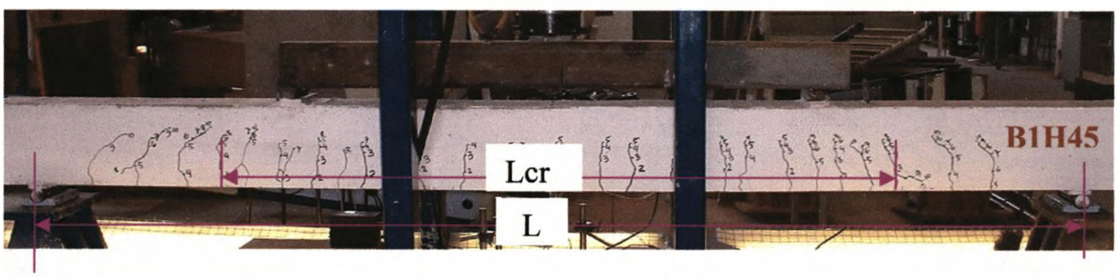

(b)

Scaling from picture (b) for load #3 :

L = 13.80 cm	actual size	L= 2.75 m
Lcr = 8.89 cm	therefore,	Lcr = 2.75x(8.89/13.80) = 1.77 m

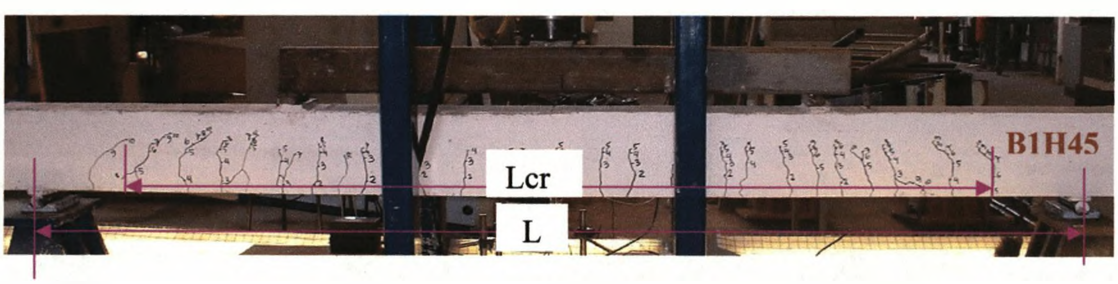

(c)

Scaling from picture (c) for load #5,6,7,8,9,10 :

L = 13.80 cm	actual size	L= 2.75 m
Lcr = 11.43 cm	therefore,	Lcr = 2.75x(11.43/13.80) = 2.28 m

Figure A-5 Experimental cracked length of beam B1H45

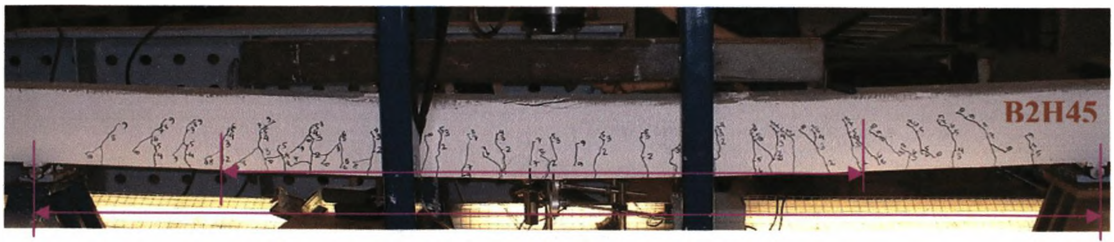

(a)

Scaling from picture (a) for load #2 :
L = 14.10 cm actual size L= 2.75 m
Lcr = 8.50 cm therefore, Lcr = 2.75x(8.50/14.10) = 1.66 m

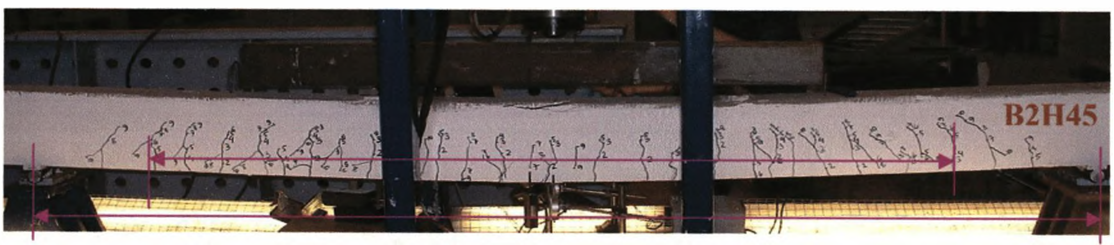

(b)

Scaling from picture (b) for load #4,5,6 :
L = 14.10 cm actual size L= 2.75 m
Lcr = 10.65 cm therefore, Lcr = 2.75x(10.65/14.10) = 2.08 m

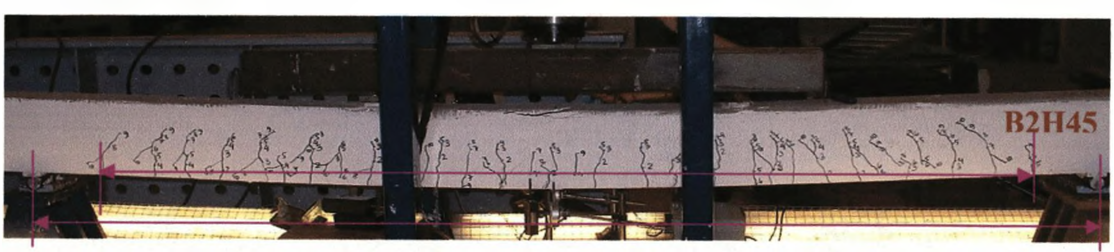

(c)

Scaling from picture (c) for load #8,9,10 :
L = 14.10 cm actual size L= 2.75 m
Lcr = 12.35 cm therefore, Lcr = 2.75x(12.35/14.10) = 2.41 m

Figure A-6 Experimental cracked length of beam B2H45

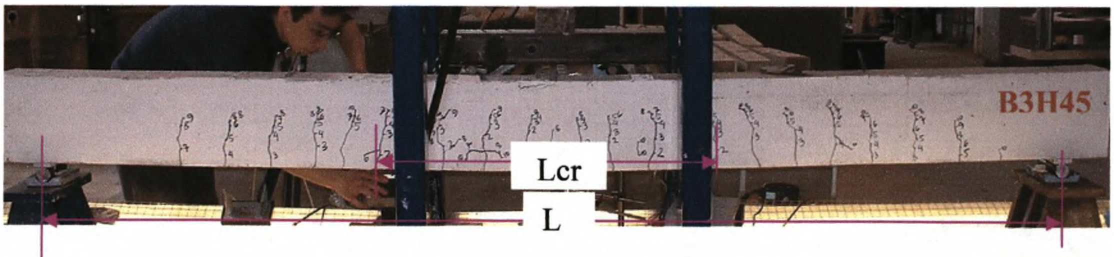

Scaling from the picture above for load #2 :

L = 13.55 cm	actual size	L= 2.75 m
Lcr = 4.50 cm	therefore,	Lcr = 2.75x(4.50/13.45) = 0.92 m

Scaling from the picture above for load #3 :

L = 13.55 cm	actual size	L= 2.75 m
Lcr = 7.94 cm	therefore,	Lcr = 2.75x(7.94/13.45) = 1.62 m

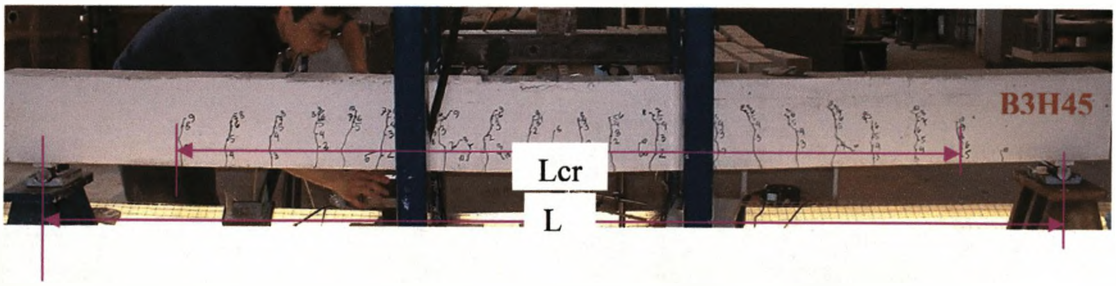

Scaling from the picture above for load #7,8,9 :

L = 13.55 cm	actual size	L= 2.75 m
Lcr = 10.34 cm	therefore,	Lcr = 2.75x(10.34/13.45) = 2.11 m

Figure A-7 Experimental cracked length of beam B3H45

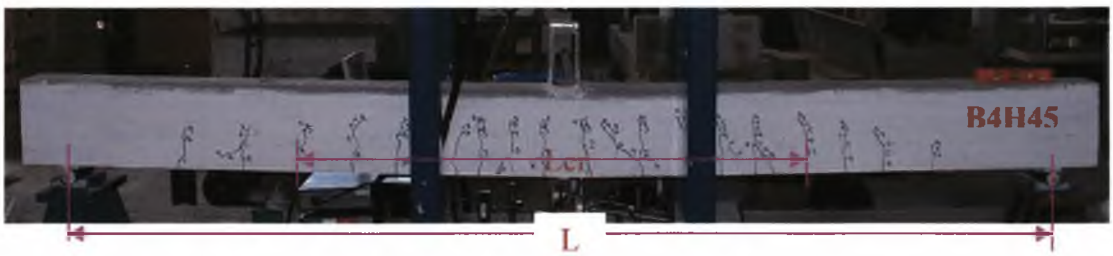

Scaling from the picture above for load #3 :

L = 13.01 cm	actual size	L= 2.75 m
Lcr = 6.75 cm	therefore,	Lcr = 2.75x(6.75/13.01) = 1.43 m

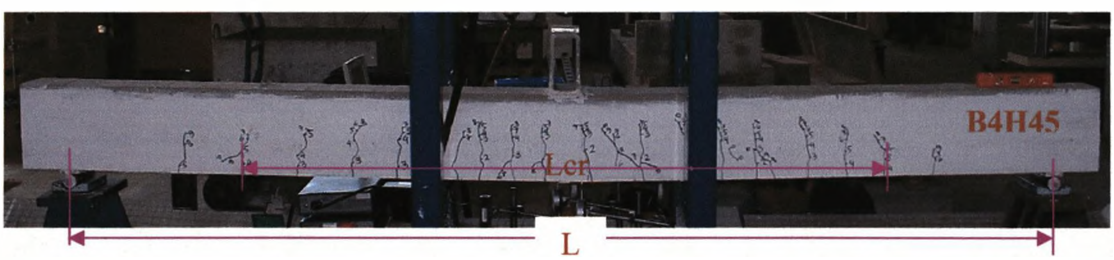

Scaling from the picture above for load #4 :

L = 13.01 cm	actual size	L= 2.75 m
Lcr = 8.57 cm	therefore,	Lcr = 2.75x(8.57/13.01) = 1.81 m

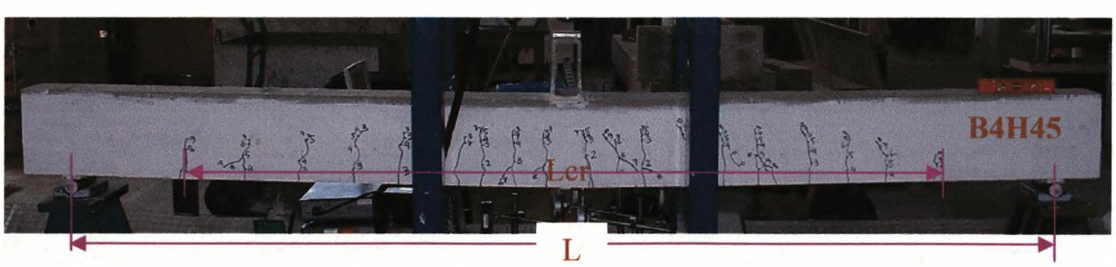

Scaling from the picture above for load #8,9 :

L = 13.01 cm	actual size	L= 2.75 m
Lcr = 10.00 cm	therefore,	Lcr = 2.75x(10.00/13.01) = 2.11 m

Figure A-8 Experimental cracked length of beam B3H45

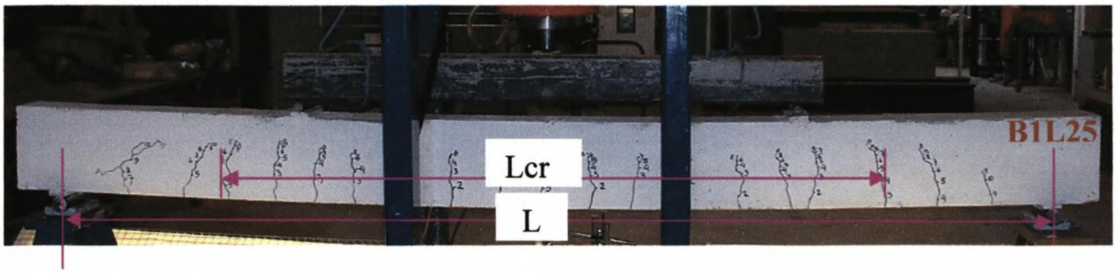

Scaling from the picture above for load #3:
L = 13.00 cm actual size L= 2.75 m
Lcr = 8.75 cm therefore, Lcr = 2.75x(8.75/13.00) = 1.85 m

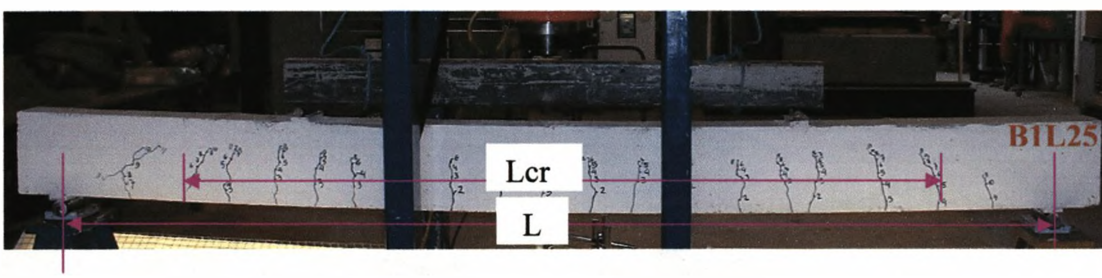

Scaling from the picture above for load #4,5,6:
L = 13.00 cm actual size L= 2.75 m
Lcr = 10.00 cm therefore, Lcr = 2.75x(10.00/13.00) = 2.12 m

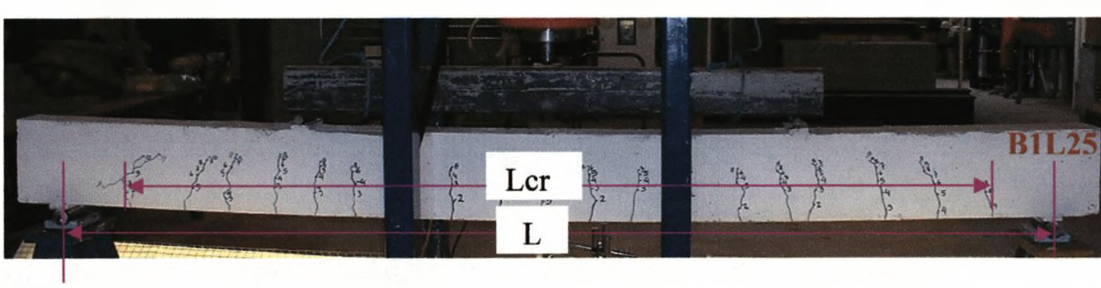

Scaling from the picture above for load #7,8,9,10:
L = 13.00 cm actual size L= 2.75 m
Lcr = 11.3 cm therefore, Lcr = 2.75x(11.30/13.00) = 2.39 m

Figure A-9 Measured cracked length of B1L25 at various load level

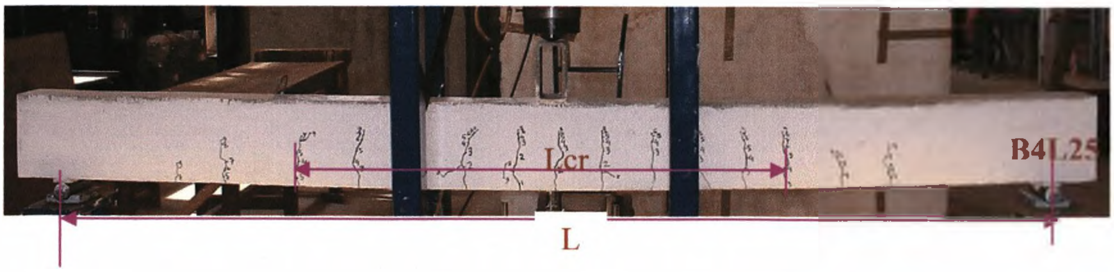

Scaling from the picture above for load #3:

L = 13.18 cm	actual size	L= 2.75 m
Lcr = 6.50 cm	therefore,	Lcr = 2.75x(6.50/13.18) = 1.36 m

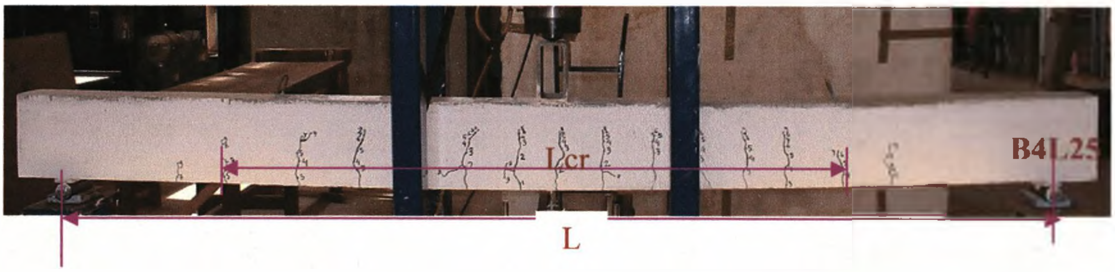

Scaling from the picture above for load #4,5:

L = 13.18 cm	actual size	L= 2.75 m
Lcr = 8.26 cm	therefore,	Lcr = 2.75x(8.26/13.18) = 1.72 m

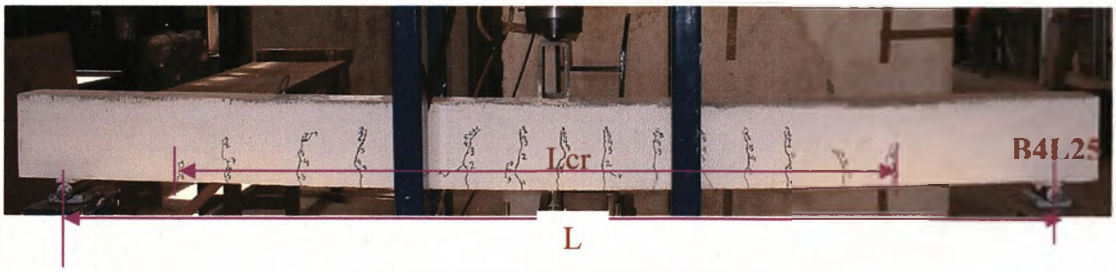

Scaling from the picture above for load #6,7,8,9:

L = 13.18 cm	actual size	L= 2.75 m
Lcr = 9.47 cm	therefore,	Lcr = 2.75x(9.47/13.18) = 1.98 m

Figure A-10 Measured cracked length of B4L25 at various load level

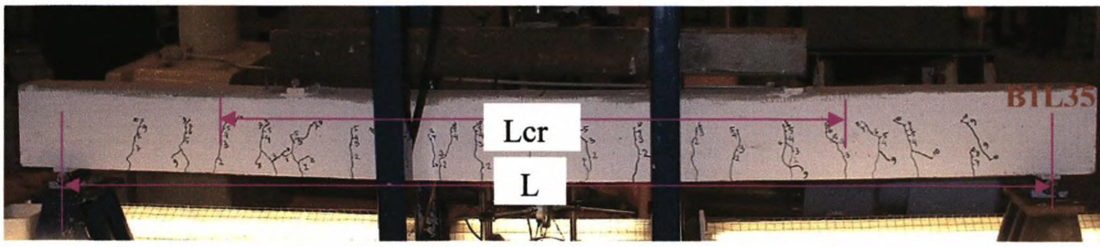

Scaling from the picture above for load #3:

L = 13.00 cm	actual size	L= 2.75 m
Lcr = 8.26 cm	therefore,	Lcr = 2.75x(8.26/13.00) = 1.75 m

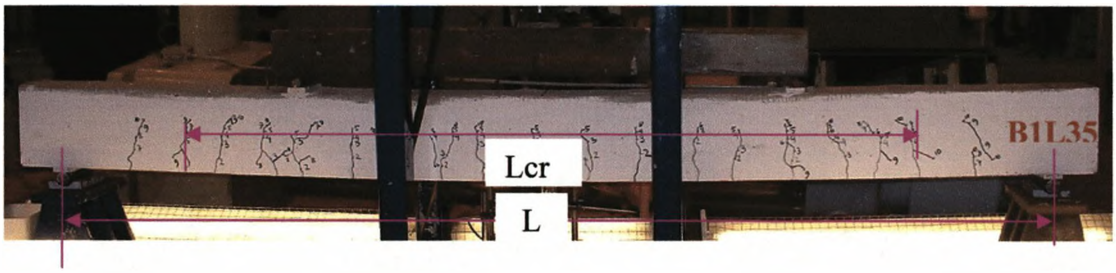

Scaling from the picture above for load # 5&6:

L = 13.00 cm	actual size	L= 2.75 m
Lcr = 9.70 cm	therefore,	Lcr = 2.75x(9.70/13.00) = 2.05 m

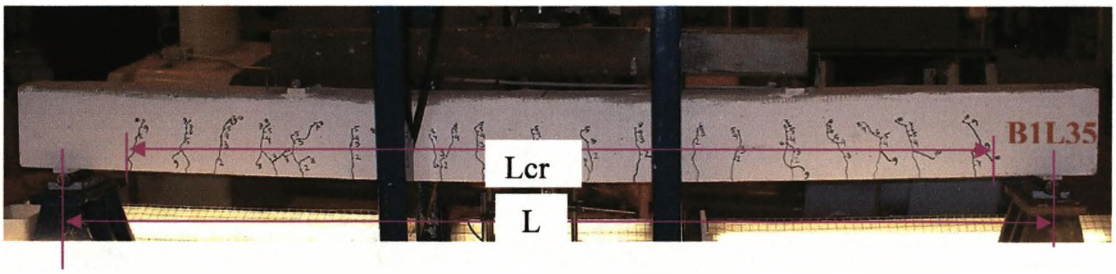

Scaling from the picture above for load #7,8,9,10:

L = 13.00 cm	actual size	L= 2.75 m
Lcr = 11.38 cm	therefore,	Lcr = 2.75x(11.38/13.00) = 2.41 m

Figure A-11 Measured cracked length of B1L35 at various load level

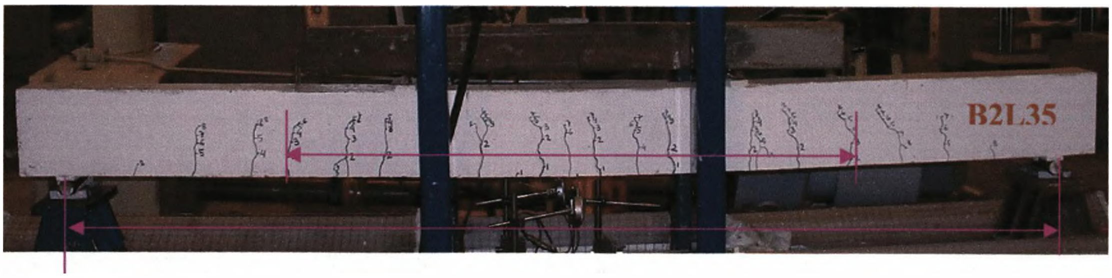

Scaling from the picture above for load #2,3:

L = 13.09 cm	actual size	L= 2.75 m
Lcr = 7.56 cm	therefore,	Lcr = 2.75x(7.56/13.09) = 1.59 m

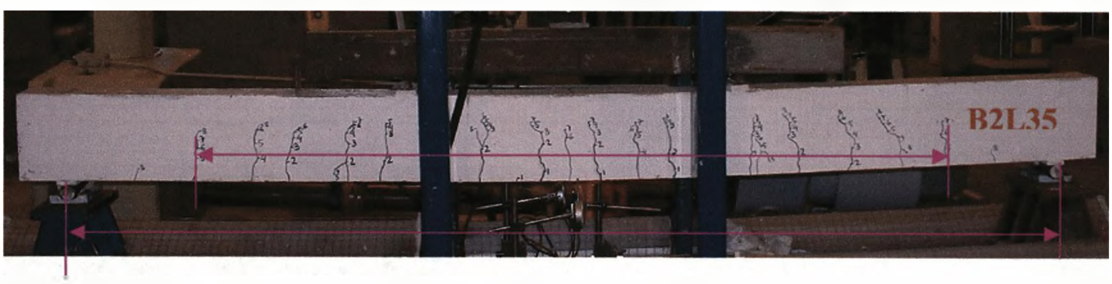

Scaling from the picture above for load #5,6,7:

L = 13.09 cm	actual size	L= 2.75 m
Lcr = 9.94 cm	therefore,	Lcr = 2.75x(9.94/13.09) = 2.09 m

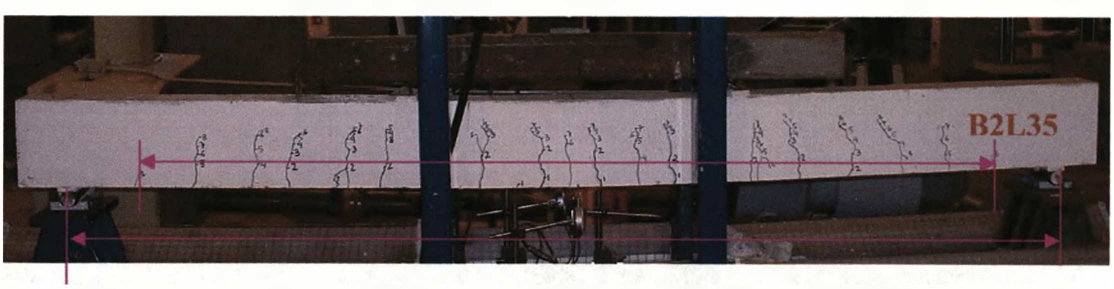

Scaling from the picture above for load #8:

L = 13.09 cm	actual size	L= 2.75 m
Lcr = 11.11 cm	therefore,	Lcr = 2.75x(11.11/13.09) = 2.33 m

Figure A-12 Measured cracked length of B2L35 at various load level

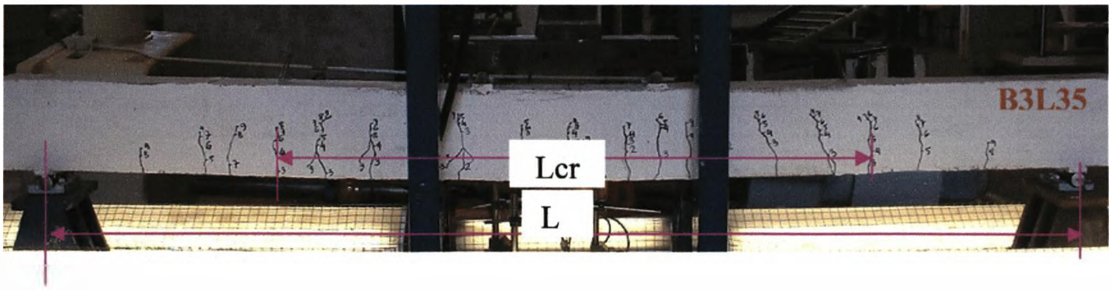

Scaling from the picture above for load #3,4:

L = 13.65 cm	actual size	L= 2.75 m
Lcr = 7.86 cm	therefore,	Lcr = 2.75x(7.86/13.65) = 1.58 m

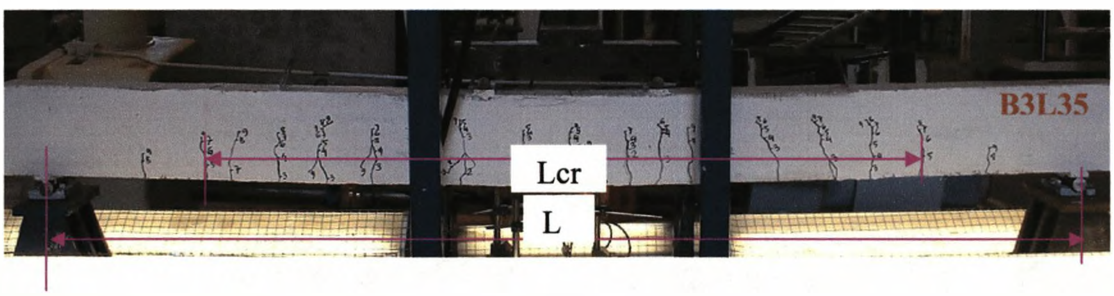

Scalaing from the picture above for load 5,6,7:

L = 13.65 cm	actual size	L= 2.75 m
Lcr = 9.45 cm	therefore,	Lcr = 2.75x(9.45/13.65) = 1.90 m

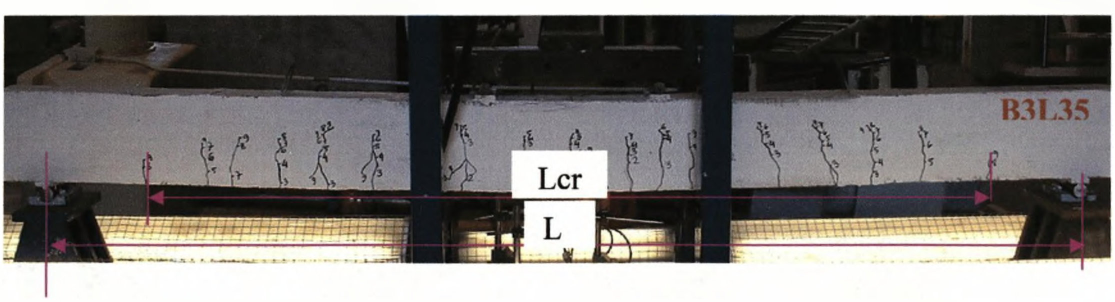

Scaling from the picture above for load #8,9:

L = 13.65 cm	actual size	L= 2.75 m
Lcr = 11.11 cm	therefore,	Lcr = 2.75x(11.11/13.65) = 2.24 m

Figure A-13 Measured cracked length of B3L35 at various load level

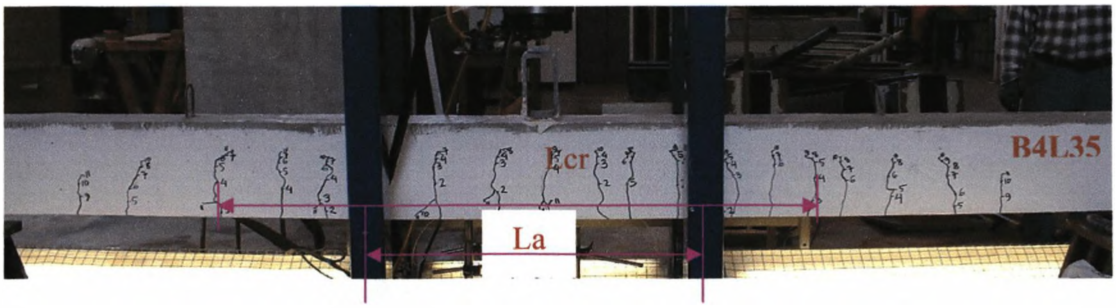

Scaling from the picture for load #3:

La = 4.45 cm	actual size	La= 0.75 m
Lcr = 7.94 cm	therefore,	Lcr = 0.75x(7.94/4.45) = 1.34 m

Scaling from the picture for load #5,6,7,8:

La = 4.45 cm	actual size	La= 0.75 m
Lcr = 10.90 cm	therefore,	Lcr = 0.75x(10.90/4.45) =1.84 m

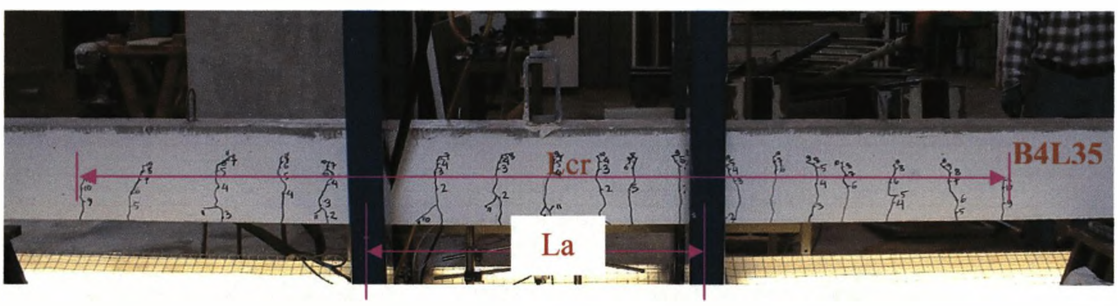

Scaling from the picture for load #9,10,11:

L = 4.45 cm	actual size	L= 0.75 m
Lcr = 12.20 cm	therefore,	Lcr = 0.75x(12.20/4.45) = 2.06 m

Figure A-14 Measured cracked length of B4L35 at various load level

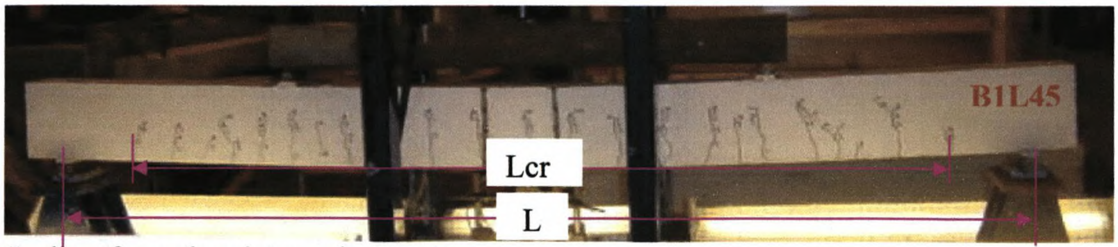

Scaling from the picture above:

L = 12.75 cm	actual size	L= 2.75 m
Lcr = 10.80 cm	therefore,	Lcr = 2.75x(10.80/12.75) = 2.33 m

Scaling from the picture above:

L = 12.80 cm	actual size	L= 2.75 m
Lcr = 10.00 cm	therefore,	Lcr = 2.75x(10.00/12.70) = 2.16 m

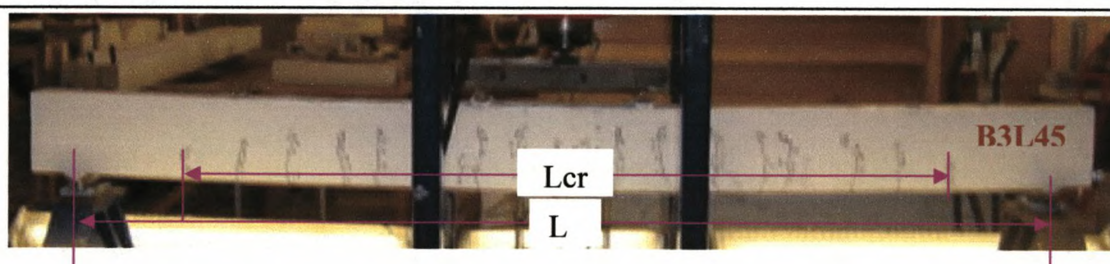

Scaling from the picture above:

L = 12.80 cm	actual size	L= 2.75 m
Lcr = 10.10 cm	therefore,	Lcr = 2.75x(10.10/12.80) = 2.15 m

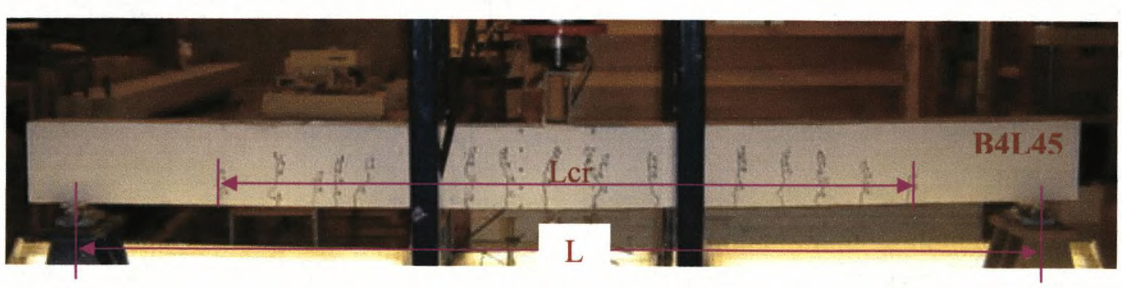

Scaling from the picture above:

L = 12.65 cm	actual size	L= 2.75 m
Lcr = 9.15 cm	therefore,	Lcr = 2.75x(9.15/12.65) = 1.99 m

Figure A-15 Measured cracked length of B1L45, B2L45, B3L45 and B4L45 at their ultimate load

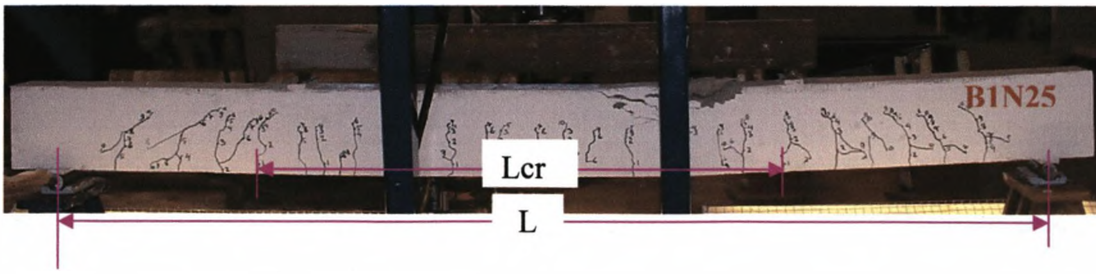

Scaling from the picture above for load #1 :

L = 13.15 cm	actual size	L= 2.75 m
Lcr = 6.99 cm	therefore,	Lcr = 2.75x(6.99/13.10) = 1.47 m

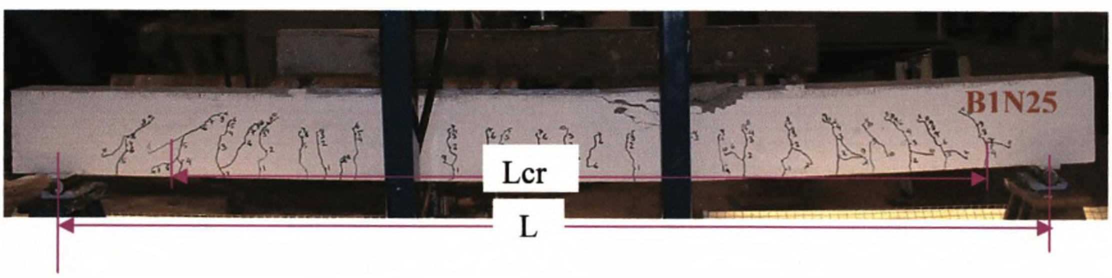

Scaling from the picture above for load #4 :

L = 13.15 cm	actual size	L= 2.75 m
Lcr = 10.80 cm	therefore,	Lcr = 2.75x(10.80/13.10) = 2.27 m

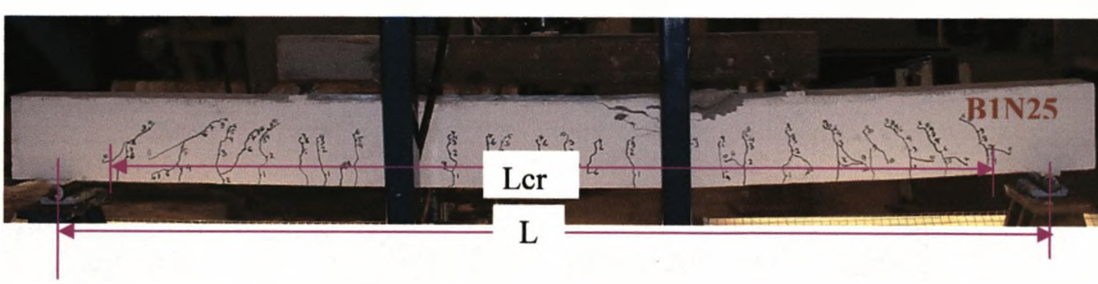

Scaling from the picture above for load #5,6,7,8,9 :

L = 13.15 cm	actual size	L= 2.75 m
Lcr = 11.68 cm	therefore,	Lcr = 2.75x(11.68/13.10) = 2.45 m

Figure A-16 Measured cracked length of B1N25 at various load level

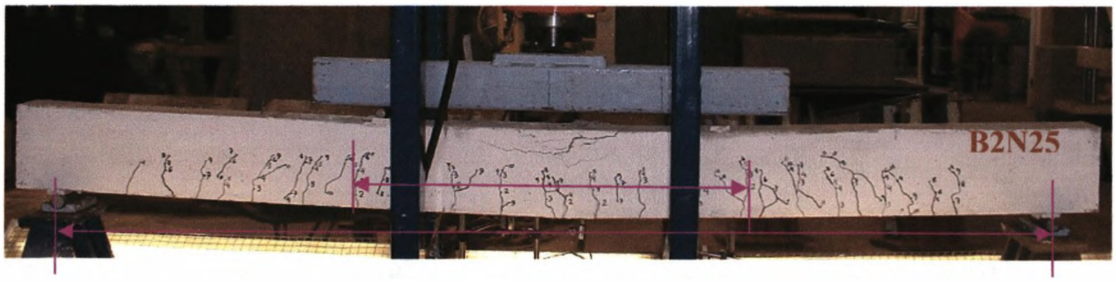

Scaling from the picture above for load #2 :

L = 13.04 cm	actual size	L= 2.75 m
Lcr = 5.20 cm	therefore,	Lcr = 2.75x(5.20/13.10) = 1.09 m

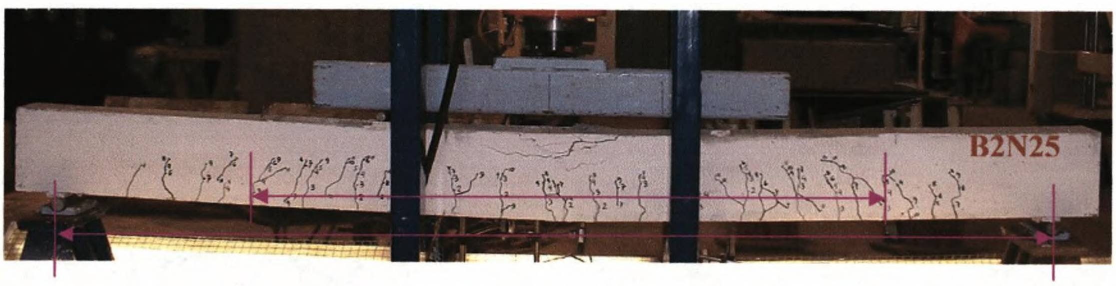

Scaling from the picture above for load #3 :

L = 13.04 cm	actual size	L= 2.75 m
Lcr = 8.35 cm	therefore,	Lcr = 2.75x(8.35/13.10) = 1.75 m

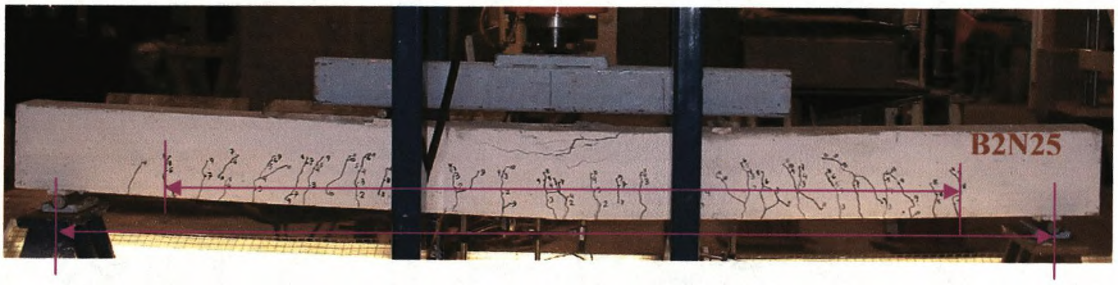

Scaling from the picture above for load #7,8,9:

L = 13.04 cm	actual size	L= 2.75 m
Lcr = 10.48 cm	therefore,	Lcr = 2.75x(11.18/13.10) = 2.36 m

Figure A-17 Measured cracked length of B2N25 at various load level

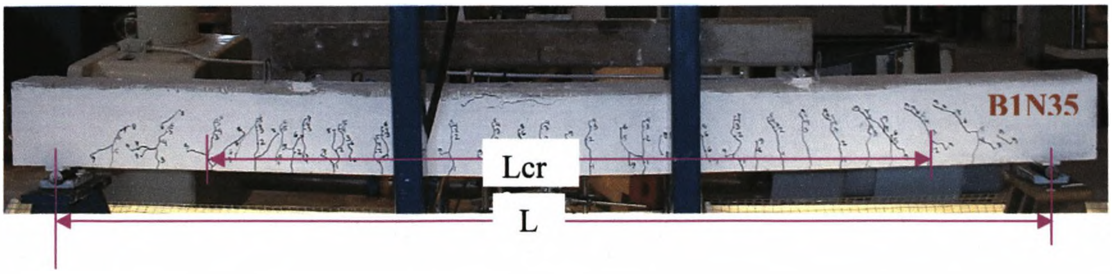

Scaling from the picture above for load #2:

L = 13.15 cm	actual size	L= 2.75 m
Lcr = 9.54 cm	therefore,	Lcr = 2.75x(9.54/13.15) = 2.00 m

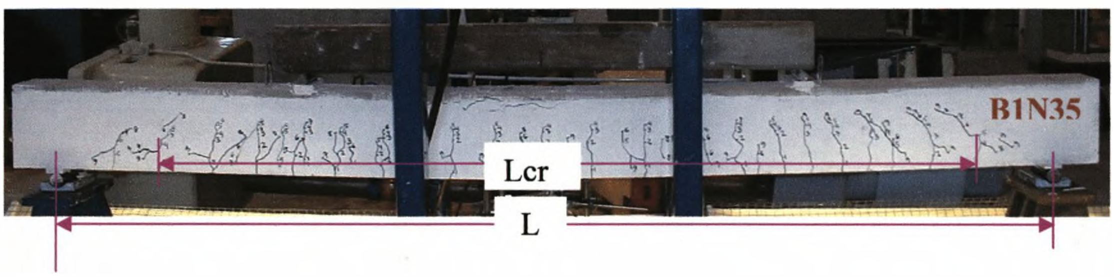

Scaling from the picture above for load #3,4:

L = 13.15 cm	actual size	L= 2.75 m
Lcr = 10.80 cm	therefore,	Lcr = 2.75x(10.80/13.15) = 2.26 m

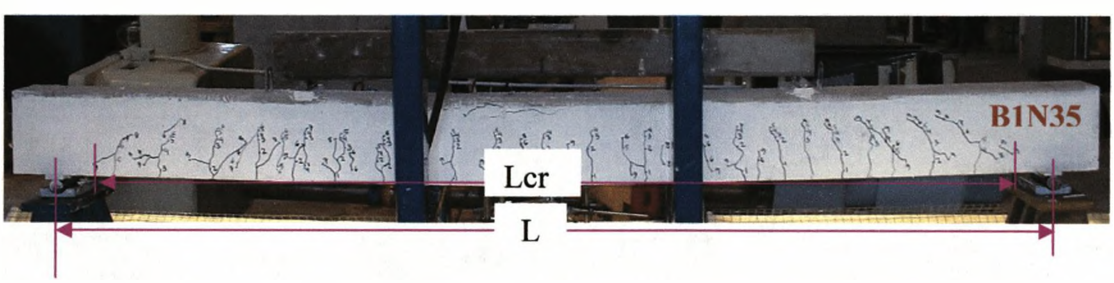

Scaling from the picture above for load #9:

L = 13.15 cm	actual size	L= 2.75 m
Lcr = 12.07 cm	therefore,	Lcr = 2.75x(12.07/13.15) = 2.52 m

Figure A-18 Measured cracked length of B1N35 at various load level

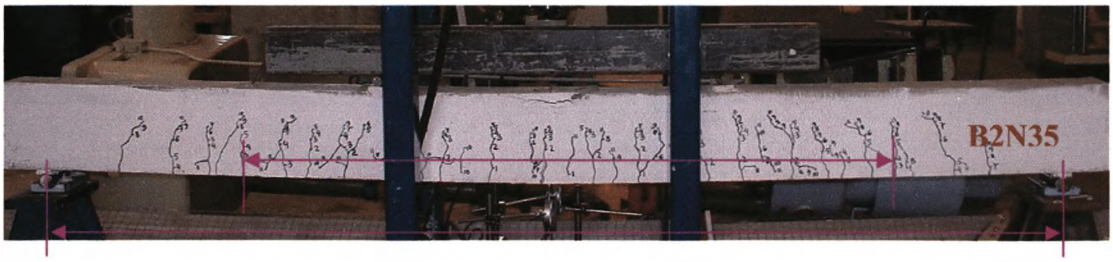

Scaling from the picture above for load #3:

L = 13.34 cm	actual size	L= 2.75 m
Lcr = 8.57 cm	therefore,	Lcr = 2.75x(8.57/13.34) = 1.77 m

Scaling from the picture above for load #4,5,6:

L = 13.34 cm	actual size	L= 2.75 m
Lcr = 10.34 cm	therefore,	Lcr = 2.75x(10.34/13.34) = 2.13 m

Scaling from the picture above for load #7,8,9:

L = 13.34 cm	actual size	L= 2.75 m
Lcr = 11.43 cm	therefore,	Lcr = 2.75x(11.43/13.34) = 2.36 m

Figure A-19 Measured cracked length of B2N35 at various load level

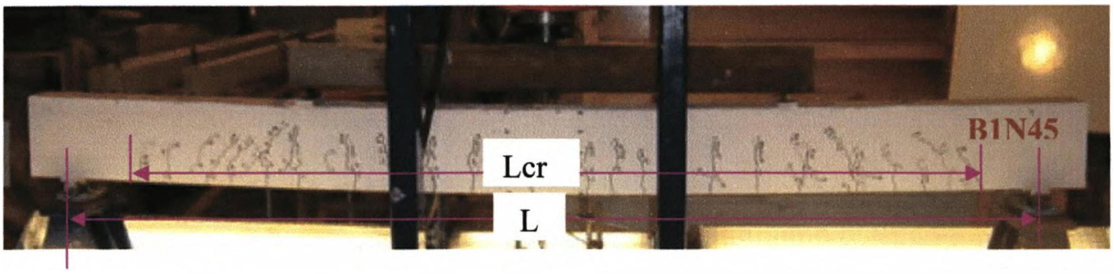

Scaling from the picture above for load # :
L = 12.75 cm actual size L= 2.75 m
Lcr = 11.20 cm therefore, Lcr = 2.75x(11.20/12.75) = 2.42 m

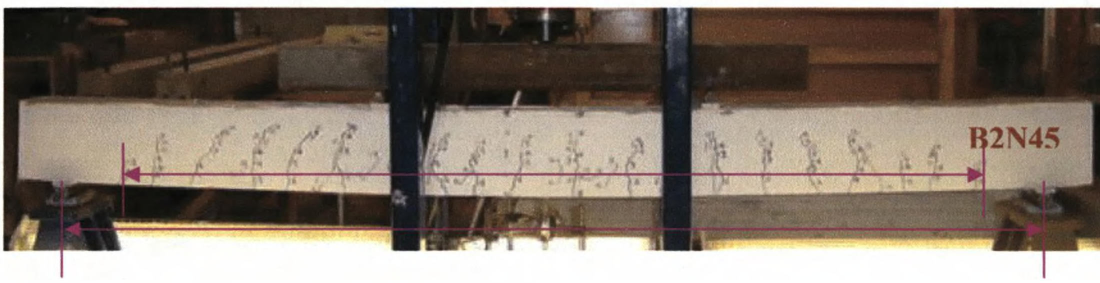

Scaling from the picture above for load # :
L = 12.90 cm actual size L= 2.75 m
Lcr = 11.35 cm therefore, Lcr = 2.75x(11.35/12.90) = 2.42 m

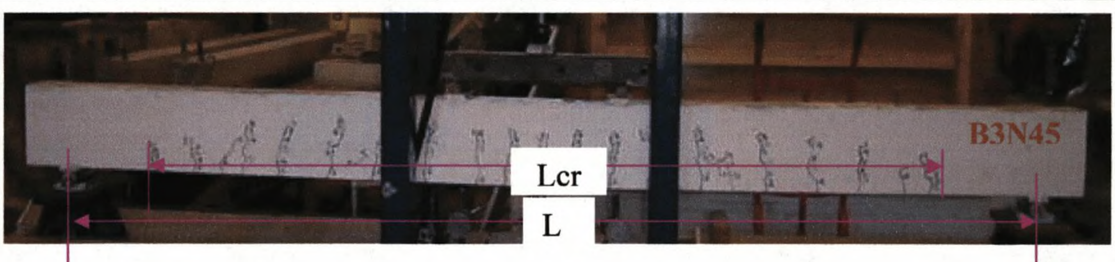

Scaling from the picture above for load # :
L = 12.70 cm actual size L= 2.75 m
Lcr = 10.50 cm therefore, Lcr = 2.75x(10.50/12.70) = 2.27 m

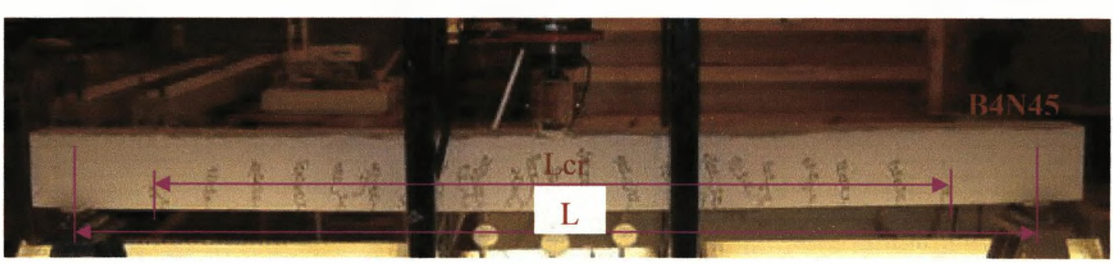

Scaling from the picture above for load # :
L = 12.70 cm actual size L= 2.75 m
Lcr = 10.50 cm therefore, Lcr = 2.75x(10.5/12.7) = 2.27 m

Figure A-20 Measured cracked length of B1N45, B2N45, B3N45 and B4N45 at their ultimate load

Appendix B

- **Derivation of deflection equation for two unsymmetrical point loads**
- **Computer programmes:**
  - Program B-1: Typical program to compute neutral axis and its output
  - Program B-2: Typical program to compute deflection using various methods for beams considered in this study and its output.
  - Program B-3: Typical program to compute deflection of beams obtained from Ref. [15] with its input and output
  - Program B-4: Typical program to compute deflection of beams obtained from data supplement of Ref. [15] and its output

- **Derivation of deflection equation for two unsymmetrical points Load**

Consider two unsymmetrical point loads acting on the beam with details as shown in Figure A-1 below.

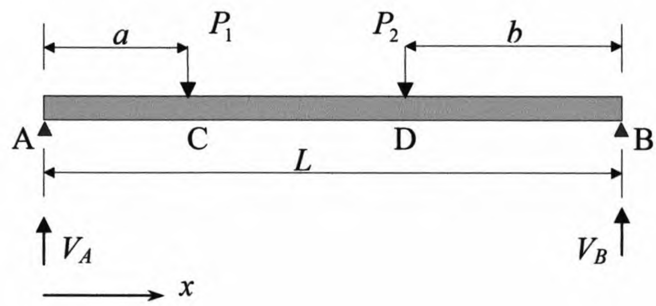

$$V_A = \frac{P_1(L-a)+P_2 b}{L} \quad ; \quad V_B = \frac{P_2(L-b)+P_1 a}{L}$$

Figure A- 1 Two unsymmetrical point loads on simply supported beam

Equations at interval A-C $[0 \le x \le a]$

$$M_x = V_A x \tag{1}$$

$$EI\frac{d^2y}{dx^2} = -M_x = -V_A x \tag{2}$$

$$EI\frac{dy}{dx} = -\tfrac{1}{2}V_A x^2 + A \tag{3}$$

$$EI\ y = -\tfrac{1}{6}V_A x^3 + Ax + B \tag{4}$$

Equations at interval C-D $[a \le x \le L\text{-}b]$

$$EI\frac{d^2y}{dx^2} = -M_x = -V_A x + P_1(x-a) \tag{5}$$

$$EI\frac{dy}{dx} = -\tfrac{1}{2}V_A x^2 + \tfrac{1}{2}P_1(x-a)^2 + A \tag{6}$$

$$EI\ y = -\tfrac{1}{6}V_A x^3 + \tfrac{1}{6}P_1(x-a)^3 + Ax + B \tag{7}$$

Equations at interval D-B [$L\text{-}b \le x \le L$]

$$EI\frac{d^2y}{dx^2} = -M_x = -V_A x + P_1(x-a) + P_2(x-L+b) \tag{8}$$

$$EI\frac{dy}{dx} = -\tfrac{1}{2}V_A x^2 + \tfrac{1}{2}P_1(x-a)^2 + \tfrac{1}{2}P_2(x-L+b)^2 + A \tag{9}$$

$$EI\ y = -\tfrac{1}{6}V_A x^3 + \tfrac{1}{6}P_1(x-a)^3 + \tfrac{1}{6}P_2(x-L+b)^3 + Ax + B \tag{10}$$

Boundary conditions:

$x = 0$; $y = 0$ Equation (4) is applied → $B = 0$

$x = L$; $y = 0$ Equation (10) is used

$$0 = -\tfrac{1}{6}V_A L^3 + \tfrac{1}{6}P_1(L-a)^3 + \tfrac{1}{6}P_2(L-L+b)^3 + AL$$

$$AL = \tfrac{1}{6}\frac{P_1(L-a)+P_2 b}{L}L^3 - \tfrac{1}{6}P_1(L-a)^3 - \tfrac{1}{6}P_2 b^3$$

$$AL = \tfrac{1}{6}P_1(L-a)L^2 + \tfrac{1}{6}P_2 bL^2 - \tfrac{1}{6}P_1(L-a)^3 - \tfrac{1}{6}P_2 b^3$$

$$A = \tfrac{1}{6}P_1(L-a)L + \tfrac{1}{6}P_2 bL - \frac{P_1}{6L}(L-a)^3 - \frac{P_2}{6L}b^3$$

$$A = \tfrac{1}{6}P_1 L^2 - \tfrac{1}{6}P_1 aL + \tfrac{1}{6}P_2 bL - \frac{P_1}{6L}(L^3 - 3aL^2 + 3a^2L - a^3) - \frac{P_2}{6L}b^3$$

$$A = \tfrac{1}{6}P_1 L^2 - \tfrac{1}{6}P_1 aL + \tfrac{1}{6}P_2 bL - \tfrac{1}{6}P_1 L^2 + \tfrac{1}{2}P_1 aL - \tfrac{1}{2}P_1 a^2 + \frac{P_1}{6L}a^3 - \frac{P_2}{6L}b^3$$

$$A = \tfrac{1}{3}P_1 aL + \tfrac{1}{6}P_2 bL - \tfrac{1}{2}P_1 a^2 + \frac{P_1}{6L}a^3 - \frac{P_2}{6L}b^3$$

Equation (3), (4), (6), (7), (9) and Equation (10) become as follows

$$EI\frac{dy}{dx} = -\tfrac{1}{2}V_A x^2 + \left(\tfrac{1}{3}P_1 aL + \tfrac{1}{6}P_2 bL - \tfrac{1}{2}P_1 a^2 + \frac{P_1}{6L}a^3 - \frac{P_2}{6L}b^3\right) \tag{11}$$

$$EI\ y = -\tfrac{1}{6}V_A x^3 + \left(\tfrac{1}{3}P_1 aL + \tfrac{1}{6}P_2 bL - \tfrac{1}{2}P_1 a^2 + \frac{P_1}{6L}a^3 - \frac{P_2}{6L}b^3\right)x \tag{12}$$

$$EI\frac{dy}{dx} = -\tfrac{1}{2}V_A x^2 + \tfrac{1}{2}P_1(x-a)^2 + \left(\tfrac{1}{3}P_1 aL + \tfrac{1}{6}P_2 bL - \tfrac{1}{2}P_1 a^2 + \frac{P_1}{6L}a^3 - \frac{P_2}{6L}b^3\right) \tag{13}$$

$$EI\ y = -\tfrac{1}{6}V_A x^3 + \tfrac{1}{6}P_1(x-a)^3 + \left(\tfrac{1}{3}P_1 aL + \tfrac{1}{6}P_2 bL - \tfrac{1}{2}P_1 a^2 + \frac{P_1}{6L}a^3 - \frac{P_2}{6L}b^3\right)x \tag{14}$$

$$EI\frac{dy}{dx} = -\tfrac{1}{2}V_A x^2 + \tfrac{1}{2}P_1(x-a)^2 + \tfrac{1}{2}P_2(x-L+b)^2$$

$$+\left(\tfrac{1}{3}P_1 aL + \tfrac{1}{6}P_2 bL - \tfrac{1}{2}P_1 a^2 + \frac{P_1}{6L}a^3 - \frac{P_2}{6L}b^3\right) \qquad \textbf{(15)}$$

$$EI\ y = -\tfrac{1}{6}V_A x^3 + \tfrac{1}{6}P_1(x-a)^3 + \tfrac{1}{6}P_2(x-L+b)^3$$

$$+\left(\tfrac{1}{3}P_1 aL + \tfrac{1}{6}P_2 bL - \tfrac{1}{2}P_1 a^2 + \frac{P_1}{6L}a^3 - \frac{P_2}{6L}b^3\right)x \qquad \textbf{(16)}$$

At position $y = y_{\max}$; $\frac{dy}{dx} = 0$

Assume at interval C-D, Equation (13) is applied

$$0 = -\tfrac{1}{2}V_A x^2 + \tfrac{1}{2}P_1(x-a)^2 + \left(\tfrac{1}{3}P_1 aL + \tfrac{1}{6}P_2 bL - \tfrac{1}{2}P_1 a^2 + \frac{P_1}{6L}a^3 - \frac{P_2}{6L}b^3\right)$$

$$0 = -\tfrac{1}{2}\frac{P_1(L-a)+P_2 b}{L}x^2 + \tfrac{1}{2}P_1(x^2 - 2ax + a^2) + \left(\tfrac{1}{3}P_1 aL + \tfrac{1}{6}P_2 bL - \tfrac{1}{2}P_1 a^2 + \frac{P_1}{6L}a^3 - \frac{P_2}{6L}b^3\right)$$

$$0 = -\tfrac{1}{2}\frac{P_1(L-a)+P_2 b}{L}x^2 + \tfrac{1}{2}P_1 x^2 - P_1 ax + \tfrac{1}{2}P_1 a^2 + \left(\tfrac{1}{3}P_1 aL + \tfrac{1}{6}P_2 bL - \tfrac{1}{2}P_1 a^2 + \frac{P_1}{6L}a^3 - \frac{P_2}{6L}b^3\right)$$

$$0 = \tfrac{1}{2}\frac{P_1 a - P_2 b}{L}x^2 - P_1 a\ x + \left(\tfrac{1}{3}P_1 aL + \tfrac{1}{6}P_2 bL + \frac{P_1}{6L}a^3 - \frac{P_2}{6L}b^3\right) \qquad \textbf{(17)}$$

$$x = \frac{P_1 a \pm \sqrt{(P_1 a)^2 - 4(\tfrac{1}{2}\frac{P_1 a - P_2 b}{L})(\tfrac{1}{3}P_1 aL + \tfrac{1}{6}P_2 bL + \frac{P_1}{6L}a^3 - \frac{P_2}{6L}b^3)}}{\frac{P_1 a - P_2 b}{L}} \qquad \textbf{(18)}$$

Check quadratic Equation (17) above by assuming two symmetrical point load acting on the beam.

Therefore,

$$a = b$$

$$P_1 = P_2 = P$$

Rewriting Equation (17) and substitute the above values

$$0 = \tfrac{1}{2}\frac{Pa - Pa}{L}x^2 - Pax + \left(\tfrac{1}{3}PaL + \tfrac{1}{6}PaL + \frac{P}{6L}a^3 - \frac{P}{6L}a^3\right)$$

$$0 = -P\ ax + \tfrac{1}{2}PaL$$

$x = \frac{1}{2}L$ ....Ok, assumption is within range $[a \le \frac{1}{2}L \le L\text{-}b]$

Maximum deflection for this condition $V_A = P$

Rewriting Equation (14) and substitute $x = \frac{1}{2}L$

$$EI\ y_{max} = -\tfrac{1}{48}V_A L^3 + \tfrac{1}{6}P(\tfrac{1}{2}L - a)^3 + \left(\tfrac{1}{3}P\,aL + \tfrac{1}{6}PaL - \tfrac{1}{2}P\,a^2\right)\tfrac{1}{2}L$$

$$EI\ y_{max} = -\tfrac{1}{48}PL^3 + \tfrac{1}{6}P(\tfrac{1}{8}L^3 - \tfrac{3}{4}aL^2 + \tfrac{3}{2}a^2L - a^3) + \left(\tfrac{1}{4}P\,aL^2 - \tfrac{1}{4}P\,a^2L\right)$$

$$EI\ y_{max} = -\tfrac{1}{48}PL^3 + \tfrac{1}{48}PL^3 - \tfrac{3}{24}PaL^2 + \tfrac{3}{12}Pa^2L - \tfrac{1}{6}Pa^3 + \tfrac{1}{4}PaL^2 - \tfrac{1}{4}Pa^2L$$

$$EI\ y_{max} = -\tfrac{3}{24}PaL^2 - \tfrac{1}{6}Pa^3 + \tfrac{1}{4}PaL^2$$

$$EI\ y_{max} = \tfrac{1}{8}PaL^2 - \tfrac{1}{6}Pa^3$$

$$y_{max} = \frac{Pa\left(3L^2 - 4a^2\right)}{24EI} \quad \text{.............. Ok}$$

or

$$y_{max} = \frac{M_a\left(3L^2 - 4a^2\right)}{24EI} \qquad \text{in which} \quad M_a = Pa \quad \text{....................Ok}$$

Therefore for two unsymmetrical point loads Equation (18) can be applied.

In this study it was designed load condition such as below

$P_1 = 0.7P$ and $P_2 = 0.3P$

$a = 0.775$ m

$b = 0.975$ m

$L = 2.75$ m

Therefore, the position of maximum deflection from support A is

$$x = \frac{0.5425P \pm \sqrt{0.17898P^2}}{0.0909P}$$

$$x = \frac{0.5425P - \sqrt{0.17898P^2}}{0.0909P}$$

$x = 1.31$ m → $[a \le \frac{1}{2}L \le L\text{-}b] = [0.775 \text{ m} \le x \le 1.775 \text{ m}]$

Thus maximum deflection is

$$y_{max} = \left\{-\tfrac{1}{6}V_A x^3 + \tfrac{1}{6}P_1(x-a)^3 + \left(\tfrac{1}{3}P_1 aL + \tfrac{1}{6}P_2 bL - \tfrac{1}{2}P_1 a^2 + \frac{P_1}{6L}a^3 - \frac{P_2}{6L}b^3\right)x\right\} \Big/ EI$$

```
%=========================================================================%
%                              PROGRAM B-1                                %
%   A TYPICAL PROGRAM TO COMPUTE NEUTRAL AXIS POSITION WITH REFERENCE TO  %
%                        THE BRITISH STANDARD                             %
%                                                                         %
% NOTE:                                                                   %
% This program reads data from input keyboard displayed on the screen,   %
% the results are stored in the file to be used latter as data input for %
% another program.                                                        %
%                                                                         %
% The value of a, ns and fcu should be replaced with the appropriate value %
% based on beam designation in Table 5.4 in Chapter 5                     %
%                                                                         %
% Here:                                                                   %
% a represents the distance between load position and end supported (m)  %
% ns is the number of tension steel                                       %
% fcu is the cube concrete strength (MPa)                                 %
% P is the total load (kN)                                                %
% dex is the measured deflection (mm)                                     %
% b is the beam width (mm)                                                %
% h is the total depth of the beam (mm)                                   %
% d is the effective depth of the beam (mm)                               %
% d1 is the distance between centroidal of compression steel and soffit   %
% Ast is the total tension steel reinforcement (mm^2)                     %
% Asc is the total compression steel (mm^2)                               %
% Es is the steel elastic modulus (MPa)                                   %
% Ec is the concrete modulus of elasticity (MPa)                          %
% C is the compression force (kN)                                         %
% F is the tension force (kN)                                             %
% xo is the initial value of neutral axis                                 %
%=========================================================================%
clear all;clc;
P = input (' P (kN):  ');
dex= input(' dexp :  ');
fprintf('\n\n\n\');
% Properties
a = 0.7;
ns= 2;
fcu = 29;
b=150;
h=230;
d=184;
d1=0;
Ast=ns*1/4*pi*12^2;
M=P/2*a;
Es=196000;  %actual steel modulus of elasticity
Ec=25800;   %actual concrete modulus of elasticity
n=Es/Ec;
Asc=b*h;
C=n*(Ast+Asc)/b;
F=n*((Ast*d)+(Asc*d1))/b;
xo=-C+((C^2)+(2*F))^0.5;
j= 1;
x=xo;
    for i=1:50
        x=x+10./j;
        fct=(h-x)./(d-x);
        fs =(M.*1e6-b.*h.*fct.*(h-x)./3)./(Ast.*(d-x./3));
```

```
        fc1=(x./(d-x)).*fs./n;
        fc2=(fs.*Ast+b*(h-x)./2.*fct)./(b.*x./2);
        f12 =abs(fc1-fc2);
        if f12 == 0.00001
           break
       end
        if fc1 < fc2
            continue
        end
        x= x-10./j;
        j=10.*j;
    end
if x > h;
   x = h;
end
% Format print out
fn=fopen('XB1L25.txt','a');
fprintf(fn,'%7.2f',P); fprintf(fn,'%7.2f',dex);
fprintf(fn,'%9.3f',x);
fprintf(fn,'%9.3f',fc1);
fprintf(fn,'%9.3f',fc2);
fprintf(fn,'\n');

replay = input(' Do you want to continue? Y/N [Y]: ','s');
end
if (isempty(replay))|(replay == 'Y')|(replay == 'y')
    replay = 'Y';
else
    replay = 'N';
    break
end
XB1L25
```

OUTPUT PROGRAM B-1

P (kN)	def(exp) (mm)	x (mm)	fc1 MPa	fc2 MPa
0.00	0.00	230.000	-144.791	3.726
5.00	0.58	230.000	-239.817	6.476
10.00	1.86	86.119	3.520	3.520
15.00	3.84	71.704	6.229	6.229
20.00	5.81	66.313	8.875	8.875
25.00	7.91	63.496	11.495	11.495
30.00	10.00	61.764	14.102	14.102
35.00	12.00	60.590	16.702	16.702
40.00	13.95	59.742	19.298	19.298
45.00	16.05	59.101	21.891	21.891
50.00	18.14	58.600	24.481	24.481
55.00	20.50	58.196	27.070	27.070
60.00	22.80	57.864	29.658	29.658
62.00	24.00	57.748	30.693	30.693

```
%====================================================================%
%                          PROGRAM B-2                                %
%    TYPICAL PROGRAM TO CALCULATE DEFLECTION OF BEAMS CONSIDERED      %
%              IN THIS STUDY USING VARIOUS METHODS                    %
% Note:                                                               %
% This program read data file obtained from PROGRAM B-1.              %
% The terms used here are similar to the terms in PROGRAM B-1.        %
%====================================================================%
clear all;clc;
load XB4N45.txt ;          % name of file input
P = XB4N45(:,1)';          % Load
dex = XB4N45(:,2)';        % measured deflection
x= XB4N45(:,3)';           % neutral axis values calculated by a separate program
ds=12;                     % bar diameter
ns=3;                      % number of steel
fcu = 47;                  % actual cube concrete strength
a = 1.375;
b = 150; h = 230; L = 2.75;
Ast=((pi*ds^2)/4)*ns;
d=h-40-(ds/2);
Es=196000;                 % actual steel modulus of elasticity
Ec=29286;                  % actual concrete modulus of elasticity
n=Es/Ec;
rho=(100*Ast)/(b*d);
Ma=(P/2*a);
%--------------------------- FIKRY'S METHOD --------------------------------%
nrho=n*rho;
if nrho < 1.9
   alpha= 0.003; beta=0.095;
   elseif nrho <5
   alpha= 0.05; beta=0.07;
   elseif nrho<17
   alpha= 0.16; beta=0.05;
    elseif nrho<=32
      alpha= 0.5; beta=0.03;
   else
      alpha=0.8; beta= 0.02;
end
Icre=(alpha+beta*nrho)*b*d^3/12;
Ig=(b*h^3)/12;
fr=0.56*sqrt(fcu);
yt=h/2;
Mcr=(fr*Ig/1e+6)/yt;
Rm=Ma./Mcr;
rho1=rho;
if rho1<1 rho1=1;
else rho1=rho1;
    end
phi=-(Rm-2*a/L)*rho1;
Ie=Icre+((Ig-Icre)*exp(phi));
delta=(Ma./Ie)*1000000*(3*(L*1000)^2-4*(a*1000)^2)/(24*Ec);
%-------------------------- BRANSON (ACI) ---------------------------------%
k=(2*n*rho/100+(n*rho/100)^2)^0.5-n*rho/100;
Icr=b*(k*d)^3/3+n*Ast*(d-k*d)^2;
y=Rm;
if Rm(1,1)<1
   y(1,1)=1;
end
```

```
y1=y;
if y(1,2)<1
   y1(1,2)=1;
end
y2=y1;
if y1(1,3)<1
   y2(1,3)=1;
end
y3=y2;
if y2(1,3)<1
   y3(1,3)=1;
end
Ie1=Icr+(Ig-Icr)*1./(y3).^3;
delta1=(Ma./Ie1)*1000000*(3*(L*1000)^2-4*(a*1000)^2)/(24*Ec);
%------------------------- BRITISH STANDARD -------------------------------%
Ig=1/12*b*h^3;
Cuc=Ma.*1e6./(Ec*Ig);           % Curvatute uncracked section
fc = XB4N45(:,4)';
Cc= fc./(x.*Ec);                % Curvatute cracked section
if Cc(1,1)<Cuc(1,1)             % check curvature (cracked or not)
   Cc(1,1)=Cuc(1,1);
end
z=Cc;
if z(1,2)<Cuc(1,2)
   z(1,2)=Cuc(1,2);
end
z1=z;
% Deflection computation
K=0.125-a^2/(6*L^2);
deltabs = z1*K*(L*1000)^2;
%-------------------------- PROPOSED MODEL ---------------------------------%
Icrn1=(0.1914-0.0012*fcu+0.3195*rho)*b*d^3/12;      % Icr Alternative 1
Icrn2=(0.1618+0.0418*nrho)*b*d^3/12;                % Icr Alternative 2
phin1=-(Rm-2*a/L)*(4.0768-1.7969*rho);              % Phi Alternative 1
phin2=-(Rm-2*a/L)*(4.4757-2.0667*rho);              % Phi Alternative 2a
phin2a=-(Rm-2*a/L)*(8.474-9.0606*rho+2.842*rho^2);  % Phi Alternative 2b
Ien1=Icrn1+((Ig-Icrn1)*exp(phin1));
Ien2=Icrn2+((Ig-Icrn2)*exp(phin2));
Ien2a=Icrn2+((Ig-Icrn2)*exp(phin2a));
deltap1=(Ma./Ien1)*1000000*(3*(L*1000)^2-4*(a*1000)^2)/(24*Ec);   % Case 1
deltap2=(Ma./Ien2)*1000000*(3*(L*1000)^2-4*(a*1000)^2)/(24*Ec);   % Case 2a
deltap2a=(Ma./Ien2a)*1000000*(3*(L*1000)^2-4*(a*1000)^2)/(24*Ec); % Case 2b
%--------------------------------------------------------------------------%
fn=fopen('DefB4N45.txt','w');
Iexp=(Ma./dex)*1000000*(3*(L*1000)^2-4*(a*1000)^2)./(24*Ec); %experimental Ie
ratio=dex./delta;
ratio1=dex./delta1;
ratio2=dex./deltabs;
ratio3=dex./deltap1;
ratio4=dex./deltap2;
ratio5=dex./deltap2a;
fprintf(fn, 'OUTPUT PROGRAM LOAD DEFLECTION\n\n');
fprintf(fn, 'BEAM PROPERTIES :\n');
fprintf(fn, ' b   ='); fprintf(fn, ' %4.2f',b'); fprintf(fn, ' mm\n');
fprintf(fn, ' h   ='); fprintf(fn, ' %4.2f',h'); fprintf(fn, ' mm\n');
fprintf(fn, ' d   ='); fprintf(fn, ' %4.2f',d'); fprintf(fn, ' mm\n');
fprintf(fn, ' L   ='); fprintf(fn, ' %4.3f',L'); fprintf(fn, ' m\n');
fprintf(fn, ' a   ='); fprintf(fn, ' %4.3f',a'); fprintf(fn, ' m\n');
fprintf(fn, ' rho ='); fprintf(fn, ' %4.2f',rho'); fprintf(fn, ' percent');
```

```
fprintf(fn, '              Es  ='); fprintf(fn,' %4.0f',Es'); fprintf(fn,...
    ' MPa\n');
fprintf(fn, ' fcu ='); fprintf(fn, ' %4.2f',fcu'); fprintf(fn, ' MPa');
fprintf(fn, '                 Ec  ='); fprintf(fn,' %4.0f',Ec'); fprintf...
(fn, ' MPa\n\n');
fprintf(fn, ' COMPARISON OF DEFLECTION USING VARIOUS METHODS                    ↙
                                   B4N45\n');
fprintf(fn, '==================================================================↙
==================================================\n');
fprintf(fn, '         Measured                                        Deflecti↙
on                  Comparison\n');
fprintf(fn, '  P(kN)    delta    Ma/Mcr    --------------------------------------↙
-------------------------------------------------\n');
fprintf(fn, '                 (mm)             Fikry     ACI      BS      Case1   Case2a   ↙
Case2b    (i)    (ii)    (iii)   (iv)    (v)    (vi)\n');
fprintf(fn, '------------------------------------------------------------------↙
--------------------------------------------------\n');
fprintf(fn, '   (1)        (2)        (3)       (4)       (5)       (6)       (7)      (8)      ↙
  (9)      (10)    (11)    (12)    (13)    (14)    (15)\n');
fprintf(fn, '------------------------------------------------------------------↙
--------------------------------------------------\n');
table(:,1) = P';
table(:,2) = dex';
table(:,3) = Rm';
table(:,4) = delta';
table(:,5) = delta1';
table(:,6) = deltabs';
table(:,7) = deltap1';
table(:,8) = deltap2';
table(:,9) = deltap2a';
table(:,10)= ratio';
table(:,11)= ratio1';
table(:,12)= ratio2';
table(:,13)= ratio3';
table(:,14)= ratio4';
table(:,15)= ratio5';
fprintf(fn, '%7.2f %7.2f %7.2f %7.2f %7.2f %7.2f %7.2f %7.2f %7.2f %6.2f %6.2f ↙
%6.2f %6.2f %6.2f %6.2f\n',table');
fprintf(fn, '==================================================================↙
==================================================\n');
fprintf(fn, 'Note :\n');
fprintf(fn, '      i   = (2)/(4)');  fprintf(fn, '          iv = (2)/(7)\n');
fprintf(fn, '      ii  = (2)/(5)');  fprintf(fn, '           v = (2)/(8)\n');
fprintf(fn, '     iii  = (2)/(6)');  fprintf(fn, '          vi = (2)/(9)\n');
status = fclose(fn);
end
subplot(2,2,1);
plot(dex,P,'om',delta,P,'-k','MarkerSize',5,'LineWidth',1.5)
h = legend('experiment','Fikry',2);
xlabel('midspan deflection (mm)'),ylabel('Load (kN)')
text(15,10,'B4N45')
subplot(2,2,2);
plot(dex,P,'om',delta1,P,'-.k','MarkerSize',5,'LineWidth',1.5)
h = legend('experiment','ACI',2);
xlabel('midspan deflection (mm)'),ylabel('Load (kN)')
text(15,10,'B4N45')
subplot(2,2,3);
plot(dex,P,'om',deltabs,P,'--k','MarkerSize',5,'LineWidth',1.5)
h = legend('experiment','BS',2);
xlabel('midspan deflection (mm)'),ylabel('Load (kN)')
```

```
text(15,10,'B4N45')
subplot(2,2,4);
plot(dex,P,'om',deltap1,P,'-k',deltap2,P,'sk',deltap2a,P,'*b',...
'MarkerSize',5,'LineWidth',1.5)
h = legend('experiment','Case1','Case2a','Case2b',2);
xlabel('midspan deflection (mm)'),ylabel('Load (kN)')
text(15,10,'B4N45')
```

OUTPUT PROGRAM LOAD DEFLECTION

BEAM PROPERTIES :
b = 150.00 mm
h = 230.00 mm
d = 184.00 mm
L = 2.750 m
a = 0.700 m
rho = 1.64 percent   Es = 196000 MPa
fcu = 30.00 MPa   Ec = 27150 MPa

COMPARISON OF DEFLECTION USING VARIOUS METHODS   B1H25

P(kN)	Measured delta (mm)	Ma/Mcr	Deflection						Comparison					
			Fikry	ACI	BS	Case1	Case2a	Case2b	(i)	(ii)	(iii)	(iv)	(v)	(vi)
(1)	(2)	(3)	(4)	(5)	(6)	(7)	(8)	(9)	(10)	(11)	(12)	(13)	(14)	(15)
0.00	0.00	0.00	0.00	0.00	0.00	0.00	0.00	0.00	NaN	NaN	NaN	NaN	NaN	NaN
9.00	1.05	0.78	0.84	0.66	0.73	0.79	0.79	0.81	1.25	1.59	1.44	1.32	1.33	1.29
18.00	2.96	1.55	2.66	2.38	2.27	2.41	2.40	2.56	1.11	1.24	1.30	1.23	1.23	1.16
27.00	4.90	2.33	4.75	4.49	3.83	4.59	4.62	4.90	1.03	1.09	1.28	1.07	1.06	1.00
36.00	6.94	3.11	6.70	6.39	5.40	6.89	7.02	7.29	1.04	1.09	1.29	1.01	0.99	0.95
45.00	9.10	3.88	8.51	8.19	6.96	9.10	9.33	9.53	1.07	1.11	1.31	1.00	0.98	0.95
54.00	11.60	4.66	10.25	9.94	8.53	11.18	11.51	11.64	1.13	1.17	1.36	1.04	1.01	1.00
63.00	13.57	5.44	11.98	11.66	10.09	13.17	13.60	13.67	1.13	1.16	1.34	1.03	1.00	0.99
72.00	15.92	6.21	13.69	13.37	11.65	15.11	15.62	15.66	1.16	1.19	1.37	1.05	1.02	1.02
81.00	18.57	6.99	15.41	15.06	13.22	17.03	17.61	17.63	1.21	1.23	1.40	1.09	1.05	1.05
90.00	21.63	7.77	17.12	16.76	14.78	18.94	19.59	19.60	1.26	1.29	1.46	1.14	1.10	1.10
99.00	25.51	8.54	18.83	18.45	16.35	20.84	21.56	21.56	1.35	1.38	1.56	1.22	1.18	1.18
104.00	30.00	8.97	19.78	19.39	17.22	21.89	22.65	22.65	1.52	1.55	1.74	1.37	1.32	1.32

Note :
i = (2)/(4)   iv = (2)/(7)
ii = (2)/(5)   v = (2)/(8)
iii = (2)/(6)   vi = (2)/(9)

OUTPUT PROGRAM LOAD DEFLECTION

BEAM PROPERTIES :

b = 150.00 mm
h = 230.00 mm
d = 184.00 mm
L = 2.750 m
a = 0.700 m
rho = 1.64 percent   Es = 196000 MPa
fcu = 39.00 MPa   Ec = 28832 MPa

COMPARISON OF DEFLECTION USING VARIOUS METHODS   B1H35

P(kN)	Measured delta (mm)	Ma/Mcr	Deflection						Comparison					
			Fikry	ACI	BS	Case1	Case2a	Case2b	(i)	(ii)	(iii)	(iv)	(v)	(vi)
(1)	(2)	(3)	(4)	(5)	(6)	(7)	(8)	(9)	(10)	(11)	(12)	(13)	(14)	(15)
0.00	0.00	0.00	0.00	0.00	0.00	0.00	0.00	0.00	NaN	NaN	NaN	NaN	NaN	NaN
8.00	1.02	0.61	0.61	0.55	0.55	0.59	0.59	0.60	1.68	1.85	1.85	1.72	1.72	1.71
16.00	2.45	1.21	1.94	1.52	1.90	1.72	1.73	1.83	1.26	1.62	1.29	1.42	1.42	1.34
24.00	4.08	1.82	3.75	3.45	3.28	3.36	3.41	3.66	1.09	1.18	1.25	1.21	1.20	1.12
32.00	5.80	2.42	5.59	5.26	4.66	5.28	5.43	5.77	1.04	1.10	1.25	1.10	1.07	1.01
40.00	7.55	3.03	7.31	6.93	6.04	7.25	7.55	7.88	1.03	1.09	1.25	1.04	1.00	0.96
48.00	9.39	3.63	8.92	8.52	7.42	9.16	9.62	9.89	1.05	1.10	1.27	1.03	0.98	0.95
56.00	11.12	4.24	10.47	10.06	8.80	10.97	11.59	11.79	1.06	1.11	1.26	1.01	0.96	0.94
64.00	13.06	4.84	12.00	11.58	10.18	12.71	13.48	13.61	1.09	1.13	1.28	1.03	0.97	0.96
72.00	14.90	5.45	13.51	13.09	11.56	14.40	15.30	15.38	1.10	1.14	1.29	1.03	0.97	0.97
80.00	16.84	6.05	15.02	14.58	12.94	16.06	17.08	17.13	1.12	1.15	1.30	1.05	0.99	0.98
88.00	18.78	6.66	16.52	16.07	14.33	17.70	18.83	18.86	1.14	1.17	1.31	1.06	1.00	1.00
96.00	20.71	7.26	18.02	17.55	15.71	19.32	20.57	20.59	1.15	1.18	1.32	1.07	1.01	1.01
100.00	22.20	7.57	18.77	18.29	16.40	20.13	21.43	21.45	1.18	1.21	1.35	1.10	1.04	1.04

Note :

i = (2)/(4)   iv = (2)/(7)
ii = (2)/(5)   v = (2)/(8)
iii = (2)/(6)   vi = (2)/(9)

OUTPUT PROGRAM LOAD DEFLECTION

BEAM PROPERTIES :

b = 150.00 mm
h = 230.00 mm
d = 184.00 mm
L = 2.750 m
a = 0.700 m
rho = 1.64 percent   Es = 196000 MPa
fcu = 50.00 MPa   Ec = 31867 MPa

COMPARISON OF DEFLECTION USING VARIOUS METHODS   B1H45

P(kN)	Measured delta (mm)	Ma/Mcr	Deflection						Comparison					
			Fikry	ACI	BS	Case1	Case2a	Case2b	(i)	(ii)	(iii)	(iv)	(v)	(vi)
(1)	(2)	(3)	(4)	(5)	(6)	(7)	(8)	(9)	(10)	(11)	(12)	(13)	(14)	(15)
0.00	0.00	0.00	0.00	0.00	0.00	0.00	0.00	0.00	NaN	NaN	NaN	NaN	NaN	NaN
10.00	1.00	0.67	0.74	0.62	0.82	0.70	0.70	0.71	1.36	1.60	1.22	1.43	1.42	1.40
20.00	2.40	1.34	2.45	2.01	2.45	2.09	2.14	2.28	0.98	1.20	0.98	1.15	1.12	1.05
30.00	4.50	2.01	4.71	4.35	4.09	4.09	4.29	4.62	0.95	1.03	1.10	1.10	1.05	0.97
40.00	6.60	2.67	6.95	6.51	5.73	6.35	6.83	7.24	0.95	1.01	1.15	1.04	0.97	0.91
50.00	9.00	3.34	9.00	8.50	7.37	8.61	9.43	9.79	1.00	1.06	1.22	1.05	0.95	0.92
60.00	11.40	4.01	10.94	10.41	9.02	10.75	11.91	12.18	1.04	1.09	1.26	1.06	0.96	0.94
70.00	13.50	4.68	12.81	12.28	10.66	12.79	14.26	14.44	1.05	1.10	1.27	1.06	0.95	0.93
80.00	15.60	5.35	14.66	14.11	12.31	14.75	16.51	16.62	1.06	1.11	1.27	1.06	0.94	0.94
90.00	18.00	6.02	16.51	15.94	13.95	16.67	18.69	18.76	1.09	1.13	1.29	1.08	0.96	0.96
100.00	20.10	6.68	18.34	17.75	15.59	18.56	20.83	20.87	1.10	1.13	1.29	1.08	0.97	0.96
110.00	23.00	7.35	20.18	19.55	17.24	20.44	22.94	22.97	1.14	1.18	1.33	1.13	1.00	1.00

Note :

i = (2)/(4)   iv = (2)/(7)
ii = (2)/(5)   v = (2)/(8)
iii = (2)/(6)   vi = (2)/(9)

OUTPUT PROGRAM LOAD DEFLECTION

BEAM PROPERTIES :

b = 150.00 mm
h = 230.00 mm
d = 184.00 mm
L = 2.750 m
a = 0.700 m
rho = 0.82 percent   Es = 196000 MPa
fcu = 29.00 MPa   Ec = 25800 MPa

COMPARISON OF DEFLECTION USING VARIOUS METHODS   B1L25

P(kN)	Measured delta (mm)	Ma/Mcr	Deflection						Comparison					
			Fikry	ACI	BS	Case1	Case2a	Case2b	(i)	(ii)	(iii)	(iv)	(v)	(vi)
(1)	(2)	(3)	(4)	(5)	(6)	(7)	(8)	(9)	(10)	(11)	(12)	(13)	(14)	(15)
0.00	0.00	0.00	0.00	0.00	0.00	0.00	0.00	0.00	NaN	NaN	NaN	NaN	NaN	NaN
5.00	0.58	0.44	0.37	0.39	0.39	0.33	0.33	0.33	1.59	1.51	1.51	1.74	1.76	1.78
10.00	1.86	0.88	1.01	0.77	1.37	1.50	1.55	1.61	1.85	2.41	1.36	1.24	1.20	1.16
15.00	3.84	1.32	1.99	2.01	2.91	3.72	3.86	4.01	1.93	1.91	1.32	1.03	0.99	0.96
20.00	5.81	1.76	3.35	4.03	4.48	6.29	6.40	6.53	1.73	1.44	1.30	0.92	0.91	0.89
25.00	7.91	2.19	5.04	6.13	6.06	8.60	8.62	8.70	1.57	1.29	1.31	0.92	0.92	0.91
30.00	10.00	2.63	6.96	8.13	7.64	10.63	10.59	10.62	1.44	1.23	1.31	0.94	0.94	0.94
35.00	12.00	3.07	8.99	10.03	9.23	12.53	12.44	12.45	1.33	1.20	1.30	0.96	0.96	0.96
40.00	13.95	3.51	11.04	11.84	10.81	14.36	14.25	14.25	1.26	1.18	1.29	0.97	0.98	0.98
45.00	16.05	3.95	13.05	13.59	12.40	16.17	16.04	16.04	1.23	1.18	1.29	0.99	1.00	1.00
50.00	18.14	4.39	14.99	15.31	13.98	17.98	17.82	17.82	1.21	1.19	1.30	1.01	1.02	1.02
55.00	20.50	4.83	16.85	16.99	15.57	19.78	19.61	19.61	1.22	1.21	1.32	1.04	1.05	1.05
60.00	22.80	5.27	18.65	18.65	17.16	21.57	21.39	21.39	1.22	1.22	1.33	1.06	1.07	1.07
62.00	24.00	5.44	19.35	19.31	17.79	22.29	22.10	22.10	1.24	1.24	1.35	1.08	1.09	1.09

Note :

i = (2)/(4)   iv = (2)/(7)
ii = (2)/(5)   v = (2)/(8)
iii = (2)/(6)   vi = (2)/(9)

OUTPUT PROGRAM LOAD DEFLECTION

BEAM PROPERTIES :

```
 b   = 150.00 mm
 h   = 230.00 mm
 d   = 184.00 mm
 L   = 2.750 m
 a   = 0.700 m
 rho = 0.82 percent          Es  = 196000 MPa
 fcu = 36.00 MPa             Ec  = 28070 MPa
```

COMPARISON OF DEFLECTION USING VARIOUS METHODS B1L35

P(kN)	Measured delta (mm)	Ma/Mcr	Deflection						Comparison					
			Fikry	ACI	BS	Case1	Case2a	Case2b	(i)	(ii)	(iii)	(iv)	(v)	(vi)
(1)	(2)	(3)	(4)	(5)	(6)	(7)	(8)	(9)	(10)	(11)	(12)	(13)	(14)	(15)
0.00	0.00	0.00	0.00	0.00	0.00	0.00	0.00	0.00	NaN	NaN	NaN	NaN	NaN	NaN
6.00	0.81	0.47	0.41	0.42	0.42	0.39	0.39	0.39	1.96	1.91	1.91	2.06	2.07	2.08
8.00	1.20	0.63	0.62	0.57	0.73	0.72	0.73	0.74	1.93	2.12	1.64	1.67	1.64	1.61
12.00	2.50	0.95	1.17	0.74	1.84	1.83	1.92	2.00	2.14	3.36	1.36	1.36	1.30	1.25
18.00	5.00	1.42	2.36	2.56	3.60	4.49	4.74	4.91	2.12	1.96	1.39	1.11	1.05	1.02
24.00	7.44	1.89	4.02	4.98	5.38	7.34	7.64	7.77	1.85	1.50	1.38	1.01	0.97	0.96
30.00	9.77	2.36	6.08	7.43	7.16	9.82	10.12	10.18	1.61	1.31	1.37	0.99	0.97	0.96
36.00	12.33	2.84	8.39	9.76	8.94	12.04	12.34	12.37	1.47	1.26	1.38	1.02	1.00	1.00
42.00	14.77	3.31	10.80	11.97	10.72	14.13	14.46	14.47	1.37	1.23	1.38	1.05	1.02	1.02
48.00	17.21	3.78	13.19	14.08	12.51	16.18	16.55	16.55	1.30	1.22	1.38	1.06	1.04	1.04
54.00	19.77	4.25	15.50	16.12	14.29	18.21	18.62	18.62	1.28	1.23	1.38	1.09	1.06	1.06
60.00	23.00	4.73	17.72	18.12	16.08	20.23	20.69	20.69	1.30	1.27	1.43	1.14	1.11	1.11

Note :

```
    i  = (2)/(4)       iv = (2)/(7)
   ii  = (2)/(5)        v = (2)/(8)
  iii  = (2)/(6)       vi = (2)/(9)
```

OUTPUT PROGRAM LOAD DEFLECTION

BEAM PROPERTIES :
b = 150.00 mm
h = 230.00 mm
d = 184.00 mm
L = 2.750 m
a = 0.700 m
rho = 0.82 percent   Es = 196000 MPa
fcu = 48.00 MPa   Ec = 31410 MPa

COMPARISON OF DEFLECTION USING VARIOUS METHODS   B1L45

P(kN)	Measured delta (mm)	Ma/Mcr	Deflection Fikry	ACI	BS	Case1	Case2a	Case2b	Comparison (i)	(ii)	(iii)	(iv)	(v)	(vi)
(1)	(2)	(3)	(4)	(5)	(6)	(7)	(8)	(9)	(10)	(11)	(12)	(13)	(14)	(15)
0.00	0.00	0.00	0.00	0.00	0.00	0.00	0.00	0.00	NaN	NaN	NaN	NaN	NaN	NaN
6.00	0.69	0.41	0.35	0.38	0.38	0.31	0.30	0.30	1.97	1.82	1.82	2.25	2.29	2.32
12.00	2.00	0.82	0.96	0.76	1.72	1.36	1.42	1.47	2.08	2.63	1.16	1.47	1.41	1.36
18.00	4.17	1.23	1.91	1.79	3.38	3.50	3.78	3.95	2.18	2.33	1.23	1.19	1.10	1.06
24.00	6.48	1.64	3.25	3.91	5.06	6.20	6.68	6.87	2.00	1.66	1.28	1.04	0.97	0.94
30.00	8.80	2.05	4.97	6.32	6.74	8.74	9.33	9.45	1.77	1.39	1.31	1.01	0.94	0.93
36.00	11.11	2.46	7.00	8.72	8.43	10.97	11.63	11.69	1.59	1.27	1.32	1.01	0.96	0.95
42.00	13.43	2.86	9.24	11.01	10.11	13.01	13.74	13.77	1.45	1.22	1.33	1.03	0.98	0.98
48.00	15.74	3.27	11.57	13.19	11.80	14.95	15.77	15.78	1.36	1.19	1.33	1.05	1.00	1.00
54.00	18.06	3.68	13.90	15.28	13.49	16.85	17.76	17.76	1.30	1.18	1.34	1.07	1.02	1.02
60.00	20.45	4.09	16.18	17.31	15.17	18.74	19.74	19.74	1.26	1.18	1.35	1.09	1.04	1.04

Note :
i = (2)/(4)   iv = (2)/(7)
ii = (2)/(5)   v = (2)/(8)
iii = (2)/(6)   vi = (2)/(9)

OUTPUT PROGRAM LOAD DEFLECTION

BEAM PROPERTIES :

b = 150.00 mm
h = 230.00 mm
d = 184.00 mm
L = 2.750 m
a = 0.700 m
rho = 1.23 percent
fcu = 31.00 MPa

Es = 196000 MPa
Ec = 26477 MPa

COMPARISON OF DEFLECTION USING VARIOUS METHODS

B1N25

P(kN)	Measured delta (mm)	Ma/Mcr	Deflection: Fikry	Deflection: ACI	Deflection: BS	Deflection: Case1	Deflection: Case2a	Deflection: Case2b	Comparison: (i)	Comparison: (ii)	Comparison: (iii)	Comparison: (iv)	Comparison: (v)	Comparison: (vi)
(1)	(2)	(3)	(4)	(5)	(6)	(7)	(8)	(9)	(10)	(11)	(12)	(13)	(14)	(15)
0.00	0.00	0.00	0.00	0.00	0.00	0.00	0.00	0.00	NaN	NaN	NaN	NaN	NaN	NaN
8.00	1.15	0.68	0.69	0.60	0.65	0.75	0.75	0.73	1.67	1.91	1.78	1.54	1.53	1.58
16.00	3.27	1.36	2.16	2.02	2.35	2.81	2.88	2.62	1.51	1.62	1.39	1.16	1.14	1.25
24.00	5.38	2.04	4.29	4.46	4.09	5.60	5.72	5.34	1.25	1.21	1.32	0.96	0.94	1.01
32.00	7.80	2.72	6.67	6.72	5.84	8.23	8.35	8.08	1.17	1.16	1.34	0.95	0.93	0.97
40.00	10.50	3.40	8.97	8.80	7.58	10.60	10.71	10.57	1.17	1.19	1.38	0.99	0.98	0.99
48.00	12.80	4.07	11.14	10.79	9.33	12.82	12.95	12.88	1.15	1.19	1.37	1.00	0.99	0.99
56.00	15.00	4.75	13.19	12.73	11.08	15.00	15.13	15.10	1.14	1.18	1.35	1.00	0.99	0.99
64.00	17.50	5.43	15.18	14.64	12.84	17.15	17.30	17.29	1.15	1.20	1.36	1.02	1.01	1.01
72.00	19.81	6.11	17.13	16.53	14.59	19.30	19.47	19.46	1.16	1.20	1.36	1.03	1.02	1.02
80.00	22.69	6.79	19.05	18.41	16.34	21.44	21.63	21.63	1.19	1.23	1.39	1.06	1.05	1.05
88.00	26.00	7.47	20.97	20.29	18.09	23.59	23.80	23.80	1.24	1.28	1.44	1.10	1.09	1.09

Note :

i = (2)/(4)
ii = (2)/(5)
iii = (2)/(6)
iv = (2)/(7)
v = (2)/(8)
vi = (2)/(9)

OUTPUT PROGRAM LOAD DEFLECTION

BEAM PROPERTIES :

```
b   = 150.00 mm
h   = 230.00 mm
d   = 184.00 mm
L   = 2.750 m
a   = 0.700 m
rho = 1.23 percent          Es  = 196000 MPa
fcu = 38.00 MPa             Ec  = 29076 MPa
```

COMPARISON OF DEFLECTION USING VARIOUS METHODS B1N35

P (kN)	Measured delta (mm)	Ma/Mcr	Deflection						Comparison					
			Fikry	ACI	BS	Case1	Case2a	Case2b	(i)	(ii)	(iii)	(iv)	(v)	(vi)
(1)	(2)	(3)	(4)	(5)	(6)	(7)	(8)	(9)	(10)	(11)	(12)	(13)	(14)	(15)
0.00	0.00	0.00	0.00	0.00	0.00	0.00	0.00	0.00	NaN	NaN	NaN	NaN	NaN	NaN
9.00	1.25	0.69	0.72	0.62	0.80	0.78	0.79	0.76	1.75	2.03	1.56	1.61	1.59	1.65
14.00	2.26	1.07	1.48	1.10	1.82	1.81	1.88	1.72	1.53	2.05	1.24	1.25	1.20	1.31
18.00	3.75	1.38	2.30	2.17	2.66	2.94	3.10	2.80	1.63	1.73	1.41	1.27	1.21	1.34
27.00	6.46	2.07	4.64	4.85	4.55	5.86	6.23	5.80	1.39	1.33	1.42	1.10	1.04	1.11
36.00	9.17	2.76	7.27	7.34	6.44	8.59	9.12	8.82	1.26	1.25	1.42	1.07	1.00	1.04
45.00	12.08	3.45	9.83	9.64	8.34	11.04	11.71	11.55	1.23	1.25	1.45	1.09	1.03	1.05
54.00	14.80	4.14	12.21	11.83	10.24	13.35	14.15	14.08	1.21	1.25	1.45	1.11	1.05	1.05
63.00	18.00	4.83	14.47	13.97	12.14	15.60	16.54	16.51	1.24	1.29	1.48	1.15	1.09	1.09
72.00	21.00	5.52	16.65	16.07	14.03	17.84	18.91	18.90	1.26	1.31	1.50	1.18	1.11	1.11
81.00	24.00	6.21	18.79	18.15	15.93	20.08	21.28	21.27	1.28	1.32	1.51	1.20	1.13	1.13
86.00	26.50	6.59	19.96	19.30	16.99	21.32	22.59	22.59	1.33	1.37	1.56	1.24	1.17	1.17

Note :

```
  i = (2)/(4)        iv = (2)/(7)
 ii = (2)/(5)         v = (2)/(8)
iii = (2)/(6)        vi = (2)/(9)
```

OUTPUT PROGRAM LOAD DEFLECTION

BEAM PROPERTIES :

```
b   = 150.00 mm
h   = 230.00 mm
d   = 184.00 mm
L   = 2.750 m
a   = 0.700 m
rho = 1.23 percent        Es  = 196000 MPa
fcu = 53.00 MPa           Ec  = 29310 MPa
```

COMPARISON OF DEFLECTION USING VARIOUS METHODS B1N45

P(kN)	Measured delta (mm)	Ma/Mcr	Deflection Fikry	ACI	BS	Case1	Case2a	Case2b	Comparison (i)	(ii)	(iii)	(iv)	(v)	(vi)
(1)	(2)	(3)	(4)	(5)	(6)	(7)	(8)	(9)	(10)	(11)	(12)	(13)	(14)	(15)
0.00	0.00	0.00	0.00	0.00	0.00	0.00	0.00	0.00	NaN	NaN	NaN	NaN	NaN	NaN
6.00	0.50	0.39	0.37	0.41	0.41	0.34	0.34	0.35	1.37	1.23	1.23	1.45	1.47	1.43
12.00	1.25	0.78	1.02	0.81	1.46	1.15	1.17	1.11	1.23	1.54	0.86	1.09	1.07	1.13
18.00	2.60	1.17	2.01	1.65	2.76	2.54	2.62	2.39	1.29	1.57	0.94	1.02	0.99	1.09
24.00	4.20	1.56	3.34	3.35	4.08	4.40	4.57	4.14	1.26	1.25	1.03	0.95	0.92	1.01
30.00	5.80	1.95	4.92	5.15	5.40	6.43	6.68	6.17	1.18	1.13	1.07	0.90	0.87	0.94
36.00	7.50	2.34	6.65	6.87	6.72	8.40	8.71	8.24	1.13	1.09	1.12	0.89	0.86	0.91
42.00	9.20	2.73	8.41	8.51	8.04	10.24	10.59	10.22	1.09	1.08	1.14	0.90	0.87	0.90
48.00	10.80	3.12	10.14	10.06	9.37	11.96	12.35	12.08	1.07	1.07	1.15	0.90	0.87	0.89
54.00	12.50	3.51	11.81	11.57	10.69	13.60	14.03	13.85	1.06	1.08	1.17	0.92	0.89	0.90
60.00	14.20	3.89	13.41	13.03	12.01	15.19	15.66	15.54	1.06	1.09	1.18	0.93	0.91	0.91
66.00	15.60	4.28	14.96	14.47	13.34	16.75	17.26	17.19	1.04	1.08	1.17	0.93	0.90	0.91
72.00	17.20	4.67	16.46	15.89	14.66	18.30	18.85	18.81	1.04	1.08	1.17	0.94	0.91	0.91
78.00	19.00	5.06	17.93	17.30	15.98	19.83	20.43	20.40	1.06	1.10	1.19	0.96	0.93	0.93
84.00	21.00	5.45	19.37	18.70	17.31	21.37	22.01	21.99	1.08	1.12	1.21	0.98	0.95	0.95
88.00	23.00	5.71	20.33	19.62	18.19	22.39	23.06	23.05	1.13	1.17	1.26	1.03	1.00	1.00

Note :

```
  i   = (2)/(4)      iv = (2)/(7)
  ii  = (2)/(5)      v  = (2)/(8)
  iii = (2)/(6)      vi = (2)/(9)
```

OUTPUT PROGRAM LOAD DEFLECTION

BEAM PROPERTIES :

b = 150.00 mm
h = 230.00 mm
d = 184.00 mm
L = 2.750 m
a = 0.920 m
rho = 1.64 percent Es = 196000 MPa
fcu = 26.00 MPa Ec = 27739 MPa

COMPARISON OF DEFLECTION USING VARIOUS METHODS B2H25

P(kN)	Measured delta (mm)	Ma/Mcr	Deflection						Comparison					
			Fikry	ACI	BS	Case1	Case2a	Case2b	(i)	(ii)	(iii)	(iv)	(v)	(vi)
(1)	(2)	(3)	(4)	(5)	(6)	(7)	(8)	(9)	(10)	(11)	(12)	(13)	(14)	(15)
0.00	0.00	0.00	0.00	0.00	0.00	0.00	0.00	0.00	NaN	NaN	NaN	NaN	NaN	NaN
7.00	1.00	0.85	0.73	0.61	0.70	0.70	0.70	0.71	1.37	1.63	1.43	1.43	1.43	1.40
14.00	3.00	1.71	2.49	2.41	2.14	2.23	2.24	2.40	1.20	1.25	1.40	1.35	1.34	1.25
21.00	5.00	2.56	4.53	4.36	3.59	4.31	4.42	4.69	1.10	1.15	1.39	1.16	1.13	1.07
28.00	7.20	3.41	6.37	6.12	5.05	6.47	6.73	6.98	1.13	1.18	1.43	1.11	1.07	1.03
35.00	9.55	4.26	8.07	7.79	6.50	8.50	8.92	9.08	1.18	1.23	1.47	1.12	1.07	1.05
42.00	11.79	5.12	9.72	9.43	7.96	10.39	10.96	11.05	1.21	1.25	1.48	1.13	1.08	1.07
49.00	14.22	5.97	11.35	11.05	9.42	12.22	12.91	12.96	1.25	1.29	1.51	1.16	1.10	1.10
56.00	16.95	6.82	12.98	12.66	10.88	14.00	14.81	14.84	1.31	1.34	1.56	1.21	1.14	1.14
63.00	19.71	7.67	14.60	14.27	12.33	15.77	16.69	16.70	1.35	1.38	1.60	1.25	1.18	1.18
70.00	23.50	8.53	16.22	15.87	13.79	17.53	18.55	18.56	1.45	1.48	1.70	1.34	1.27	1.27

Note :

i = (2)/(4) iv = (2)/(7)
ii = (2)/(5) v = (2)/(8)
iii = (2)/(6) vi = (2)/(9)

OUTPUT PROGRAM LOAD DEFLECTION

BEAM PROPERTIES :

```
 b   = 150.00 mm
 h   = 230.00 mm
 d   = 184.00 mm
 L   = 2.750 m
 a   = 0.920 m
 rho = 1.64 percent          Es  = 196000 MPa
 fcu = 37.00 MPa             Ec  = 27400 MPa
```

COMPARISON OF DEFLECTION USING VARIOUS METHODS B2H35

P(kN)	Measured delta (mm)	Ma/Mcr	Deflection						Comparison					
			Fikry	ACI	BS	Case1	Case2a	Case2b	(i)	(ii)	(iii)	(iv)	(v)	(vi)
(1)	(2)	(3)	(4)	(5)	(6)	(7)	(8)	(9)	(10)	(11)	(12)	(13)	(14)	(15)
0.00	0.00	0.00	0.00	0.00	0.00	0.00	0.00	0.00	NaN	NaN	NaN	NaN	NaN	NaN
6.00	0.83	0.61	0.50	0.53	0.53	0.51	0.51	0.51	1.65	1.56	1.56	1.63	1.62	1.63
12.00	2.08	1.23	1.69	1.48	1.82	1.54	1.53	1.60	1.23	1.41	1.14	1.35	1.36	1.30
18.00	3.63	1.84	3.38	3.28	3.15	3.08	3.07	3.28	1.07	1.11	1.15	1.18	1.18	1.11
24.00	5.19	2.45	5.13	4.95	4.48	4.95	4.96	5.27	1.01	1.05	1.16	1.05	1.05	0.99
30.00	6.85	3.06	6.75	6.49	5.82	6.88	6.95	7.27	1.01	1.06	1.18	1.00	0.99	0.94
36.00	8.51	3.68	8.27	7.96	7.15	8.75	8.90	9.16	1.03	1.07	1.19	0.97	0.96	0.93
42.00	10.17	4.29	9.72	9.39	8.49	10.52	10.75	10.94	1.05	1.08	1.20	0.97	0.95	0.93
48.00	12.04	4.90	11.14	10.80	9.82	12.22	12.52	12.64	1.08	1.11	1.23	0.99	0.96	0.95
54.00	13.70	5.51	12.54	12.20	11.16	13.85	14.22	14.30	1.09	1.12	1.23	0.99	0.96	0.96
60.00	15.36	6.13	13.94	13.59	12.49	15.45	15.88	15.93	1.10	1.13	1.23	0.99	0.97	0.96
66.00	17.43	6.74	15.33	14.97	13.83	17.03	17.51	17.54	1.14	1.16	1.26	1.02	1.00	0.99
72.00	19.30	7.35	16.73	16.36	15.16	18.60	19.12	19.14	1.15	1.18	1.27	1.04	1.01	1.01
78.00	21.17	7.96	18.12	17.73	16.50	20.16	20.73	20.74	1.17	1.19	1.28	1.05	1.02	1.02
84.00	23.86	8.58	19.52	19.11	17.83	21.71	22.33	22.34	1.22	1.25	1.34	1.10	1.07	1.07
90.00	27.00	9.19	20.91	20.48	19.17	23.26	23.93	23.94	1.29	1.32	1.41	1.16	1.13	1.13

Note :

```
   i = (2)/(4)        iv = (2)/(7)
  ii = (2)/(5)         v = (2)/(8)
 iii = (2)/(6)        vi = (2)/(9)
```

OUTPUT PROGRAM LOAD DEFLECTION

BEAM PROPERTIES :

b = 150.00 mm
h = 230.00 mm
d = 184.00 mm
L = 2.750 m
a = 0.920 m
rho = 1.64 percent   Es = 196000 MPa
fcu = 48.00 MPa   Ec = 30639 MPa

COMPARISON OF DEFLECTION USING VARIOUS METHODS   B2H45

P(kN)	Measured delta (mm)	Ma/Mcr	Deflection						Comparison					
			Fikry	ACI	BS	Case1	Case2a	Case2b	(i)	(ii)	(iii)	(iv)	(v)	(vi)
(1)	(2)	(3)	(4)	(5)	(6)	(7)	(8)	(9)	(10)	(11)	(12)	(13)	(14)	(15)
0.00	0.00	0.00	0.00	0.00	0.00	0.00	0.00	0.00	NaN	NaN	NaN	NaN	NaN	NaN
5.52	0.61	0.49	0.36	0.44	0.44	0.38	0.38	0.37	1.69	1.39	1.39	1.59	1.59	1.63
9.00	1.20	0.81	0.82	0.71	1.08	0.79	0.79	0.80	1.46	1.68	1.11	1.52	1.52	1.49
18.00	3.20	1.61	2.93	2.79	2.95	2.53	2.57	2.76	1.09	1.15	1.08	1.26	1.24	1.16
27.00	5.60	2.42	5.54	5.30	4.83	5.01	5.23	5.59	1.01	1.06	1.16	1.12	1.07	1.00
36.00	8.00	3.23	7.94	7.55	6.71	7.66	8.16	8.53	1.01	1.06	1.19	1.04	0.98	0.94
45.00	10.40	4.03	10.12	9.68	8.60	10.17	10.99	11.26	1.03	1.07	1.21	1.02	0.95	0.92
54.00	12.80	4.84	12.21	11.75	10.48	12.52	13.63	13.79	1.05	1.09	1.22	1.02	0.94	0.93
63.00	15.40	5.65	14.27	13.78	12.36	14.75	16.12	16.21	1.08	1.12	1.25	1.04	0.96	0.95
72.00	18.00	6.45	16.31	15.80	14.25	16.93	18.53	18.58	1.10	1.14	1.26	1.06	0.97	0.97
81.00	20.80	7.26	18.35	17.81	16.13	19.08	20.89	20.92	1.13	1.17	1.29	1.09	1.00	0.99
90.00	24.20	8.07	20.39	19.82	18.01	21.22	23.24	23.25	1.19	1.22	1.34	1.14	1.04	1.04
94.00	26.20	8.43	21.30	20.71	18.85	22.16	24.28	24.29	1.23	1.27	1.39	1.18	1.08	1.08

Note :

i = (2)/(4)   iv = (2)/(7)
ii = (2)/(5)   v = (2)/(8)
iii = (2)/(6)   vi = (2)/(9)

OUTPUT PROGRAM LOAD DEFLECTION

BEAM PROPERTIES :

```
 b   = 150.00 mm
 h   = 230.00 mm
 d   = 184.00 mm
 L   = 2.750 m
 a   = 0.920 m
 rho = 0.82 percent          Es  = 196000 MPa
 fcu = 29.00 MPa             Ec  = 26452 MPa
```

COMPARISON OF DEFLECTION USING VARIOUS METHODS B2L25

P(kN)	Measured delta (mm)	Ma/Mcr	Deflection Fikry	ACI	BS	Case1	Case2a	Case2b	Comparison (i)	(ii)	(iii)	(iv)	(v)	(vi)
(1)	(2)	(3)	(4)	(5)	(6)	(7)	(8)	(9)	(10)	(11)	(12)	(13)	(14)	(15)
0.00	0.00	0.00	0.00	0.00	0.00	0.00	0.00	0.00	NaN	NaN	NaN	NaN	NaN	NaN
4.00	0.40	0.46	0.31	0.37	0.37	0.24	0.23	0.22	1.28	1.09	1.09	1.70	1.76	1.81
6.00	1.50	0.69	0.56	0.55	0.68	0.58	0.58	0.58	2.67	2.72	2.22	2.59	2.59	2.58
8.00	2.43	0.92	0.89	0.61	1.35	1.19	1.22	1.26	2.74	3.99	1.81	2.05	1.99	1.93
12.00	4.35	1.38	1.81	2.10	2.77	3.28	3.44	3.58	2.41	2.07	1.57	1.33	1.26	1.21
16.00	6.45	1.85	3.11	4.10	4.21	5.86	6.06	6.21	2.07	1.57	1.53	1.10	1.06	1.04
20.00	8.60	2.31	4.77	6.13	5.66	8.16	8.32	8.40	1.80	1.40	1.52	1.05	1.03	1.02
24.00	10.70	2.77	6.67	8.06	7.11	10.14	10.26	10.29	1.60	1.33	1.50	1.05	1.04	1.04
28.00	12.80	3.23	8.69	9.88	8.57	11.96	12.06	12.08	1.47	1.30	1.49	1.07	1.06	1.06
32.00	14.90	3.69	10.72	11.62	10.02	13.72	13.82	13.82	1.39	1.28	1.49	1.09	1.08	1.08
35.00	16.50	4.04	12.21	12.90	11.11	15.01	15.12	15.12	1.35	1.28	1.48	1.10	1.09	1.09
36.00	17.22	4.15	12.69	13.31	11.48	15.45	15.55	15.55	1.36	1.29	1.50	1.11	1.11	1.11
38.00	19.20	4.38	13.65	14.14	12.20	16.31	16.42	16.42	1.41	1.36	1.57	1.18	1.17	1.17

Note :

```
    i   = (2)/(4)        iv = (2)/(7)
    ii  = (2)/(5)         v = (2)/(8)
    iii = (2)/(6)        vi = (2)/(9)
```

OUTPUT PROGRAM LOAD DEFLECTION

BEAM PROPERTIES :

```
b   = 150.00 mm
h   = 230.00 mm
d   = 184.00 mm
L   = 2.750 m
a   = 0.920 m
rho = 0.82 percent          Es  = 196000 MPa
fcu = 38.00 MPa             Ec  = 27349 MPa
```

COMPARISON OF DEFLECTION USING VARIOUS METHODS B2L35

P(kN)	Measured delta (mm)	Ma/Mcr	Deflection						Comparison					
			Fikry	ACI	BS	Case1	Case2a	Case2b	(i)	(ii)	(iii)	(iv)	(v)	(vi)
(1)	(2)	(3)	(4)	(5)	(6)	(7)	(8)	(9)	(10)	(11)	(12)	(13)	(14)	(15)
0.00	0.00	0.00	0.00	0.00	0.00	0.00	0.00	0.00	NaN	NaN	NaN	NaN	NaN	NaN
5.00	0.78	0.50	0.39	0.44	0.44	0.31	0.30	0.30	2.00	1.75	1.75	2.50	2.56	2.63
10.00	2.61	1.01	1.14	0.91	2.08	1.66	1.72	1.78	2.29	2.88	1.26	1.57	1.52	1.47
15.00	4.70	1.51	2.37	2.94	3.92	4.49	4.69	4.87	1.98	1.60	1.20	1.05	1.00	0.97
20.00	7.13	2.02	4.12	5.46	5.79	7.65	7.83	7.97	1.73	1.31	1.23	0.93	0.91	0.90
25.00	9.57	2.52	6.30	7.94	7.65	10.34	10.43	10.49	1.52	1.20	1.25	0.93	0.92	0.91
30.00	12.00	3.02	8.74	10.28	9.52	12.68	12.73	12.75	1.37	1.17	1.26	0.95	0.94	0.94
35.00	14.26	3.53	11.26	12.48	11.38	14.88	14.91	14.92	1.27	1.14	1.25	0.96	0.96	0.96
40.00	16.70	4.03	13.74	14.61	13.25	17.04	17.05	17.06	1.22	1.14	1.26	0.98	0.98	0.98
44.00	19.00	4.43	15.65	16.26	14.75	18.75	18.76	18.76	1.21	1.17	1.29	1.01	1.01	1.01

Note :

```
   i  = (2)/(4)      iv = (2)/(7)
   ii = (2)/(5)       v = (2)/(8)
  iii = (2)/(6)      vi = (2)/(9)
```

OUTPUT PROGRAM LOAD DEFLECTION

BEAM PROPERTIES :

```
 b   = 150.00 mm
 h   = 230.00 mm
 d   = 184.00 mm
 L   = 2.750 m
 a   = 0.920 m
 rho = 0.82 percent            Es  = 196000 MPa
 fcu = 49.00 MPa               Ec  = 29898 MPa
```

COMPARISON OF DEFLECTION USING VARIOUS METHODS — B2L45

P(kN)	Measured delta (mm)	Ma/Mcr	Deflection Fikry	ACI	BS	Case1	Case2a	Case2b	Comparison (i)	(ii)	(iii)	(iv)	(v)	(vi)
(1)	(2)	(3)	(4)	(5)	(6)	(7)	(8)	(9)	(10)	(11)	(12)	(13)	(14)	(15)
0.00	0.00	0.00	0.00	0.00	0.00	0.00	0.00	0.00	NaN	NaN	NaN	NaN	NaN	NaN
4.00	0.61	0.35	0.25	0.33	0.33	0.16	0.15	0.15	2.41	1.87	1.87	3.77	3.97	4.18
8.00	1.30	0.71	0.67	0.65	1.29	0.71	0.71	0.72	1.94	2.00	1.01	1.84	1.83	1.82
12.00	3.00	1.06	1.31	1.13	2.70	2.01	2.10	2.19	2.29	2.66	1.11	1.50	1.43	1.37
16.00	5.00	1.42	2.21	2.66	4.13	4.13	4.38	4.57	2.26	1.88	1.21	1.21	1.14	1.09
20.00	7.00	1.77	3.41	4.57	5.57	6.59	6.93	7.13	2.06	1.53	1.26	1.06	1.01	0.98
24.00	8.91	2.13	4.87	6.57	7.02	8.89	9.23	9.36	1.83	1.36	1.27	1.00	0.97	0.95
28.00	10.83	2.48	6.57	8.53	8.46	10.90	11.22	11.30	1.65	1.27	1.28	0.99	0.96	0.96
32.00	12.75	2.84	8.44	10.40	9.91	12.72	13.03	13.07	1.51	1.23	1.29	1.00	0.98	0.98
36.00	14.67	3.19	10.39	12.20	11.35	14.42	14.75	14.77	1.41	1.20	1.29	1.02	0.99	0.99
40.00	16.42	3.55	12.36	13.93	12.80	16.08	16.43	16.44	1.33	1.18	1.28	1.02	1.00	1.00
44.00	18.50	3.90	14.31	15.62	14.25	17.71	18.09	18.09	1.29	1.18	1.30	1.04	1.02	1.02
48.00	20.50	4.26	16.20	17.26	15.69	19.33	19.74	19.74	1.27	1.19	1.31	1.06	1.04	1.04

Note :

```
    i   = (2)/(4)          iv = (2)/(7)
    ii  = (2)/(5)           v = (2)/(8)
    iii = (2)/(6)          vi = (2)/(9)
```

OUTPUT PROGRAM LOAD DEFLECTION

BEAM PROPERTIES :

b = 150.00 mm
h = 230.00 mm
d = 184.00 mm
L = 2.750 m
a = 0.920 m
rho = 1.23 percent   Es = 196000 MPa
fcu = 28.00 MPa   Ec = 26562 MPa

COMPARISON OF DEFLECTION USING VARIOUS METHODS   B2N25

P(kN)	Measured delta (mm)	Ma/Mcr	Deflection Fikry	ACI	BS	Case1	Case2a	Case2b	Comparison (i)	(ii)	(iii)	(iv)	(v)	(vi)
(1)	(2)	(3)	(4)	(5)	(6)	(7)	(8)	(9)	(10)	(11)	(12)	(13)	(14)	(15)
0.00	0.00	0.00	0.00	0.00	0.00	0.00	0.00	0.00	NaN	NaN	NaN	NaN	NaN	NaN
6.00	1.05	0.70	0.57	0.55	0.59	0.58	0.58	0.57	1.86	1.91	1.78	1.82	1.82	1.83
12.00	2.62	1.41	1.86	1.94	2.21	2.38	2.44	2.23	1.41	1.35	1.18	1.10	1.07	1.18
18.00	4.71	2.11	3.83	4.17	3.88	4.99	5.13	4.77	1.23	1.13	1.21	0.94	0.92	0.99
24.00	6.94	2.82	6.05	6.22	5.55	7.45	7.62	7.36	1.15	1.12	1.25	0.93	0.91	0.94
30.00	9.30	3.52	8.21	8.11	7.22	9.63	9.82	9.68	1.13	1.15	1.29	0.97	0.95	0.96
36.00	11.26	4.23	10.21	9.92	8.90	11.66	11.87	11.81	1.10	1.13	1.27	0.97	0.95	0.95
42.00	13.61	4.93	12.10	11.70	10.57	13.63	13.88	13.85	1.12	1.16	1.29	1.00	0.98	0.98
48.00	15.71	5.63	13.93	13.44	12.24	15.59	15.87	15.86	1.13	1.17	1.28	1.01	0.99	0.99
54.00	18.32	6.34	15.71	15.18	13.92	17.54	17.85	17.85	1.17	1.21	1.32	1.04	1.03	1.03
60.00	21.20	7.04	17.48	16.90	15.59	19.49	19.84	19.84	1.21	1.25	1.36	1.09	1.07	1.07
66.00	24.00	7.75	19.23	18.62	17.27	21.44	21.82	21.82	1.25	1.29	1.39	1.12	1.10	1.10

Note :

i = (2)/(4)   iv = (2)/(7)
ii = (2)/(5)   v = (2)/(8)
iii = (2)/(6)   vi = (2)/(9)

OUTPUT PROGRAM LOAD DEFLECTION

BEAM PROPERTIES :

b = 150.00 mm
h = 230.00 mm
d = 184.00 mm
L = 2.750 m
a = 0.920 m
rho = 1.23 percent Es = 196000 MPa
fcu = 38.00 MPa Ec = 27180 MPa

COMPARISON OF DEFLECTION USING VARIOUS METHODS B2N35

P(kN)	Measured delta (mm)	Ma/Mcr	Deflection						Comparison					
			Fikry	ACI	BS	Case1	Case2a	Case2b	(i)	(ii)	(iii)	(iv)	(v)	(vi)
(1)	(2)	(3)	(4)	(5)	(6)	(7)	(8)	(9)	(10)	(11)	(12)	(13)	(14)	(15)
0.00	0.00	0.00	0.00	0.00	0.00	0.00	0.00	0.00	NaN	NaN	NaN	NaN	NaN	NaN
6.00	0.77	0.60	0.51	0.54	0.58	0.49	0.49	0.50	1.52	1.43	1.33	1.57	1.57	1.55
9.30	1.40	0.94	1.03	0.83	1.45	1.16	1.18	1.12	1.36	1.68	0.97	1.20	1.19	1.25
12.00	2.58	1.21	1.62	1.53	2.18	1.99	2.03	1.87	1.60	1.69	1.18	1.30	1.27	1.38
18.00	4.64	1.81	3.37	3.73	3.83	4.46	4.58	4.18	1.38	1.24	1.21	1.04	1.01	1.11
24.00	6.96	2.42	5.52	5.87	5.48	7.08	7.23	6.83	1.26	1.19	1.27	0.98	0.96	1.02
30.00	9.02	3.02	7.73	7.84	7.14	9.43	9.58	9.31	1.17	1.15	1.26	0.96	0.94	0.97
36.00	11.34	3.63	9.85	9.70	8.80	11.56	11.72	11.57	1.15	1.17	1.29	0.98	0.97	0.98
42.00	13.66	4.23	11.84	11.50	10.45	13.59	13.75	13.68	1.15	1.19	1.31	1.01	0.99	1.00
48.00	15.98	4.84	13.73	13.27	12.11	15.56	15.75	15.71	1.16	1.20	1.32	1.03	1.01	1.02
54.00	18.20	5.44	15.55	15.01	13.76	17.52	17.73	17.71	1.17	1.21	1.32	1.04	1.03	1.03
60.00	20.50	6.05	17.33	16.74	15.42	19.47	19.70	19.69	1.18	1.22	1.33	1.05	1.04	1.04
66.00	23.00	6.65	19.10	18.46	17.08	21.42	21.67	21.67	1.20	1.25	1.35	1.07	1.06	1.06
68.00	25.00	6.85	19.68	19.03	17.63	22.07	22.33	22.33	1.27	1.31	1.42	1.13	1.12	1.12

Note :

i = (2)/(4) iv = (2)/(7)
ii = (2)/(5) v = (2)/(8)
iii = (2)/(6) vi = (2)/(9)

OUTPUT PROGRAM LOAD DEFLECTION

BEAM PROPERTIES :
b = 150.00 mm
h = 230.00 mm
d = 184.00 mm
L = 2.750 m
a = 0.920 m
rho = 1.23 percent   Es = 196000 MPa
fcu = 50.00 MPa   Ec = 29848 MPa

COMPARISON OF DEFLECTION USING VARIOUS METHODS   B2N45

P(kN)	Measured delta (mm)	Ma/Mcr	Deflection Fikry	ACI	BS	Case1	Case2a	Case2b	Comparison (i)	(ii)	(iii)	(iv)	(v)	(vi)
(1)	(2)	(3)	(4)	(5)	(6)	(7)	(8)	(9)	(10)	(11)	(12)	(13)	(14)	(15)
0.00	0.00	0.00	0.00	0.00	0.00	0.00	0.00	0.00	NaN	NaN	NaN	NaN	NaN	NaN
5.00	0.52	0.44	0.33	0.41	0.41	0.29	0.29	0.30	1.57	1.28	1.28	1.78	1.81	1.71
10.00	1.31	0.88	0.97	0.81	1.56	1.07	1.08	1.04	1.35	1.61	0.84	1.23	1.21	1.26
15.00	2.88	1.32	2.01	2.02	2.87	2.51	2.61	2.38	1.44	1.42	1.00	1.15	1.10	1.21
20.00	4.70	1.76	3.43	3.83	4.19	4.47	4.71	4.27	1.37	1.23	1.12	1.05	1.00	1.10
25.00	6.50	2.20	5.13	5.62	5.51	6.56	6.92	6.42	1.27	1.16	1.18	0.99	0.94	1.01
30.00	8.20	2.64	6.95	7.30	6.84	8.52	8.98	8.56	1.18	1.12	1.20	0.96	0.91	0.96
35.00	10.20	3.07	8.76	8.90	8.16	10.31	10.86	10.55	1.16	1.15	1.25	0.99	0.94	0.97
40.00	11.80	3.51	10.51	10.43	9.49	11.99	12.60	12.40	1.12	1.13	1.24	0.98	0.94	0.95
45.00	13.80	3.95	12.18	11.92	10.81	13.58	14.28	14.15	1.13	1.16	1.28	1.02	0.97	0.98
50.00	15.20	4.39	13.77	13.38	12.14	15.14	15.91	15.84	1.10	1.14	1.25	1.00	0.96	0.96
55.00	17.00	4.83	15.31	14.82	13.46	16.68	17.52	17.48	1.11	1.15	1.26	1.02	0.97	0.97
60.00	19.00	5.27	16.80	16.24	14.79	18.21	19.12	19.10	1.13	1.17	1.28	1.04	0.99	0.99
65.00	21.00	5.71	18.26	17.66	16.11	19.73	20.72	20.71	1.15	1.19	1.30	1.06	1.01	1.01
69.00	22.77	6.06	19.42	18.78	17.18	20.95	22.00	21.99	1.17	1.21	1.33	1.09	1.04	1.04

Note :
i = (2)/(4)   iv = (2)/(7)
ii = (2)/(5)   v = (2)/(8)
iii = (2)/(6)   vi = (2)/(9)

OUTPUT PROGRAM LOAD DEFLECTION

BEAM PROPERTIES :
b = 150.00 mm
h = 230.00 mm
d = 184.00 mm
L = 2.750 m
a = 1.150 m
rho = 1.64 percent   Es = 196000 MPa
fcu = 26.00 MPa   Ec = 25200 MPa

COMPARISON OF DEFLECTION USING VARIOUS METHODS   B3H25

P (kN)	Measured delta (mm)	Ma/Mcr	Deflection Comparison											
			Fikry	ACI	BS	Case1	Case2a	Case2b	(i)	(ii)	(iii)	(iv)	(v)	(vi)
(1)	(2)	(3)	(4)	(5)	(6)	(7)	(8)	(9)	(10)	(11)	(12)	(13)	(14)	(15)
0.00	0.00	0.00	0.00	0.00	0.00	0.00	0.00	0.00	NaN	NaN	NaN	NaN	NaN	NaN
5.00	0.70	0.76	0.50	0.54	0.54	0.51	0.52	0.51	1.39	1.29	1.29	1.36	1.36	1.37
10.00	2.00	1.52	1.81	1.88	1.81	1.68	1.65	1.73	1.10	1.07	1.10	1.19	1.22	1.15
15.00	3.20	2.28	3.52	3.53	3.10	3.42	3.34	3.55	0.91	0.91	1.03	0.93	0.96	0.90
20.00	5.00	3.05	5.13	5.02	4.39	5.39	5.25	5.50	0.97	1.00	1.14	0.93	0.95	0.91
25.00	7.00	3.81	6.59	6.42	5.68	7.29	7.13	7.33	1.06	1.09	1.23	0.96	0.98	0.96
30.00	9.35	4.57	7.97	7.79	6.97	9.07	8.90	9.02	1.17	1.20	1.34	1.03	1.05	1.04
35.00	11.50	5.33	9.31	9.13	8.26	10.75	10.56	10.63	1.23	1.26	1.39	1.07	1.09	1.08
40.00	13.80	6.09	10.65	10.47	9.55	12.36	12.16	12.20	1.30	1.32	1.44	1.12	1.14	1.13
45.00	16.15	6.85	11.99	11.80	10.84	13.95	13.72	13.75	1.35	1.37	1.49	1.16	1.18	1.17
50.00	18.70	7.61	13.32	13.13	12.13	15.52	15.27	15.28	1.40	1.42	1.54	1.21	1.22	1.22
55.00	21.50	8.37	14.65	14.45	13.42	17.08	16.81	16.81	1.47	1.49	1.60	1.26	1.28	1.28
56.00	22.00	8.53	14.92	14.72	13.68	17.39	17.12	17.12	1.47	1.49	1.61	1.27	1.29	1.28

Note :
i = (2)/(4)   iv = (2)/(7)
ii = (2)/(5)   v = (2)/(8)
iii = (2)/(6)   vi = (2)/(9)

OUTPUT PROGRAM LOAD DEFLECTION

BEAM PROPERTIES :

b = 150.00 mm
h = 230.00 mm
d = 184.00 mm
L = 2.750 m
a = 1.150 m
rho = 1.64 percent   Es = 196000 MPa
fcu = 39.00 MPa   Ec = 27985 MPa

COMPARISON OF DEFLECTION USING VARIOUS METHODS   B3H35

P(kN)	Measured delta (mm)	Ma/Mcr	Deflection						Comparison					
			Fikry	ACI	BS	Case1	Case2a	Case2b	(i)	(ii)	(iii)	(iv)	(v)	(vi)
(1)	(2)	(3)	(4)	(5)	(6)	(7)	(8)	(9)	(10)	(11)	(12)	(13)	(14)	(15)
0.00	0.00	0.00	0.00	0.00	0.00	0.00	0.00	0.00	NaN	NaN	NaN	NaN	NaN	NaN
5.00	0.60	0.62	0.39	0.49	0.50	0.41	0.42	0.41	1.55	1.23	1.19	1.45	1.44	1.48
10.00	2.00	1.24	1.41	1.39	1.71	1.29	1.29	1.34	1.42	1.44	1.17	1.55	1.55	1.49
15.00	3.70	1.86	2.99	3.07	2.93	2.68	2.68	2.87	1.24	1.21	1.26	1.38	1.38	1.29
20.00	5.37	2.49	4.69	4.62	4.15	4.41	4.45	4.75	1.14	1.16	1.29	1.22	1.21	1.13
25.00	7.09	3.11	6.26	6.06	5.38	6.24	6.36	6.67	1.13	1.17	1.32	1.14	1.12	1.06
30.00	8.92	3.73	7.71	7.43	6.61	8.00	8.22	8.49	1.16	1.20	1.35	1.11	1.08	1.05
35.00	10.54	4.35	9.07	8.77	7.83	9.67	9.99	10.18	1.16	1.20	1.35	1.09	1.06	1.04
40.00	12.20	4.97	10.40	10.08	9.06	11.25	11.66	11.79	1.17	1.21	1.35	1.08	1.05	1.03
45.00	14.00	5.59	11.72	11.39	10.29	12.77	13.26	13.35	1.19	1.23	1.36	1.10	1.06	1.05
50.00	16.01	6.22	13.03	12.68	11.51	14.25	14.82	14.87	1.23	1.26	1.39	1.12	1.08	1.08
55.00	18.00	6.84	14.33	13.98	12.74	15.71	16.35	16.38	1.26	1.29	1.41	1.15	1.10	1.10
60.00	20.27	7.46	15.64	15.26	13.97	17.15	17.86	17.88	1.30	1.33	1.45	1.18	1.14	1.13
65.00	23.00	8.08	16.94	16.55	15.20	18.59	19.36	19.37	1.36	1.39	1.51	1.24	1.19	1.19

Note :

i = (2)/(4)   iv = (2)/(7)
ii = (2)/(5)   v = (2)/(8)
iii = (2)/(6)   vi = (2)/(9)

OUTPUT PROGRAM LOAD DEFLECTION

BEAM PROPERTIES :

```
b   = 150.00 mm
h   = 230.00 mm
d   = 184.00 mm
L   = 2.750 m
a   = 1.150 m
rho = 1.64 percent          Es  = 196000 MPa
fcu = 49.00 MPa             Ec  = 31316 MPa
```

COMPARISON OF DEFLECTION USING VARIOUS METHODS B3H45

P(kN)	Measured delta (mm)	Ma/Mcr	Deflection						Comparison					
			Fikry	ACI	BS	Case1	Case2a	Case2b	(i)	(ii)	(iii)	(iv)	(v)	(vi)
(1)	(2)	(3)	(4)	(5)	(6)	(7)	(8)	(9)	(10)	(11)	(12)	(13)	(14)	(15)
0.00	0.00	0.00	0.00	0.00	0.00	0.00	0.00	0.00	NaN	NaN	NaN	NaN	NaN	NaN
7.00	0.80	0.78	0.57	0.61	0.91	0.59	0.59	0.58	1.39	1.31	0.88	1.37	1.37	1.38
14.00	2.20	1.55	2.24	2.33	2.51	1.94	1.97	2.09	0.98	0.95	0.88	1.13	1.12	1.05
21.00	4.30	2.33	4.58	4.54	4.12	4.01	4.18	4.49	0.94	0.95	1.04	1.07	1.03	0.96
28.00	6.40	3.11	6.80	6.53	5.74	6.33	6.78	7.15	0.94	0.98	1.12	1.01	0.94	0.89
35.00	8.50	3.88	8.78	8.40	7.35	8.58	9.35	9.65	0.97	1.01	1.16	0.99	0.91	0.88
42.00	10.80	4.66	10.63	10.21	8.97	10.66	11.73	11.93	1.02	1.06	1.20	1.01	0.92	0.91
49.00	12.80	5.43	12.43	11.99	10.58	12.62	13.96	14.08	1.03	1.07	1.21	1.01	0.92	0.91
56.00	14.90	6.21	14.22	13.75	12.19	14.52	16.10	16.16	1.05	1.08	1.22	1.03	0.93	0.92
63.00	17.20	6.99	16.00	15.50	13.81	16.38	18.18	18.21	1.07	1.11	1.25	1.05	0.95	0.94
70.00	19.60	7.76	17.78	17.25	15.42	18.22	20.23	20.25	1.10	1.14	1.27	1.08	0.97	0.97
74.00	21.00	8.21	18.80	18.25	16.35	19.26	21.40	21.41	1.12	1.15	1.28	1.09	0.98	0.98

Note :

```
    i   = (2)/(4)        iv = (2)/(7)
    ii  = (2)/(5)         v = (2)/(8)
    iii = (2)/(6)        vi = (2)/(9)
```

OUTPUT PROGRAM LOAD DEFLECTION

BEAM PROPERTIES :

```
 b   = 150.00 mm
 h   = 230.00 mm
 d   = 184.00 mm
 L   = 2.750 m
 a   = 1.150 m
 rho = 0.82 percent          Es  = 196000 MPa
 fcu = 28.00 MPa             Ec  = 26883 MPa
```

COMPARISON OF DEFLECTION USING VARIOUS METHODS B3L25

P(kN)	Measured delta (mm)	Ma/Mcr	Deflection						Comparison					
			Fikry	ACI	BS	Case1	Case2a	Case2b	(i)	(ii)	(iii)	(iv)	(v)	(vi)
(1)	(2)	(3)	(4)	(5)	(6)	(7)	(8)	(9)	(10)	(11)	(12)	(13)	(14)	(15)
0.00	0.00	0.00	0.00	0.00	0.00	0.00	0.00	0.00	NaN	NaN	NaN	NaN	NaN	NaN
4.00	0.78	0.59	0.34	0.41	0.41	0.24	0.23	0.22	2.33	1.91	1.91	3.29	3.43	3.56
8.00	2.20	1.17	1.04	1.15	1.82	1.51	1.57	1.63	2.11	1.91	1.21	1.46	1.40	1.35
12.00	4.50	1.76	2.27	3.26	3.41	4.28	4.51	4.67	1.98	1.38	1.32	1.05	1.00	0.96
16.00	6.96	2.35	4.04	5.55	5.02	7.09	7.33	7.42	1.72	1.26	1.39	0.98	0.95	0.94
20.00	9.39	2.93	6.20	7.69	6.63	9.34	9.57	9.60	1.51	1.22	1.42	1.00	0.98	0.98
24.00	11.65	3.52	8.52	9.69	8.24	11.35	11.59	11.60	1.37	1.20	1.41	1.03	1.01	1.00
28.00	14.09	4.11	10.82	11.60	9.85	13.28	13.54	13.54	1.30	1.21	1.43	1.06	1.04	1.04
32.00	16.70	4.70	13.00	13.46	11.47	15.18	15.48	15.48	1.29	1.24	1.46	1.10	1.08	1.08
37.00	20.00	5.43	15.55	15.73	13.48	17.56	17.90	17.90	1.29	1.27	1.48	1.14	1.12	1.12

Note :

```
    i   = (2)/(4)        iv = (2)/(7)
    ii  = (2)/(5)         v = (2)/(8)
    iii = (2)/(6)        vi = (2)/(9)
```

OUTPUT PROGRAM LOAD DEFLECTION

BEAM PROPERTIES :

b = 150.00 mm
h = 230.00 mm
d = 184.00 mm
L = 2.750 m
a = 1.150 m
rho = 0.82 percent   Es = 196000 MPa
fcu = 39.00 MPa   Ec = 28585 MPa

COMPARISON OF DEFLECTION USING VARIOUS METHODS   B3L35

P(kN)	Measured delta (mm)	Ma/Mcr	Deflection Fikry	ACI	BS	Case1	Case2a	Case2b	Comparison (i)	(ii)	(iii)	(iv)	(v)	(vi)
(1)	(2)	(3)	(4)	(5)	(6)	(7)	(8)	(9)	(10)	(11)	(12)	(13)	(14)	(15)
0.00	0.00	0.00	0.00	0.00	0.00	0.00	0.00	0.00	NaN	NaN	NaN	NaN	NaN	NaN
4.00	0.61	0.50	0.29	0.38	0.38	0.18	0.17	0.16	2.09	1.59	1.59	3.38	3.58	3.78
6.00	1.03	0.75	0.54	0.58	1.02	0.48	0.47	0.46	1.92	1.79	1.01	2.17	2.20	2.23
8.00	2.00	0.99	0.87	0.76	1.79	1.05	1.07	1.09	2.31	2.64	1.12	1.91	1.87	1.83
12.00	4.17	1.49	1.83	2.51	3.38	3.27	3.47	3.62	2.28	1.66	1.23	1.27	1.20	1.15
16.00	6.26	1.99	3.26	4.76	4.99	6.20	6.52	6.69	1.92	1.32	1.25	1.01	0.96	0.94
20.00	8.52	2.49	5.12	6.99	6.60	8.76	9.08	9.17	1.66	1.22	1.29	0.97	0.94	0.93
24.00	10.65	2.98	7.28	9.09	8.21	10.90	11.22	11.25	1.46	1.17	1.30	0.98	0.95	0.95
28.00	12.87	3.48	9.56	11.08	9.82	12.85	13.18	13.20	1.35	1.16	1.31	1.00	0.98	0.98
32.00	14.96	3.98	11.84	12.99	11.43	14.73	15.10	15.10	1.26	1.15	1.31	1.02	0.99	0.99
36.00	17.39	4.48	14.02	14.84	13.04	16.58	16.99	16.99	1.24	1.17	1.33	1.05	1.02	1.02
37.00	19.00	4.60	14.55	15.30	13.44	17.04	17.46	17.46	1.31	1.24	1.41	1.11	1.09	1.09

Note :

i = (2)/(4)   iv = (2)/(7)
ii = (2)/(5)   v = (2)/(8)
iii = (2)/(6)   vi = (2)/(9)

OUTPUT PROGRAM LOAD DEFLECTION

BEAM PROPERTIES :

b = 150.00 mm
h = 230.00 mm
d = 184.00 mm
L = 2.750 m
a = 1.150 m
rho = 0.82 percent   Es = 196000 MPa
fcu = 50.00 MPa   Ec = 30764 MPa

COMPARISON OF DEFLECTION USING VARIOUS METHODS   B3L45

P(kN)	Measured delta (mm)	Ma/Mcr	Deflection						Comparison					
			Fikry	ACI	BS	Case1	Case2a	Case2b	(i)	(ii)	(iii)	(iv)	(v)	(vi)
(1)	(2)	(3)	(4)	(5)	(6)	(7)	(8)	(9)	(10)	(11)	(12)	(13)	(14)	(15)
0.00	0.00	0.00	0.00	0.00	0.00	0.00	0.00	0.00	NaN	NaN	NaN	NaN	NaN	NaN
3.00	0.35	0.33	0.18	0.27	0.27	0.08	0.08	0.07	1.99	1.31	1.31	4.18	4.58	4.98
6.00	1.05	0.66	0.46	0.53	0.98	0.36	0.35	0.34	2.26	1.96	1.07	2.89	2.98	3.06
9.00	2.01	0.99	0.90	0.78	2.13	1.08	1.11	1.13	2.23	2.58	0.94	1.85	1.81	1.78
12.00	3.41	1.32	1.53	1.92	3.31	2.49	2.63	2.75	2.23	1.77	1.03	1.37	1.29	1.24
15.00	4.98	1.65	2.37	3.45	4.49	4.48	4.79	4.99	2.10	1.45	1.11	1.11	1.04	1.00
18.00	6.60	1.98	3.44	5.12	5.67	6.62	7.02	7.22	1.92	1.29	1.16	1.00	0.94	0.91
21.00	8.20	2.31	4.72	6.79	6.86	8.55	8.99	9.12	1.74	1.21	1.20	0.96	0.91	0.90
24.00	9.80	2.64	6.19	8.41	8.05	10.24	10.69	10.77	1.58	1.17	1.22	0.96	0.92	0.91
27.00	11.40	2.96	7.78	9.96	9.23	11.76	12.23	12.27	1.46	1.14	1.23	0.97	0.93	0.93
30.00	13.00	3.29	9.45	11.46	10.42	13.19	13.67	13.69	1.38	1.13	1.25	0.99	0.95	0.95
33.00	14.40	3.62	11.14	12.91	11.61	14.56	15.08	15.09	1.29	1.12	1.24	0.99	0.95	0.95
36.00	16.00	3.95	12.81	14.32	12.80	15.91	16.47	16.47	1.25	1.12	1.25	1.01	0.97	0.97
40.00	18.00	4.39	14.97	16.16	14.38	17.69	18.31	18.31	1.20	1.11	1.25	1.02	0.98	0.98

Note :

i = (2)/(4)   iv = (2)/(7)
ii = (2)/(5)   v = (2)/(8)
iii = (2)/(6)   vi = (2)/(9)

OUTPUT PROGRAM LOAD DEFLECTION

BEAM PROPERTIES :

```
 b   = 150.00 mm
 h   = 230.00 mm
 d   = 184.00 mm
 L   = 2.750 m
 a   = 1.150 m
 rho = 1.23 percent              Es  = 196000 MPa
 fcu = 31.00 MPa                 Ec  = 26200 MPa
```

COMPARISON OF DEFLECTION USING VARIOUS METHODS B3N25

P(kN)	Measured delta (mm)	Ma/Mcr	Deflection						Comparison					
			Fikry	ACI	BS	Case1	Case2a	Case2b	(i)	(ii)	(iii)	(iv)	(v)	(vi)
(1)	(2)	(3)	(4)	(5)	(6)	(7)	(8)	(9)	(10)	(11)	(12)	(13)	(14)	(15)
0.00	0.00	0.00	0.00	0.00	0.00	0.00	0.00	0.00	NaN	NaN	NaN	NaN	NaN	NaN
5.00	0.70	0.70	0.46	0.52	0.58	0.43	0.43	0.44	1.51	1.34	1.20	1.62	1.64	1.58
10.00	2.50	1.39	1.58	1.82	2.07	1.96	2.00	1.84	1.58	1.37	1.21	1.28	1.25	1.36
15.00	4.50	2.09	3.39	3.92	3.59	4.49	4.57	4.21	1.33	1.15	1.25	1.00	0.98	1.07
20.00	6.80	2.79	5.52	5.85	5.11	7.00	7.06	6.76	1.23	1.16	1.33	0.97	0.96	1.01
25.00	8.90	3.49	7.61	7.64	6.63	9.17	9.21	9.04	1.17	1.17	1.34	0.97	0.97	0.98
30.00	11.20	4.18	9.55	9.35	8.16	11.15	11.18	11.10	1.17	1.20	1.37	1.00	1.00	1.01
35.00	13.00	4.88	11.37	11.02	9.68	13.06	13.08	13.05	1.14	1.18	1.34	1.00	0.99	1.00
40.00	15.00	5.58	13.10	12.66	11.20	14.94	14.96	14.94	1.14	1.18	1.34	1.00	1.00	1.00
45.00	17.20	6.28	14.79	14.30	12.73	16.81	16.83	16.83	1.16	1.20	1.35	1.02	1.02	1.02
50.00	19.20	6.97	16.46	15.92	14.25	18.68	18.70	18.70	1.17	1.21	1.35	1.03	1.03	1.03
55.00	21.50	7.67	18.12	17.54	15.78	20.54	20.57	20.57	1.19	1.23	1.36	1.05	1.05	1.05

Note :

```
      i   = (2)/(4)        iv = (2)/(7)
      ii  = (2)/(5)         v = (2)/(8)
      iii = (2)/(6)        vi = (2)/(9)
```

OUTPUT PROGRAM LOAD DEFLECTION

BEAM PROPERTIES :
b = 150.00 mm
h = 230.00 mm
d = 184.00 mm
L = 2.750 m
a = 1.150 m
rho = 1.23 percent   Es = 196000 MPa
fcu = 41.00 MPa   Ec = 27787 MPa

COMPARISON OF DEFLECTION USING VARIOUS METHODS   B3N35

P(kN)	Measured delta (mm)	Ma/Mcr	Deflection						Comparison					
			Fikry	ACI	BS	Case1	Case2a	Case2b	(i)	(ii)	(iii)	(iv)	(v)	(vi)
(1)	(2)	(3)	(4)	(5)	(6)	(7)	(8)	(9)	(10)	(11)	(12)	(13)	(14)	(15)
0.00	0.00	0.00	0.00	0.00	0.00	0.00	0.00	0.00	NaN	NaN	NaN	NaN	NaN	NaN
5.00	0.65	0.61	0.40	0.49	0.57	0.35	0.35	0.37	1.62	1.32	1.14	1.83	1.86	1.76
10.00	2.00	1.21	1.33	1.41	2.05	1.56	1.59	1.48	1.51	1.42	0.98	1.28	1.26	1.35
15.00	4.00	1.82	2.89	3.47	3.56	3.80	3.92	3.56	1.38	1.15	1.12	1.05	1.02	1.12
20.00	6.60	2.43	4.90	5.47	5.08	6.34	6.53	6.10	1.35	1.21	1.30	1.04	1.01	1.08
25.00	9.10	3.03	7.03	7.31	6.60	8.62	8.84	8.54	1.29	1.24	1.38	1.06	1.03	1.07
30.00	11.25	3.64	9.07	9.05	8.12	10.65	10.89	10.72	1.24	1.24	1.39	1.06	1.03	1.05
35.00	13.50	4.24	10.98	10.74	9.64	12.55	12.81	12.73	1.23	1.26	1.40	1.08	1.05	1.06
40.00	15.81	4.85	12.77	12.38	11.16	14.38	14.68	14.64	1.24	1.28	1.42	1.10	1.08	1.08
45.00	18.14	5.46	14.49	14.01	12.68	16.20	16.53	16.51	1.25	1.29	1.43	1.12	1.10	1.10

Note :
i = (2)/(4)   iv = (2)/(7)
ii = (2)/(5)   v = (2)/(8)
iii = (2)/(6)   vi = (2)/(9)

OUTPUT PROGRAM LOAD DEFLECTION

BEAM PROPERTIES :

b = 150.00 mm
h = 230.00 mm
d = 184.00 mm
L = 2.750 m
a = 1.150 m
rho = 1.23 percent   Es = 196000 MPa
fcu = 52.00 MPa   Ec = 29775 MPa

COMPARISON OF DEFLECTION USING VARIOUS METHODS   B3N45

P(kN)	Measured delta (mm)	Ma/Mcr	Deflection						Comparison					
			Fikry	ACI	BS	Case1	Case2a	Case2b	(i)	(ii)	(iii)	(iv)	(v)	(vi)
(1)	(2)	(3)	(4)	(5)	(6)	(7)	(8)	(9)	(10)	(11)	(12)	(13)	(14)	(15)
0.00	0.00	0.00	0.00	0.00	0.00	0.00	0.00	0.00	NaN	NaN	NaN	NaN	NaN	NaN
4.00	0.48	0.43	0.25	0.37	0.37	0.20	0.20	0.22	1.90	1.30	1.30	2.39	2.46	2.21
8.00	1.07	0.86	0.75	0.74	1.41	0.76	0.76	0.76	1.42	1.45	0.76	1.40	1.40	1.41
12.00	2.14	1.29	1.59	1.77	2.59	1.90	1.96	1.81	1.35	1.21	0.83	1.12	1.09	1.18
16.00	3.57	1.72	2.79	3.39	3.79	3.62	3.78	3.41	1.28	1.05	0.94	0.99	0.95	1.05
20.00	5.24	2.15	4.28	5.01	4.98	5.58	5.86	5.37	1.22	1.05	1.05	0.94	0.89	0.98
24.00	6.80	2.58	5.94	6.54	6.18	7.48	7.85	7.39	1.15	1.04	1.10	0.91	0.87	0.92
28.00	8.50	3.01	7.63	7.99	7.38	9.22	9.65	9.29	1.11	1.06	1.15	0.92	0.88	0.91
32.00	10.00	3.45	9.27	9.38	8.57	10.80	11.29	11.05	1.08	1.07	1.17	0.93	0.89	0.91
36.00	11.70	3.88	10.83	10.73	9.77	12.29	12.84	12.68	1.08	1.09	1.20	0.95	0.91	0.92
40.00	13.20	4.31	12.31	12.05	10.97	13.72	14.33	14.24	1.07	1.10	1.20	0.96	0.92	0.93
44.00	14.60	4.74	13.73	13.35	12.17	15.13	15.79	15.74	1.06	1.09	1.20	0.96	0.92	0.93
48.00	16.00	5.17	15.10	14.64	13.36	16.52	17.24	17.21	1.06	1.09	1.20	0.97	0.93	0.93
52.00	17.60	5.60	16.44	15.91	14.56	17.91	18.69	18.67	1.07	1.11	1.21	0.98	0.94	0.94
54.00	19.00	5.81	17.10	16.55	15.16	18.60	19.41	19.40	1.11	1.15	1.25	1.02	0.98	0.98

Note :

i = (2)/(4)   iv = (2)/(7)
ii = (2)/(5)   v = (2)/(8)
iii = (2)/(6)   vi = (2)/(9)

OUTPUT PROGRAM LOAD DEFLECTION

BEAM PROPERTIES :

b = 150.00 mm
h = 230.00 mm
d = 184.00 mm
L = 2.750 m
a = 1.375 m
rho = 1.64 percent   Es = 196000 MPa
fcu = 26.00 MPa   Ec = 26629 MPa

COMPARISON OF DEFLECTION USING VARIOUS METHODS   B4H25

P(kN)	Measured delta (mm)	Ma/Mcr	Deflection						Comparison					
			Fikry	ACI	BS	Case1	Case2a	Case2b	(i)	(ii)	(iii)	(iv)	(v)	(vi)
(1)	(2)	(3)	(4)	(5)	(6)	(7)	(8)	(9)	(10)	(11)	(12)	(13)	(14)	(15)
0.00	0.00	0.00	0.00	0.00	0.00	0.00	0.00	0.00	NaN	NaN	NaN	NaN	NaN	NaN
4.00	0.40	0.73	0.32	0.43	0.43	0.35	0.35	0.34	1.25	0.93	0.93	1.15	1.15	1.19
8.00	1.70	1.46	1.26	1.44	1.40	1.16	1.15	1.20	1.35	1.18	1.22	1.47	1.47	1.41
12.00	3.10	2.18	2.68	2.82	2.41	2.47	2.46	2.62	1.15	1.10	1.29	1.26	1.26	1.18
16.00	4.50	2.91	4.10	4.06	3.42	4.03	4.04	4.27	1.10	1.11	1.31	1.12	1.11	1.05
20.00	6.00	3.64	5.37	5.22	4.44	5.59	5.66	5.87	1.12	1.15	1.35	1.07	1.06	1.02
24.00	7.60	4.37	6.53	6.35	5.46	7.04	7.17	7.32	1.16	1.20	1.39	1.08	1.06	1.04
28.00	9.20	5.10	7.65	7.46	6.47	8.40	8.59	8.69	1.20	1.23	1.42	1.09	1.07	1.06
32.00	10.80	5.83	8.76	8.55	7.49	9.70	9.94	9.99	1.23	1.26	1.44	1.11	1.09	1.08
36.00	12.56	6.55	9.85	9.64	8.50	10.96	11.24	11.27	1.27	1.30	1.48	1.15	1.12	1.11
40.00	14.50	7.28	10.95	10.73	9.52	12.20	12.52	12.54	1.32	1.35	1.52	1.19	1.16	1.16
44.00	16.40	8.01	12.05	11.82	10.54	13.43	13.79	13.80	1.36	1.39	1.56	1.22	1.19	1.19
48.00	18.60	8.74	13.14	12.90	11.55	14.66	15.05	15.06	1.42	1.44	1.61	1.27	1.24	1.24
50.00	21.00	9.10	13.69	13.44	12.06	15.27	15.68	15.68	1.53	1.56	1.74	1.37	1.34	1.34

Note :

i = (2)/(4)   iv = (2)/(7)
ii = (2)/(5)   v = (2)/(8)
iii = (2)/(6)   vi = (2)/(9)

OUTPUT PROGRAM LOAD DEFLECTION

BEAM PROPERTIES :

```
 b   = 150.00 mm
 h   = 230.00 mm
 d   = 184.00 mm
 L   = 2.750 m
 a   = 1.375 m
 rho = 1.64 percent          Es  = 196000 MPa
 fcu = 39.00 MPa             Ec  = 27800 MPa
```

COMPARISON OF DEFLECTION USING VARIOUS METHODS B4H35

P(kN)	Measured delta (mm)	Ma/Mcr	Deflection						Comparison					
			Fikry	ACI	BS	Case1	Case2a	Case2b	(i)	(ii)	(iii)	(iv)	(v)	(vi)
(1)	(2)	(3)	(4)	(5)	(6)	(7)	(8)	(9)	(10)	(11)	(12)	(13)	(14)	(15)
0.00	0.00	0.00	0.00	0.00	0.00	0.00	0.00	0.00	NaN	NaN	NaN	NaN	NaN	NaN
5.00	0.65	0.74	0.39	0.51	0.64	0.42	0.42	0.41	1.68	1.27	1.01	1.55	1.54	1.59
10.00	2.00	1.49	1.56	1.79	1.91	1.42	1.41	1.48	1.28	1.12	1.05	1.41	1.41	1.35
15.00	3.80	2.23	3.34	3.49	3.19	3.04	3.04	3.25	1.14	1.09	1.19	1.25	1.25	1.17
20.00	5.70	2.97	5.09	5.01	4.47	4.97	5.02	5.31	1.12	1.14	1.27	1.15	1.14	1.07
25.00	7.50	3.72	6.65	6.45	5.76	6.88	7.02	7.28	1.13	1.16	1.30	1.09	1.07	1.03
30.00	9.50	4.46	8.09	7.84	7.04	8.65	8.89	9.07	1.17	1.21	1.35	1.10	1.07	1.05
35.00	11.40	5.20	9.48	9.20	8.33	10.31	10.64	10.75	1.20	1.24	1.37	1.11	1.07	1.06
40.00	13.40	5.95	10.85	10.56	9.61	11.89	12.30	12.37	1.24	1.27	1.39	1.13	1.09	1.08
45.00	15.20	6.69	12.21	11.90	10.89	13.44	13.91	13.94	1.25	1.28	1.40	1.13	1.09	1.09
50.00	17.70	7.43	13.56	13.25	12.18	14.95	15.49	15.51	1.31	1.34	1.45	1.18	1.14	1.14
55.00	19.80	8.18	14.92	14.59	13.46	16.46	17.06	17.07	1.33	1.36	1.47	1.20	1.16	1.16

Note :

```
     i   = (2)/(4)        iv = (2)/(7)
     ii  = (2)/(5)         v = (2)/(8)
     iii = (2)/(6)        vi = (2)/(9)
```

OUTPUT PROGRAM LOAD DEFLECTION

BEAM PROPERTIES :

b = 150.00 mm
h = 230.00 mm
d = 184.00 mm
L = 2.750 m
a = 1.375 m
rho = 1.64 percent
fcu = 48.00 MPa
Es = 196000 MPa
Ec = 32852 MPa

COMPARISON OF DEFLECTION USING VARIOUS METHODS — B4H45

P(kN)	Measured delta (mm)	Ma/Mcr	Deflection						Comparison					
			Fikry	ACI	BS	Case1	Case2a	Case2b	(i)	(ii)	(iii)	(iv)	(v)	(vi)
(1)	(2)	(3)	(4)	(5)	(6)	(7)	(8)	(9)	(10)	(11)	(12)	(13)	(14)	(15)
0.00	0.00	0.00	0.00	0.00	0.00	0.00	0.00	0.00	NaN	NaN	NaN	NaN	NaN	NaN
6.00	0.82	0.80	0.42	0.52	0.78	0.45	0.45	0.43	1.97	1.58	1.05	1.84	1.84	1.89
12.00	1.87	1.61	1.80	2.08	2.15	1.55	1.58	1.67	1.04	0.90	0.87	1.20	1.18	1.12
18.00	3.50	2.41	3.92	4.02	3.52	3.31	3.51	3.79	0.89	0.87	1.00	1.06	1.00	0.92
24.00	5.60	3.22	5.95	5.76	4.89	5.33	5.85	6.20	0.94	0.97	1.15	1.05	0.96	0.90
30.00	7.50	4.02	7.72	7.40	6.26	7.26	8.17	8.45	0.97	1.01	1.20	1.03	0.92	0.89
36.00	9.40	4.82	9.36	8.98	7.63	9.04	10.30	10.48	1.00	1.05	1.23	1.04	0.91	0.90
42.00	11.40	5.63	10.95	10.55	9.00	10.71	12.27	12.38	1.04	1.08	1.27	1.06	0.93	0.92
48.00	13.40	6.43	12.52	12.10	10.37	12.31	14.16	14.21	1.07	1.11	1.29	1.09	0.95	0.94
54.00	15.20	7.24	14.09	13.64	11.74	13.89	15.99	16.01	1.08	1.11	1.29	1.09	0.95	0.95
60.00	17.27	8.04	15.66	15.18	13.12	15.45	17.79	17.80	1.10	1.14	1.32	1.12	0.97	0.97
64.00	19.50	8.58	16.70	16.20	14.03	16.48	18.99	18.99	1.17	1.20	1.39	1.18	1.03	1.03

Note :

i = (2)/(4)
ii = (2)/(5)
iii = (2)/(6)
iv = (2)/(7)
v = (2)/(8)
vi = (2)/(9)

OUTPUT PROGRAM LOAD DEFLECTION

BEAM PROPERTIES :

```
b   = 150.00 mm
h   = 230.00 mm
d   = 184.00 mm
L   = 2.750 m
a   = 1.375 m
rho = 0.82 percent          Es  = 196000 MPa
fcu = 31.00 MPa             Ec  = 25778 MPa
```

COMPARISON OF DEFLECTION USING VARIOUS METHODS B4L25

P(kN)	Measured delta (mm)	Ma/Mcr	Deflection						Comparison					
			Fikry	ACI	BS	Case1	Case2a	Case2b	(i)	(ii)	(iii)	(iv)	(v)	(vi)
(1)	(2)	(3)	(4)	(5)	(6)	(7)	(8)	(9)	(10)	(11)	(12)	(13)	(14)	(15)
0.00	0.00	0.00	0.00	0.00	0.00	0.00	0.00	0.00	NaN	NaN	NaN	NaN	NaN	NaN
3.00	0.35	0.50	0.22	0.33	0.33	0.11	0.10	0.09	1.57	1.06	1.06	3.28	3.55	3.86
6.00	1.20	1.00	0.66	0.66	1.35	0.66	0.66	0.66	1.81	1.81	0.89	1.81	1.81	1.81
9.00	3.00	1.50	1.42	2.13	2.64	2.33	2.42	2.52	2.12	1.41	1.13	1.29	1.24	1.19
12.00	4.70	2.00	2.55	3.93	3.95	4.89	5.01	5.16	1.84	1.20	1.19	0.96	0.94	0.91
15.00	6.70	2.50	4.04	5.69	5.26	7.24	7.26	7.35	1.66	1.18	1.27	0.92	0.92	0.91
18.00	8.60	3.00	5.78	7.34	6.57	9.15	9.08	9.11	1.49	1.17	1.31	0.94	0.95	0.94
21.00	10.40	3.50	7.64	8.91	7.88	10.84	10.70	10.71	1.36	1.17	1.32	0.96	0.97	0.97
24.00	12.10	4.00	9.50	10.41	9.19	12.43	12.26	12.26	1.27	1.16	1.32	0.97	0.99	0.99
27.00	14.00	4.50	11.29	11.88	10.50	14.00	13.80	13.80	1.24	1.18	1.33	1.00	1.01	1.01
30.00	15.50	5.00	12.99	13.32	11.81	15.56	15.33	15.33	1.19	1.16	1.31	1.00	1.01	1.01
33.00	17.00	5.50	14.60	14.74	13.12	17.12	16.87	16.87	1.16	1.15	1.30	0.99	1.01	1.01

Note :

```
  i = (2)/(4)      iv = (2)/(7)
 ii = (2)/(5)       v = (2)/(8)
iii = (2)/(6)      vi = (2)/(9)
```

OUTPUT PROGRAM LOAD DEFLECTION

BEAM PROPERTIES :

```
b    = 150.00 mm
h    = 230.00 mm
d    = 184.00 mm
L    = 2.750 m
a    = 1.375 m
rho  = 0.82 percent          Es  = 196000 MPa
fcu  = 38.00 MPa             Ec  = 28006 MPa
```

COMPARISON OF DEFLECTION USING VARIOUS METHODS B4L35

P(kN)	Measured delta (mm)	Ma/Mcr	Deflection						Comparison					
			Fikry	ACI	BS	Case1	Case2a	Case2b	(i)	(ii)	(iii)	(iv)	(v)	(vi)
(1)	(2)	(3)	(4)	(5)	(6)	(7)	(8)	(9)	(10)	(11)	(12)	(13)	(14)	(15)
0.00	0.00	0.00	0.00	0.00	0.00	0.00	0.00	0.00	NaN	NaN	NaN	NaN	NaN	NaN
3.00	0.36	0.45	0.20	0.31	0.31	0.09	0.08	0.07	1.84	1.18	1.18	4.14	4.55	4.98
5.00	0.80	0.75	0.42	0.51	0.90	0.30	0.28	0.27	1.91	1.57	0.89	2.70	2.81	2.92
6.00	1.14	0.90	0.57	0.48	1.30	0.50	0.49	0.48	2.01	2.38	0.87	2.29	2.32	2.36
9.00	2.43	1.36	1.19	1.70	2.56	1.75	1.83	1.89	2.04	1.43	0.95	1.39	1.33	1.28
12.00	4.14	1.81	2.13	3.41	3.84	4.00	4.21	4.38	1.94	1.22	1.08	1.04	0.98	0.94
15.00	6.00	2.26	3.41	5.18	5.12	6.40	6.65	6.79	1.76	1.16	1.17	0.94	0.90	0.88
18.00	8.00	2.71	4.97	6.87	6.40	8.40	8.62	8.69	1.61	1.16	1.25	0.95	0.93	0.92
21.00	9.70	3.16	6.73	8.48	7.68	10.10	10.29	10.32	1.44	1.14	1.26	0.96	0.94	0.94
24.00	11.50	3.61	8.56	10.01	8.96	11.65	11.84	11.85	1.34	1.15	1.28	0.99	0.97	0.97
27.00	13.20	4.07	10.38	11.49	10.24	13.14	13.35	13.35	1.27	1.15	1.29	1.00	0.99	0.99
30.00	14.80	4.52	12.13	12.93	11.52	14.62	14.84	14.84	1.22	1.14	1.28	1.01	1.00	1.00
34.00	17.50	5.12	14.33	14.82	13.23	16.57	16.82	16.82	1.22	1.18	1.32	1.06	1.04	1.04

Note :

```
  i   = (2)/(4)        iv = (2)/(7)
  ii  = (2)/(5)         v = (2)/(8)
  iii = (2)/(6)        vi = (2)/(9)
```

OUTPUT PROGRAM LOAD DEFLECTION

BEAM PROPERTIES :

```
b    = 150.00 mm
h    = 230.00 mm
d    = 184.00 mm
L    = 2.750 m
a    = 1.375 m
rho = 0.82 percent        Es  = 196000 MPa
fcu = 52.00 MPa           Ec  = 29024 MPa
```

COMPARISON OF DEFLECTION USING VARIOUS METHODS B4L45

P(kN)	Measured delta (mm)	Ma/Mcr	Deflection						Comparison					
			Fikry	ACI	BS	Case1	Case2a	Case2b	(i)	(ii)	(iii)	(iv)	(v)	(vi)
(1)	(2)	(3)	(4)	(5)	(6)	(7)	(8)	(9)	(10)	(11)	(12)	(13)	(14)	(15)
0.00	0.00	0.00	0.00	0.00	0.00	0.00	0.00	0.00	NaN	NaN	NaN	NaN	NaN	NaN
3.00	0.57	0.39	0.18	0.29	0.29	0.07	0.06	0.06	3.21	1.94	1.94	8.04	8.92	9.89
6.00	1.43	0.77	0.49	0.59	1.31	0.36	0.35	0.33	2.91	2.43	1.09	4.00	4.14	4.29
9.00	2.64	1.16	1.00	1.22	2.60	1.21	1.24	1.26	2.65	2.16	1.02	2.18	2.14	2.09
12.00	4.14	1.54	1.75	2.72	3.90	2.99	3.13	3.26	2.37	1.52	1.06	1.38	1.32	1.27
15.00	5.71	1.93	2.78	4.47	5.20	5.43	5.64	5.84	2.05	1.28	1.10	1.05	1.01	0.98
18.00	7.40	2.32	4.09	6.22	6.51	7.82	7.97	8.12	1.81	1.19	1.14	0.95	0.93	0.91
21.00	9.00	2.70	5.65	7.91	7.82	9.83	9.90	9.98	1.59	1.14	1.15	0.92	0.91	0.90
24.00	10.60	3.09	7.37	9.51	9.13	11.57	11.57	11.61	1.44	1.11	1.16	0.92	0.92	0.91
27.00	12.30	3.48	9.17	11.05	10.43	13.16	13.11	13.13	1.34	1.11	1.18	0.93	0.94	0.94
30.00	14.00	3.86	10.99	12.54	11.74	14.68	14.61	14.62	1.27	1.12	1.19	0.95	0.96	0.96
31.00	15.00	3.99	11.59	13.03	12.18	15.18	15.10	15.11	1.29	1.15	1.23	0.99	0.99	0.99

Note :

```
  i   = (2)/(4)      iv = (2)/(7)
  ii  = (2)/(5)       v = (2)/(8)
  iii = (2)/(6)      vi = (2)/(9)
```

OUTPUT PROGRAM LOAD DEFLECTION

BEAM PROPERTIES :

```
b   = 150.00 mm
h   = 230.00 mm
d   = 184.00 mm
L   = 2.750 m
a   = 1.375 m
rho = 1.23 percent       Es = 196000 MPa
fcu = 28.00 MPa          Ec = 26670 MPa
```

COMPARISON OF DEFLECTION USING VARIOUS METHODS B4N25

P(kN)	Measured delta (mm)	Ma/Mcr	Deflection Fikry	ACI	BS	Case1	Case2a	Case2b	Comparison (i)	(ii)	(iii)	(iv)	(v)	(vi)
(1)	(2)	(3)	(4)	(5)	(6)	(7)	(8)	(9)	(10)	(11)	(12)	(13)	(14)	(15)
0.00	0.00	0.00	0.00	0.00	0.00	0.00	0.00	0.00	NaN	NaN	NaN	NaN	NaN	NaN
4.00	0.65	0.70	0.33	0.43	0.45	0.28	0.27	0.29	1.98	1.52	1.46	2.34	2.38	2.21
8.00	1.50	1.40	1.17	1.51	1.65	1.38	1.41	1.31	1.28	1.00	0.91	1.09	1.07	1.14
12.00	3.48	2.11	2.62	3.25	2.89	3.44	3.55	3.24	1.33	1.07	1.20	1.01	0.98	1.07
16.00	5.22	2.81	4.41	4.84	4.14	5.58	5.73	5.44	1.18	1.08	1.26	0.94	0.91	0.96
20.00	7.00	3.51	6.20	6.32	5.38	7.40	7.58	7.41	1.13	1.11	1.30	0.95	0.92	0.94
24.00	8.90	4.21	7.85	7.74	6.63	9.04	9.23	9.15	1.13	1.15	1.34	0.98	0.96	0.97
28.00	10.80	4.91	9.38	9.12	7.87	10.59	10.81	10.78	1.15	1.18	1.37	1.02	1.00	1.00
32.00	12.50	5.61	10.83	10.48	9.12	12.12	12.37	12.36	1.15	1.19	1.37	1.03	1.01	1.01
36.00	13.91	6.32	12.24	11.83	10.36	13.64	13.92	13.92	1.14	1.18	1.34	1.02	1.00	1.00
40.00	15.65	7.02	13.62	13.18	11.61	15.16	15.47	15.47	1.15	1.19	1.35	1.03	1.01	1.01
44.00	17.39	7.72	15.00	14.52	12.85	16.67	17.02	17.02	1.16	1.20	1.35	1.04	1.02	1.02
48.00	20.00	8.42	16.37	15.86	14.10	18.19	18.56	18.56	1.22	1.26	1.42	1.10	1.08	1.08

Note :

```
  i = (2)/(4)     iv = (2)/(7)
 ii = (2)/(5)      v = (2)/(8)
iii = (2)/(6)     vi = (2)/(9)
```

OUTPUT PROGRAM LOAD DEFLECTION

BEAM PROPERTIES :

```
b    = 150.00 mm
h    = 230.00 mm
d    = 184.00 mm
L    = 2.750 m
a    = 1.375 m
rho = 1.23 percent          Es   = 196000 MPa
fcu = 37.00 MPa             Ec   = 27400 MPa
```

COMPARISON OF DEFLECTION USING VARIOUS METHODS B4N35

P(kN)	Measured delta (mm)	Ma/Mcr	Deflection						Comparison					
			Fikry	ACI	BS	Case1	Case2a	Case2b	(i)	(ii)	(iii)	(iv)	(v)	(vi)
(1)	(2)	(3)	(4)	(5)	(6)	(7)	(8)	(9)	(10)	(11)	(12)	(13)	(14)	(15)
0.00	0.00	0.00	0.00	0.00	0.00	0.00	0.00	0.00	NaN	NaN	NaN	NaN	NaN	NaN
4.00	0.58	0.61	0.29	0.42	0.45	0.23	0.23	0.25	1.99	1.39	1.30	2.47	2.54	2.30
8.00	1.31	1.22	1.00	1.20	1.69	1.10	1.11	1.07	1.32	1.09	0.78	1.19	1.18	1.23
12.00	2.84	1.83	2.24	2.92	2.96	2.90	2.99	2.72	1.27	0.97	0.96	0.98	0.95	1.04
16.00	4.66	2.44	3.92	4.58	4.24	5.11	5.27	4.89	1.19	1.02	1.10	0.91	0.88	0.95
20.00	6.70	3.05	5.73	6.12	5.53	7.12	7.30	7.01	1.17	1.10	1.21	0.94	0.92	0.96
24.00	8.74	3.66	7.49	7.57	6.81	8.87	9.07	8.90	1.17	1.16	1.28	0.99	0.96	0.98
28.00	10.63	4.27	9.11	8.97	8.09	10.47	10.69	10.60	1.17	1.19	1.31	1.01	0.99	1.00
32.00	12.52	4.88	10.63	10.34	9.37	12.02	12.26	12.22	1.18	1.21	1.34	1.04	1.02	1.02
36.00	14.50	5.49	12.08	11.70	10.66	13.54	13.80	13.79	1.20	1.24	1.36	1.07	1.05	1.05
40.00	16.80	6.10	13.49	13.04	11.94	15.05	15.34	15.33	1.25	1.29	1.41	1.12	1.10	1.10
44.00	18.90	6.71	14.87	14.38	13.22	16.55	16.88	16.87	1.27	1.31	1.43	1.14	1.12	1.12

Note :

```
  i  = (2)/(4)       iv = (2)/(7)
  ii = (2)/(5)        v = (2)/(8)
 iii = (2)/(6)       vi = (2)/(9)
```

OUTPUT PROGRAM LOAD DEFLECTION

BEAM PROPERTIES :

```
 b   = 150.00 mm
 h   = 230.00 mm
 d   = 184.00 mm
 L   = 2.750 m
 a   = 1.375 m
 rho = 1.23 percent          Es  = 196000 MPa
 fcu = 47.00 MPa             Ec  = 29286 MPa
```

COMPARISON OF DEFLECTION USING VARIOUS METHODS — B4N45

P(kN)	Measured delta (mm)	Ma/Mcr	Deflection: Fikry	ACI	BS	Case1	Case2a	Case2b	Comparison: (i)	(ii)	(iii)	(iv)	(v)	(vi)
(1)	(2)	(3)	(4)	(5)	(6)	(7)	(8)	(9)	(10)	(11)	(12)	(13)	(14)	(15)
0.00	0.00	0.00	0.00	0.00	0.00	0.00	0.00	0.00	NaN	NaN	NaN	NaN	NaN	NaN
3.00	0.30	0.41	0.17	0.29	0.29	0.12	0.11	0.13	1.81	1.03	1.03	2.55	2.67	2.27
6.00	0.60	0.81	0.49	0.58	1.03	0.45	0.44	0.46	1.22	1.03	0.58	1.34	1.36	1.30
9.00	1.20	1.22	1.05	1.27	1.97	1.16	1.18	1.13	1.14	0.94	0.61	1.04	1.02	1.07
12.00	2.22	1.62	1.88	2.52	2.91	2.35	2.43	2.22	1.18	0.88	0.76	0.95	0.91	1.00
15.00	3.40	2.03	2.97	3.80	3.86	3.87	4.06	3.68	1.15	0.89	0.88	0.88	0.84	0.92
18.00	4.80	2.44	4.24	5.02	4.81	5.47	5.74	5.31	1.13	0.96	1.00	0.88	0.84	0.90
21.00	6.30	2.84	5.58	6.17	5.75	6.96	7.30	6.91	1.13	1.02	1.09	0.91	0.86	0.91
24.00	7.50	3.25	6.93	7.28	6.70	8.30	8.70	8.40	1.08	1.03	1.12	0.90	0.86	0.89
27.00	8.80	3.66	8.22	8.34	7.65	9.54	9.98	9.78	1.07	1.05	1.15	0.92	0.88	0.90
30.00	10.00	4.06	9.45	9.39	8.60	10.70	11.19	11.06	1.06	1.07	1.16	0.93	0.89	0.90
33.00	11.20	4.47	10.61	10.41	9.55	11.83	12.35	12.28	1.06	1.08	1.17	0.95	0.91	0.91
36.00	12.40	4.87	11.73	11.42	10.50	12.93	13.50	13.46	1.06	1.09	1.18	0.96	0.92	0.92
39.00	13.50	5.28	12.81	12.43	11.45	14.03	14.64	14.61	1.05	1.09	1.18	0.96	0.92	0.92
42.00	14.60	5.69	13.86	13.43	12.40	15.11	15.77	15.76	1.05	1.09	1.18	0.97	0.93	0.93
45.00	15.80	6.09	14.89	14.42	13.35	16.20	16.90	16.89	1.06	1.10	1.18	0.98	0.93	0.94
46.00	17.80	6.23	15.24	14.75	13.66	16.56	17.28	17.27	1.17	1.21	1.30	1.08	1.03	1.03

Note :

```
     i   = (2)/(4)        iv = (2)/(7)
     ii  = (2)/(5)         v = (2)/(8)
     iii = (2)/(6)        vi = (2)/(9)
```

```
%=============================================================================%
%                              PROGRAM B-3                                    %
%        TYPICAL PROGRAM TO CALCULATE DEFLECTION OF BEAMS OBTAINED            %
%                        FROM BEEBY'S REPORT [15]                             %
%                                                                             %
% Note:                                                                       %
% The terms used here are similar to the terms PROGRAM B-1                    %
%=============================================================================%
% Read data file
clear all;clc;
load cera05.txt      %File name of data input at 50% Pu taken from Ref. [15]
nobeam = cera05 (:,1)';
b = cera05 (:,2)';
h = cera05 (:,3)';
d = cera05 (:,4)';
L = cera05 (:,5)';
rho = cera05 (:,6)';
Ma = cera05 (:,7)';
fcu = cera05 (:,8)';
fy = cera05 (:,9)';
dex = cera05 (:,10)';
a = 0.28.*L;
Es=200000;
Ec=(20+0.2.*fcu).*1000;
n=Es./Ec;
As= rho./100.*b.*d;
Es=200000;
Ec=(20+0.2.*fcu).*1000;
n=Es./Ec;
%----------------------------- FIKRY'S METHOD -------------------------------%
nrho=n.*rho;
if nrho < 1.9
   alpha= 0.003; beta=0.095;
   elseif nrho <5
   alpha= 0.05; beta=0.07;
   elseif nrho<17
   alpha= 0.16; beta=0.05;
    elseif nrho<=32
      alpha= 0.5; beta=0.03;
   else
      alpha=0.8; beta= 0.02;
end
alpha; beta;
Icre=(alpha+beta.*nrho).*b.*d.^3./12;
Ig=(b.*h.^3)./12;
fr=0.56.*(fcu).^0.5;
yt=h./2;
Mcr=(fr.*Ig./1e+6)./yt;
Rm=Ma./Mcr;
if rho(:,1) < 1
   phi=-(Rm-2.*a./L);
else
    phi=-(Rm-2.*a./L).*rho;
    end
Ie=Icre+((Ig-Icre).*exp(phi));
delta=(Ma./Ie).*1000000.*(3.*(L.*1000).^2-4.*(a.*1000).^2)./(24.*Ec);
```

```
%--------------------------- BRANSON (ACI) ---------------------------------%
k=(2.*nrho./100+(nrho./100).^2).^0.5-nrho./100;
Icr=b.*(k.*d).^3./3+n.*As.*(d-k.*d).^2;
Ie1=Icr+(Ig-Icr).*1/Rm.^3;
delta1=(Ma./Ie1).*1000000.*(3.*(L.*1000).^2-4.*(a.*1000).^2)./(24.*Ec);
%--------------------------- BRITISH STANDARD ------------------------------%
x = cera05 (:,11)';
fc= cera05 (:,12)';
Cuc=Ma.*1e6./(Ec.*Ig);          % Curvatute uncracked section
Cc= fc./(x.*Ec);               % Curvatute cracked section
K=0.125-a.^2/(6.*L.^2);
if Cc(:,1)<Cuc(:,1)   % argument to check curvature (cracked or not)
   deltabs = Cuc.*K.*(L*1000).^2;
else
    deltabs= Cc.*K.*(L*1000).^2;
end
%--------------------------- PROPOSED MODEL---------------------------------%
Icrn1=(0.1914-0.0012.*fcu+0.3195.*rho).*b.*d.^3./12;
Icrn2=(0.1618+0.0418.*nrho).*b.*d.^3./12;
phin1=-(Rm-2.*a./L).*(4.0768-1.7969.*rho);
phin2=-(Rm-2.*a./L).*(4.4757-2.0667.*rho);
phin2a=-(Rm-2.*a./L).*(8.474-9.0606.*rho+2.842.*rho.^2);
Ien1=Icrn1+((Ig-Icrn1).*exp(phin1));
Ien2=Icrn2+((Ig-Icrn2).*exp(phin2));
Ien2a=Icrn2+((Ig-Icrn2).*exp(phin2a));
% Case 1
deltap1=(Ma./Ien1).*1000000.*(3.*(L.*1000).^2-4.*(a.*1000).^2)./(24.*Ec);
% Case 2a
deltap2=(Ma./Ien2).*1000000.*(3.*(L.*1000).^2-4.*(a.*1000).^2)./(24.*Ec);
% Case 2b
deltap2a=(Ma./Ien2a).*1000000.*(3.*(L.*1000).^2-4.*(a.*1000).^2)./(24.*Ec);
%===========================================================================%
fn=fopen('ceraout05a.txt','w');
fprintf(fn, '                                   OUTPUT PROGRAM B-3\n\n');
fprintf(fn, '     COMPARISON BETWEEN MEASURED AND ANALYTICAL DEFLECTION\n');
fprintf(fn, '                                USING VARIOUS METHOD\n');
fprintf(fn, '=============================================================\n');
fprintf(fn, '                measd                       Deflection (mm)       \n');
fprintf(fn, ' Beam     rho     def.   -------------------------------------\n');
fprintf(fn, '  #               (mm)  Fikry   ACI    BS   Case1  Case2a  Case2b\n');
fprintf(fn, '-------------------------------------------------------------\n');
fprintf(fn, '  (1)     (2)     (3)     (4)     (5)    (6)  (7)     (8)     (9)\n');
fprintf(fn, '-------------------------------------------------------------\n');
table(:,1) = nobeam';
table(:,2) = rho';
table(:,3) = dex';
table(:,4) = delta';
table(:,5) = delta1';
table(:,6) = deltabs';
table(:,7) = deltap1';
table(:,8) = deltap2';
table(:,9) = deltap2a';
fprintf(fn, '%6.0f %6.2f %7.2f %7.2f %7.2f %6.2f %6.2f %6.2f %6.2f\n',table');
fprintf(fn, '=============================================================\n');
status = fclose(fn);
end
```

INPUT PROGRAM B-3
DATA AT 50% Pu TAKEN FROM REF.[15]

Beam #	b (mm)	h (mm)	d (mm)	L (m)	rho (%)	Ma (kNm)	fcu (MPa)	fy (MPa)	dex (mm)	x (mm)	fc1 (MPa)	fc2 (MPa)
1	203.20	384.18	333.38	4.57	2.33	69.60	36.68	319.93	9.58	152.80	16.05	16.05
2	203.20	384.18	333.38	4.57	2.33	101.23	34.82	393.02	0.00	151.32	23.46	23.46
3	203.20	384.18	333.38	4.57	2.33	93.66	37.23	421.97	13.11	150.78	21.78	21.78
4	203.20	384.18	333.38	4.57	2.33	98.07	36.89	420.60	11.46	150.68	22.81	22.81
5	203.20	384.18	333.38	4.57	2.33	97.45	34.34	420.60	9.65	151.70	22.54	22.54
6	203.20	384.18	333.38	4.57	2.33	96.83	35.72	427.49	0.00	151.19	22.46	22.46
7	203.20	384.18	333.38	4.57	2.33	62.65	31.72	319.93	8.08	155.51	14.26	14.26
8	203.20	384.18	333.38	4.57	2.33	86.04	31.58	393.02	11.46	153.44	19.73	19.73
9	203.20	384.18	333.38	4.57	2.33	92.87	31.72	421.97	9.88	152.97	21.34	21.34
10	203.20	384.18	333.38	4.57	2.33	87.34	31.17	420.60	11.61	153.52	20.02	20.02
11	203.20	384.18	333.38	4.57	2.33	80.67	31.37	420.60	11.33	153.90	18.47	18.47
12	203.20	384.18	333.38	4.57	2.33	89.82	31.72	427.49	9.80	153.15	20.63	20.63
13	203.20	400.05	333.38	4.57	2.29	63.27	34.06	324.07	5.23	154.80	14.39	14.39
14	203.20	400.05	333.38	4.57	2.29	85.42	33.37	393.02	11.38	152.71	19.62	19.62
15	203.20	400.05	333.38	4.57	2.29	107.34	33.85	409.56	11.02	151.18	24.83	24.83
16	203.20	400.05	333.38	4.57	2.29	89.82	33.16	468.86	12.68	152.47	20.65	20.65
17	203.20	400.05	333.38	4.57	2.29	86.04	34.06	421.97	0.00	152.39	19.79	19.79
18	203.20	400.05	333.38	4.57	2.29	85.42	33.65	421.97	12.04	152.60	19.63	19.63
19	203.20	400.05	333.38	4.57	2.29	63.27	33.85	324.07	8.31	154.88	14.39	14.39
20	203.20	400.05	333.38	4.57	2.29	92.37	33.85	393.02	12.75	152.02	21.28	21.28
21	203.20	400.05	333.38	4.57	2.29	87.34	32.96	409.56	12.12	152.72	20.05	20.05
22	203.20	400.05	333.38	4.57	2.29	92.99	32.75	468.86	13.95	152.41	21.38	21.38
23	203.20	400.05	333.38	4.57	2.29	91.12	33.58	421.97	12.78	152.21	20.97	20.97
24	203.20	400.05	333.38	4.57	2.29	92.37	33.30	421.97	11.68	152.24	21.26	21.26
25	203.20	406.40	342.90	4.57	2.18	74.68	30.61	296.49	9.20	156.65	16.29	16.29
26	203.20	406.40	342.90	4.57	2.18	90.50	30.20	394.39	11.74	155.43	19.84	19.84
27	203.20	406.40	342.90	4.57	2.18	91.12	30.41	410.94	12.45	155.30	19.99	19.99
28	203.20	406.40	342.90	4.57	2.18	93.66	29.65	489.55	12.27	155.44	20.52	20.52
29	203.20	406.40	342.90	4.57	2.18	92.37	29.92	413.70	12.75	155.42	20.25	20.25
30	203.20	406.40	342.90	4.57	2.18	81.01	30.61	413.70	11.74	156.03	17.72	17.72
31	203.20	406.40	352.43	4.57	2.13	77.85	38.75	296.49	9.73	155.81	16.57	16.57
32	203.20	406.40	352.43	4.57	2.13	94.91	37.85	394.39	11.94	154.82	20.26	20.26

33	203.20	406.40	352.43	4.57	2.13	93.66	38.20	410.94	13.31	154.76	20.01	20.01
34	203.20	406.40	352.43	4.57	2.13	94.29	37.58	489.55	11.79	154.96	20.12	20.12
35	203.20	406.40	352.43	4.57	2.13	91.12	38.47	413.70	11.43	154.83	19.46	19.46
36	203.20	406.40	352.43	4.57	2.13	86.04	39.58	413.70	11.20	154.77	18.39	18.39
37	203.20	384.18	333.38	4.57	2.29	60.11	26.50	324.07	9.40	157.06	13.57	13.57
38	203.20	384.18	333.38	4.57	2.29	59.49	26.50	324.07	8.61	157.15	13.43	13.43
39	203.20	400.05	333.38	4.57	2.29	68.36	26.50	324.07	8.66	157.16	15.35	15.35
40	203.20	400.05	333.38	4.57	2.29	62.03	26.50	324.07	8.92	158.02	13.87	13.87
41	203.20	384.18	333.38	4.57	2.29	85.42	28.79	434.39	13.89	153.70	19.57	19.57
42	203.20	384.18	333.38	4.57	2.29	89.82	28.89	434.39	13.89	153.38	20.60	20.60
43	203.20	400.05	333.38	4.57	2.29	81.01	28.98	434.39	11.81	154.83	18.39	18.39
44	203.20	400.05	333.38	4.57	2.29	86.66	29.07	434.39	11.91	154.33	19.72	19.72
45	203.20	400.05	333.38	4.57	2.29	86.04	33.23	436.45	11.43	152.72	19.76	19.76
46	203.20	400.05	333.38	4.57	2.29	89.82	33.58	436.45	14.45	152.30	20.67	20.67
47	203.20	400.05	333.38	4.57	2.29	93.66	33.79	436.45	12.22	151.96	21.58	21.58
48	158.75	406.40	333.38	4.57	2.67	62.65	29.79	295.11	9.14	163.13	17.40	17.40
49	203.20	406.40	334.01	4.57	2.25	71.52	31.37	295.11	9.20	154.59	16.21	16.21
50	247.65	406.40	333.38	4.57	1.84	72.76	31.03	295.11	8.74	145.81	14.27	14.27
51	203.20	400.05	333.38	4.57	2.29	83.50	36.34	434.39	13.69	151.71	19.28	19.28
52	203.20	400.05	333.38	4.57	2.29	89.82	36.68	434.39	12.14	151.10	20.80	20.80
53	203.20	400.05	333.38	4.57	2.29	89.82	34.82	434.39	11.81	151.82	20.72	20.72
54	158.75	406.40	333.38	4.57	2.67	84.80	35.92	455.07	11.63	158.72	24.08	24.08
55	203.20	406.40	333.38	4.57	2.25	84.80	36.54	455.07	11.76	150.97	19.63	19.63
56	247.65	406.40	333.38	4.57	1.84	98.69	36.82	455.07	12.55	140.90	19.89	19.89
57	203.20	434.98	333.38	4.57	2.29	92.99	26.20	434.39	12.62	157.05	20.65	20.65
58	203.20	434.98	333.38	4.57	2.29	81.01	26.75	434.39	11.51	158.07	17.88	17.88
59	203.20	409.58	333.38	4.57	2.29	88.58	27.24	434.39	12.24	155.47	19.99	19.99
60	203.20	409.58	333.38	4.57	2.29	81.63	27.58	434.39	12.22	155.93	18.38	18.38
61	203.20	377.83	333.38	4.57	2.29	85.42	28.89	434.39	12.52	153.34	19.62	19.62
62	203.20	377.83	333.38	4.57	2.29	82.87	29.23	434.39	11.91	153.37	19.04	19.04
63	203.20	377.83	333.38	4.57	2.29	81.63	31.72	436.45	13.03	152.45	18.85	18.85
64	203.20	400.05	333.38	4.57	2.29	82.25	33.10	436.45	15.60	153.07	18.85	18.85
65	203.20	400.05	333.38	4.57	2.29	82.25	33.44	436.45	7.42	152.94	18.87	18.87
66	203.20	377.83	333.38	4.57	2.29	72.76	33.44	434.39	9.96	152.46	16.82	16.82
67	203.20	400.05	333.38	4.57	2.29	79.09	34.13	434.39	12.68	152.94	18.15	18.15
68	203.20	400.05	333.38	4.57	2.29	92.37	35.58	434.39	12.95	151.35	21.36	21.36
69	203.20	400.05	333.38	4.57	2.29	68.98	20.34	434.39	10.31	159.72	15.27	15.27

70	203.20	400.05	333.38	4.57	2.29	70.84	20.58	434.39	12.29	159.40	15.71	15.71
71	203.20	400.05	333.38	4.57	2.29	82.25	34.20	434.39	11.79	152.64	18.90	18.90
72	203.20	400.05	333.38	4.57	2.29	65.81	19.51	434.39	13.03	160.49	14.52	14.52
73	203.20	400.05	333.38	4.57	2.29	74.68	23.96	434.39	11.56	157.52	16.72	16.72
74	203.20	400.05	333.38	4.57	2.29	82.87	33.79	434.39	13.01	152.75	19.03	19.03
75	203.20	406.40	333.38	4.57	2.25	72.14	32.89	295.11	9.30	153.64	16.47	16.47
76	203.20	406.40	333.38	4.57	1.68	58.19	34.34	295.11	6.38	140.27	14.39	14.39
77	203.20	406.40	333.38	4.57	1.12	37.34	34.82	295.11	7.52	127.14	10.14	10.14
78	203.20	400.05	333.38	4.57	2.29	62.65	32.41	322.69	7.54	155.53	14.20	14.20
79	203.20	400.05	333.38	4.57	1.68	48.08	31.03	322.69	9.14	143.16	11.73	11.73
80	203.20	400.05	333.38	4.57	1.17	36.72	34.06	322.69	6.76	128.80	9.89	9.89
81	203.20	406.40	333.38	4.57	2.25	91.12	33.44	492.99	11.96	151.68	21.01	21.01
82	203.20	406.40	333.38	4.57	1.68	84.80	32.92	492.99	15.85	137.46	21.27	21.27
83	203.20	406.40	333.38	4.57	1.12	56.32	34.61	492.99	13.67	121.25	15.84	15.84
84	203.20	400.05	333.38	4.57	2.29	89.82	35.79	448.18	13.01	151.44	20.76	20.76
85	203.20	400.05	333.38	4.57	1.68	69.60	34.20	434.39	11.46	138.13	17.44	17.44
86	203.20	400.05	333.38	4.57	1.17	45.53	33.79	406.81	10.80	125.55	12.49	12.49
87	203.20	406.40	333.38	4.57	2.25	77.17	29.92	492.99	12.37	154.27	17.55	17.55
88	203.20	406.40	333.38	4.57	1.68	72.76	28.61	492.99	11.38	140.29	17.95	17.95
89	203.20	406.40	333.38	4.57	1.12	55.70	31.30	492.99	10.54	122.51	15.53	15.53
90	203.20	400.05	333.38	4.57	2.29	81.01	28.17	434.39	10.49	155.16	18.36	18.36
91	203.20	400.05	333.38	4.57	2.29	86.04	27.91	434.39	10.08	154.86	19.53	19.53
92	203.20	400.05	333.38	4.57	2.29	72.14	28.61	434.39	14.20	155.85	16.30	16.30
93	203.20	400.05	333.38	4.57	2.29	94.29	29.50	434.39	14.05	153.63	21.53	21.53
94	203.20	400.05	333.38	4.57	2.29	81.01	23.51	434.39	11.05	157.12	18.17	18.17
95	203.20	400.05	333.38	4.57	2.29	84.80	30.34	434.39	12.40	153.96	19.34	19.34
96	203.20	400.05	333.38	4.57	2.29	92.37	32.20	434.39	12.22	152.67	21.21	21.21
97	203.20	400.05	333.38	4.57	2.29	87.68	30.06	434.39	12.22	153.86	20.00	20.00
98	203.20	400.05	333.38	4.57	2.29	85.02	30.06	434.39	11.94	154.06	19.38	19.38
99	203.20	400.05	333.38	4.57	2.29	81.12	30.06	434.39	10.90	154.38	18.46	18.46
100	203.20	400.05	355.60	4.57	1.05	55.70	28.13	434.39	11.41	127.43	14.12	14.12
101	203.20	400.05	355.60	4.57	1.05	58.87	27.99	434.39	10.03	126.93	14.95	14.95
102	203.20	400.05	355.60	4.57	1.05	56.94	27.03	434.39	9.68	127.62	14.41	14.41
103	158.75	406.40	365.13	4.57	1.34	55.70	27.86	434.39	11.38	141.14	15.97	15.97
104	203.20	406.40	365.13	4.57	1.05	56.94	28.34	434.39	9.65	130.74	13.72	13.72
105	247.65	406.40	365.13	4.57	0.86	63.27	27.17	434.39	9.58	122.63	13.30	13.30
106	177.80	387.35	342.90	4.57	0.93	40.51	30.48	410.25	9.37	117.87	13.14	13.14

107	177.80	387.35	342.90	4.57	0.93	42.37	31.99	410.25	9.73	116.86	13.84	13.84
108	177.80	387.35	342.90	4.57	0.93	32.88	30.61	317.17	7.47	120.52	10.53	10.53
109	177.80	387.35	342.90	4.57	0.93	34.18	31.37	317.17	7.21	119.71	11.00	11.00
110	177.80	387.35	342.90	4.57	0.93	42.37	30.06	410.25	9.12	117.52	13.76	13.76
111	177.80	387.35	342.90	4.57	0.93	42.37	31.30	410.25	9.80	117.10	13.81	13.81
112	177.80	387.35	342.90	4.57	0.93	34.18	30.61	317.17	7.26	119.97	10.98	10.98
113	177.80	387.35	342.90	4.57	0.93	32.88	31.44	317.17	6.33	120.23	10.55	10.55
114	177.80	387.35	342.90	4.57	0.93	42.37	27.24	410.25	10.31	118.50	13.66	13.66
115	177.80	387.35	342.90	4.57	0.93	41.75	28.41	410.25	9.78	118.25	13.49	13.49
116	177.80	387.35	342.90	4.57	0.93	32.88	26.89	317.17	6.88	121.82	10.43	10.43
117	177.80	387.35	342.90	4.57	0.93	34.80	28.75	317.17	7.95	120.36	11.13	11.13
118	177.80	387.35	342.90	4.57	0.93	39.88	29.30	410.25	9.42	118.46	12.89	12.89
119	177.80	387.35	342.90	4.57	0.93	41.13	29.79	410.25	9.50	117.94	13.33	13.33
120	177.80	387.35	342.90	4.57	0.93	34.18	29.37	317.17	7.37	120.39	10.94	10.94
121	177.80	387.35	342.90	4.57	0.93	33.56	29.92	317.17	7.44	120.46	10.74	10.74
122	177.80	387.35	342.90	4.57	0.93	41.13	32.20	410.25	8.87	117.12	13.42	13.42
123	177.80	387.35	342.90	4.57	0.93	41.13	33.72	410.25	0.00	116.61	13.47	13.47
124	177.80	387.35	342.90	4.57	0.93	33.56	31.72	317.17	7.44	119.85	10.79	10.79
125	177.80	387.35	342.90	4.57	0.93	33.56	33.58	317.17	6.73	119.22	10.84	10.84
126	177.80	387.35	342.90	4.57	0.93	41.13	27.51	410.25	9.37	118.73	13.25	13.25
127	177.80	387.35	342.90	4.57	0.93	41.13	30.13	410.25	9.63	117.82	13.34	13.34
128	177.80	387.35	342.90	4.57	0.93	32.88	28.55	317.17	7.52	121.23	10.47	10.47
129	177.80	387.35	342.90	4.57	0.93	34.18	29.79	317.17	7.37	120.25	10.95	10.95
130	177.80	387.35	342.90	4.57	0.93	41.13	27.86	455.07	10.54	118.61	13.26	13.26
131	177.80	387.35	342.90	4.57	0.93	42.37	27.86	455.07	10.85	118.28	13.68	13.68
132	177.80	387.35	342.90	4.57	0.93	42.37	27.86	455.07	10.08	118.28	13.68	13.68
133	177.80	387.35	342.90	4.57	0.93	42.37	27.86	455.07	10.67	118.28	13.68	13.68

INPUT PROGRAM B-3

DATA AT 70% Pu TAKEN FROM REF.[15]

Beam #	b (mm)	h (mm)	d (mm)	L (m)	rho (%)	Ma (kNm)	fcu (MPa)	fy (MPa)	dex (mm)	x (mm)	fc1 (MPa)	fc2 (MPa)
1	203.20	384.18	333.38	4.57	2.33	97.44	36.68	319.93	13.82	150.79	22.65	22.65
2	203.20	384.18	333.38	4.57	2.33	141.73	34.82	393.02	0.00	149.97	33.02	33.02
3	203.20	384.18	333.38	4.57	2.33	131.13	37.23	421.97	19.28	149.32	30.67	30.67
4	203.20	384.18	333.38	4.57	2.33	137.30	36.89	420.60	17.12	149.28	32.11	32.11
5	203.20	384.18	333.38	4.57	2.33	136.43	34.34	420.60	15.04	150.29	31.73	31.73
6	203.20	384.18	333.38	4.57	2.33	135.56	35.72	427.49	0.00	149.78	31.62	31.62
7	203.20	384.18	333.38	4.57	2.33	87.71	31.72	319.93	12.27	153.28	20.13	20.13
8	203.20	384.18	333.38	4.57	2.33	120.45	31.58	393.02	17.20	151.85	27.80	27.80
9	203.20	384.18	333.38	4.57	2.33	130.02	31.72	421.97	15.14	151.50	30.05	30.05
10	203.20	384.18	333.38	4.57	2.33	122.27	31.17	420.60	17.09	151.95	28.20	28.20
11	203.20	384.18	333.38	4.57	2.33	112.94	31.37	420.60	14.68	152.19	26.03	26.03
12	203.20	384.18	333.38	4.57	2.33	125.75	31.72	427.49	15.65	151.62	29.05	29.05
13	203.20	400.05	333.38	4.57	2.29	88.58	34.06	324.07	9.12	152.20	20.39	20.39
14	203.20	400.05	333.38	4.57	2.29	119.58	33.37	393.02	16.97	150.83	27.69	27.69
15	203.20	400.05	333.38	4.57	2.29	150.27	33.85	409.56	17.91	149.71	34.99	34.99
16	203.20	400.05	333.38	4.57	2.29	125.75	33.16	468.86	18.87	150.69	29.14	29.14
17	203.20	400.05	333.38	4.57	2.29	120.45	34.06	421.97	0.00	150.53	27.94	27.94
18	203.20	400.05	333.38	4.57	2.29	119.58	33.65	421.97	17.98	150.72	27.71	27.71
19	203.20	400.05	333.38	4.57	2.29	88.58	33.85	324.07	12.60	152.28	20.38	20.38
20	203.20	400.05	333.38	4.57	2.29	129.31	33.85	393.02	19.18	150.30	30.03	30.03
21	203.20	400.05	333.38	4.57	2.29	122.27	32.96	409.56	18.11	150.89	28.31	28.31
22	203.20	400.05	333.38	4.57	2.29	130.18	32.75	468.86	20.30	150.70	30.16	30.16
23	203.20	400.05	333.38	4.57	2.29	127.57	33.58	421.97	19.48	150.46	29.60	29.60
24	203.20	400.05	333.38	4.57	2.29	129.31	33.30	421.97	17.55	150.51	29.99	29.99
25	203.20	406.40	342.90	4.57	2.18	104.56	30.61	296.49	13.18	154.39	23.03	23.03
26	203.20	406.40	342.90	4.57	2.18	126.70	30.20	394.39	17.98	153.59	27.99	27.99
27	203.20	406.40	342.90	4.57	2.18	127.57	30.41	410.94	18.26	153.47	28.20	28.20
28	203.20	406.40	342.90	4.57	2.18	131.13	29.65	489.55	18.64	153.67	28.95	28.95
29	203.20	406.40	342.90	4.57	2.18	129.31	29.92	413.70	20.47	153.62	28.56	28.56
30	203.20	406.40	342.90	4.57	2.18	113.41	30.61	413.70	17.48	153.96	25.02	25.02
31	203.20	406.40	352.43	4.57	2.13	108.99	38.75	296.49	14.25	153.68	23.39	23.39
32	203.20	406.40	352.43	4.57	2.13	132.87	37.85	394.39	17.98	153.09	28.56	28.56

33	203.20	406.40	352.43	4.57	2.13	131.13	38.20	410.94	19.74	153.01	28.20	28.20
34	203.20	406.40	352.43	4.57	2.13	132.00	37.58	489.55	17.48	153.22	28.35	28.35
35	203.20	406.40	352.43	4.57	2.13	127.57	38.47	413.70	16.99	153.02	27.44	27.44
36	203.20	406.40	352.43	4.57	2.13	120.45	39.58	413.70	16.66	152.85	25.94	25.94
37	203.20	384.18	333.38	4.57	2.29	84.15	26.50	324.07	14.73	154.73	19.17	19.17
38	203.20	384.18	333.38	4.57	2.29	83.28	26.50	324.07	14.10	154.79	18.97	18.97
39	203.20	400.05	333.38	4.57	2.29	95.70	26.50	324.07	14.40	154.78	21.71	21.71
40	203.20	400.05	333.38	4.57	2.29	86.84	26.50	324.07	13.46	155.38	19.65	19.65
41	203.20	384.18	333.38	4.57	2.29	119.58	28.79	434.39	21.62	152.09	27.56	27.56
42	203.20	384.18	333.38	4.57	2.29	125.75	28.89	434.39	20.73	151.85	29.01	29.01
43	203.20	400.05	333.38	4.57	2.29	113.41	28.98	434.39	21.06	152.85	25.98	25.98
44	203.20	400.05	333.38	4.57	2.29	121.32	29.07	434.39	17.04	152.49	27.84	27.84
45	203.20	400.05	333.38	4.57	2.29	120.45	33.23	436.45	17.45	150.86	27.89	27.89
46	203.20	400.05	333.38	4.57	2.29	125.75	33.58	436.45	18.09	150.53	29.17	29.17
47	203.20	400.05	333.38	4.57	2.29	131.13	33.79	436.45	18.67	150.26	30.45	30.45
48	158.75	406.40	333.38	4.57	2.67	87.71	29.79	295.11	14.17	161.02	24.60	24.60
49	203.20	406.40	334.01	4.57	2.25	100.13	31.37	295.11	13.92	152.18	22.96	22.96
50	247.65	406.40	333.38	4.57	1.84	101.87	31.03	295.11	12.93	142.85	20.29	20.29
51	203.20	400.05	333.38	4.57	2.29	116.89	36.34	434.39	19.03	149.79	27.23	27.23
52	203.20	400.05	333.38	4.57	2.29	125.75	36.68	434.39	18.34	149.32	29.36	29.36
53	203.20	400.05	333.38	4.57	2.29	125.75	34.82	434.39	18.06	150.04	29.25	29.25
54	158.75	406.40	333.38	4.57	2.67	118.71	35.92	455.07	18.01	157.19	33.94	33.94
55	203.20	406.40	333.38	4.57	2.25	118.71	36.54	455.07	18.14	148.96	27.75	27.75
56	247.65	406.40	333.38	4.57	1.84	138.17	36.82	455.07	19.00	138.79	28.15	28.15
57	203.20	434.98	333.38	4.57	2.29	130.18	26.20	434.39	18.87	154.71	29.31	29.31
58	203.20	434.98	333.38	4.57	2.29	113.41	26.75	434.39	17.53	155.34	25.43	25.43
59	203.20	409.58	333.38	4.57	2.29	124.01	27.24	434.39	18.57	153.51	28.25	28.25
60	203.20	409.58	333.38	4.57	2.29	114.28	27.58	434.39	18.39	153.78	26.00	26.00
61	203.20	377.83	333.38	4.57	2.29	119.58	28.89	434.39	19.33	151.83	27.62	27.62
62	203.20	377.83	333.38	4.57	2.29	116.02	29.23	434.39	18.39	151.81	26.80	26.80
63	203.20	377.83	333.38	4.57	2.29	114.28	31.72	436.45	19.46	150.87	26.54	26.54
64	203.20	400.05	333.38	4.57	2.29	115.15	33.10	436.45	19.58	151.12	26.63	26.63
65	203.20	400.05	333.38	4.57	2.29	115.15	33.44	436.45	9.91	150.99	26.65	26.65
66	203.20	377.83	333.38	4.57	2.29	101.87	33.44	434.39	14.91	150.67	23.71	23.71
67	203.20	400.05	333.38	4.57	2.29	110.73	34.13	434.39	19.05	150.91	25.64	25.64
68	203.20	400.05	333.38	4.57	2.29	129.31	35.58	434.39	18.52	149.63	30.14	30.14
69	203.20	400.05	333.38	4.57	2.29	96.57	20.34	434.39	16.33	157.38	21.61	21.61

70	203.20	400.05	333.38	4.57	2.29	99.18	20.58	434.39	18.59	157.12	22.22	22.22
71	203.20	400.05	333.38	4.57	2.29	115.15	34.20	434.39	15.19	150.69	26.70	26.70
72	203.20	400.05	333.38	4.57	2.29	92.14	19.51	434.39	19.13	158.02	20.55	20.55
73	203.20	400.05	333.38	4.57	2.29	104.56	23.96	434.39	17.50	155.36	23.64	23.64
74	203.20	400.05	333.38	4.57	2.29	116.02	33.79	434.39	19.51	150.81	26.88	26.88
75	203.20	406.40	333.38	4.57	2.25	101.00	32.89	295.11	14.17	151.25	23.33	23.33
76	203.20	406.40	333.38	4.57	1.68	81.46	34.34	295.11	9.88	137.23	20.47	20.47
77	203.20	406.40	333.38	4.57	1.12	52.28	34.82	295.11	11.76	122.05	14.64	14.64
78	203.20	400.05	333.38	4.57	2.29	87.71	32.41	322.69	14.22	152.91	20.11	20.11
79	203.20	400.05	333.38	4.57	1.68	67.31	31.03	322.69	12.75	139.60	16.72	16.72
80	203.20	400.05	333.38	4.57	1.17	51.41	34.06	322.69	10.06	123.92	14.24	14.24
81	203.20	406.40	333.38	4.57	2.25	127.57	33.44	492.99	18.54	149.82	29.67	29.67
82	203.20	406.40	333.38	4.57	1.68	118.71	32.92	492.99	23.14	135.46	30.09	30.09
83	203.20	406.40	333.38	4.57	1.12	78.85	34.61	492.99	19.76	118.15	22.60	22.60
84	203.20	400.05	333.38	4.57	2.29	125.75	35.79	448.18	19.58	149.67	29.31	29.31
85	203.20	400.05	333.38	4.57	1.68	97.44	34.20	434.39	17.12	135.78	24.71	24.71
86	203.20	400.05	333.38	4.57	1.17	63.75	33.79	406.81	16.21	121.79	17.87	17.87
87	203.20	406.40	333.38	4.57	2.25	108.04	29.92	492.99	14.05	152.06	24.84	24.84
88	203.20	406.40	333.38	4.57	1.68	101.87	28.61	492.99	18.01	137.92	25.45	25.45
89	203.20	406.40	333.38	4.57	1.12	77.98	31.30	492.99	17.68	119.36	22.15	22.15
90	203.20	400.05	333.38	4.57	2.29	113.41	28.17	434.39	16.82	153.18	25.93	25.93
91	203.20	400.05	333.38	4.57	2.29	120.45	27.91	434.39	21.79	153.00	27.56	27.56
92	203.20	400.05	333.38	4.57	2.29	101.00	28.61	434.39	19.41	153.60	23.06	23.06
93	203.20	400.05	333.38	4.57	2.29	132.00	29.50	434.39	21.08	151.95	30.37	30.37
94	203.20	400.05	333.38	4.57	2.29	113.41	23.51	434.39	20.19	155.14	25.66	25.66
95	203.20	400.05	333.38	4.57	2.29	118.71	30.34	434.39	18.47	152.08	27.31	27.31
96	203.20	400.05	333.38	4.57	2.29	129.31	32.20	434.39	19.28	150.95	29.92	29.92
97	203.20	400.05	333.38	4.57	2.29	122.75	30.06	434.39	18.67	152.04	28.24	28.24
98	203.20	400.05	333.38	4.57	2.29	119.03	30.06	434.39	18.77	152.18	27.36	27.36
99	203.20	400.05	333.38	4.57	2.29	113.57	30.06	434.39	19.05	152.40	26.08	26.08
100	203.20	400.05	355.60	4.57	1.05	77.98	28.13	434.39	17.02	117.20	22.55	22.55
101	203.20	400.05	355.60	4.57	1.05	82.41	27.99	434.39	15.04	116.86	23.87	23.87
102	203.20	400.05	355.60	4.57	1.05	79.72	27.03	434.39	14.48	117.43	23.00	23.00
103	158.75	406.40	365.13	4.57	1.34	77.98	27.86	434.39	17.50	138.81	22.54	22.54
104	203.20	406.40	365.13	4.57	1.05	79.72	28.34	434.39	15.34	127.79	19.45	19.45
105	247.65	406.40	365.13	4.57	0.86	88.58	27.17	434.39	15.32	119.39	18.89	18.89
106	177.80	387.35	342.90	4.57	0.93	56.71	30.48	410.25	14.71	114.69	18.69	18.69

107	177.80	387.35	342.90	4.57	0.93	59.32	31.99	410.25	15.32	113.84	19.66	19.66
108	177.80	387.35	342.90	4.57	0.93	46.03	30.61	317.17	11.51	116.48	15.04	15.04
109	177.80	387.35	342.90	4.57	0.93	47.85	31.37	317.17	11.66	115.84	15.69	15.69
110	177.80	387.35	342.90	4.57	0.93	59.32	30.06	410.25	15.16	114.49	19.56	19.56
111	177.80	387.35	342.90	4.57	0.93	59.32	31.30	410.25	15.72	114.07	19.62	19.62
112	177.80	387.35	342.90	4.57	0.93	47.85	30.61	317.17	11.79	116.10	15.66	15.66
113	177.80	387.35	342.90	4.57	0.93	46.03	31.44	317.17	10.49	116.19	15.07	15.07
114	177.80	387.35	342.90	4.57	0.93	59.32	27.24	410.25	16.03	115.47	19.41	19.41
115	177.80	387.35	342.90	4.57	0.93	58.45	28.41	410.25	15.32	115.17	19.18	19.18
116	177.80	387.35	342.90	4.57	0.93	46.03	26.89	317.17	11.18	117.77	14.89	14.89
117	177.80	387.35	342.90	4.57	0.93	48.72	28.75	317.17	12.62	116.57	15.88	15.88
118	177.80	387.35	342.90	4.57	0.93	55.84	29.30	410.25	14.58	115.22	18.33	18.33
119	177.80	387.35	342.90	4.57	0.93	57.58	29.79	410.25	14.78	114.81	18.95	18.95
120	177.80	387.35	342.90	4.57	0.93	47.85	29.37	317.17	11.84	116.53	15.61	15.61
121	177.80	387.35	342.90	4.57	0.93	46.98	29.92	317.17	11.96	116.51	15.34	15.34
122	177.80	387.35	342.90	4.57	0.93	57.58	32.20	410.25	14.07	113.99	19.07	19.07
123	177.80	387.35	342.90	4.57	0.93	57.58	33.72	410.25	0.00	113.49	19.15	19.15
124	177.80	387.35	342.90	4.57	0.93	46.98	31.72	317.17	11.76	115.90	15.41	15.41
125	177.80	387.35	342.90	4.57	0.93	46.98	33.58	317.17	10.87	115.28	15.49	15.49
126	177.80	387.35	342.90	4.57	0.93	57.58	27.51	410.25	14.83	115.60	18.83	18.83
127	177.80	387.35	342.90	4.57	0.93	57.58	30.13	410.25	15.01	114.69	18.97	18.97
128	177.80	387.35	342.90	4.57	0.93	46.03	28.55	317.17	11.94	117.19	14.96	14.96
129	177.80	387.35	342.90	4.57	0.93	47.85	29.79	317.17	12.12	116.38	15.63	15.63
130	177.80	387.35	342.90	4.57	0.93	57.58	27.86	455.07	16.23	115.48	18.85	18.85
131	177.80	387.35	342.90	4.57	0.93	59.32	27.86	455.07	16.71	115.25	19.44	19.44
132	177.80	387.35	342.90	4.57	0.93	59.32	27.86	455.07	16.26	115.25	19.44	19.44
133	177.80	387.35	342.90	4.57	0.93	59.32	27.86	455.07	16.46	115.25	19.44	19.44

OUTPUT PROGRAM B-3

COMPARISON BETWEEN MEASURED AND ANALYTICAL DEFLECTION
USING VARIOUS METHOD

Beam #	rho	measd def. (mm)	Deflection (mm)					
			Fikry	ACI	BS	Case1	Case2a	Case2b
(1)	(2)	(3)	(4)	(5)	(6)	(7)	(8)	(9)
1	2.33	9.58	9.38	9.60	8.98	5.17	3.10	10.85
2	2.33	0.00	13.73	14.04	13.44	6.76	2.71	15.82
3	2.33	13.11	12.60	12.91	12.30	6.39	2.90	14.59
4	2.33	11.46	13.21	13.53	12.93	6.59	2.82	15.28
5	2.33	9.65	13.24	13.53	12.93	6.61	2.76	15.24
6	2.33	0.00	13.09	13.40	12.79	6.56	2.81	15.11
7	2.33	8.08	8.60	8.76	8.14	4.87	3.05	9.83
8	2.33	11.46	11.81	12.03	11.42	6.14	2.88	13.51
9	2.33	9.88	12.74	12.98	12.38	6.46	2.77	14.57
10	2.33	11.61	12.01	12.23	11.62	6.21	2.85	13.72
11	2.33	11.33	11.08	11.29	10.68	5.88	2.95	12.67
12	2.33	9.80	12.33	12.56	11.95	6.32	2.82	14.10
13	2.29	5.23	8.68	8.89	8.10	4.80	3.23	10.04
14	2.29	11.38	11.75	12.02	11.26	6.35	3.46	13.57
15	2.29	11.02	14.74	15.09	14.34	7.76	3.40	17.04
16	2.29	12.68	12.37	12.65	11.89	6.65	3.46	14.27
17	2.29	0.00	11.81	12.09	11.32	6.37	3.47	13.65
18	2.29	12.04	11.74	12.02	11.25	6.34	3.46	13.56
19	2.29	8.31	8.68	8.90	8.11	4.81	3.23	10.04
20	2.29	12.75	12.69	12.99	12.22	6.79	3.47	14.66
21	2.29	12.12	12.04	12.31	11.54	6.50	3.46	13.88
22	2.29	13.95	12.82	13.11	12.35	6.88	3.45	14.78
23	2.29	12.78	12.53	12.82	12.06	6.72	3.47	14.47
24	2.29	11.68	12.71	13.00	12.25	6.82	3.46	14.67
25	2.18	9.20	9.78	10.05	9.31	7.54	5.56	11.39
26	2.18	11.74	11.87	12.20	11.46	9.63	6.67	13.81
27	2.18	12.45	11.94	12.27	11.54	9.69	6.70	13.90
28	2.18	12.27	12.31	12.64	11.90	10.12	6.91	14.30
29	2.18	12.75	12.13	12.46	11.72	9.91	6.81	14.10
30	2.18	11.74	10.61	10.91	10.16	8.34	6.00	12.35
31	2.13	9.73	9.21	9.61	8.96	7.86	6.46	11.00
32	2.13	11.94	11.27	11.74	11.10	10.20	8.14	13.44
33	2.13	13.31	11.10	11.58	10.94	9.99	7.99	13.26
34	2.13	11.79	11.20	11.67	11.03	10.14	8.10	13.36
35	2.13	11.43	10.79	11.26	10.61	9.62	7.73	12.89
36	2.13	11.20	10.15	10.60	9.95	8.85	7.18	12.15
37	2.29	9.40	8.49	8.62	7.98	5.45	3.59	9.64
38	2.29	8.61	8.40	8.53	7.90	5.40	3.58	9.54
39	2.29	8.66	9.65	9.80	9.02	5.42	3.27	10.96
40	2.29	8.92	8.76	8.89	8.11	4.95	3.19	9.94
41	2.29	13.89	11.96	12.17	11.56	7.40	3.81	13.65
42	2.29	13.89	12.57	12.79	12.18	7.74	3.80	14.35
43	2.29	11.81	11.33	11.54	10.76	6.22	3.39	12.94
44	2.29	11.91	12.12	12.34	11.57	6.60	3.39	13.85
45	2.29	11.43	11.85	12.12	11.35	6.40	3.46	13.67
46	2.29	14.45	12.35	12.64	11.88	6.64	3.47	14.26

(1)	(2)	(3)	(4)	(5)	(6)	(7)	(8)	(9)
47	2.29	12.22	12.87	13.17	12.41	6.88	3.47	14.87
48	2.67	9.14	10.30	10.32	9.61	0.69	0.19	11.27
49	2.25	9.20	9.94	10.18	9.33	5.94	3.90	11.49
50	1.84	8.74	9.17	9.79	8.73	9.87	9.39	11.07
51	2.29	13.69	11.36	11.66	10.90	6.11	3.48	13.21
52	2.29	12.14	12.21	12.54	11.77	6.51	3.50	14.20
53	2.29	11.81	12.29	12.60	11.83	6.59	3.48	14.24
54	2.67	11.63	13.66	13.73	13.05	0.41	0.08	15.14
55	2.25	11.76	11.63	11.98	11.13	6.83	4.20	13.60
56	1.84	12.55	12.19	13.10	12.06	13.83	13.54	15.11
57	2.29	12.62	13.14	13.35	12.18	5.56	2.71	14.92
58	2.29	11.51	11.42	11.61	10.43	4.90	2.72	12.98
59	2.29	12.24	12.47	12.68	11.81	6.34	3.15	14.19
60	2.29	12.22	11.48	11.67	10.80	5.88	3.16	13.07
61	2.29	12.52	11.95	12.17	11.60	7.80	4.03	13.65
62	2.29	11.91	11.58	11.79	11.23	7.57	4.04	13.24
63	2.29	13.03	11.30	11.54	10.97	7.35	4.08	12.99
64	2.29	15.60	11.33	11.59	10.81	6.15	3.44	13.07
65	2.29	7.42	11.31	11.58	10.81	6.13	3.45	13.06
66	2.29	9.96	10.01	10.24	9.66	6.54	4.02	11.55
67	2.29	12.68	10.85	11.11	10.34	5.89	3.43	12.55
68	2.29	12.95	12.61	12.93	12.17	6.72	3.49	14.63
69	2.29	10.31	9.97	10.07	9.29	5.67	3.15	11.16
70	2.29	12.29	10.23	10.33	9.55	5.80	3.16	11.45
71	2.29	11.79	11.28	11.55	10.78	6.11	3.45	13.05
72	2.29	13.03	9.54	9.63	8.85	5.46	3.11	10.66
73	2.29	11.56	10.65	10.79	10.01	5.96	3.27	12.02
74	2.29	13.01	11.38	11.65	10.88	6.16	3.45	13.15
75	2.25	9.30	10.03	10.29	9.43	5.92	3.90	11.63
76	1.68	6.38	9.10	10.07	8.93	10.65	10.53	11.13
77	1.12	7.52	5.40	8.65	6.91	9.03	9.14	8.72
78	2.29	7.54	8.65	8.84	8.06	4.81	3.22	9.96
79	1.68	9.14	7.57	8.39	7.31	8.72	8.53	9.07
80	1.17	6.76	5.51	8.25	6.69	8.72	8.80	8.37
81	2.25	11.96	12.65	12.97	12.13	7.57	4.35	14.68
82	1.68	15.85	13.51	14.73	13.61	16.92	16.80	17.08
83	1.12	13.67	9.57	13.05	11.34	15.13	15.12	14.96
84	2.29	13.01	12.25	12.57	11.80	6.55	3.49	14.22
85	1.68	11.46	11.00	12.05	11.00	13.48	13.40	13.81
86	1.17	10.80	7.43	10.23	8.69	11.59	11.61	11.29
87	2.25	12.37	10.85	11.09	10.23	6.53	4.06	12.49
88	1.68	11.38	11.80	12.76	11.63	14.76	14.39	14.70
89	1.12	10.54	9.73	12.99	11.28	15.27	15.11	14.98
90	2.29	10.49	11.37	11.56	10.79	6.25	3.37	12.96
91	2.29	10.08	12.08	12.29	11.52	6.61	3.37	13.77
92	2.29	14.20	10.10	10.28	9.51	5.61	3.33	11.53
93	2.29	14.05	13.16	13.41	12.65	7.10	3.38	15.06
94	2.29	11.05	11.57	11.72	10.94	6.43	3.25	13.04
95	2.29	12.40	11.80	12.03	11.27	6.43	3.42	13.52
96	2.29	12.22	12.77	13.04	12.28	6.86	3.44	14.69
97	2.29	12.22	12.21	12.45	11.68	6.63	3.41	13.99
98	2.29	11.94	11.84	12.07	11.31	6.45	3.41	13.56
99	2.29	10.90	11.30	11.52	10.75	6.19	3.40	12.94
100	1.05	11.41	8.58	11.32	10.11	13.49	13.20	13.18

(1)	(2)	(3)	(4)	(5)	(6)	(7)	(8)	(9)
101	1.05	10.03	9.14	11.96	10.76	14.28	13.97	13.95
102	1.05	9.68	8.87	11.59	10.39	13.88	13.54	13.52
103	1.34	11.38	9.66	11.19	10.34	13.46	13.15	13.10
104	1.05	9.65	8.10	10.69	9.56	12.72	12.46	12.43
105	0.86	9.58	7.48	11.38	9.97	13.31	13.00	13.00
106	0.93	9.37	7.66	11.42	9.99	13.35	13.15	13.14
107	0.93	9.73	7.99	11.91	10.49	13.87	13.71	13.70
108	0.93	7.47	5.82	9.26	7.82	10.62	10.51	10.49
109	0.93	7.21	6.07	9.62	8.18	11.03	10.93	10.92
110	0.93	9.12	8.14	11.95	10.52	14.02	13.79	13.79
111	0.93	9.80	8.04	11.92	10.50	13.92	13.74	13.73
112	0.93	7.26	6.13	9.63	8.19	11.09	10.97	10.95
113	0.93	6.33	5.76	9.25	7.80	10.55	10.47	10.45
114	0.93	10.31	8.38	12.01	10.59	14.25	13.91	13.91
115	0.93	9.78	8.13	11.81	10.38	13.94	13.66	13.65
116	0.93	6.88	6.08	9.33	7.89	10.91	10.69	10.68
117	0.93	7.95	6.41	9.84	8.40	11.47	11.28	11.26
118	0.93	9.42	7.60	11.26	9.84	13.22	12.99	12.98
119	0.93	9.50	7.87	11.61	10.18	13.62	13.39	13.38
120	0.93	7.37	6.22	9.65	8.21	11.19	11.03	11.02
121	0.93	7.44	6.03	9.47	8.02	10.92	10.79	10.77
122	0.93	8.87	7.68	11.56	10.13	13.43	13.28	13.27
123	0.93	0.00	7.56	11.52	10.10	13.31	13.22	13.21
124	0.93	7.44	5.90	9.44	7.99	10.78	10.70	10.68
125	0.93	6.73	5.78	9.41	7.96	10.63	10.60	10.58
126	0.93	9.37	8.05	11.66	10.23	13.80	13.49	13.48
127	0.93	9.63	7.84	11.60	10.17	13.59	13.37	13.37
128	0.93	7.52	5.96	9.30	7.85	10.78	10.61	10.60
129	0.93	7.37	6.19	9.65	8.20	11.16	11.01	11.00
130	0.93	10.54	8.02	11.65	10.22	13.77	13.47	13.47
131	0.93	10.85	8.32	12.00	10.57	14.20	13.89	13.88
132	0.93	10.08	8.32	12.00	10.57	14.20	13.89	13.88
133	0.93	10.67	8.32	12.00	10.57	14.20	13.89	13.88

OUTPUT PROGRAM B-3

COMPARISON BETWEEN MEASURED AND ANALYTICAL DEFLECTION
USING VARIOUS METHOD AT 70% Pu

Beam #	rho	measd def. (mm)	Deflection (mm) Fikry	ACI	BS	Case1	Case2a	Case2b
(1)	(2)	(3)	(4)	(5)	(6)	(7)	(8)	(9)
1	2.33	13.82	13.13	13.49	12.85	6.57	2.83	15.19
2	2.33	0.00	19.23	19.72	19.09	8.06	1.82	22.15
3	2.33	19.28	17.64	18.13	17.49	7.78	2.15	20.43
4	2.33	17.12	18.49	19.00	18.37	7.95	2.01	21.40
5	2.33	15.04	18.54	19.01	18.37	7.93	1.92	21.33
6	2.33	0.00	18.33	18.82	18.18	7.90	2.00	21.16
7	2.33	12.27	12.04	12.30	11.65	6.22	2.86	13.76
8	2.33	17.20	16.54	16.90	16.26	7.49	2.16	18.91
9	2.33	15.14	17.84	18.24	17.60	7.76	1.94	20.41
10	2.33	17.09	16.81	17.18	16.54	7.54	2.10	19.20
11	2.33	14.68	15.52	15.86	15.22	7.24	2.32	17.73
12	2.33	15.65	17.26	17.64	17.00	7.64	2.04	19.73
13	2.29	9.12	12.16	12.49	11.68	6.53	3.47	14.05
14	2.29	16.97	16.45	16.89	16.09	8.54	3.26	18.99
15	2.29	17.91	20.64	21.20	20.41	10.32	2.81	23.85
16	2.29	18.87	17.32	17.77	16.97	8.93	3.17	19.98
17	2.29	0.00	16.53	16.98	16.18	8.56	3.27	19.11
18	2.29	17.98	16.44	16.88	16.08	8.53	3.27	18.98
19	2.29	12.60	12.17	12.50	11.69	6.54	3.47	14.06
20	2.29	19.18	17.76	18.24	17.45	9.11	3.15	20.52
21	2.29	18.11	16.85	17.29	16.49	8.73	3.21	19.43
22	2.29	20.30	17.95	18.42	17.62	9.21	3.09	20.69
23	2.29	19.48	17.54	18.01	17.21	9.02	3.16	20.25
24	2.29	17.55	17.80	18.27	17.47	9.13	3.13	20.54
25	2.18	13.18	13.70	14.12	13.35	11.51	7.58	15.95
26	2.18	17.98	16.62	17.13	16.36	14.79	9.03	19.33
27	2.18	18.26	16.72	17.24	16.47	14.88	9.07	19.46
28	2.18	18.64	17.24	17.76	16.98	15.56	9.34	20.03
29	2.18	20.47	16.98	17.50	16.73	15.23	9.21	19.74
30	2.18	17.48	14.86	15.32	14.54	12.77	8.16	17.30
31	2.13	14.25	12.90	13.50	12.82	12.06	9.47	15.42
32	2.13	17.98	15.77	16.49	15.82	15.64	12.04	18.82
33	2.13	19.74	15.55	16.26	15.59	15.33	11.82	18.56
34	2.13	17.48	15.69	16.39	15.72	15.55	11.97	18.70
35	2.13	16.99	15.11	15.81	15.14	14.76	11.41	18.05
36	2.13	16.66	14.21	14.89	14.21	13.58	10.57	17.02
37	2.29	14.73	11.88	12.11	11.45	7.41	3.76	13.49
38	2.29	14.10	11.76	11.98	11.32	7.34	3.76	13.35
39	2.29	14.40	13.51	13.77	12.96	7.32	3.28	15.34
40	2.29	13.46	12.26	12.49	11.69	6.72	3.33	13.92
41	2.29	21.62	16.74	17.10	16.45	9.94	3.39	19.11
42	2.29	20.73	17.59	17.97	17.33	10.37	3.28	20.10
43	2.29	21.06	15.86	16.21	15.40	8.36	3.18	18.12
44	2.29	17.04	16.96	17.33	16.53	8.85	3.07	19.38
45	2.29	17.45	16.58	17.02	16.22	8.60	3.25	19.13
46	2.29	18.09	17.29	17.75	16.96	8.91	3.19	19.97

(1)	(2)	(3)	(4)	(5)	(6)	(7)	(8)	(9)
47	2.29	18.67	18.02	18.50	17.70	9.22	3.12	20.81
48	2.67	14.17	14.42	14.50	13.76	0.26	0.04	15.77
49	2.25	13.92	13.93	14.30	13.42	8.54	4.49	16.09
50	1.84	12.93	12.89	13.76	12.67	15.18	14.66	15.82
51	2.29	19.03	15.91	16.39	15.58	8.24	3.38	18.49
52	2.29	18.34	17.09	17.61	16.81	8.76	3.29	19.88
53	2.29	18.06	17.21	17.70	16.90	8.85	3.23	19.93
54	2.67	18.01	19.12	19.30	18.57	0.11	0.01	21.19
55	2.25	18.14	16.29	16.83	15.95	9.84	4.69	19.04
56	1.84	19.00	17.09	18.41	17.33	20.53	20.51	21.31
57	2.29	18.87	18.40	18.75	17.55	7.40	2.44	20.88
58	2.29	17.53	16.00	16.31	15.10	6.58	2.63	18.18
59	2.29	18.57	17.46	17.81	16.91	8.47	2.81	19.86
60	2.29	18.39	16.07	16.39	15.49	7.89	2.96	18.30
61	2.29	19.33	16.73	17.09	16.50	10.49	3.56	19.11
62	2.29	18.39	16.21	16.57	15.97	10.20	3.65	18.53
63	2.29	19.46	15.82	16.21	15.61	9.93	3.79	18.19
64	2.29	19.58	15.86	16.28	15.48	8.28	3.31	18.29
65	2.29	9.91	15.84	16.26	15.46	8.27	3.32	18.29
66	2.29	14.91	14.01	14.39	13.78	8.88	4.02	16.18
67	2.29	19.05	15.19	15.61	14.81	7.96	3.38	17.57
68	2.29	18.52	17.65	18.16	17.37	9.02	3.21	20.47
69	2.29	16.33	13.96	14.14	13.34	7.62	2.96	15.62
70	2.29	18.59	14.32	14.51	13.71	7.79	2.94	16.03
71	2.29	15.19	15.80	16.23	15.43	8.23	3.34	18.27
72	2.29	19.13	13.36	13.53	12.72	7.35	2.97	14.92
73	2.29	17.50	14.91	15.15	14.35	8.01	3.06	16.82
74	2.29	19.51	15.94	16.37	15.57	8.30	3.32	18.42
75	2.25	14.17	14.05	14.45	13.57	8.51	4.50	16.28
76	1.68	9.88	12.89	14.16	12.98	16.01	15.97	16.31
77	1.12	11.76	8.67	12.18	10.40	13.91	13.93	13.71
78	2.29	14.22	12.11	12.42	11.61	6.54	3.45	13.95
79	1.68	12.75	10.79	11.79	10.68	13.32	13.09	13.46
80	1.17	10.06	8.67	11.61	10.02	13.32	13.32	13.09
81	2.25	18.54	17.71	18.23	17.35	10.95	4.70	20.55
82	1.68	23.14	18.92	20.70	19.53	24.09	24.02	24.09
83	1.12	19.76	14.24	18.37	16.61	21.47	21.40	21.37
84	2.29	19.58	17.15	17.65	16.86	8.80	3.26	19.90
85	1.68	17.12	15.45	16.95	15.85	19.53	19.53	19.69
86	1.17	16.21	11.24	14.40	12.82	16.83	16.76	16.66
87	2.25	14.05	15.19	15.58	14.70	9.41	4.55	17.49
88	1.68	18.01	16.54	17.95	16.77	21.17	20.72	20.82
89	1.12	17.68	14.38	18.29	16.52	21.61	21.33	21.31
90	2.29	16.82	15.91	16.24	15.44	8.40	3.14	18.14
91	2.29	21.79	16.92	17.26	16.46	8.85	3.03	19.27
92	2.29	19.41	14.15	14.45	13.64	7.58	3.30	16.15
93	2.29	21.08	18.43	18.84	18.04	9.48	2.92	21.08
94	2.29	20.19	16.20	16.46	15.65	8.60	2.90	18.26
95	2.29	18.47	16.52	16.90	16.10	8.63	3.16	18.93
96	2.29	19.28	17.87	18.32	17.53	9.19	3.08	20.57
97	2.29	18.67	17.10	17.49	16.69	8.89	3.09	19.58
98	2.29	18.77	16.58	16.96	16.16	8.66	3.15	18.99
99	2.29	19.05	15.82	16.18	15.38	8.32	3.22	18.12
100	1.05	17.02	12.40	15.92	17.55	18.94	18.52	18.52

(1)	(2)	(3)	(4)	(5)	(6)	(7)	(8)	(9)
101	1.05	15.04	13.15	16.83	18.65	20.04	19.58	19.58
102	1.05	14.48	12.78	16.31	18.02	19.48	18.99	18.99
103	1.34	17.50	13.59	15.73	14.84	18.88	18.45	18.44
104	1.05	15.34	11.70	15.03	13.86	17.87	17.48	17.48
105	0.86	15.32	11.15	15.99	14.54	18.69	18.23	18.23
106	0.93	14.71	11.49	16.09	14.60	18.81	18.49	18.49
107	0.93	15.32	11.95	16.79	15.29	19.53	19.27	19.27
108	0.93	11.51	8.97	13.06	11.56	15.22	14.98	14.98
109	0.93	11.66	9.34	13.56	12.05	15.77	15.55	15.55
110	0.93	15.16	12.12	16.85	15.35	19.72	19.37	19.37
111	0.93	15.72	12.01	16.81	15.31	19.60	19.30	19.30
112	0.93	11.79	9.41	13.58	12.07	15.83	15.58	15.58
113	0.93	10.49	8.91	13.04	11.53	15.15	14.95	14.94
114	0.93	16.03	12.38	16.93	15.44	20.01	19.52	19.52
115	0.93	15.32	12.08	16.65	15.16	19.59	19.17	19.17
116	0.93	11.18	9.29	13.15	11.65	15.53	15.15	15.14
117	0.93	12.62	9.77	13.87	12.37	16.29	15.95	15.95
118	0.93	14.58	11.39	15.88	14.38	18.63	18.27	18.27
119	0.93	14.78	11.75	16.36	14.86	19.17	18.81	18.81
120	0.93	11.84	9.51	13.61	12.10	15.94	15.64	15.64
121	0.93	11.96	9.26	13.35	11.85	15.60	15.33	15.32
122	0.93	14.07	11.53	16.29	14.79	18.93	18.69	18.69
123	0.93	0.00	11.40	16.25	14.75	18.79	18.61	18.61
124	0.93	11.76	9.11	13.30	11.80	15.45	15.25	15.24
125	0.93	10.87	8.95	13.26	11.76	15.30	15.16	15.16
126	0.93	14.83	11.96	16.43	14.93	19.39	18.93	18.93
127	0.93	15.01	11.72	16.35	14.86	19.13	18.80	18.80
128	0.93	11.94	9.15	13.11	11.61	15.39	15.07	15.07
129	0.93	12.12	9.48	13.60	12.09	15.90	15.62	15.62
130	0.93	16.23	11.92	16.42	14.92	19.36	18.91	18.91
131	0.93	16.71	12.33	16.92	15.42	19.94	19.49	19.48
132	0.93	16.26	12.33	16.92	15.42	19.94	19.49	19.48
133	0.93	16.46	12.33	16.92	15.42	19.94	19.49	19.48

```
%==========================================================================%
%                              PROGRAM B-4                                 %
%        TYPICAL PROGRAM TO CALCULATE DEFLECTION OF BEAMS OBTAINED         %
%                      FROM DATA SUPPLEENT OF REF.[15]                     %
%                                                                          %
% Note:                                                                    %
% The terms used here are similar to the terms in PROGRAM B-1.             %
%==========================================================================%
% Read data file
clear all;clc;
load lain.txt
nobeam = lain (:,1)';
b = lain (:,2)';
h = lain (:,3)';
d = lain (:,4)';
L = lain (:,5)';
rho = lain (:,6)';
Ma = lain (:,7)';
fcu = lain (:,8)';
dex = lain (:,9)';
al = lain (:,10)';
a = al.*L;
Es=200000;
Ec=(20+0.2.*fcu).*1000;
n=Es./Ec;
As= rho./100.*b.*d;
Es=200000;
Ec=(20+0.2.*fcu).*1000;
n=Es./Ec;
%---------------------------- FIKRY'S METHOD -------------------------------%
nrho=n.*rho;
if nrho < 1.9
   alpha= 0.003; beta=0.095;
   elseif nrho <5
   alpha= 0.05; beta=0.07;
   elseif nrho<17
   alpha= 0.16; beta=0.05;
    elseif nrho<=32
      alpha= 0.5; beta=0.03;
   else
      alpha=0.8; beta= 0.02;
end
alpha; beta;
Icre=(alpha+beta.*nrho).*b.*d.^3./12;
Ig=(b.*h.^3)./12;
fr=0.56.*(fcu).^0.5;
yt=h./2;
Mcr=(fr.*Ig./1e+6)./yt;
Rm=Ma./Mcr;
if rho(:,1) < 1
   phi=-(Rm-2.*a./L);
else
    phi=-(Rm-2.*a./L).*rho;
    end
Ie=Icre+((Ig-Icre).*exp(phi));
delta=(Ma./Ie).*1000000.*(3.*(L.*1000).^2-4.*(a.*1000).^2)./(24.*Ec);
```

```
%-------------------------- BRANSON (ACI) --------------------------------%
k=(2.*nrho./100+(nrho./100).^2).^0.5-nrho./100;
Icr=b.*(k.*d).^3./3+n.*As.*(d-k.*d).^2;
Ie1=Icr+(Ig-Icr).*1/Rm.^3;
delta1=(Ma./Ie1).*1000000.*(3.*(L.*1000).^2-4.*(a.*1000).^2)./(24.*Ec);
%-------------------------- BRITISH STANDARD -----------------------------%
x = lain (:,11)';
fc= lain (:,12)';
Cuc=Ma.*1e6./(Ec.*Ig);           % Curvatute uncracked section
Cc= fc./(x.*Ec);                % Curvatute cracked section
K=0.125-a.^2/(6.*L.^2);
if Cc(:,1)<Cuc(:,1)    % argument to check curvature (cracked or not)
   deltabs = Cuc.*K.*(L*1000).^2;
else
    deltabs= Cc.*K.*(L*1000).^2;
end
%-------------------------- PROPOSED MODEL--------------------------------%
Icrn1=(0.1914-0.0012.*fcu+0.3195.*rho).*b.*d.^3./12;
Icrn2=(0.1618+0.0418.*nrho).*b.*d.^3./12;
phin1=-(Rm-2.*a./L).*(4.0768-1.7969.*rho);
phin2=-(Rm-2.*a./L).*(4.4757-2.0667.*rho);
phin2a=-(Rm-2.*a./L).*(8.474-9.0606.*rho+2.842.*rho.^2);
Ien1=Icrn1+((Ig-Icrn1).*exp(phin1));
Ien2=Icrn2+((Ig-Icrn2).*exp(phin2));
Ien2a=Icrn2+((Ig-Icrn2).*exp(phin2a));
% Case 1
deltap1=(Ma./Ien1).*1000000.*(3.*(L.*1000).^2-4.*(a.*1000).^2)./(24.*Ec);
% Case 2a
deltap2=(Ma./Ien2).*1000000.*(3.*(L.*1000).^2-4.*(a.*1000).^2)./(24.*Ec);
% Case 2b
deltap2a=(Ma./Ien2a).*1000000.*(3.*(L.*1000).^2-4.*(a.*1000).^2)./(24.*Ec);
%=========================================================================%
fn=fopen('lainout.txt','w');
fprintf(fn, '                          OUTPUT PROGRAM B-4\n\n');
fprintf(fn, '     COMPARISON BETWEEN MEASURED AND ANALYTICAL DEFLECTION\n');
fprintf(fn, '                       USING VARIOUS METHOD\n');
fprintf(fn, '============================================================\n');
fprintf(fn, '                measd                Deflection (mm)        \n');
fprintf(fn, ' Beam    rho     def. ------------------------------------\n');
fprintf(fn, '  #              (mm)  Fikry  ACI  BS  Case1  Case2a  Case2b\n');
fprintf(fn, '------------------------------------------------------------\n');
fprintf(fn, '  (1)    (2)     (3)    (4)    (5)  (6)   (7)     (8)    (9)\n');
fprintf(fn, '------------------------------------------------------------\n');
table(:,1) = nobeam';
table(:,2) = rho';
table(:,3) = dex';
table(:,4) = delta';
table(:,5) = delta1';
table(:,6) = deltabs';
table(:,7) = deltap1';
table(:,8) = deltap2';
table(:,9) = deltap2a';
fprintf(fn, '%6.0f %6.2f %7.2f %7.2f %7.2f %6.2f %6.2f %6.2f %6.2f\n',table');
fprintf(fn, '============================================================\n');
status = fclose(fn);
end
```

OUTPUT PROGRAM B-4

COMPARISON BETWEEN MEASURED AND ANALYTICAL DEFLECTION USING VARIOUS METHOD

Beam #	rho	measd def. (mm)	Deflection (mm)					
			Fikry	ACI	BS	Case1	Case2a	Case2b
(1)	(2)	(3)	(4)	(5)	(6)	(7)	(8)	(9)
1	3.20	8.46	7.15	7.14	9.45	0.00	0.00	7.44
2	1.31	5.56	4.66	5.59	7.11	6.50	6.53	6.51
4	3.25	9.91	7.52	7.52	9.97	0.00	0.00	7.91
5	3.25	5.33	4.69	4.69	6.12	0.00	0.00	4.85
6	2.50	5.33	4.68	4.75	6.14	0.96	0.29	5.25
7	0.81	4.32	3.22	5.48	6.62	6.14	6.09	6.10
9	3.26	5.84	4.76	4.76	6.22	0.00	0.00	4.85
10	2.50	5.08	5.27	5.36	6.98	0.89	0.22	5.95
11	2.50	8.89	5.09	5.19	6.74	0.94	0.26	5.77
12	2.50	1.78	1.33	1.35	1.76	0.21	0.05	1.49
13	0.81	2.03	1.20	1.84	2.30	2.10	2.07	2.07
91	0.48	5.72	3.27	10.90	8.70	10.52	10.31	10.44
91	0.48	4.62	3.79	12.12	9.90	11.84	11.56	11.63
91	0.48	7.32	2.55	9.09	6.93	8.40	8.33	8.65
92	0.48	4.42	2.51	9.01	6.84	8.27	8.21	8.55
92	0.48	5.72	3.22	10.81	8.62	10.41	10.20	10.34
92	0.48	9.09	3.72	12.02	9.80	11.71	11.44	11.51
93	0.48	4.12	2.53	8.85	6.71	8.25	8.20	8.49
93	0.48	6.99	3.24	10.60	8.44	10.31	10.12	10.24
93	0.48	8.81	3.75	11.77	9.61	11.57	11.32	11.38
94	0.68	6.81	5.35	10.66	9.11	11.62	11.47	11.48
94	0.68	10.72	7.83	14.22	12.63	15.55	15.32	15.32
95	0.68	10.52	4.82	10.21	8.66	10.95	10.86	10.89
95	0.68	13.06	6.94	13.36	11.77	14.42	14.26	14.27
96	0.68	10.16	5.06	10.54	8.99	11.34	11.23	11.26
96	0.68	13.06	7.43	14.02	12.43	15.16	14.99	14.99
97	0.99	9.53	7.88	10.80	9.71	12.52	12.43	12.42
97	0.99	12.78	10.70	14.37	13.23	16.67	16.54	16.54
98	0.99	8.33	7.52	10.49	9.41	12.06	12.04	12.04
98	0.99	11.53	10.30	14.00	12.87	16.11	16.08	16.08
99	0.99	9.37	7.68	10.55	9.46	12.23	12.14	12.14
99	0.99	12.78	10.47	14.07	12.94	16.33	16.20	16.20
100	1.21	9.68	7.79	9.69	9.00	11.26	11.30	11.28
100	1.21	13.06	10.46	12.91	12.25	15.02	15.07	15.06
101	1.21	9.68	8.12	10.07	9.39	11.72	11.75	11.73
101	1.21	13.34	10.89	13.42	12.76	15.64	15.67	15.67
102	1.21	9.68	8.10	9.82	9.14	11.70	11.49	11.47
102	1.21	13.34	10.84	13.09	12.44	15.60	15.32	15.31
103	1.48	10.16	9.37	10.57	9.78	12.55	12.35	12.33
103	1.48	13.95	12.50	14.10	13.27	16.75	16.48	16.48
104	1.48	10.72	8.65	10.02	9.24	11.44	11.68	11.64
104	1.48	14.63	11.54	13.35	12.52	15.30	15.62	15.61
105	1.48	11.10	8.59	9.95	9.17	11.36	11.59	11.56
105	1.48	15.01	11.46	13.25	12.43	15.19	15.51	15.50
106	1.83	11.53	10.80	11.71	11.01	13.09	13.28	13.57
106	1.83	15.80	12.63	13.69	12.96	15.41	15.70	15.87
107	1.83	13.06	10.73	11.65	10.94	12.98	13.20	13.50

107	1.83	17.68	14.29	15.51	14.76	17.47	17.88	17.99
108	1.83	11.33	10.69	11.48	10.79	13.08	13.04	13.27
108	1.83	15.01	14.25	15.31	14.56	17.59	17.62	17.69
109	2.80	10.72	12.54	12.63	12.10	0.01	0.00	13.71
109	2.80	18.75	16.68	16.80	16.22	0.00	0.00	18.24
110	2.80	13.95	12.58	12.72	12.19	0.02	0.00	13.95
110	2.80	18.75	16.76	16.94	16.36	0.00	0.00	18.58
111	2.80	13.64	12.03	12.14	11.62	0.02	0.00	13.28
111	2.80	18.75	15.99	16.15	15.58	0.00	0.00	17.65
112	0.33	2.01	1.28	7.49	4.18	4.11	4.30	5.53
112	0.33	5.18	1.83	10.00	6.60	7.47	7.55	8.28
113	0.33	1.80	1.47	8.07	4.74	5.43	5.62	6.60
113	0.33	4.47	2.11	10.75	7.34	8.82	8.80	9.17
114	0.33	1.91	1.20	7.84	4.49	3.40	3.55	4.85
114	0.33	4.42	1.70	10.43	7.02	6.78	6.83	8.01
115	0.68	7.42	3.63	8.82	7.17	9.10	9.11	9.24
115	0.68	10.52	5.45	11.74	10.03	12.48	12.39	12.42
116	0.68	7.24	3.58	8.33	6.70	8.78	8.75	8.86
116	0.68	10.34	5.37	11.11	9.43	12.02	11.89	11.91
117	0.68	8.23	3.92	9.08	7.43	9.57	9.53	9.63
117	0.68	11.10	5.86	12.10	10.39	13.00	12.88	12.89
118	1.00	6.99	6.25	8.86	7.80	10.18	10.16	10.15
118	1.00	10.34	8.65	11.80	10.71	13.61	13.57	13.57
119	1.00	7.24	6.45	8.79	7.74	10.35	10.15	10.15
119	1.00	9.68	8.86	11.72	10.63	13.82	13.55	13.55
120	1.00	8.23	6.84	9.21	8.16	10.88	10.65	10.65
120	1.00	11.10	9.34	12.27	11.17	14.51	14.20	14.20
121	1.23	6.81	7.17	8.78	7.75	10.40	10.24	10.17
121	1.23	9.53	9.69	11.69	10.63	13.91	13.68	13.66
122	1.23	11.53	7.94	9.68	8.63	11.48	11.30	11.25
122	1.23	14.63	10.70	12.89	11.81	15.33	15.08	15.07
123	1.23	9.68	6.90	9.05	8.00	10.09	10.40	10.24
123	1.23	11.99	9.49	12.07	11.00	13.63	14.03	13.98
124	1.55	9.83	8.00	9.32	8.51	10.23	10.70	10.69
124	1.55	13.06	10.67	12.38	11.54	13.78	14.44	14.44
125	1.55	10.16	8.05	9.39	8.58	10.28	10.78	10.77
125	1.55	13.34	10.78	12.54	11.68	13.91	14.63	14.62
126	1.55	10.52	8.57	9.77	8.96	11.09	11.32	11.32
126	1.55	13.95	11.44	13.02	12.16	14.89	15.21	15.21
127	1.91	10.16	8.89	9.39	8.66	10.42	9.94	10.76
127	1.91	13.06	11.85	12.51	11.74	14.34	13.88	14.34
128	1.91	11.10	9.10	9.71	8.97	10.45	10.15	11.18
128	1.91	13.34	12.14	12.95	12.17	14.47	14.32	14.92
129	1.91	10.01	9.19	9.78	9.04	10.65	10.30	11.24
129	1.91	12.78	12.23	13.01	12.23	14.66	14.43	14.97
130	2.82	13.06	10.72	10.78	10.28	0.02	0.00	11.67
130	2.82	17.65	14.30	14.38	13.84	0.00	0.00	15.56
131	2.82	8.23	11.18	11.21	10.70	0.01	0.00	11.99
131	2.82	10.52	14.86	14.90	14.36	0.00	0.00	15.94
132	2.82	6.66	10.70	10.75	10.25	0.02	0.00	11.57
132	2.82	9.37	14.27	14.33	13.79	0.00	0.00	15.42
133	0.33	4.19	2.15	11.39	8.12	8.99	8.87	9.35
133	0.33	7.60	3.11	15.16	11.81	12.89	12.44	12.53
134	0.33	5.41	2.19	11.63	8.36	9.23	9.09	9.54
134	0.33	9.22	3.18	15.48	12.12	13.15	12.67	12.76
135	0.33	6.33	2.87	14.08	10.76	11.92	11.57	11.70
135	0.33	7.90	3.30	15.65	12.29	13.39	12.94	13.01

136	0.68	5.89	4.14	9.25	7.69	9.85	9.79	9.86
136	0.68	8.46	6.17	12.33	10.74	13.32	13.17	13.18
137	0.68	5.00	4.10	9.34	7.77	9.87	9.83	9.90
137	0.68	8.56	6.12	12.43	10.85	13.35	13.23	13.24
138	0.68	5.51	4.50	9.87	8.31	10.54	10.47	10.52
138	0.68	8.33	6.69	13.15	11.56	14.18	14.03	14.04
139	1.00	7.14	5.16	7.50	6.56	8.51	8.56	8.53
139	1.00	10.16	7.18	9.97	9.00	11.40	11.44	11.43
140	1.00	6.20	5.48	7.79	6.84	8.93	8.92	8.91
140	1.00	8.56	7.57	10.35	9.38	11.93	11.90	11.90
141	1.00	6.33	5.66	7.86	6.92	9.14	9.04	9.03
141	1.00	9.22	7.81	10.49	9.52	12.23	12.09	12.09
142	1.22	6.81	6.75	8.38	7.41	9.83	9.75	9.68
142	1.22	9.83	9.17	11.18	10.18	13.20	13.07	13.05
143	1.22	7.70	6.37	8.00	7.04	9.32	9.28	9.19
143	1.22	11.10	8.68	10.66	9.66	12.51	12.45	12.42
144	1.22	7.90	6.68	8.26	7.30	9.74	9.62	9.55
144	1.22	10.90	9.02	10.96	9.97	12.99	12.81	12.80
145	1.55	7.32	6.66	7.45	6.72	8.65	8.54	8.54
145	1.55	10.72	8.90	9.93	9.16	11.68	11.54	11.54
146	1.55	7.32	6.26	7.64	6.90	7.74	8.33	8.31
146	1.55	10.52	8.48	10.19	9.42	10.76	11.68	11.67
147	1.55	8.23	6.57	7.81	7.06	8.24	8.71	8.69
147	1.55	11.53	8.85	10.40	9.63	11.32	12.03	12.02
148	1.80	8.46	7.58	8.33	7.69	8.95	9.13	9.63
148	1.80	10.72	10.10	11.09	10.41	12.25	12.63	12.88
149	1.80	8.23	6.93	7.65	7.03	8.01	8.20	8.82
149	1.80	10.52	9.23	10.18	9.52	11.06	11.47	11.83
150	1.80	7.80	7.38	8.03	7.40	8.79	8.83	9.27
150	1.80	10.52	9.85	10.71	10.04	12.03	12.20	12.41
151	2.76	11.10	10.72	10.83	10.33	0.07	0.01	11.87
151	2.76	15.01	14.29	14.44	13.90	0.01	0.00	15.82
152	2.76	13.06	10.89	10.95	10.45	0.04	0.00	11.87
152	2.76	16.21	14.54	14.62	14.08	0.00	0.00	15.84
153	2.76	9.83	10.50	10.58	10.08	0.06	0.01	11.51
153	2.76	13.06	13.95	14.05	13.51	0.01	0.00	15.29
154	0.42	5.99	3.18	22.75	10.06	7.24	7.67	10.55
154	0.42	9.83	3.85	26.46	13.81	11.23	11.93	16.56
155	0.42	2.11	3.24	23.24	10.55	7.48	7.92	10.93
155	0.42	6.12	3.93	27.07	14.41	11.66	12.38	17.16
156	0.42	6.38	3.30	23.31	10.61	7.93	8.42	11.66
156	0.42	12.50	4.01	27.15	14.48	12.32	13.10	18.03
157	0.44	2.90	3.45	24.92	10.17	8.98	9.59	13.38
157	0.44	5.61	4.20	28.98	14.30	13.94	14.91	20.45
158	0.44	2.62	3.06	23.69	9.03	6.54	6.93	9.41
158	0.44	6.53	3.74	27.72	12.97	10.43	11.14	15.63
159	0.44	3.58	3.22	24.70	9.99	7.40	7.86	10.83
159	0.44	7.70	3.92	28.72	14.10	11.59	12.39	17.35
160	0.82	6.66	10.07	25.94	19.30	25.32	26.02	26.62
160	0.82	24.00	12.93	30.27	23.66	31.91	32.44	32.86
161	0.82	15.39	8.98	25.58	18.98	22.64	23.63	24.37
161	0.82	19.99	11.52	29.85	23.28	29.39	30.35	30.96
162	0.82	15.39	9.30	25.76	19.14	23.48	24.41	25.12
162	0.82	22.23	11.97	30.11	23.52	30.31	31.17	31.72
163	0.90	16.21	11.76	29.84	20.85	29.09	29.87	29.90
163	0.90	21.44	15.40	34.79	25.87	37.17	37.70	37.73
164	0.90	15.80	10.23	27.54	18.49	25.13	25.97	26.01
164	0.90	19.99	13.32	32.04	23.05	32.77	33.45	33.48

165	0.90	13.06	10.94	28.94	19.99	27.06	27.95	27.98
165	0.90	15.80	13.02	31.96	22.97	32.17	32.96	32.99
166	0.38	3.99	2.20	14.98	8.38	3.63	3.77	4.81
166	0.38	7.80	2.67	17.51	11.08	6.09	6.41	8.82
167	0.38	2.79	2.20	14.47	7.86	3.82	3.98	5.15
167	0.38	5.26	2.67	16.90	10.44	6.35	6.71	9.22
168	0.37	2.08	1.95	14.63	7.88	2.51	2.56	2.94
168	0.37	3.56	2.36	17.09	10.50	4.20	4.38	5.76
169	0.37	1.45	2.15	15.19	8.45	3.39	3.51	4.41
169	0.37	2.26	2.60	17.73	11.19	5.68	5.97	8.24
170	0.37	1.27	2.37	15.16	8.44	4.95	5.22	7.12
170	0.37	3.99	2.94	17.97	11.45	8.51	9.01	12.23
171	0.37	4.80	2.44	15.27	8.55	5.45	5.77	7.93
171	0.37	8.56	2.97	17.85	11.34	8.90	9.42	12.65
172	0.38	6.12	1.95	13.58	2.48	2.00	2.01	2.04
172	0.38	12.78	2.33	15.90	4.10	2.99	3.05	3.48
173	0.37	2.85	3.46	24.86	11.86	7.08	7.41	10.12
173	0.37	5.41	4.16	29.01	15.84	11.01	11.56	16.15
174	0.37	3.53	4.58	26.46	13.40	15.21	16.05	20.68
174	0.37	7.49	5.56	30.86	17.65	21.63	22.44	26.48
175	0.36	1.73	3.80	25.91	12.52	9.39	9.92	13.90
175	0.36	2.03	4.60	30.27	16.74	14.44	15.21	20.64
176	0.36	4.52	3.59	24.64	11.29	8.21	8.65	12.08
176	0.36	4.95	4.32	28.73	15.27	12.63	13.33	18.41
177	0.36	6.38	3.85	25.36	12.02	9.91	10.49	14.66
177	0.36	9.22	4.65	29.61	16.10	15.09	15.90	21.23
178	0.38	4.34	4.75	26.25	13.57	16.21	17.04	21.40
178	0.38	8.23	5.78	30.62	17.82	22.69	23.43	27.00
179	0.38	4.72	4.55	26.64	13.94	14.37	15.16	19.89
179	0.38	6.60	5.54	31.12	18.27	20.81	21.63	26.09
180	0.38	3.58	4.44	26.12	13.44	13.66	14.43	19.09
180	0.38	5.82	5.41	30.53	17.70	19.95	20.79	25.35
181	1.98	7.24	6.56	7.11	6.49	6.42	6.11	8.17
181	1.98	10.34	8.77	9.47	8.83	9.27	8.98	10.96
182	1.98	6.60	6.52	7.08	6.47	6.32	6.03	8.14
182	1.98	11.10	8.70	9.44	8.80	9.13	8.87	10.93
183	1.98	7.32	6.49	7.07	6.45	6.27	5.99	8.12
183	1.98	10.34	8.68	9.42	8.78	9.07	8.82	10.91
184	1.98	7.80	6.64	7.13	6.52	6.62	6.27	8.19
184	1.98	11.10	8.81	9.45	8.81	9.46	9.10	10.91
185	1.98	7.42	6.64	7.13	6.52	6.63	6.28	8.20
185	1.98	10.72	8.81	9.45	8.82	9.47	9.11	10.91
186	1.98	7.70	6.58	7.10	6.48	6.49	6.16	8.16
186	1.98	11.10	8.73	9.40	8.77	9.28	8.96	10.87
187	2.00	10.01	8.94	9.63	9.00	9.36	8.94	11.13
187	2.00	13.34	11.91	12.83	12.16	13.23	12.99	14.84
188	2.00	10.72	8.91	9.61	8.97	9.28	8.87	11.11
188	2.00	15.01	11.86	12.80	12.13	13.13	12.91	14.81
189	2.00	9.83	9.09	9.72	9.09	9.70	9.21	11.21
189	2.00	16.66	12.10	12.94	12.28	13.63	13.30	14.93
190	2.14	9.37	7.65	8.11	7.52	6.44	5.20	9.32
190	2.14	13.64	10.18	10.80	10.17	9.24	7.15	12.41
191	2.14	9.68	7.74	8.17	7.58	6.63	5.33	9.37
191	2.14	14.28	10.29	10.87	10.25	9.50	7.32	12.47
192	2.24	9.53	8.71	9.12	8.38	5.33	3.38	10.40
192	2.24	13.95	11.59	12.13	11.37	7.33	3.86	13.84
193	2.14	9.83	9.07	9.52	8.78	7.33	5.58	10.89
193	2.14	13.95	12.31	12.94	12.15	11.00	7.90	14.79
194	2.14	11.33	9.02	9.49	8.75	7.23	5.52	10.87

194	2.14	16.66	12.25	12.89	12.11	10.85	7.81	14.76
195	2.14	13.06	9.03	9.50	8.75	7.25	5.53	10.87
195	2.14	13.64	12.26	12.90	12.12	10.87	7.82	14.77
196	2.09	8.69	8.30	8.73	7.96	7.24	6.00	9.99
196	2.09	12.24	11.08	11.66	10.85	10.66	8.70	13.34
197	2.09	8.81	8.00	8.54	7.77	6.55	5.51	9.83
197	2.09	11.53	10.69	11.40	10.60	9.67	7.99	13.15
198	2.09	7.90	8.00	8.55	7.78	6.56	5.52	9.83
198	2.09	11.33	10.69	11.41	10.60	9.68	7.99	13.15

Appendix C

- **Comparison between measured and calculated deflection curves for all test beams**

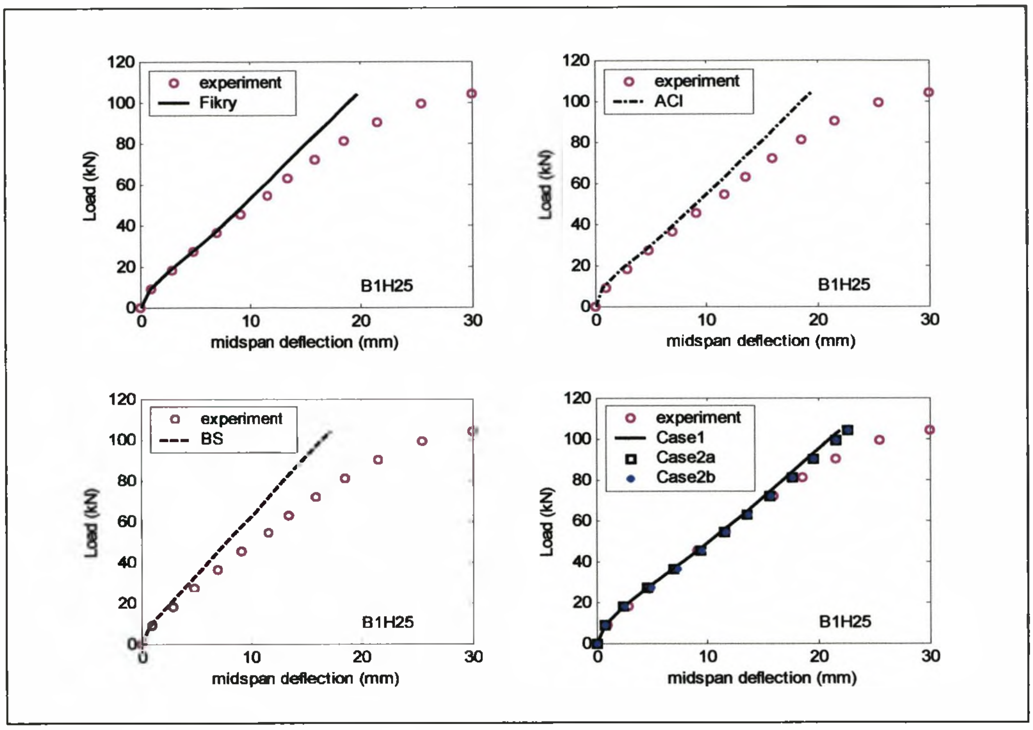

Figure C-1 Comparison between measured and predicted deflection of B1H25 with various methods

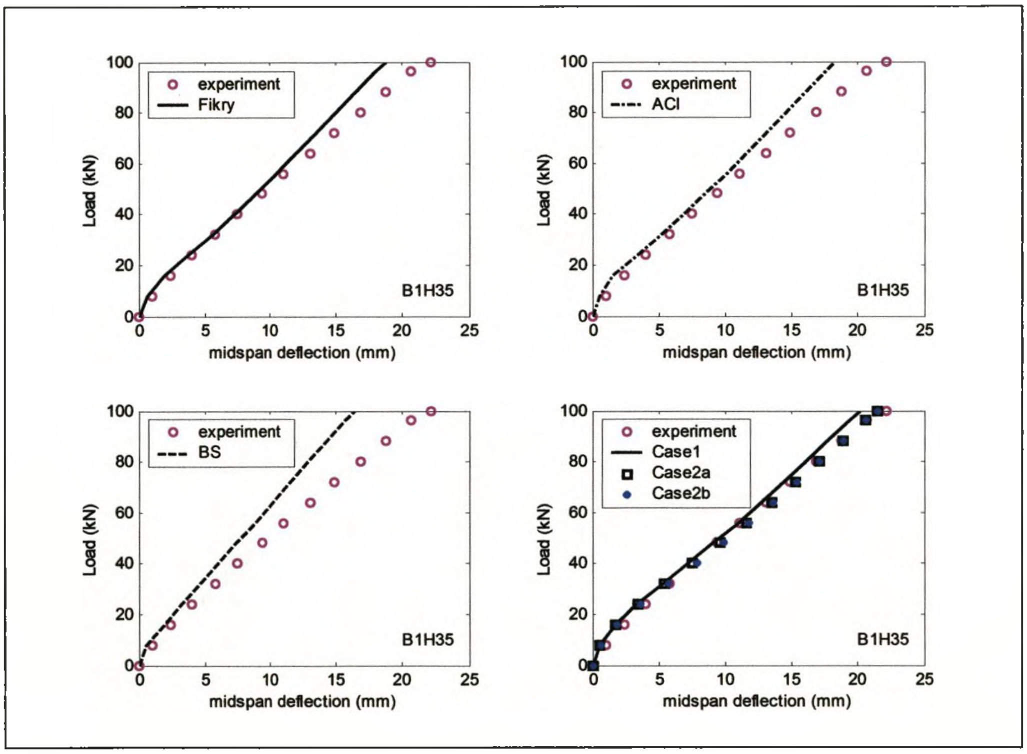

Figure C-2 Comparison between measured and predicted deflection of B1H35 with various methods

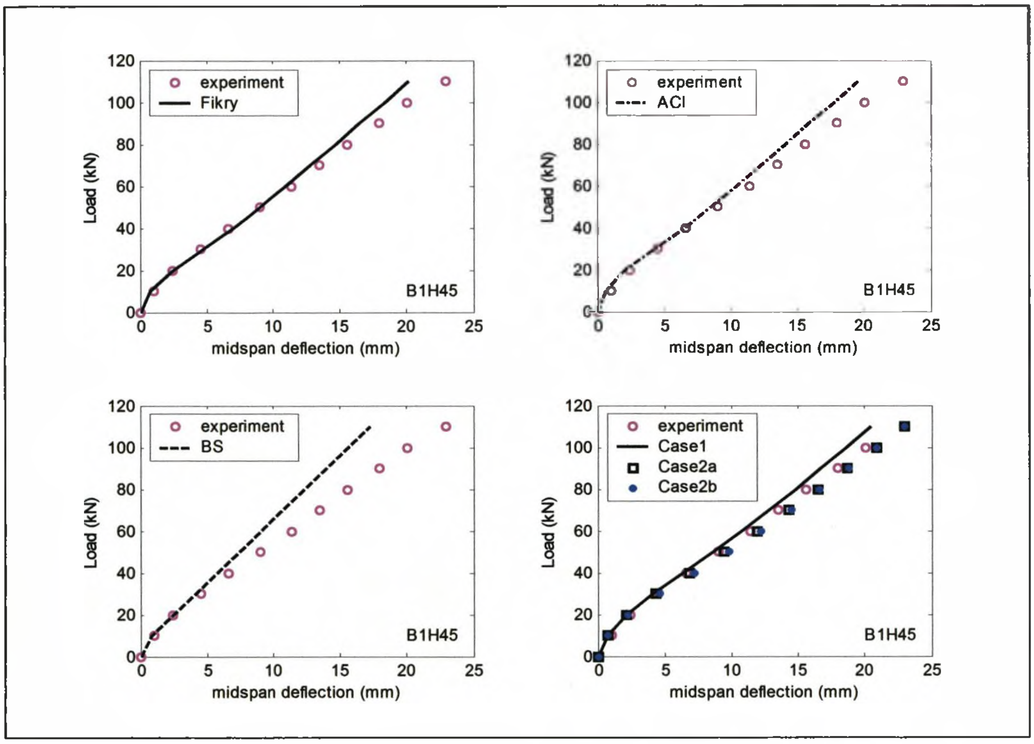

Figure C-3 Comparison between measured and predicted deflection of B1H45 with various methods

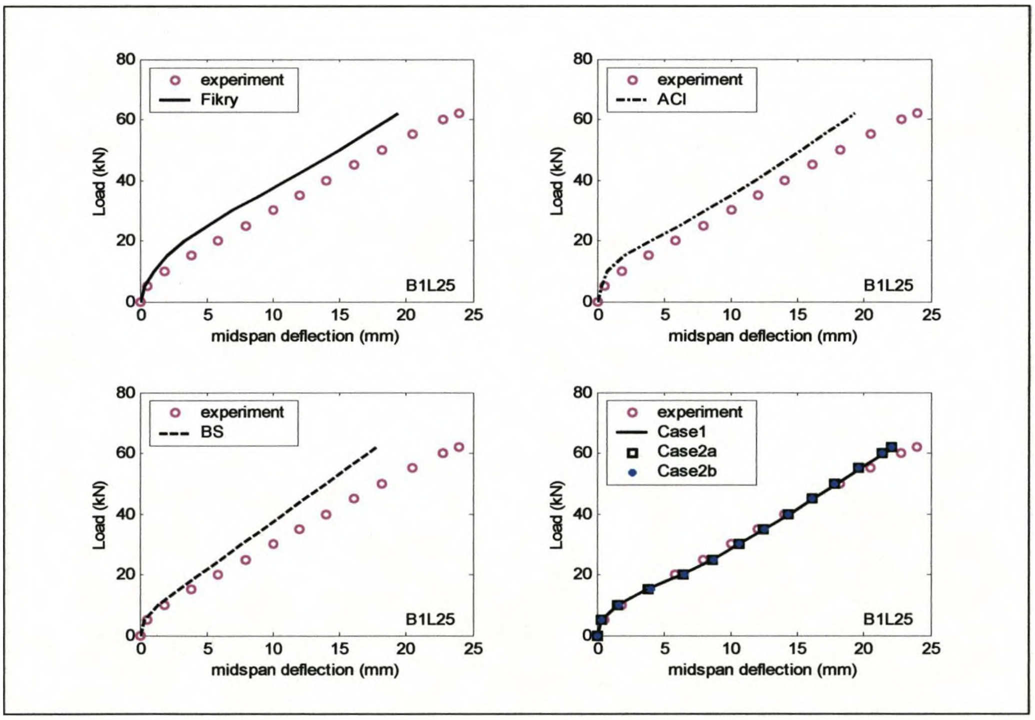

Figure C- 4 Comparison between measured and predicted deflection of B1L25 with various methods

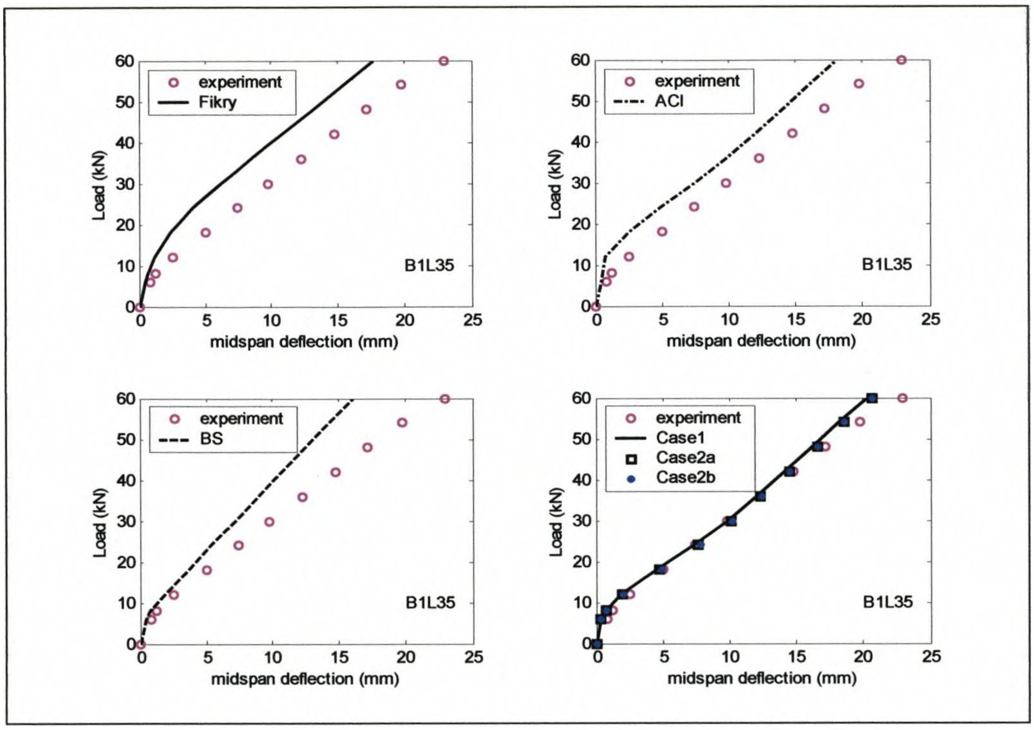

Figure C-5 Comparison between measured and predicted deflection of B1L35 with various methods

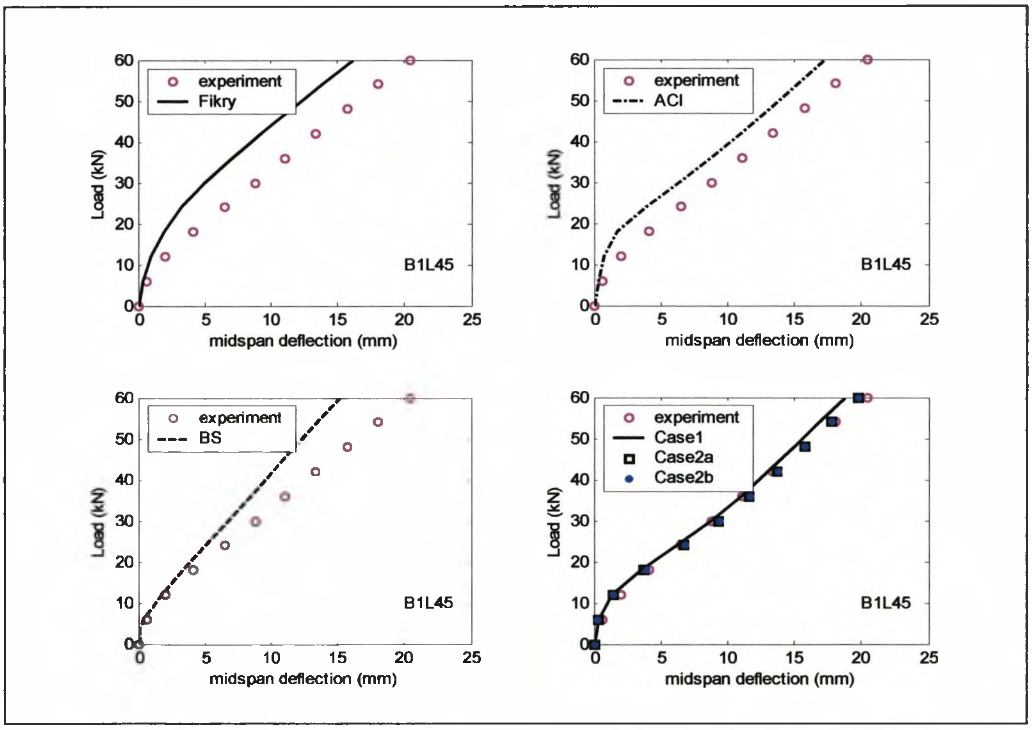

Figure C-6 Comparison between measured and predicted deflection of B1L45 with various methods

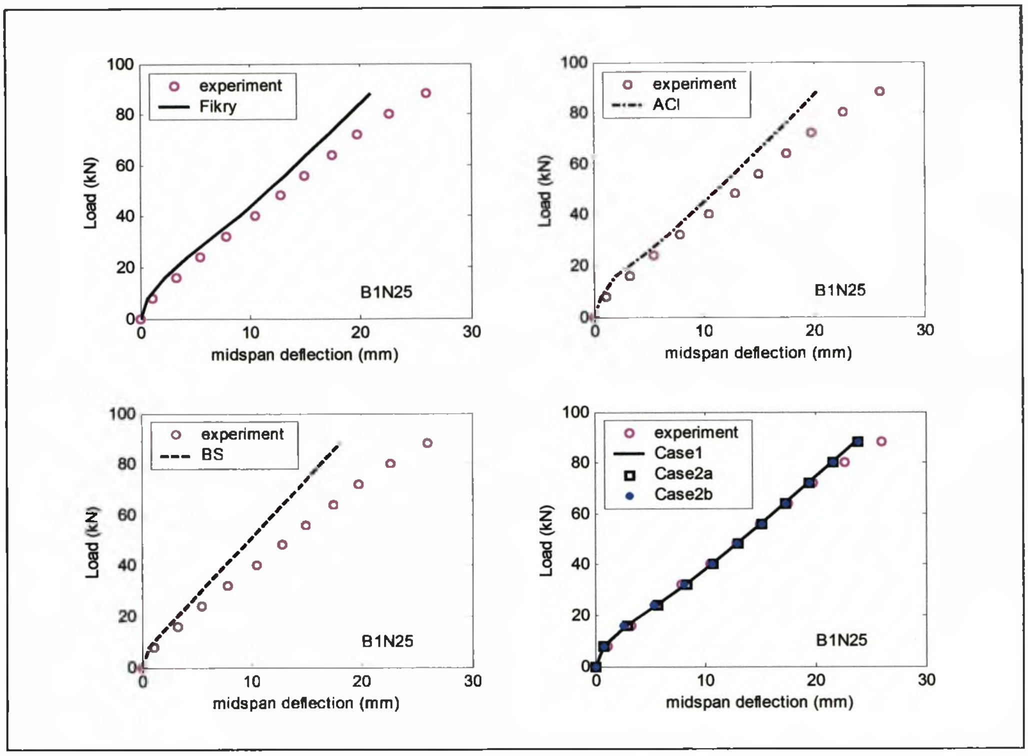

Figure C-7 Comparison between measured and predicted deflection of B1N25 with various methods

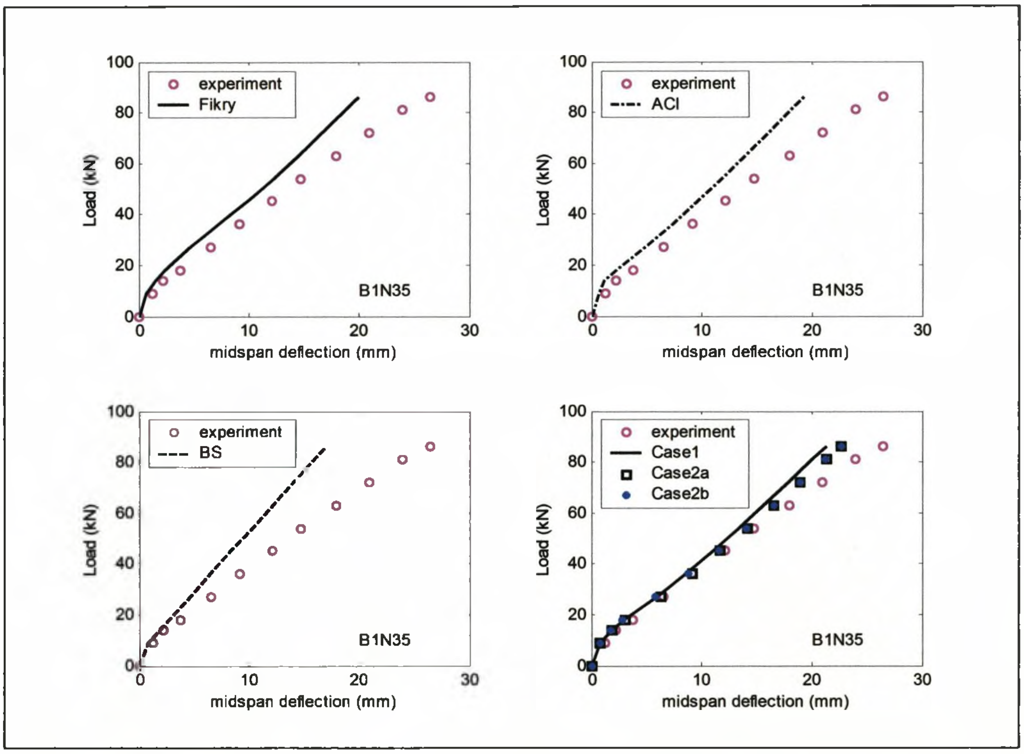

Figure C-8 Comparison between measured and predicted deflection of B1N35 with various methods

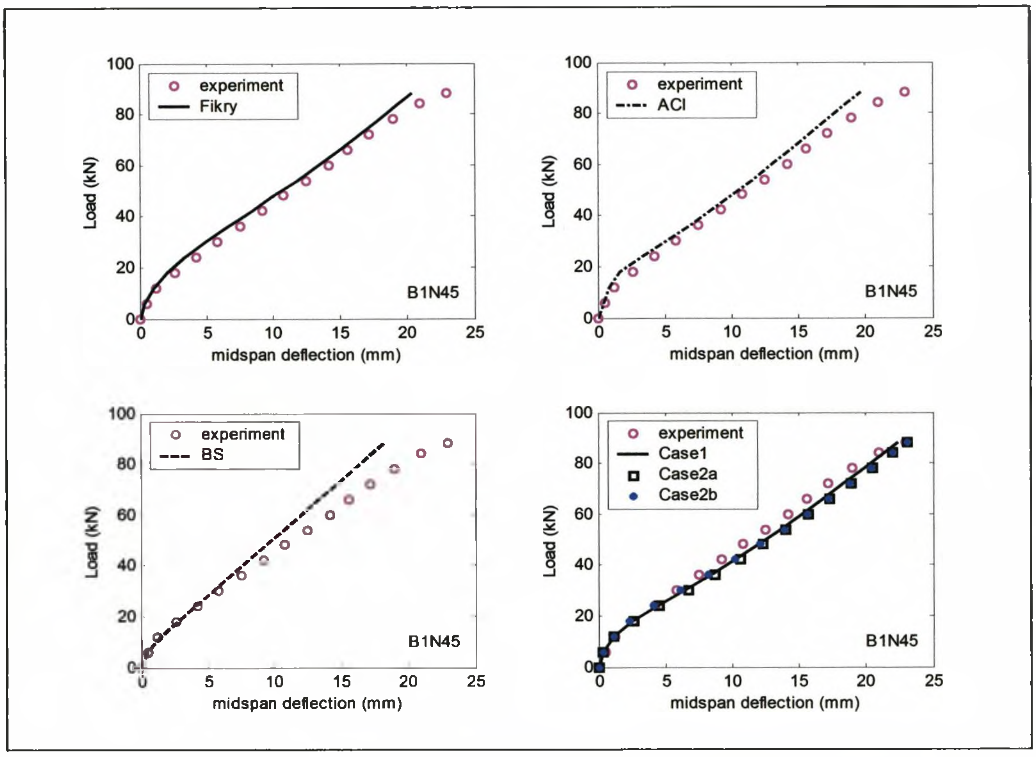

Figure C-9 Comparison between measured and predicted deflection of B1N45 with various methods

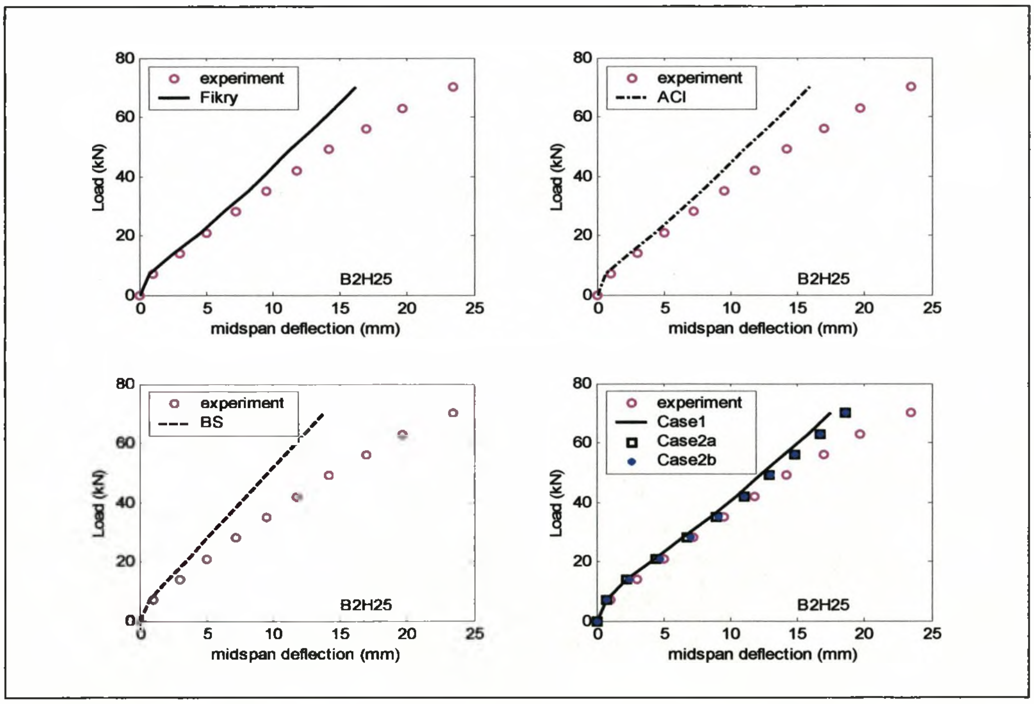

Figure C-10 Comparison between measured and predicted deflection of B2H25 with various methods

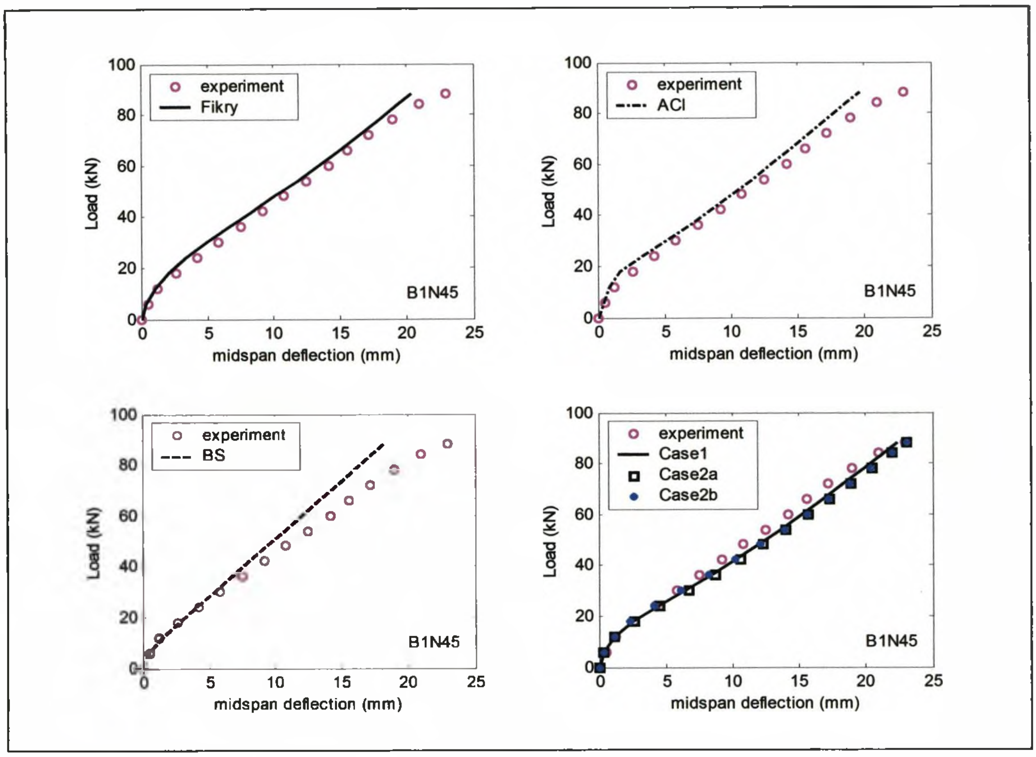

Figure C-11 Comparison between measured and predicted deflection of B2H35 with various methods

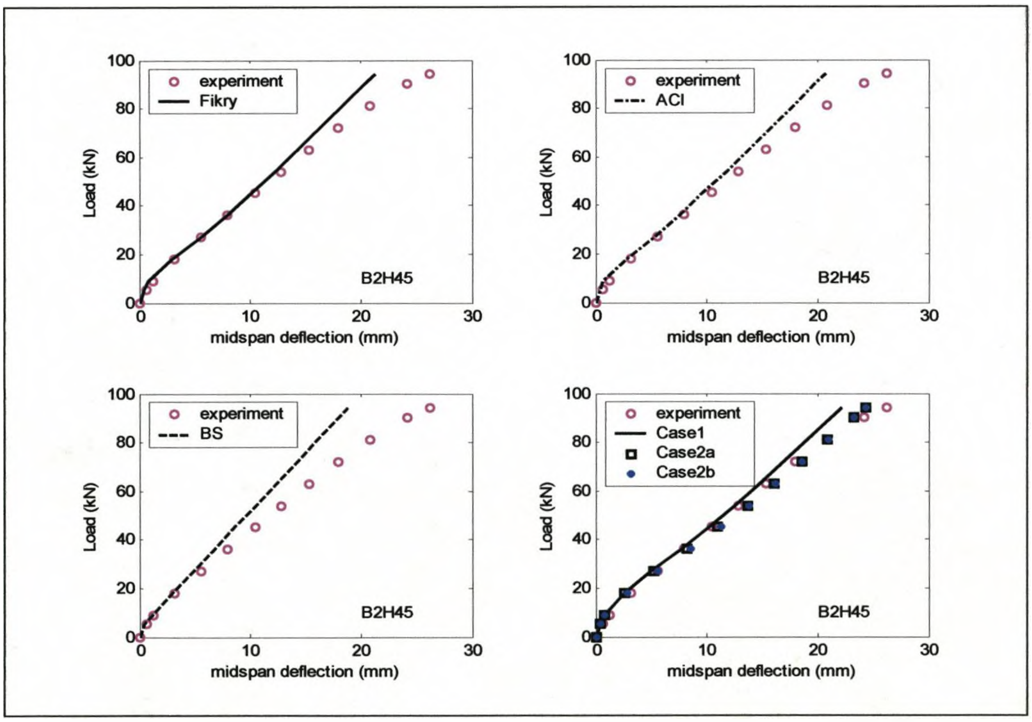

Figure C-12 Comparison between measured and predicted deflection of B2H45 with various methods

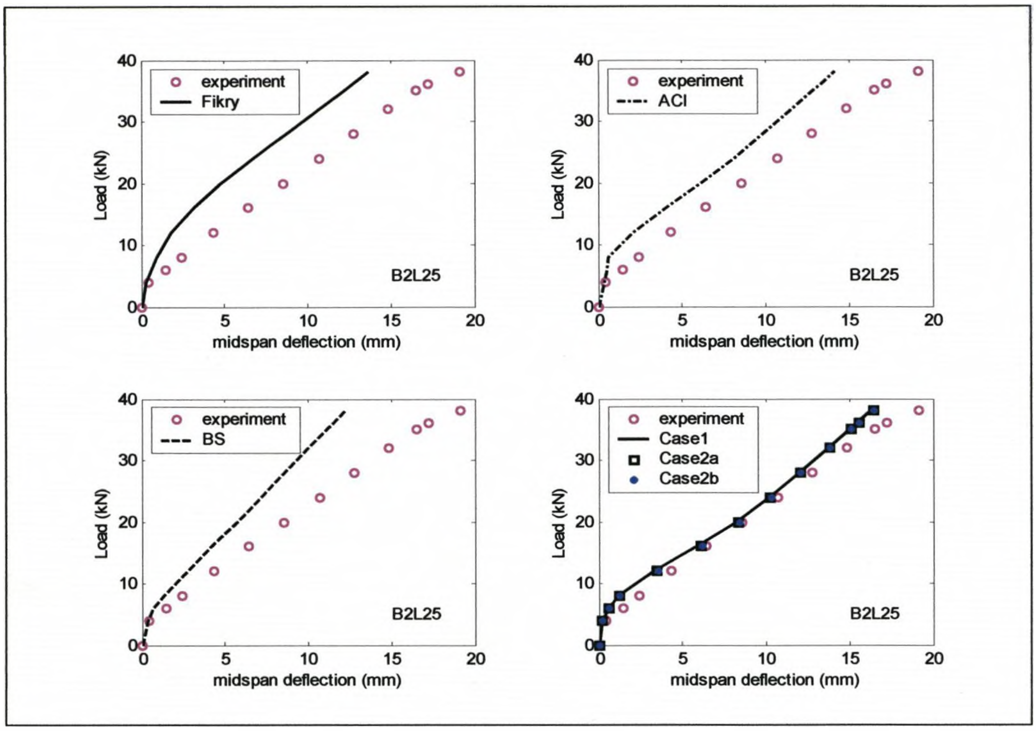

Figure C-13 Comparison between measured and predicted deflection of B2L25 with various methods

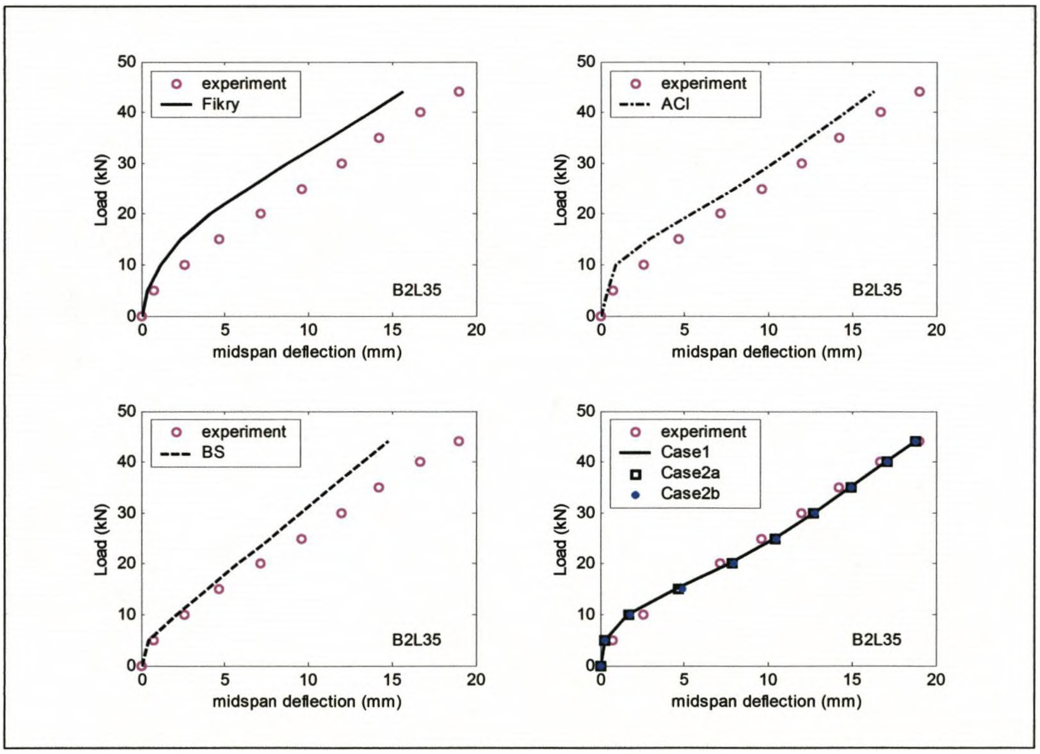

Figure C-14 Comparison between measured and predicted deflection of B2L35 with various methods

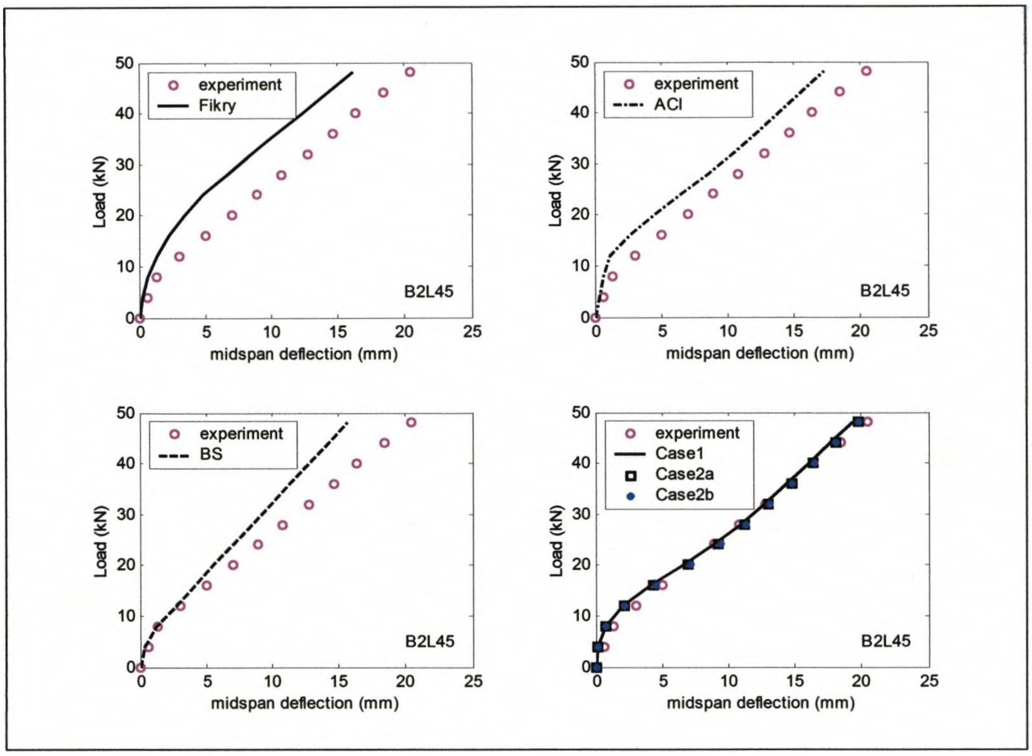

Figure C-15 Comparison between measured and predicted deflection of B2L45 with various methods

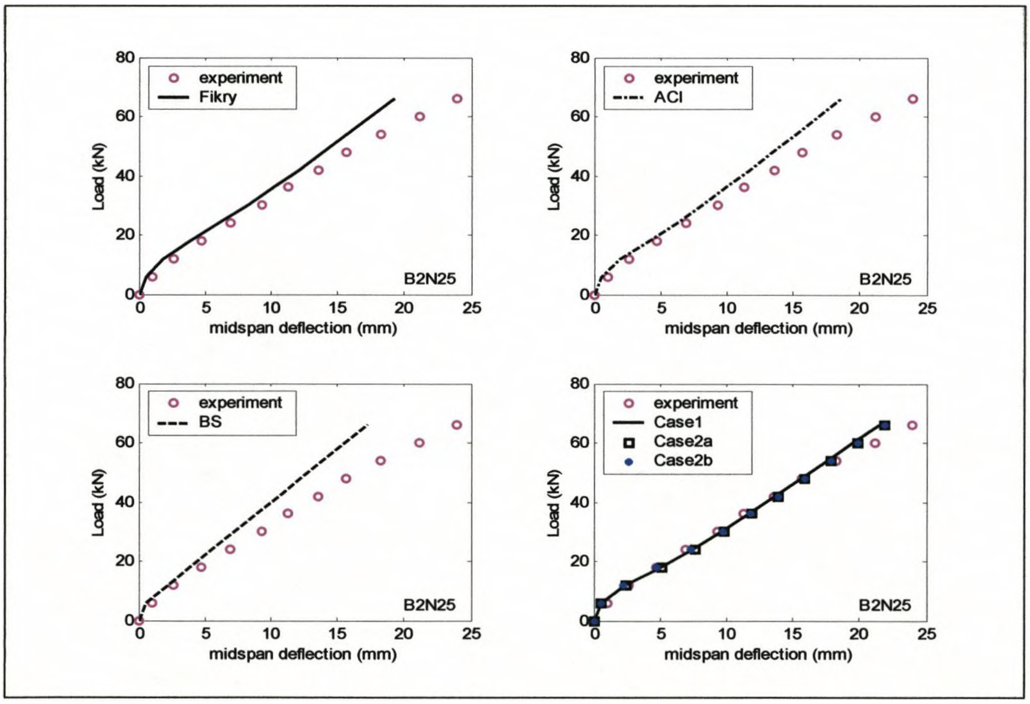

Figure C-16 Comparison between measured and predicted deflection of B2N25 with various methods

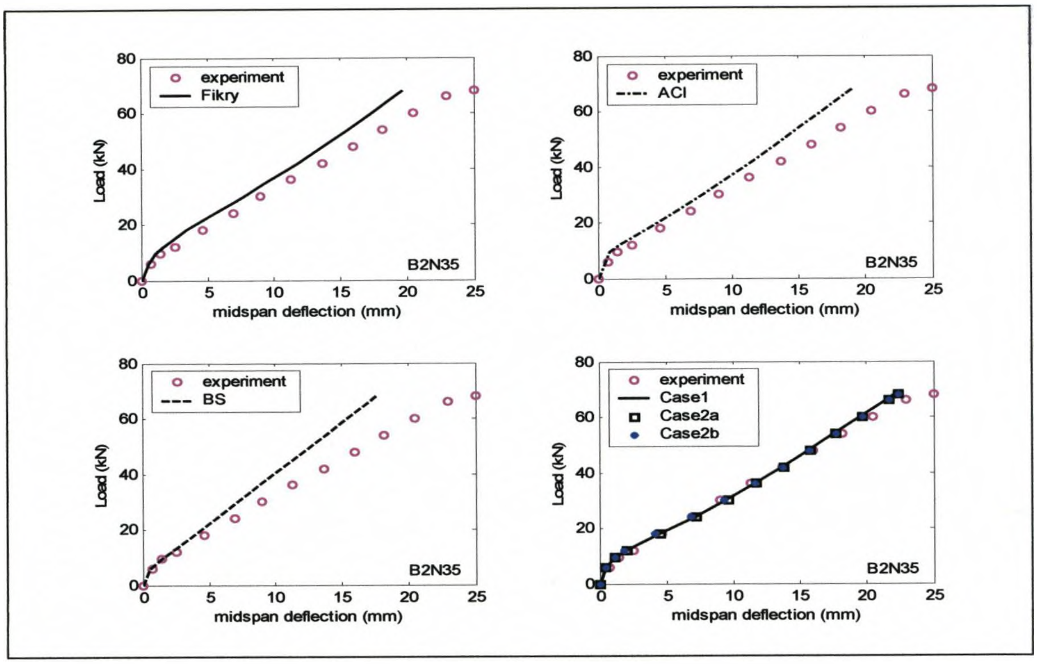

Figure C-17 Comparison between measured and predicted deflection of B2N35 with various methods

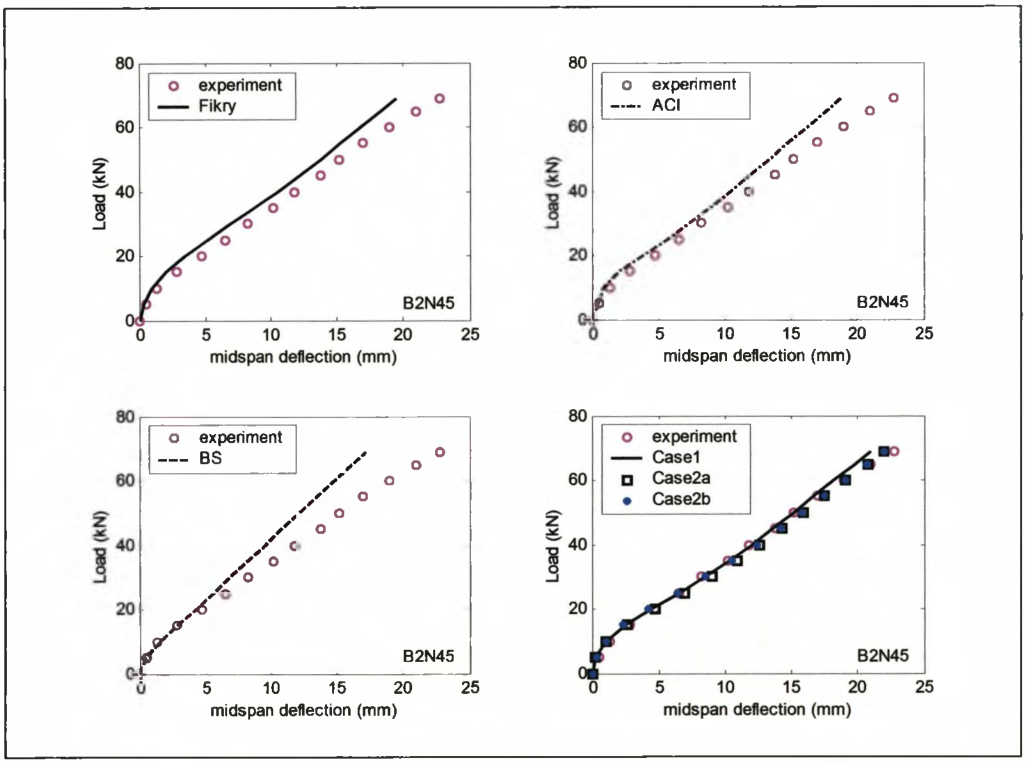

Figure C-18 Comparison between measured and predicted deflection of B2N45 with various methods

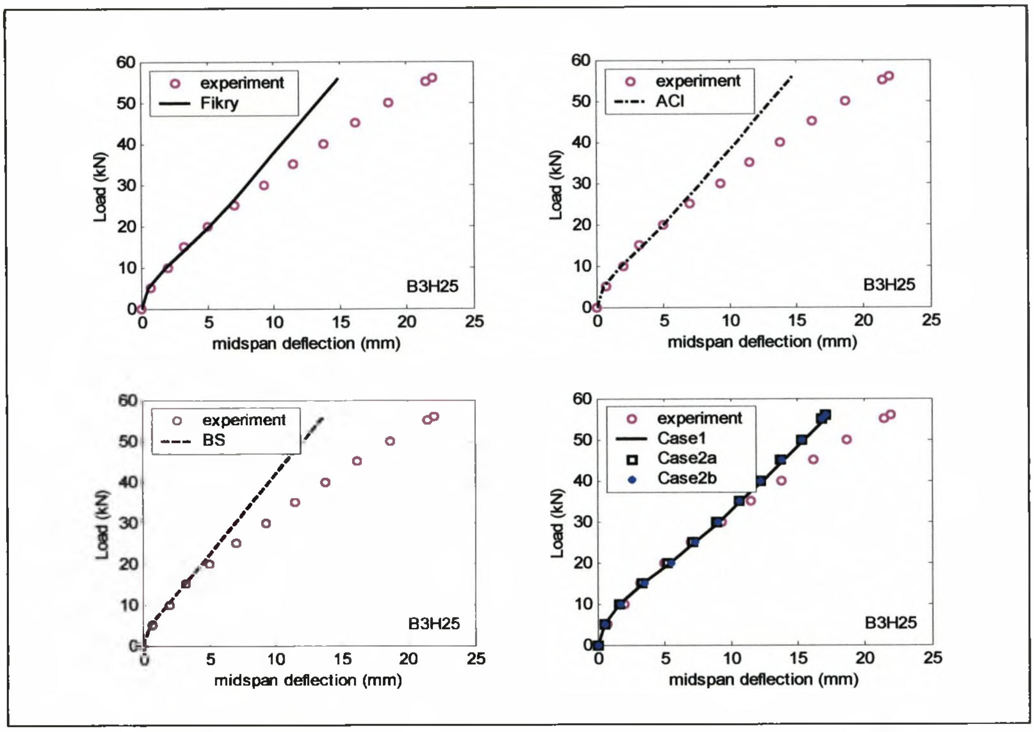

Figure C-19 Comparison between measured and predicted deflection of B3H25 with various methods

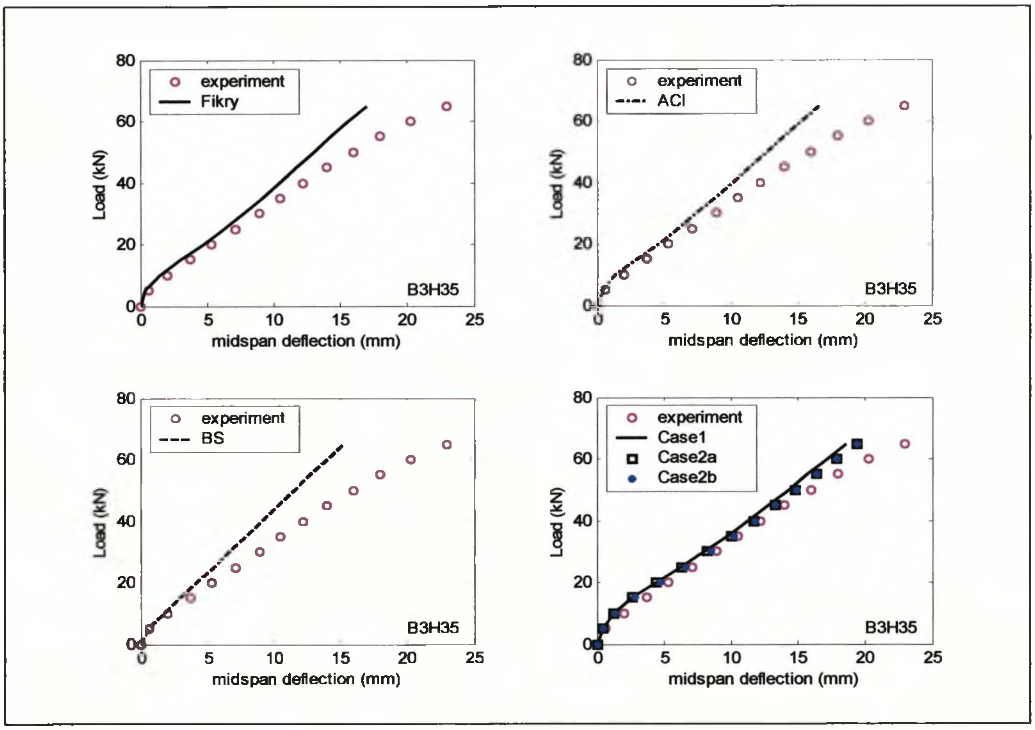

Figure C-20 Comparison between measured and predicted deflection of B3H35 with various methods

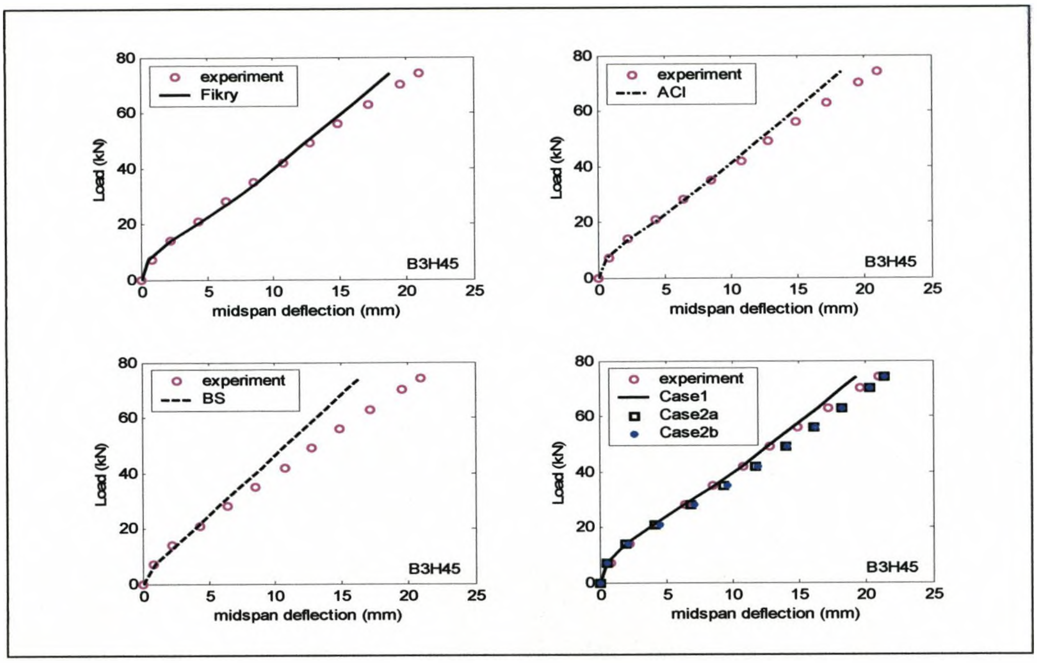

Figure C-21 Comparison between measured and predicted deflection of B3H45 with various methods

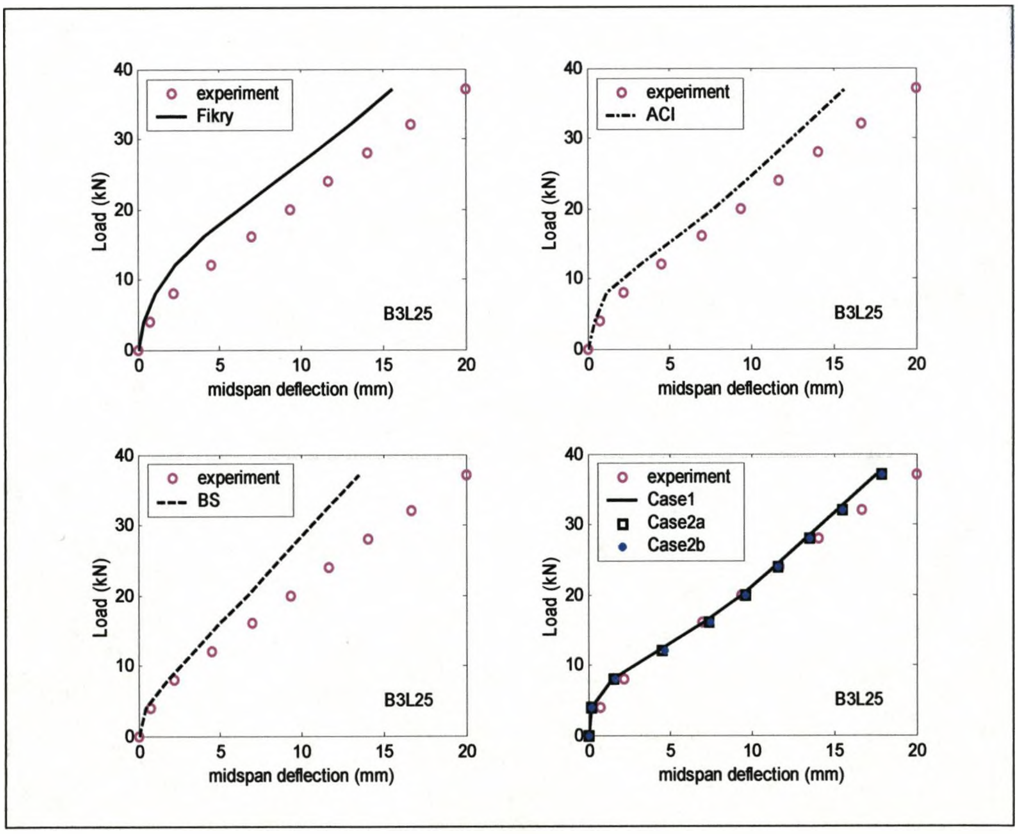

Figure C-22 Comparison between measured and predicted deflection of B3L25 with various methods

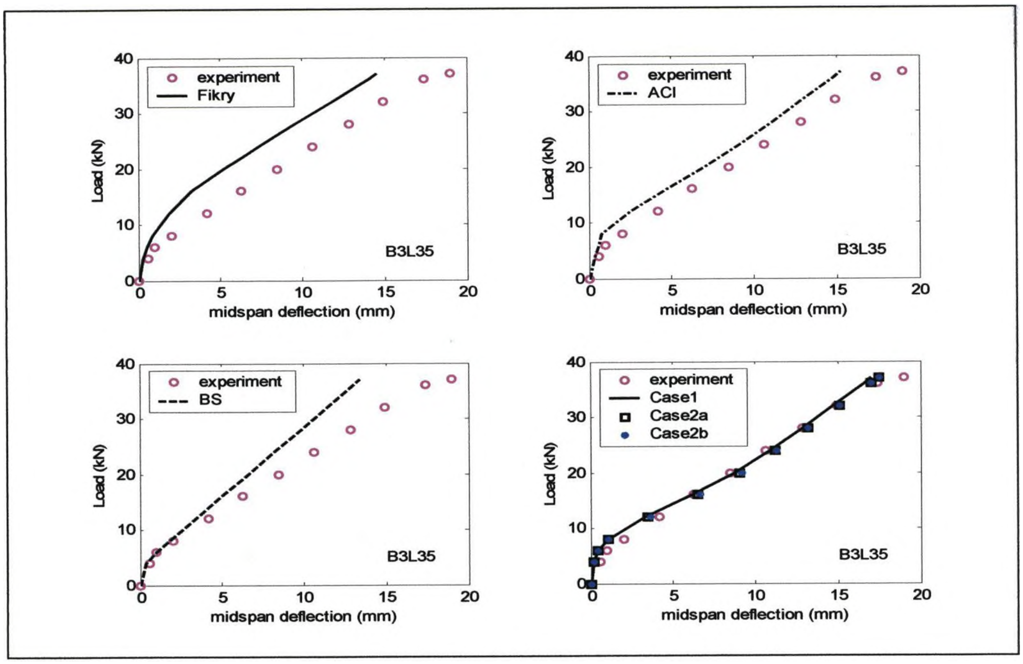

Figure C-23 Comparison between measured and predicted deflection of B3L35 with various methods

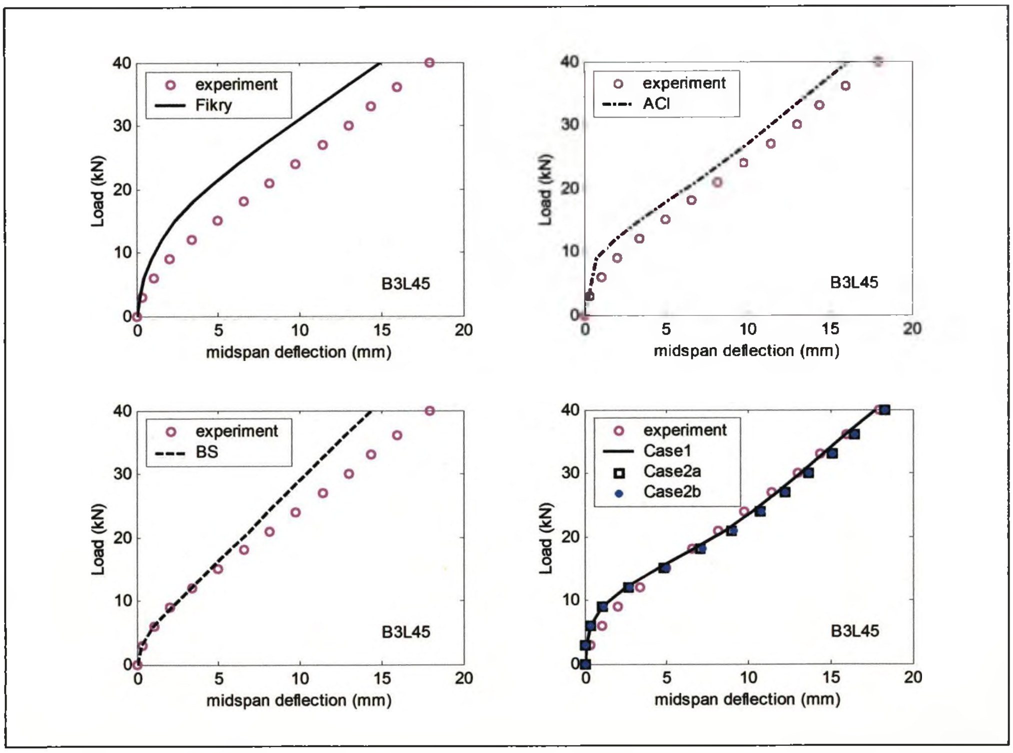

Figure C-24 Comparison between measured and predicted deflection of B3L45 with various methods

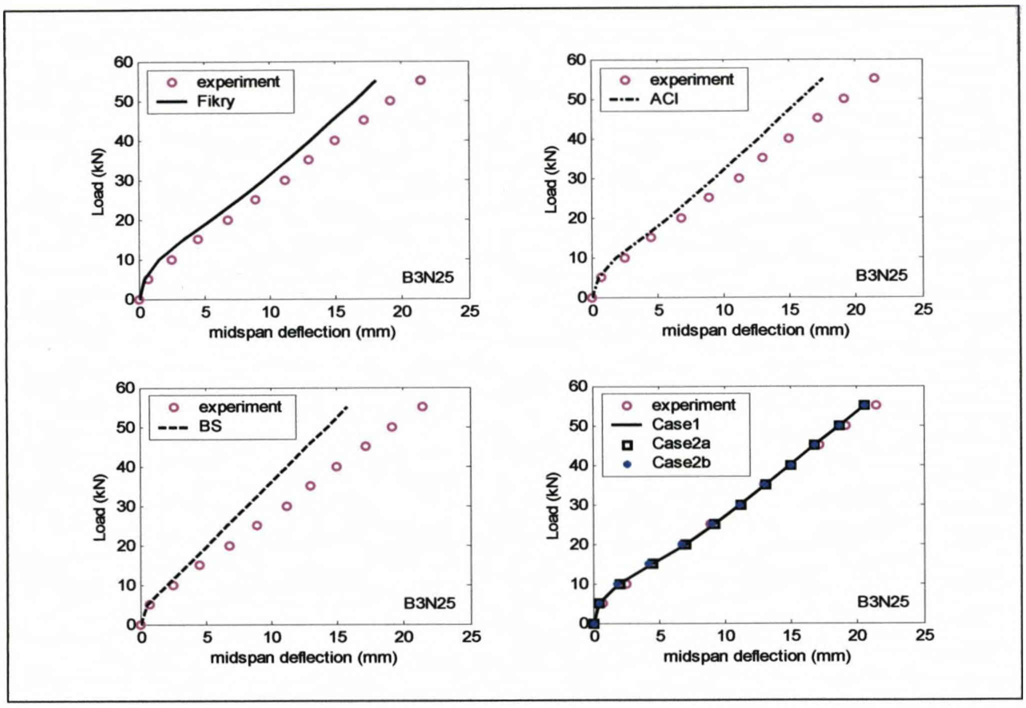

Figure C-25 Comparison between measured and predicted deflection of B3N25 with various methods

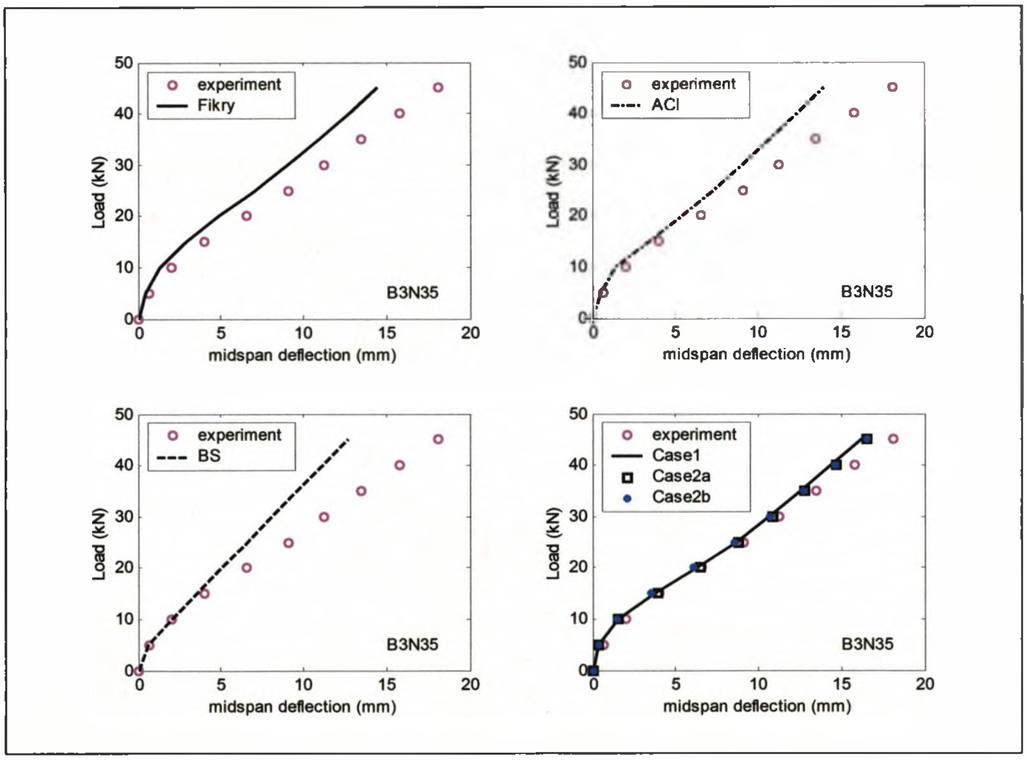

Figure C-26 Comparison between measured and predicted deflection of B3N35 with various methods

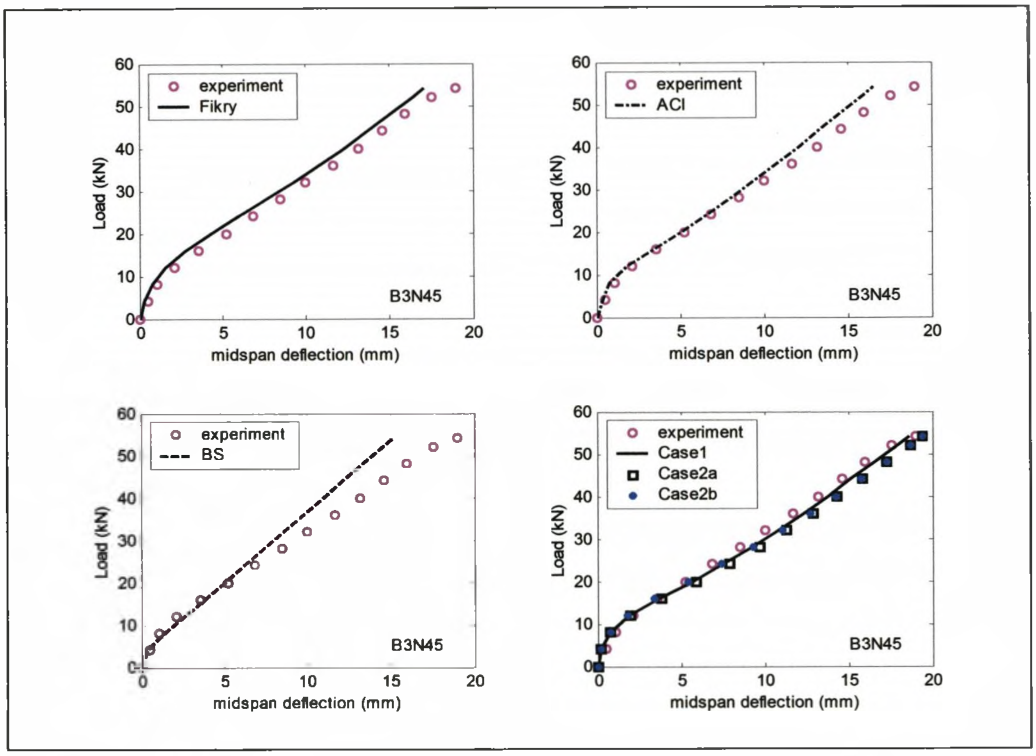

Figure C-27 Comparison between measured and predicted deflection of B3N45 with various methods

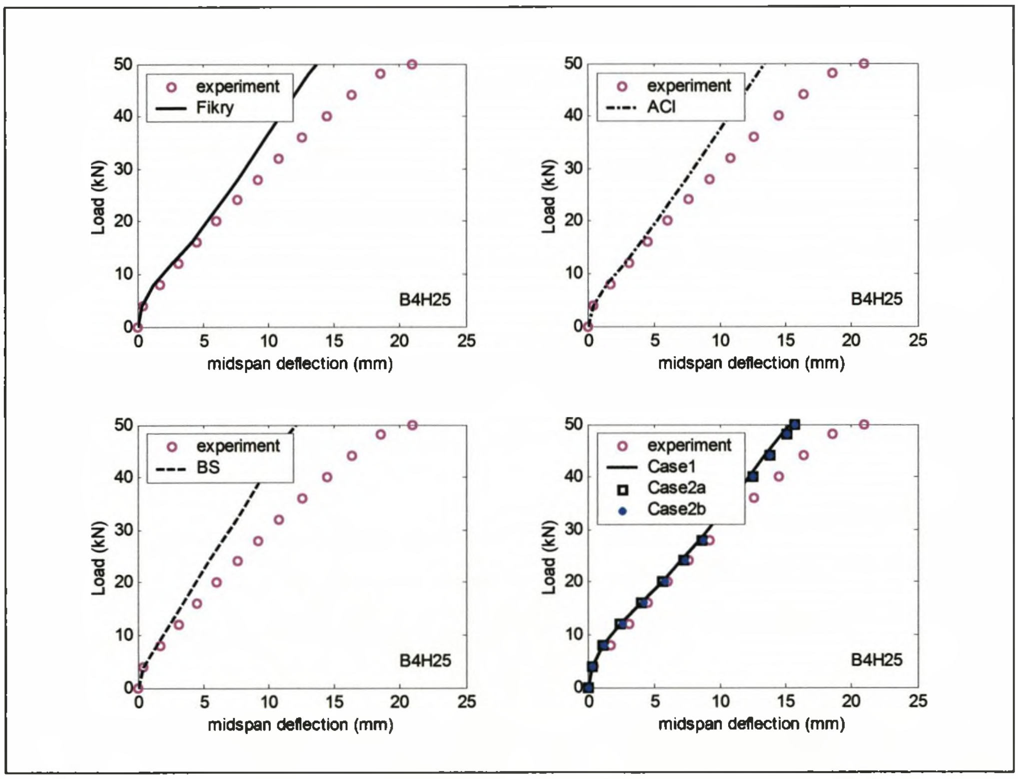

Figure C-28 Comparison between measured and predicted deflection of B4H25 with various methods

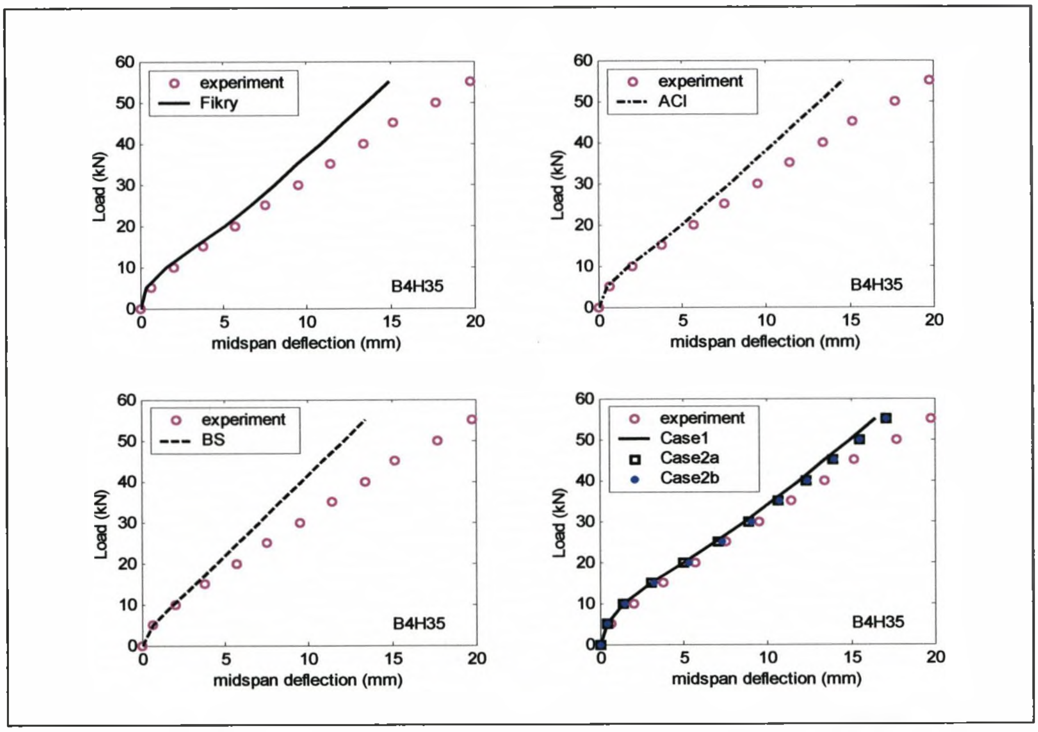

Figure C-29 Comparison between measured and predicted deflection of B4H35 with various methods

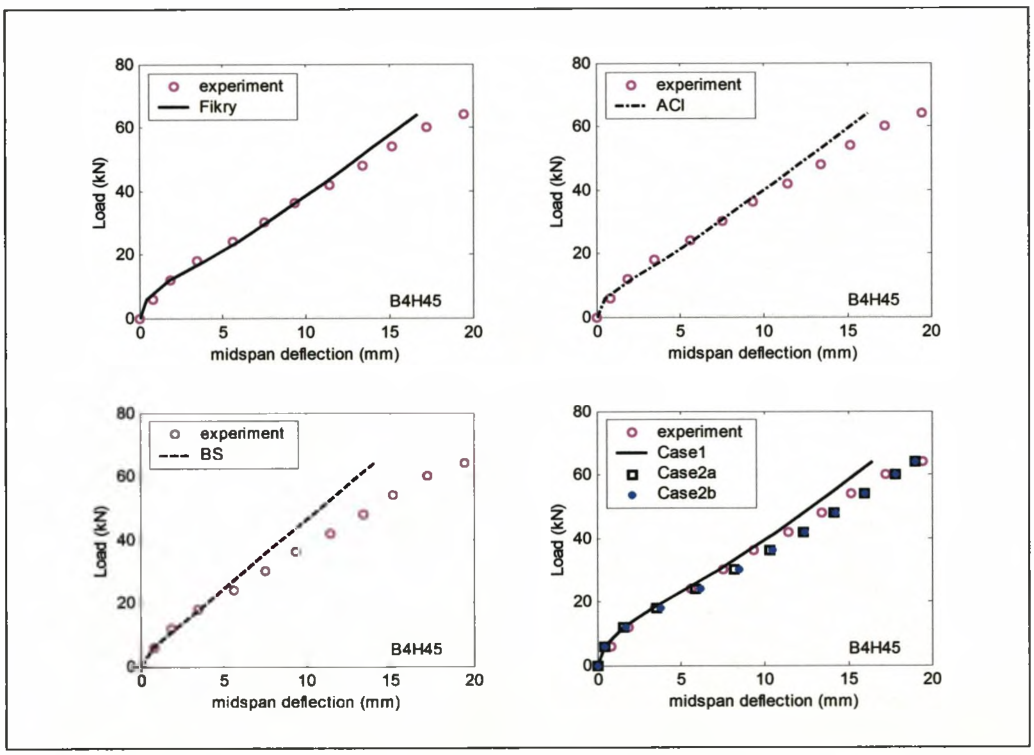

Figure C-30 Comparison between measured and predicted deflection of B4H45 with various methods

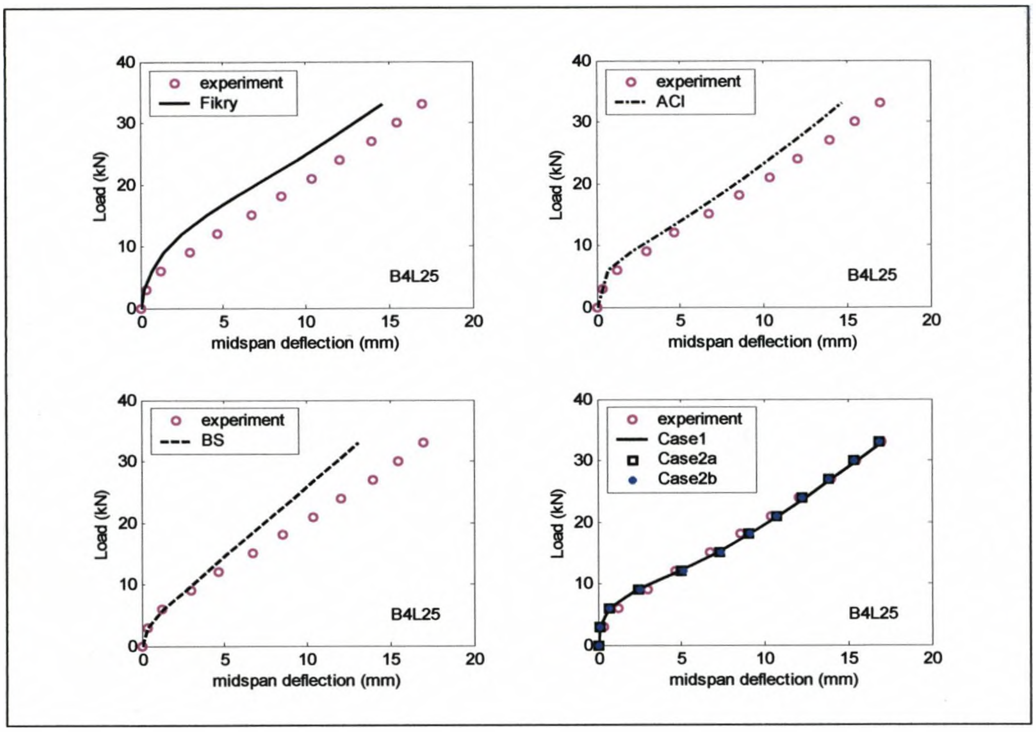

Figure C-31 Comparison between measured and predicted deflection of B4L25 with various methods

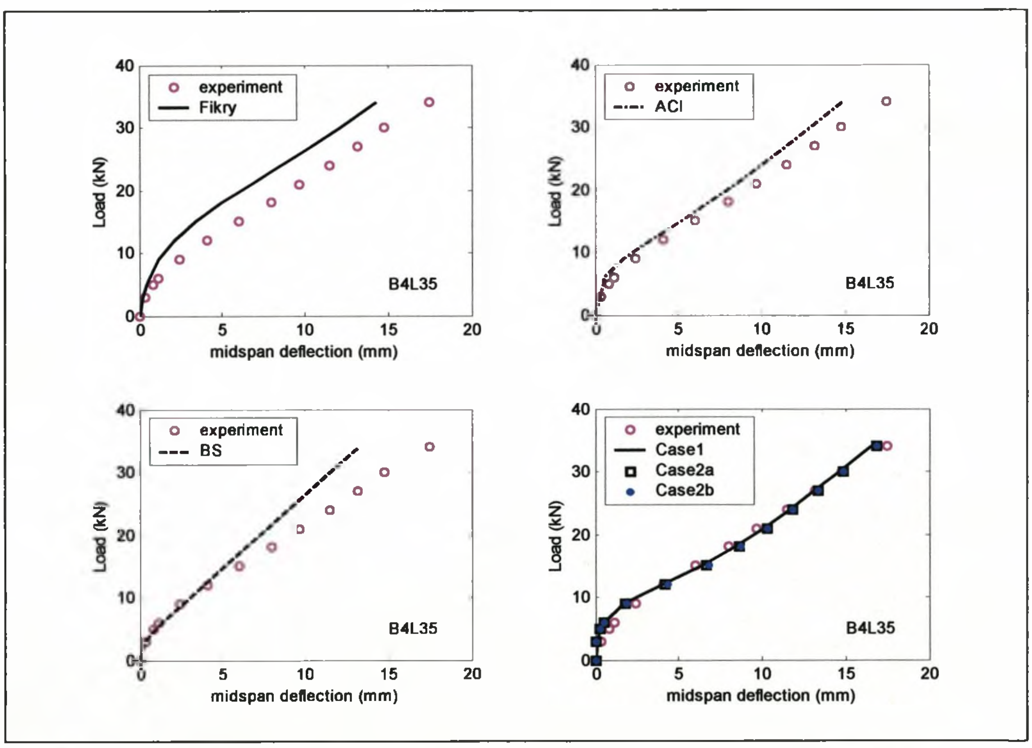

Figure C-32 Comparison between measured and predicted deflection of B4L35 with various methods

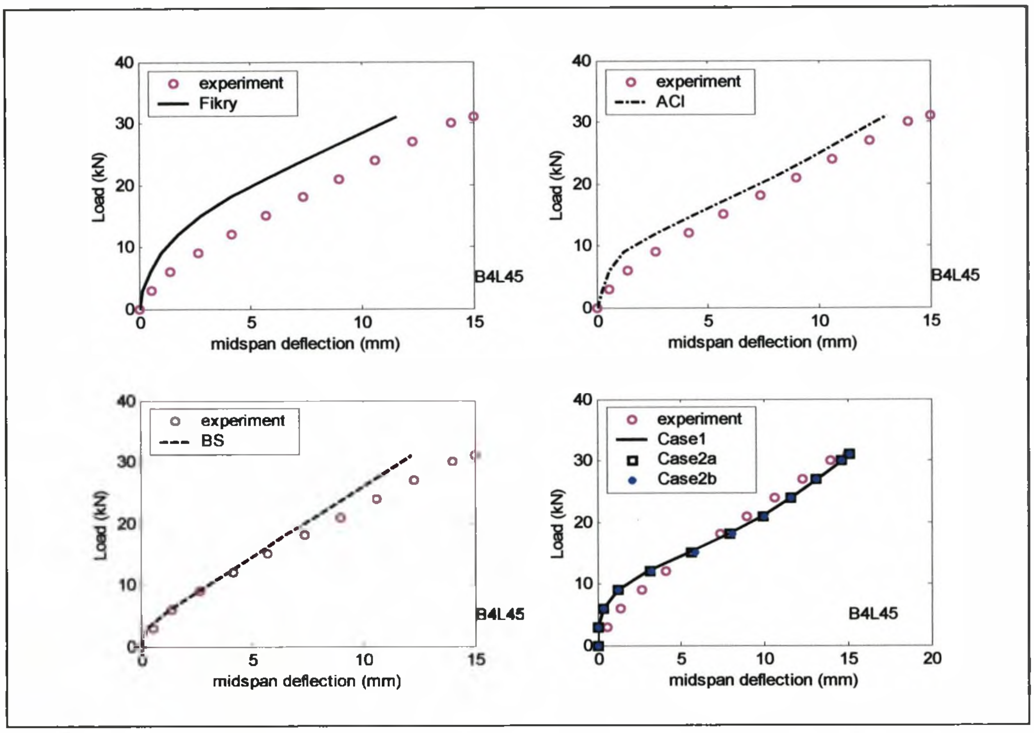

Figure C-33 Comparison between measured and predicted deflection of B4L45 with various methods

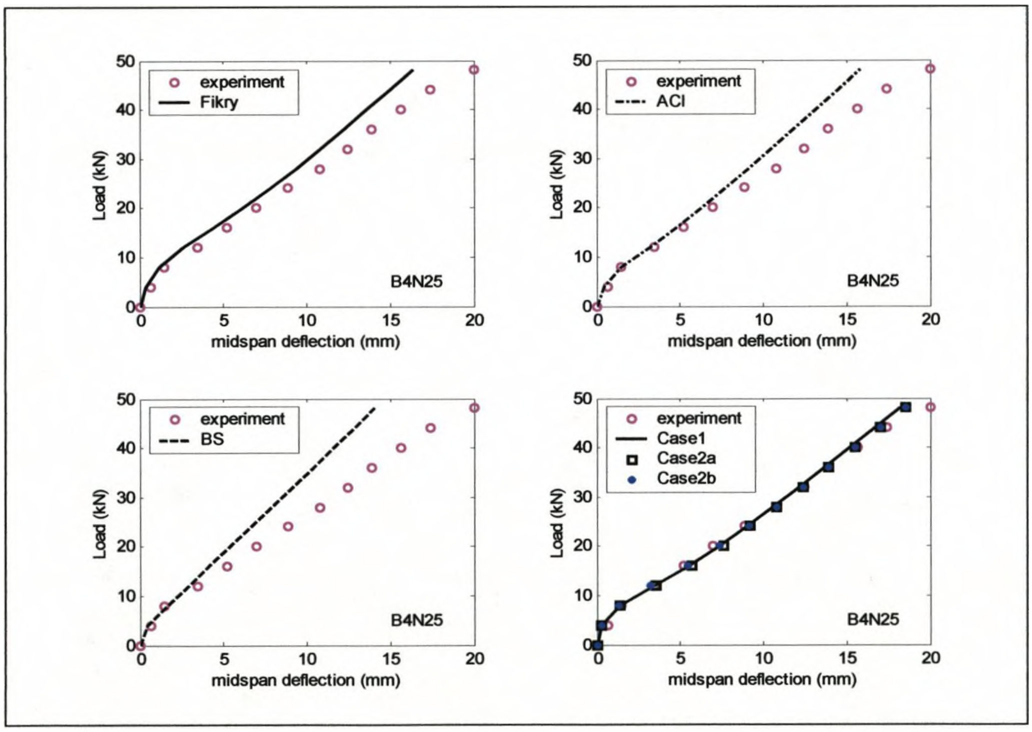

Figure C-34 Comparison between measured and predicted deflection of B4N25 with various methods

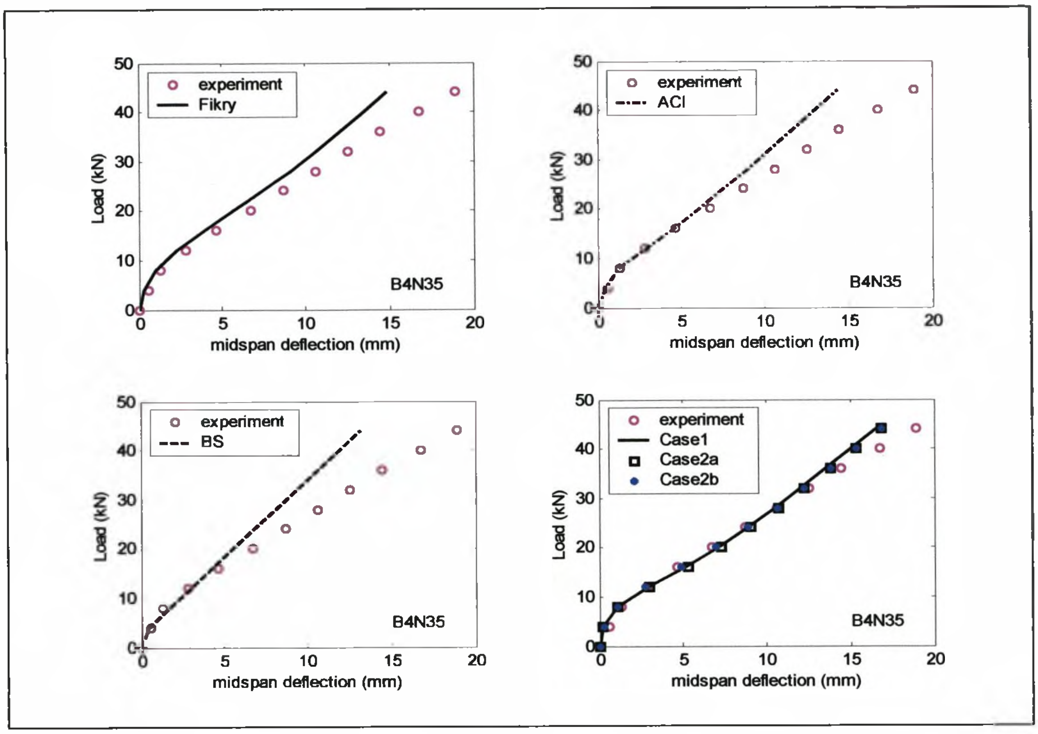

Figure C-35 Comparison between measured and predicted deflection of B4N35 with various methods

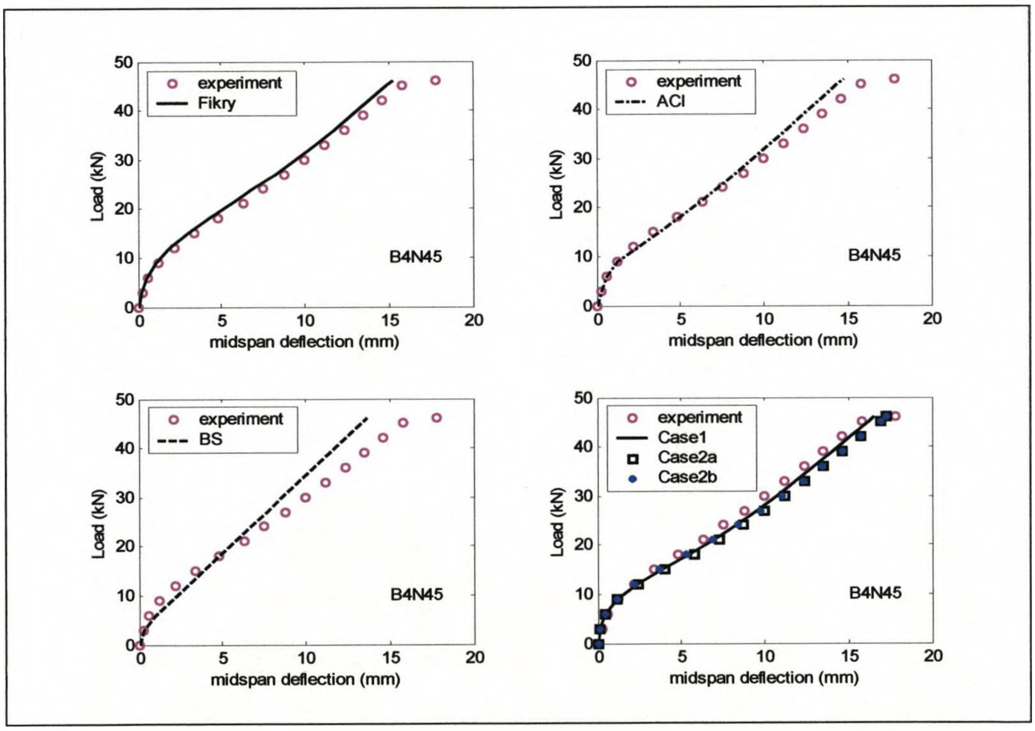

Figure C-36 Comparison between measured and predicted deflection of B4N45 with various methods